Universidade Federal do Rio de Janeiro

Instituto de Bioquímica Médica

Fausto Stauffer Junqueira de Souza

FUSÃO DE MEMBRANAS COMO ALVO PARA INATIVAÇÃO VIRAL E DESENVOLVIMENTO DE VACINAS

Rio de Janeiro

2007

Fausto Stauffer Junqueira de Souza

FUSÃO DE MEMBRANAS COMO ALVO PARA INATIVAÇÃO VIRAL E DESENVOLVIMENTO DE VACINAS

Tese de doutorado apresentada ao Programa de Pós-graduação em Química Biológica, Instituto de Bioquímica Médica, Universidade Federal do Rio de Janeiro, como parte dos requisitos necessários à obtenção do título de Doutor em Química Biológica.

Orientadora: Andrea Thompson Da Poian

Rio de Janeiro

2007

FICHA CATALOGRÁFICA

Stauffer, Fausto.

Fusão de membranas como alvo para inativação viral e desenvolvimento de vacinas / Fausto Stauffer Junqueira de Souza. – Rio de Janeiro, 2007.

161 f.: il.

Dissertação (Doutorado em Química Biológica) – Universidade Federal do Rio de Janeiro, Instituto de Bioquímica Médica, 2007.

Orientadora: Andrea Thompson Da Poian

1. Fusão de Membranas. 2. Inativação Viral. 3. Dietilpirocarbonato. 4. Vacina. I. Da Poian, Andrea T. (Orient.). II. Universidade Federal do Rio de Janeiro. Instituto de Bioquímica Médica. III. Título.

AGRADECIMENTOS

À Andrea, minha orientadora, pelo apoio durante todos esses anos. Muito obrigado pelo voto de confiança no momento que mais precisei. Tenho certeza que nossos laços de amizade irão perdurar apesar do término do doutorado.

À Fabiana, pela amizade e orientação durante minha iniciação científica até os dias atuais.

Ao prof. Miguel, meu orientador em Portugal, pela hospitalidade e amizade.

Aos meus alunos de iniciação científica: Carol, Fernando, Marcos, Nathalia, Sabrina e Vitor.

Ao Joari, pelo valioso apoio no início do doutorado.

Ao prof. Ronaldo e à Ada, meus colaboradores, pela ajuda no desenvolvimento desta tese.

Aos meus outros colaboradores: prof. Gilberto Weissmüller, prof[a]. Gisele Fabrino, prof[a]. Lucia Bianconi e prof. Luiz Juliano.

Ao prof. Paulo Mourão, por revisar esta tese e “batalhar” pelo sucesso do programa MD-PhD.

Ao pessoal do meu laboratório: Ana Paula, Aninha, Beth, Carla, Eliesier, Fernanda, Flávia, Iranaia, Leandro, Luíza, Mariana, Marina, Marisa, Rogério, Rosângela, Tatiana e Thaís.

Ao pessoal do laboratório e amigos de Portugal: David, Guida, Isabel, Manuel, Salomé, Silvia, Sónia.

Ao pessoal do laboratório do Ronaldo: Chico, Diego, Emerson e Marcela.

Aos membros da banca, pela disposição em aceitar o convite.

À minha grande amiga Carol e aos meus amigos Alberto, Flávio, Karina e Lê.

À Mel, minha namorada, por tudo.

Aos pais da Mel, Fernando e Adelaide.

Aos meus pais, por todo o apoio e compreensão que foram imprescindíveis durante o doutorado.

RESUMO

STAUFFER, Fausto Junqueira de Souza. Fusão de membranas como alvo para inativação viral e desenvolvimento de vacinas. Rio de Janeiro, 2007. Dissertação (Doutorado em Química Biológica) – Instituto de Bioquímica Médica, Centro de Ciências da Saúde, Universidade Federal do Rio de Janeiro, Rio de Janeiro, 2007.

A fusão de membranas é uma etapa essencial para a entrada dos vírus envelopados na célula alvo. Este processo é catalisado pelas glicoproteínas do envelope viral, que sofrem uma mudança conformacional desencadeada pela interação do vírus com seu receptor celular específico ou exposição ao pH ácido do meio endossomal. Nesta reestruturação da proteína de superfície viral, ocorre a exposição do peptídeo de fusão, que desestabiliza a membrana, iniciando a reação de fusão. A elucidação dos mecanismos moleculares envolvidos na reação de fusão de membranas pode auxiliar no desenvolvimento de novos compostos de inativação viral. Com este objetivo, foi investigada a interação dos vírus da estomatite vesicular e da dengue com vesículas lipídicas, estudando as mudanças conformacionais das glicoproteínas virais e o processo de fusão. Os resultados obtidos com o vírus da dengue indicam que o peptídeo de fusão da glicoproteína E possui alta afinidade por vesículas compostas de lipídeos aniônicos e que a interação é de natureza eletrostática. Tanto o coeficiente de partição quanto a reação de fusão possuem maior intensidade na presença de fosfolipídios carregados negativamente e da oligomerização do peptídeo. No caso do vírus da estomatite vesicular (VSV), estudos prévios haviam demonstrado que a fusão de membranas ocorre numa faixa estreita de pH, entre 6.2 e 5.8, sugerindo que a protonação de resíduos de histidina seria necessária para este processo. A fim de investigar o papel desses aminoácidos na fusão mediada pelo VSV, modificamos quimicamente estes resíduos com dietilpirocarbonato (DEPC). Demonstramos que a fusão de membrana mediada pelo VSV era inibida pela modificação dos resíduos de histidina. Medidas de fluorescência mostraram que a modificação do vírus com DEPC abolia as mudanças conformacionais da proteína G, sugerindo que a protonação de resíduos de histidina dirige a interação entre a glicoproteína viral e a membrana alvo no pH ácido do meio endossomal. Baseado nestes resultados, decidimos avaliar se o tratamento com DEPC era capaz de inativar o vírus e o potencial uso deste composto como inativador viral para o desenvolvimento de vacinas. A infectividade do VSV em células BHK_{21} e a patogenicidade em camundongos Balb/c foram abolidas através do tratamento viral com DEPC 0.5 mM. Além disso, a modificação com DEPC não alterou a integridade conformacional das proteínas de superfície do VSV inativado como observado por microscopia eletrônica e ELISA de competição. Os anticorpos produzidos nos camundongos após imunização intraperitoneal com VSV inativado pelo DEPC misturado com adjuvantes foram capazes de reconhecer e neutralizar o vírus nativo, além de proteger de forma eficiente os animais do desafio com doses letais de VSV. Esses resultados em conjunto sugerem que a inativação viral com DEPC baseada na inibição da fusão de membranas é um método adequado para o desenvolvimento de vacinas.

Palavras chave: fusão de membranas / inativação viral / dietilpirocarbonato

ABSTRACT

STAUFFER, Fausto Junqueira de Souza. Fusão de membranas como alvo para inativação viral e desenvolvimento de vacinas. Rio de Janeiro, 2007. Dissertação (Doutorado em Química Biológica) – Instituto de Bioquímica Médica, Centro de Ciências da Saúde, Universidade Federal do Rio de Janeiro, Rio de Janeiro, 2007.

Membrane fusion is an essential step in the entry of enveloped viruses into their host cells. This process is catalyzed by viral surface glycoproteins that undergo a conformational changes triggered by interaction with specific cellular receptors or by the exposition to low pH of endossomal medium. The structural reorganization of the viral glycoproteins leads to the exposure of the fusion peptide, a specific segment of these proteins, which destabilizes the lipid bilayers, initiating the fusion reaction. Understanding the virus induced membrane fusion at the molecular level should provide means to develop new viral inactivating compounds. For this purpose, we evaluated the interaction of vesicular stomatitis and dengue viruses with lipid vesicles, studying the conformational changes in viral glycoproteins and the membrane fusion process. In dengue virus studies, our results indicate that E glycoprotein fusion peptide has a high affinity to vesicles composed of anionic lipids and that the interaction is mainly electrostatic. Both partition coefficient and fusion index are enhanced by negatively charged phospholipids and peptide oligomerization. In the case of vesicular stomatitis virus (VSV), previous studies have shown that membrane fusion occurs at a very narrow pH range, between 6.2 and 5.8, suggesting that His protonation is required for this process. To investigate the role of His in VSV fusion, we chemically modified these residues using diethypyrocarbonate (DEPC). We found that membrane fusion mediated by VSV was inhibited by His modification. Fluorescence measurements showed that VSV modification abolished pH-induced conformational changes in G protein, suggesting that His protonation drives G protein interaction with the target membrane at acidic pH. Based on these results, we decided to assess whether treatment with DEPC was able to inactivate the virus and its potential use as a viral inactivating chemical agent for the development of useful vaccines. VSV infectivity in BHK_{21} cells and pathogenicity in Balb/c mice were abolished by viral treatment with 0.5mM DEPC. In addition, DEPC treatment did not alter the conformational integrity of surface proteins of inactivated VSV as demonstrated by transmission electron microscopy and competitive ELISA. Antibodies elicited in mice by intraperitoneal immunization with DEPC-inactivated VSV mixed with adjuvants were able to recognize and neutralize the native virus and efficiently protected animals against the challenge with lethal doses of VSV. These results together suggest that viral inactivation with DEPC based on membrane fusion inhibition seems to be a suitable method for the development of vaccines.

Keywords: membrane fusion / viral inactivation / diethypyrocarbonate

LISTA DE FIGURAS

LISTA DE TABELAS

LISTA DE ABREVIATURAS

BHK	do inglês: *baby hamster kidney*
C-terminal	Carboxi-terminal
DEN	Vírus da dengue
DEPC	Dietilpirocarbonato
ELISA	do inglês: *enzyme-linked immunosorbent assay*
GAG	Glicosaminoglicano
GP	Glicoproteína
HIV	Vírus da imunodefiência humana
HS	Heparan sulfato
IgG	Imunoglobulinas do tipo G
IgM	Imunoglobulinas do tipo M
INPI	Instituto Nacional da Propriedade Industrial
N-terminal	Amino-terminal
PS	Fosfatidilserina
RNA	do inglês: *ribonucleic acid*
TBE	do inglês: *tick born encephalitis*
UV	Ultra-violeta
VSHV	Vírus da septicemia hemorrágica viral
VSV	Vírus da estomatite vesicular
VSV-NJ	Vírus da estomatite vesicular New Jersey
VSV-IN	Vírus da estomatite vesicular Indiana

LISTA DE AMINOÁCIDOS

Ala	A	Alanina
Cys	C	Cisteína
Asp	D	Ácido Aspártico
Glu	E	Ácido Glutâmico
Phe	F	Fenilalanina
Gly	G	Glicina
His	H	Histidina
Ile	I	Isoleucina
Lys	K	Lisina
Leu	L	Leucina
Met	M	Metionina
Asn	N	Asparagina
Pro	P	Prolina
Gln	Q	Glutamina
Arg	R	Arginina
Ser	S	Serina
Thr	T	Treonina
Val	V	Valina
Trp	W	Triptofano
Tyr	Y	Tirosina

SUMÁRIO

INTRODUÇÃO

1 Introdução

1.1 Aspectos gerais da infecção viral

Os vírus são os menores organismos que podem se replicar e são classicamente conhecidos pela sua habilidade de atravessar filtros que retêm até as menores bactérias. Na sua forma mais básica, as partículas virais são compostas por um material genético, que é revestido por uma capa protéica, conhecida como capsídeo. Em alguns casos, a partícula viral pode ainda ser envolvida por uma membrana lipídica, conhecida como envelope, que contém as glicoproteínas virais. Apesar desta simplicidade, os vírus apresentam grande variação quanto ao tamanho, forma e composição e podem infectar uma gama de organismos na natureza.

A infecção da célula hospedeira é essencial para a replicação viral, já que os vírus não possuem metabolismo próprio e dependem da maquinaria enzimática celular para este processo. Em uma primeira etapa da infecção viral, os vírus aderem às células por meio de regiões específicas das proteínas de sua superfície interagindo com moléculas presentes na superfície celular que passam a funcionar como receptores. Estas moléculas podem ser proteínas, carboidratos ou lipídeos. Após aderirem à superfície celular, os vírus iniciam sua entrada nas células utilizando diferentes mecanismos, levando à liberação do genoma viral no citoplasma ou no núcleo da célula hospedeira.

O genoma viral pode ser liberado no citoplasma tanto como moléculas de ácido nucléico livre, como acontece para alguns vírus RNA, quanto como complexos de ácido nucléico e proteínas. Coincidindo com, ou imediatamente após a entrada na célula, começa um processo de desmontagem dos componentes virais, levando à replicação do genoma viral, com a formação de novas partículas virais.

A liberação destas partículas recém formadas da célula hospedeira pode ocorrer de diferentes formas. Os vírus envelopados podem sair da célula por brotamento através da membrana plasmática ou pela fusão de vesículas secretoras contendo partículas virais com a membrana plasmática. Os vírus não envelopados são geralmente liberados por lise da membrana celular.

1.2 Fusão de membranas

Tanto os vírus envelopados quanto os não envelopados compartilham as principais etapas do processo de entrada nas células hospedeiras, que se inicia pela ligação na célula hospedeira e termina com a liberação do material genético viral no citoplasma (Dimitrov,

2004). A principal diferença está na etapa de penetração do nucleocapsídeo no citoplasma: para os vírus envelopados, ocorre a fusão de membranas, enquanto que para os não envelopados, ocorre a formação de poros ou lise de membranas (Marsh e Helenius, 2006).

A fusão de membranas, um processo celular essencial para fagocitose, pinocitose e tráfego de vesículas, é o mecanismo básico de entrada dos vírus envelopados nas células hospedeiras. É um método "elegante e efetivo" para liberar o genoma viral no citoplasma e iniciar a infecção (Smith e Helenius, 2004). A reação de fusão do envelope viral pode ser direta com a membrana plasmática da célula ou com a membrana do compartimento endossomal após a internalização da partícula viral por endocitose mediada por receptor (Earp *et al.*, 2005; Harrison, 2005; Kielian e Rey, 2006) (fig.1). As vias de endocitose utilizadas podem ser dependente de clatrina (mais comum), dependente de caveolina ou independente de clatrina e caveolina (Sieczkarski e Whittaker, 2002; Marsh e Helenius, 2006). Dentre os vírus que são capazes de fundir-se diretamente com a membrana plasmática podemos citar como exemplo os paramixovírus, os retrovírus e os herpesvírus. Já os alfavírus, os flavivírus, os rabdovírus e o vírus influenza são exemplos de vírus que penetram na célula hospedeira através de endocitose mediada por receptor, seguida pela fusão da membrana viral com a endossomal (Dimitrov, 2004).

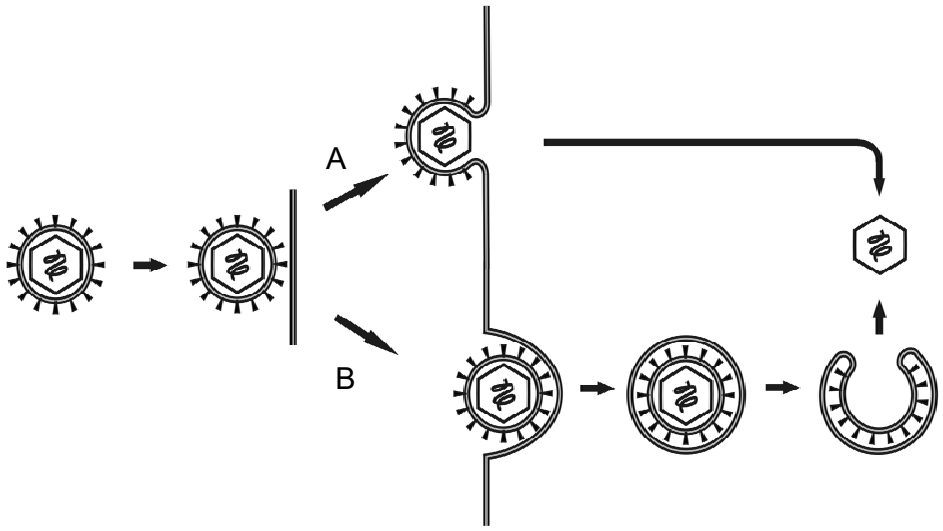

Figura 1: Mecanismos de entrada dos vírus envelopados nas células hospedeiras: **(A)** fusão direta das membranas viral e plasmática; **(B)** endocitose mediada por receptor, com posterior acidificação do endossoma e fusão de membranas. Extraído de Da Poian *et al.* (2005).

A fusão de membranas induzida pelos vírus envelopados é mediada pelas proteínas de superfície (Kielian e Rey, 2006), que sofrem uma dramática mudança conformacional

desencadeada pela interação com o receptor na membrana alvo em pH neutro ou pela exposição ao pH ácido do meio endossomal (Earp *et al.*, 2005; Sieczkarski e Whittaker, 2005). Outras formas de ativação do processo de fusão têm sido propostas, como a combinação de interação da glicoproteína viral com seu receptor associada à exposição ao pH ácido (Mothes *et al.*, 2000; Matsuyama *et al.*, 2004) e a clivagem proteolítica dessas glicoproteínas por proteases do endossoma ativadas pelo pH ácido (Chandran *et al.*, 2005).

1.2.1 Glicoproteínas Virais

As glicoproteínas dos vírus envelopados, tipicamente proteínas integrais de membrana tipo I, são codificadas pelo material genético viral e sintetizadas utilizando-se a maquinaria de síntese protéica da célula infectada. Após o processamento destas proteínas, elas são ancoradas em membranas da célula hospedeira e incorporadas às partículas virais durante a montagem e brotamento dos novos vírus. Na superfície viral, podemos observar que estas proteínas formam oligômeros altamente organizados e são glicosiladas (Eckert e Kim, 2001).

A fusão de membranas, etapa essencial para infecção dos vírus envelopados, é mediada por estas proteínas transmembrana (Kielian e Rey, 2006), que por esta razão são denominadas proteínas de fusão. Estas glicoproteínas contêm uma seqüência de aminoácidos com grande número de resíduos hidrofóbicos e de glicinas, capaz de interagir com a membrana alvo, conhecida como peptídeo de fusão (Eckert e Kim, 2001). São sintetizadas numa conformação metaestável de alta energia na superfície viral, na qual seu peptídeo de fusão encontra-se "escondido" no interior do oligômero formado pelas glicoproteínas (Hernandez *et al.*, 1996). No entanto, é proposto que a ligação ao receptor ou a exposição ao pH ácido acarretaria na transição da glicoproteína viral para a conformação fusogênica de baixa energia, expondo o peptídeo de fusão e liberando a energia necessária para o processo de fusão (Carr *et al.*, 1997; Epand, 2003; Dimitrov, 2004).

As características em comum das proteínas de fusão são: (a) a maior parte de sua massa é composta da porção externa à membrana viral, (b) o N-terminal está sempre localizado no domínio externo, (c) os domínios transmembrana e C-terminal são relativamente pequenos, (d) contêm carboidratos N-ligados, (d) formam oligômeros, e (e) estão presentes em alta densidade na membrana viral (Eckert e Kim, 2001).

Embora possuam estas semelhanças, com base em critérios estruturais, principalmente no estado conformacional pós-fusão, foram definidas até o momento duas classes de proteínas de fusão (fig. 2) (Heinz e Allison, 2001; Lescar *et al.*, 2001; Weissenhorn *et al.*, 2007). Entretanto, as proteínas de fusão de alguns vírus possuem características que não as

enquadram em classe I ou II e provavelmente representam uma nova classe de proteínas de fusão, que recentemente vem sendo referida como classe III, como é o caso dos rabdovírus (fig. 2) (Da Poian *et al.*, 2005; Heldwein *et al.*, 2006; Roche *et al.*, 2006; Weissenhorn *et al.*, 2007).

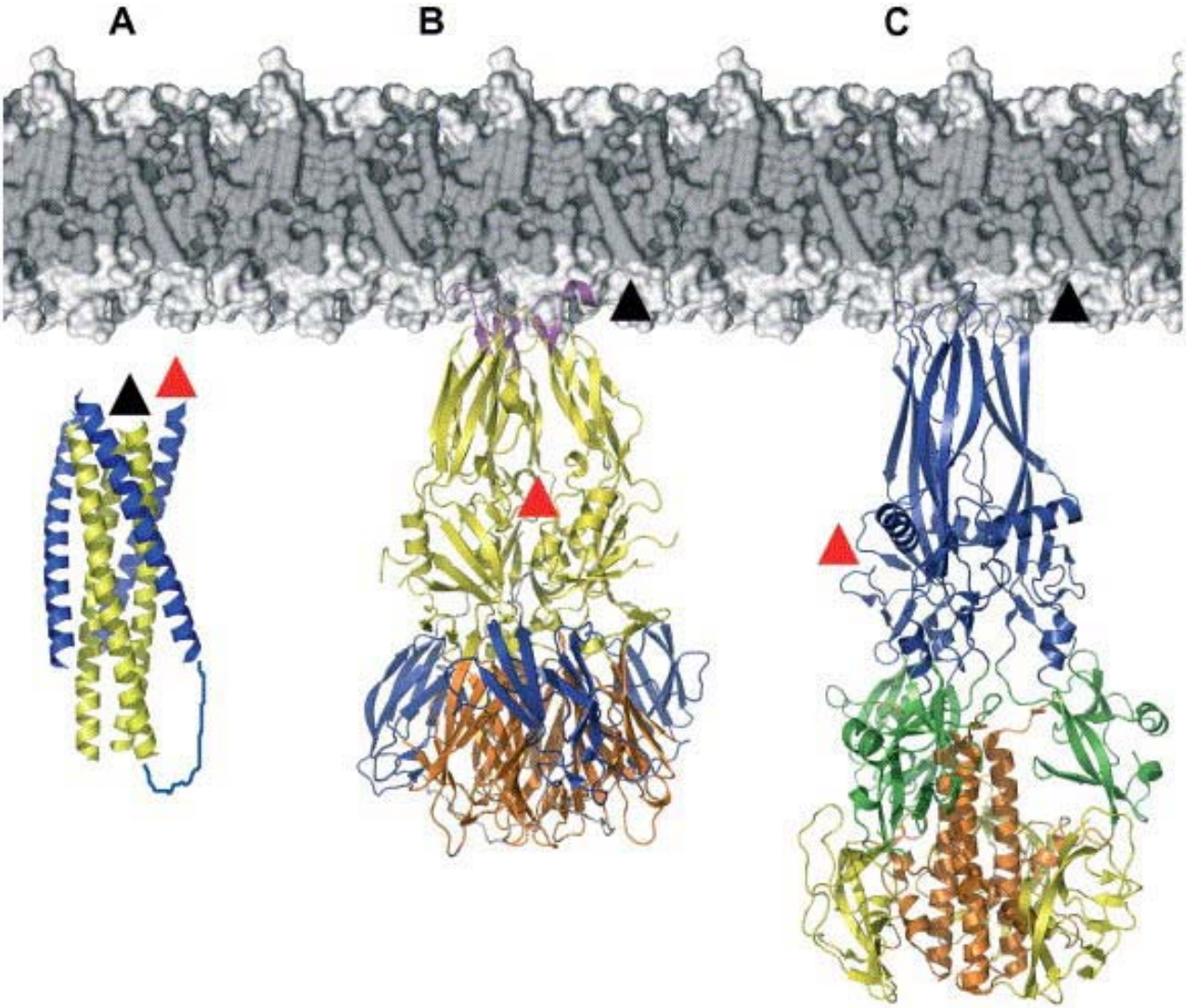

Figura 2: Representação esquemática das estruturas das proteínas de fusão de classes I, II e III no estado conformacional pós-fusogênico. **(A)** Proteína gp41 do HIV-1 (classe I); **(B)** Proteína E dos flavivírus (classe II); **(C)** Glicoproteína G do VSV (classe III). As posições da porção transmembrana (seta vermelha) e do peptídeo de fusão (seta preta) estão indicadas. Adaptado de (Weissenhorn *et al.*, 2007).

As proteínas de classe I são exemplificadas pelas proteínas de fusão dos ortomixovírus (Wilson *et al.*, 1981; Bullough *et al.*, 1994), retrovírus (Fass *et al.*, 1996), coronavirus (Xu *et al.*, 2004a; Xu *et al.*, 2004b), filovírus (Weissenhorn *et al.*, 1998) e paramixovírus (Chen *et al.*, 2001; Yin *et al.*, 2005; Yin *et al.*, 2006). Elas formam espículas triméricas no envelope viral, com estrutura predominantemente em α-hélices. São sintetizadas como uma proteína precursora, que após uma clivagem proteolítica gera duas subunidades que permanecem

ligadas entre si, seja por pontes dissulfeto ou ligações não covalentes. Uma das subunidades é responsável pela interação inicial com o receptor na membrana alvo. Já a outra, que se encontra ancorada no envelope viral, contém na extremidade N-terminal uma seqüência de aminoácidos hidrofóbicos, que está diretamente relacionada com a fusão de membranas. Após a ligação ao receptor celular ou a exposição ao baixo pH, a proteína de fusão muda parcialmente de conformação, mantendo-se em trímeros, e o peptídeo de fusão é então inserido na membrana alvo, catalisando a reação de fusão. A conformação pós-fusão apresenta uma estrutura bastante típica, conhecida como *hairpin*, ou grampo de cabelo (fig. 2).

As proteínas de fusão de classe II são exemplificadas pelos alfavírus (Lescar *et al.*, 2001; Gibbons *et al.*, 2004) e flavivírus (Rey *et al.*, 1995; Modis *et al.*, 2003; Modis *et al.*, 2004). Elas possuem três domínios, que estão principalmente organizados em folhas-β, que também formam *hairpins*. Estas proteínas formam homo ou heterodímeros, que se encontram paralelos ao envelope viral. O peptídeo de fusão está localizado em um *loop* entre duas fitas β, que se localiza na interface interna do dímero. Ao contrário das proteínas de classe I, as proteínas de classe II não sofrem clivagem proteolítica durante sua maturação. No entanto, é necessária a clivagem de proteínas de membrana que se encontram associadas a estas proteínas de fusão. Após a exposição ao pH ácido, a proteína se reorganiza em trímeros perpendiculares à membrana viral, expondo o peptídeo de fusão, catalisando a fusão de membranas.

As principais características dessas duas classes de proteínas de fusão estão listadas na tabela 1.

Tabela 1: Comparação entre as proteínas de fusão de classes I e II

Característica	Classe I	Classe II
Mudança conformacional durante a fusão	Trímero metaestável para estável da proteína de fusão	Dímero metaestável para trímero estável da proteína de fusão
Estrutura secundária predominante	alfa hélice	folha beta
Estrutura pós fusão	Trímero de hairpins com uma região central em alfa hélice	Trímero de hairpins compostos de estrutura beta
Maturação para o conformação pré fusão	Clivagem proteolítica da proteína de fusão	Clivagem proteolítica da proteína acessória
Localização do peptídeo de fusão	Peptídeo localizado na porção N-terminal no interior do trímero	Loop hidrofófico no interior do dímero

As proteínas de classe III também apresentam trímeros de *hairpins*, mas combinam elementos estruturais de ambas as classes de proteínas de fusão. Semelhante às proteínas de classe I, apresentam uma região central em α-hélice. No entanto, cada domínio de fusão está localizado na ponta de folhas-β alongadas, característica marcante das proteínas de classe II. Além disso, a glicoproteína dos rabdovírus não sofre clivagem proteolítica e nem é sintetizada associada a alguma outra proteína durante seu processo de maturação, características presentes nas proteínas de classes I e II, respectivamente. Por último, as mudanças conformacionais induzidas por baixo pH nesta proteína são reversíveis, enquanto que nas demais proteínas de fusão são irreversíveis.

Apesar das proteínas de fusão de classes I e II apresentarem importantes diferenças estruturais, os mecanismos de fusão propostos são bastante similares (fig. 3) (Weissenhorn *et al.*, 1999; Skehel e Wiley, 2000; Bressanelli *et al.*, 2004; Modis *et al.*, 2004; Weissenhorn *et al.*, 2007) e as mudanças conformacionais induzidas durante a ativação da forma não fusogênica para a forma fusogênica são irreversíveis (Carr *et al.*, 1997; Lescar *et al.*, 2001; Stiasny *et al.*, 2001).

A reação de fusão induzida pelas proteínas de classe I (fig. 3A) é iniciada pela ligação do vírus ao seu receptor específico na membrana alvo ou pela exposição ao pH ácido no meio endossomal, sendo desencadeadas mudanças conformacionais que resultam na projeção e inserção do peptídeo de fusão na membrana alvo. Assim, a proteína de fusão fica ancorada nas membranas celular e viral. Subsequentemente, ocorre uma reestruturação da proteína, que se "dobra", forçando a aproximação da porção N-terminal, que contém o peptídeo de fusão inserido na membrana alvo, com a porção C-terminal transmembrana, que está ancorada no envelope viral, acarretando a aproximação dessas duas membranas (Harrison, 2005).

Já o processo de fusão induzido pelas proteínas de fusão de classe II (fig. 3B) inicia-se com a reorganização da proteína em trímeros desencadeada pela exposição ao pH ácido do meio endossomal. Durante este processo, ocorre um rearranjo da orientação relativa dos domínios II e III da glicoproteína, que acarreta na exposição do peptídeo de fusão, que se insere na membrana alvo, com o ancoramento da proteína nas membranas celular e viral, como já havia sido descrito para as proteínas de classe I. Posteriormente, ocorre uma reestruturação do domínio III, que traz o peptídeo de fusão e o domínio transmembrana C-terminal para posições justapostas, ocasionando a aproximação das membranas viral e celular (Harrison, 2005).

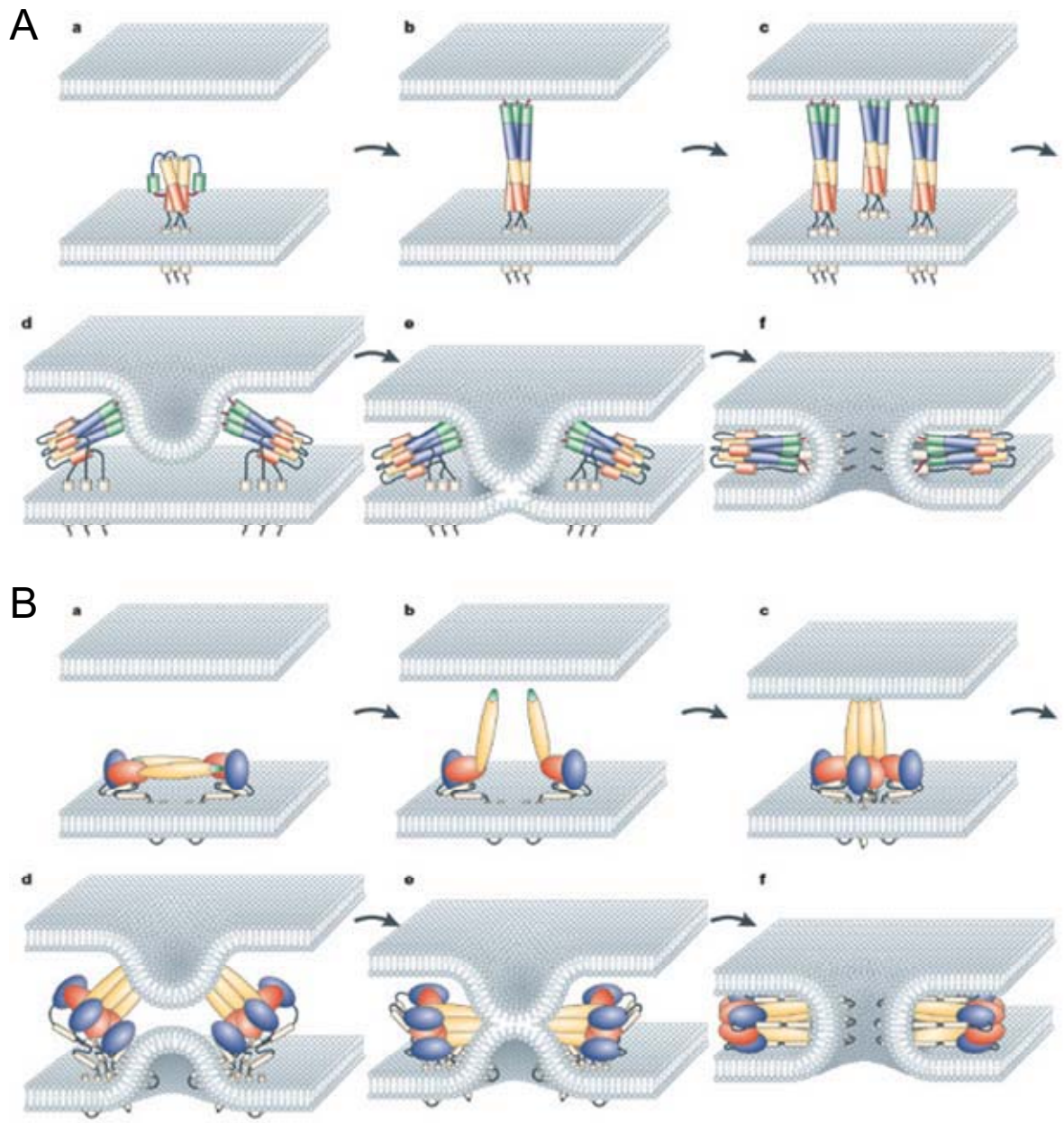

Figura 3: Mecanismos propostos para o processo de fusão catalisado pelas glicoproteínas virais. (A) Proteína de classe I. O trímero da proteína de fusão na sua forma metaestável é representado ancorado no envelope viral, com seu peptídeo de fusão em rosa escuro (a). Após a ligação ao receptor celular ou exposição ao pH ácido do meio endossomal, a proteína de fusão adquire uma conformação estendida e o peptídeo de fusão é inserido na membrana alvo (b). Vários trímeros estão envolvidos no processo (c). A reestruturação da proteína continua, com o "dobramento" da molécula, que aproxima as membranas viral e celular (d). É formada a haste de hemifusão (e) e finalmente o poro de fusão (f) após o total rearranjo da proteína de fusão, que adquiriu sua conformação mais estável, onde o peptídeo de fusão e o domínio transmembrana se encontram justapostos. **(B) Proteína de classe II.** O dímero é representado na superfície viral, com o seu peptídeo de fusão interno em verde, domínio I em vermelho, II em amarelo e III em azul (a). A proteína se liga ao receptor específico e é internalizada por endocitose. Após exposição ao pH ácido do meio endossomal, ocorre um rearranjo na orientação relativa dos domínios II e III, expondo o peptídeo de fusão (b) e permitindo a formação de trímeros e a inserção do peptídeo de fusão na membrana alvo (c). A reestruturação da proteína continua, com o "dobramento" do domínio III, que aproxima as membranas viral e endossomal (c). É formada a haste de hemifusão (d) e finalmente o poro de fusão (f) após o total rearranjo trimérico da proteína de fusão, onde o peptídeo de fusão e a porção transmembrana se encontram próximos. Extraído de Mukhopadhyay *et al.* (2005).

A desestabilização da membrana alvo pelo peptídeo de fusão e a aproximação com o envelope viral são os processos essenciais para formação da haste de hemifusão (intermediário do processo de fusão, onde as monocamadas externas encontram-se fusionadas, enquanto que as internas não) (Jahn *et al.*, 2003). Este intermediário se forma durante a aproximação das membranas viral e celular. No final da reestruturação das proteínas de fusão de classes I e II, ocorre a formação do poro de fusão que permite a liberação do nucleocapsídeo viral no citoplasma (Harrison, 2005).

1.3 Modelo de estudo I: o vírus da estomatite vesicular

O vírus da estomatite vesicular (VSV) pertence ao gênero *Vesiculovirus*, da família Rhabdoviridae, um grupo de vírus com grande abrangência de hospedeiros (plantas, animais invertebrados e vertebrados) (Rose e Whitt, 2001). Dentre os rabdovírus, o VSV é o mais estudado e é o agente responsável pela estomatite vesicular. Esta doença afeta bovinos, eqüinos e suínos, e suas manifestações clínicas incluem vesiculação e/ou ulceração grave na língua e nos tecidos orais, podendo, às vezes, provocar lesões nos pés e nas tetas dos animais acometidos, o que resulta em uma substancial perda de produtividade (Letchworth *et al.*, 1999). Os sintomas desta doença são indistinguíveis daqueles observados na febre aftosa, exceto por afetar também eqüinos. A infecção em humanos tem sido observada em pessoas expostas a animais infectados ou inadvertidamente expostas em laboratório (Johnson *et al.*, 1966; Fields e Hawkins, 1967; Quiroz *et al.*, 1988). Em humanos, a infecção pode ser assintomática ou se manifestar com sinais e sintomas de um resfriado comum.

A estomatite vesicular causada pelo VSV é endêmica no continente americano, ocorrendo desde o sudeste dos Estados Unidos até o norte da América do Sul, passando pelo México e por toda a América Central (Wilks, 1994; Letchworth *et al.*, 1999; Rodriguez, 2002). Nestas regiões, os sorotipos predominantes são VSV New Jersey (VSV-NJ) e VSV Indiana (VSV-IN) (Cotton, 1926; Cotton, 1927). No Brasil, é endêmico o sorotipo Indiana 3, ou Alagoas (Federer *et al.*, 1967; Tesh *et al.*, 1987). Outros vesiculovírus também já foram encontrados na Índia e na África (Hanson, 1968). Nos Estados Unidos, os dois surtos mais recentes ocorreram em 1997 e 1998, afetando principalmente eqüinos (Mccluskey *et al.*, 1999). Em 1995, um grande surto atingiu rebanhos bovinos causando um impacto significativo na indústria de carne do Colorado (Bridges *et al.*, 1997).

O diagnóstico de infecção por VSV pode ser confirmado através de sorologia por ELISA nas fases sintomática e de convalescença (Allende e Germano, 1993). Tem sido

descrito também o uso de RT-PCR para detecção do VSV em amostras clínicas (Rodriguez *et al.*, 1993; Hofner *et al.*, 1994). Atualmente, não existe vacina disponível contra a estomatite vesicular.

1.3.1 A Estrutura dos Rabdovírus

Os rabdovírus são formados por um capsídeo ribonucléico helicoidal envolto por uma membrana lipídica (Wagner, 1987). O nucleocapsídeo é composto pelo genoma viral, uma fita simples RNA, polaridade negativa, fortemente associado à proteína N e às proteínas L e P, que juntas constituem a RNA polimerase viral. Envolvendo este conjunto, temos o envelope lipídico, que está associado a duas proteínas: a glicoproteína G, integral à membrana, cujos trímeros formam as espículas virais, e a proteína M, que interage com a face interna da membrana e com o capsídeo ribonucléico (fig. 4).

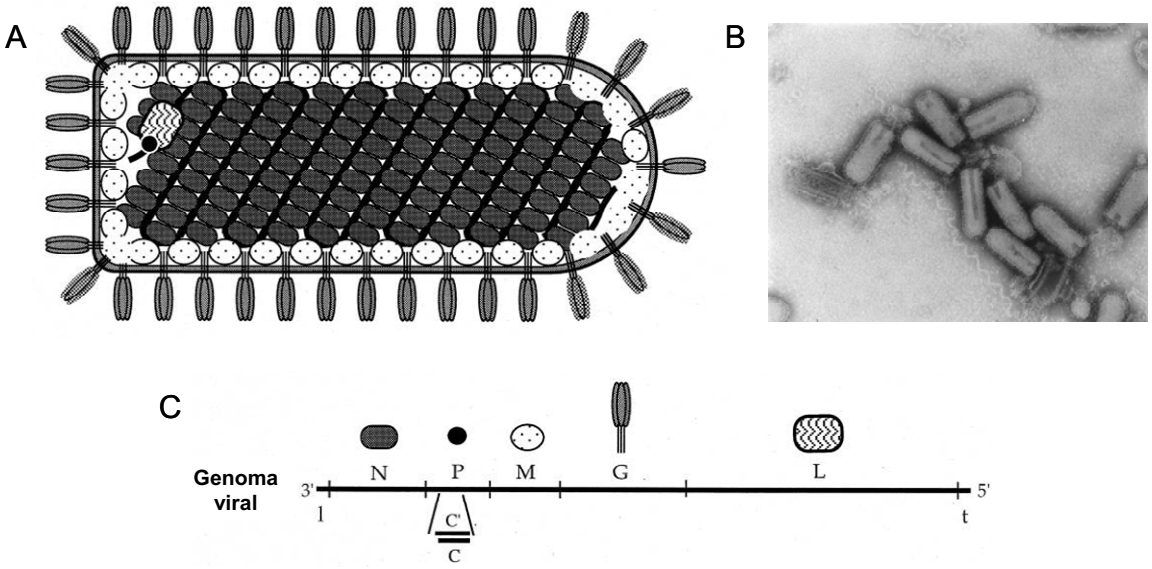

Figura 4: Representação esquemática do VSV. (A) Neste esquema observamos os dois maiores componentes estruturais do VSV: o nucleocapsídeo, contendo o RNA envolto, principalmente, pela proteína N, e pelas proteínas L e P; e a membrana lipídica que contém a glicoproteína transmembrana (G) e a proteína periférica de matriz (M), que adere na superfície interna da membrana e liga-se ao nucleocapsídeo. **(B)** Micrografia eletrônica do vírus. **(C)** Seqüência do genoma viral com os símbolos representando as proteínas expressas. Adaptado de Rose e Whitt (2001).

1.3.2 Ciclo de Replicação dos Rabdovírus

Após a interação com receptores celulares específicos, ocorre a endocitose da partícula viral (Matlin *et al.*, 1982). Durante o processo de acidificação do meio endossomal, é desencadeada a reação de fusão do envelope viral com a membrana do endossoma, com conseqüente liberação do nucleocapsídeo no citoplasma (fig. 5). Em seguida, ocorre a

dissociação do capsídeo viral, liberando o genoma viral que é então transcrito, traduzido e replicado. Após a síntese de novas proteínas virais, inicia-se o processo de montagem viral. As proteínas N, L e P são agrupadas com o RNA genômico formando o nucleocapsídeo. Este se associa à proteína M, que então interage com o domínio citoplasmático da proteína G, levando ao brotamento dos novos vírus (Rose e Whitt, 2001).

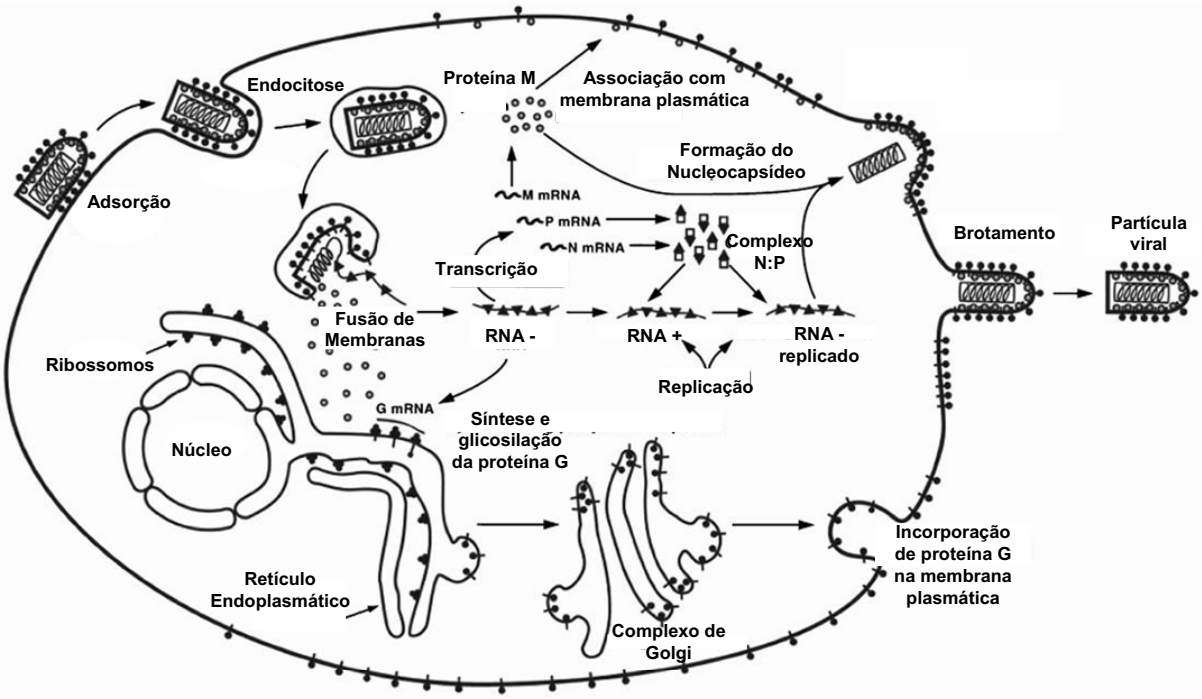

Figura 5: Ciclo de replicação do VSV. Adaptado de Rose e Whitt (2001).

1.3.3 Fusão de membranas mediada pelo VSV

A membrana do VSV possui aproximadamente 1.200 moléculas da proteína G, a glicoproteína de superfície deste vírus, sendo essa proteína envolvida em pelo menos dois passos importantes do processo de infecção do VSV (White *et al.*, 1983): o reconhecimento da célula com conseqüente adsorção à superfície desta, e o processo de fusão de membranas, fundamental à liberação do genoma viral no citoplasma.

A fusão de membranas mediada pela proteína G depende da diminuição do pH (White *et al.*, 1981; Eidelman *et al.*, 1984; Puri *et al.*, 1988). Durante a entrada na célula hospedeira, similar a outras proteínas de fusão, a glicoproteína do VSV sofre mudanças conformacionais, que são essenciais para a aquisição da conformação fusogênica e têm sido motivo de vários estudos. Pelo menos três estados conformacionais podem ser adotados dependendo do pH do meio no qual a proteína se encontra (Pak *et al.*, 1997; Carneiro *et al.*, 2001): estado pré-fusogênico, em pH neutro; estado fusogênico (ativo), em pH ácido, que inicia a reação de fusão; e estado pós-fusogênico, também em pH ácido, que é inativo. Após a endocitose da

partícula viral, ocorre a acidificação do meio endossomal. À medida que o pH diminui no interior do endossoma, uma dramática mudança conformacional na proteína ocorre. Primeiramente, há a exposição de um domínio hidrofóbico que interage com a membrana alvo, e em seguida ocorre perda de estruturas secundária e terciária, que, em pHs mais baixos ainda, se reorganizam em uma nova estrutura (Carneiro *et al.*, 2001). Estes três estados da proteína G se encontram em equilíbrio, que é deslocado para a conformação pós-fusogênica após a exposição ao pH ácido, como observado em estudo realizado com a glicoproteína do vírus da raiva (Roche e Gaudin, 2002).

Recentemente, as estruturas tridimensionais do ectodomínio da proteína G (seqüência de aminoácidos de 17 a 426, indicada na figura 6) na sua conformação pré-fusão (pH neutro) e pós fusão (pH ácido) foram determinadas (Roche *et al.*, 2006; Roche *et al.*, 2007) e podem ser observadas na figura 7. A conformação pós-fusogênica mostra a clássica conformação de *hairpin* observada em outras proteínas de fusão. Como uma proteína de classe I, exibe α-hélices centrais com o domínio de fusão no N-terminal e o domínio transmembrana no C-terminal. Cada domínio de fusão contém dois *loops* de fusão localizados na ponta de uma folha-β, característica similar a uma proteína de classe II. Sendo assim, foi postulado que estas similaridades estruturais são resultados de uma evolução convergente (Roche *et al.*, 2006).

```
1   M K C L L Y L A F L F I G V N C K F T I V F P H N Q K G N W K N V P S N Y H Y C
41  P S S S D L N W H N D L I G T A I Q V K M P K S H K A I Q A D G W M C H A S K W
81  V T T C D F R W Y G P K Y I W Q S I R S F T P S V E Q C K E S I E Q T K Q G T W
121 L N P G F P P Q S C G Y A T V T D A E A V I V Q V T P H H V L V D E Y T G E W V
161 D S Q F I N G K C S N Y I C P T V H N S T T W H S D Y K V K G L C D S N L I S M
201 D I T F F S E D G E L S S L G K E G T G F R S N Y F A Y E T G G K A C K M Q Y C
241 K H W G V R L P S G V W F E M A D K D L F A A A R F P E C P E G S S I S A P S Q
281 T S V D V S L I Q D V E R I L D Y S L C Q E T W S K I R A G L P I S P V D L S Y
321 L A P K N P G T G P A F T I I N G T L K Y F E T R Y I R V D I A A P I L S R M V
361 G M I S G T T T E R E L W D D W A P Y E D V E I G P N G V L R T S S G Y K F P L
401 Y M I G H G M L D S D L H L S S K A Q V F E H P H I Q D A A S Q L P D D E S L F
441 F G D T G L S K N P I E L V E G W F S S W K S S I A S F F F I I G L I I G L F L
481 V L R V G I H L C I K L K H T K K R Q I Y T D I E M N R L G K
```

Figura 6: Seqüência de aminoácidos da proteína G do VSV. O ectodomínio (aa 17-426) está grifado de cinza, sendo que o domínio de fusão (aa 69-188) está de amarelo. Os resíduos de His estão assinalados em vermelho. O segmento 1-511 corresponde ao precursor da glicoproteína G, 17-511 a glicoproteína madura, 1-16 ao peptídeo sinalizador.

A proteína G possui em sua estrutura quatro domínios (fig. 7), que foram determinados pela conformação tridimensional e não pela seqüência linear de aminoácidos. O domínio I, localizado lateralmente no topo da molécula, é composto de aproximadamente 90

resíduos em dois segmentos (resíduos 17-33 e 326-398)[1], principalmente organizados em folhas-β. O domínio II, localizado na região central no topo da molécula, é composto de três segmentos (resíduos 34-51, 275-325 e 399-421), principalmente estruturado em α-hélices. Este domínio está envolvido na formação do trímero. O domínio III é composto de dois segmentos (resíduos 52-62 e 197-274), que estão inseridos no domínio II. Possui duas α-hélices e duas folhas-β. O domínio IV (resíduos 69-188) está inserido num *loop* do domínio III. É uma estrutura composta de folhas-β, contendo dois *loops* onde são encontrados resíduos aromáticos (W88, Y89, Y132, A133).

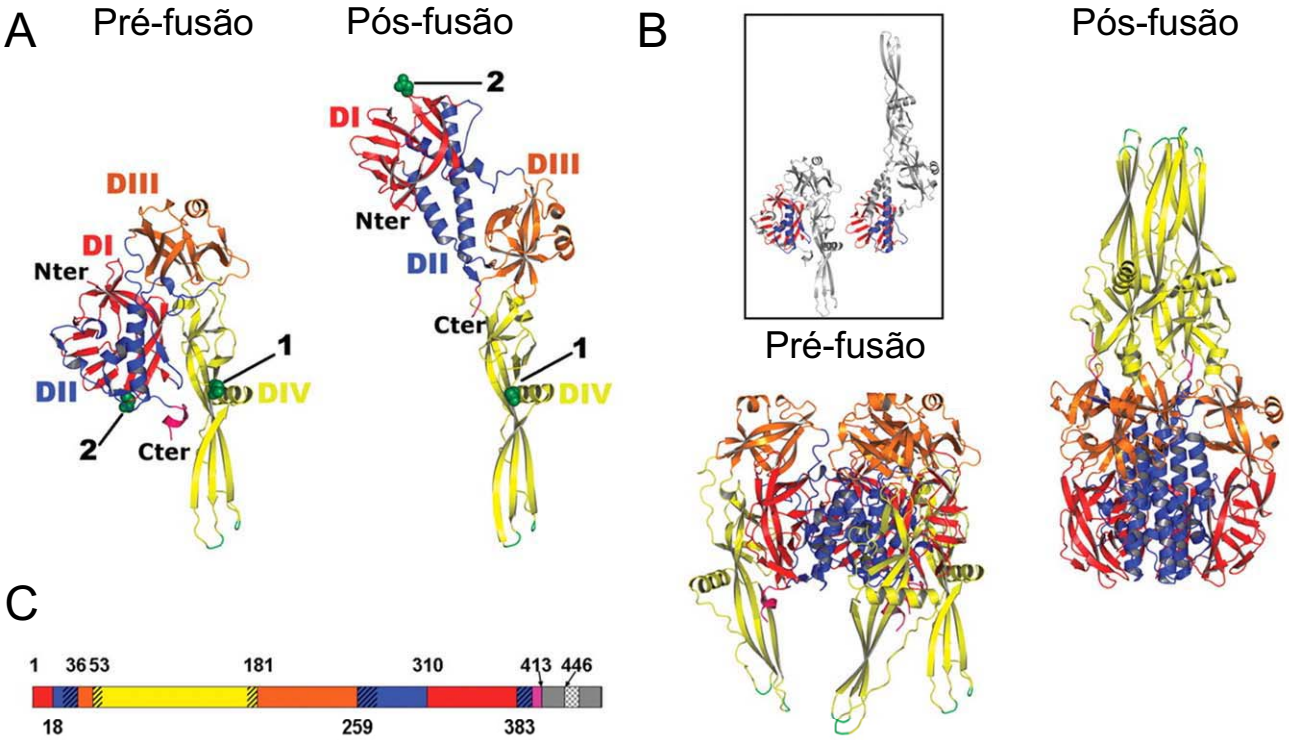

Figura 7: Estrutura cristalográfica da proteína G do VSV nas conformações pré e pós fusogênica. (A) Visão do monômero. **(B)** Visão do trímero. **(C)** Diagrama linear mostrando os resíduos de aminoácidos correspondentes a cada domínio. *Loops* de fusão em verde escuro, domínio I em vermelho, domínio II em azul, domínio III em laranja, domínio IV em amarelo e porção C-terminal em rosa. Os números 1 e 2 representam os sítios de glicosilação. Cter indica a porção C-terminal e Nter a porção N-terminal. Extraído de Roche *et al.* (2007).

O domínio IV é denominado domínio de fusão, visto que a presença de uma grande quantidade de resíduos aromáticos por trímero é provavelmente capaz de desestabilizar a membrana, iniciando o processo de fusão (Roche *et al.*, 2006). Esta idéia é reforçada por antigos experimentos de substituições de aminoácidos em regiões do ectodomínio da proteína

[1] A numeração usada nesta tese inclui os 16 resíduos que contituem o peptídeo sinal, ao contrário da numeração usada nos artigos de Roche et al, 2006 e 2007, que começou a numeração no resíduo 17.

G que eram utilizados como estratégia de localização do peptídeo de fusão do VSV. Mutações em resíduos presentes na região 117-137, que são altamente conservadas nos vesiculovírus, aboliram a fusão de membranas mediada pela glicoproteína, sugerindo que esta região continha o domínio de fusão (Zhang e Ghosh, 1994; Fredericksen e Whitt, 1995). Além disso, já havia sido demonstrado que o segmento contendo os aminoácidos 59-221 tornava-se capaz de interagir com membranas durante as transições conformacionais decorrentes da acidificação (Durrer *et al.*, 1995).

Outras regiões já foram previamente relacionadas com a fusão de membranas catalisadas pelo VSV, estando indiretamente envolvidas com o processo. Este é o caso do segmento contendo os aminoácidos 395-418 (Shokralla *et al.*, 1998) e do domínio transmembrana (Odell *et al.*, 1997; Cleverley e Lenard, 1998; Jeetendra *et al.*, 2003).

A reorganização da proteína G que ocorre após a exposição ao pH ácido está representada na figura 8 (Roche *et al.*, 2007). Resumidamente, ocorre inicialmente a projeção do domínio de fusão para o topo da molécula pela conjugação de dois movimentos: rotação do domínio de fusão (IV) em relação ao domínio III e reposicionamento do domínio III no topo do domínio II, permitindo a interação inicial dos *loops* de fusão com a membrana alvo (fig. 8C). Em seguida, ocorre a reestruturação do domínio II, fazendo com que ocorra uma movimentação da porção C-terminal para a mesma extremidade em que se encontram os *loops* de fusão, acarretando na aproximação das membranas viral e endossomal. Sendo assim, apesar de haver uma grande mudança conformacional da proteína G, somente o domínio II sofre uma grande reestruturação (fig. 8B), pois os domínios I, III e IV mantêm sua estrutura inicial, sofrendo apenas uma reorientação através de movimentos de rotação (fig. 8A).

As características e a termodinâmica da interação entre a proteína G e vesículas de diferentes composições lipídicas foram estudadas previamente por nós através do uso da microscopia de força atômica, calorimetria e espectroscopia de fluorescência (Carneiro *et al.*, 2002) (anexo A). Mostramos que, em diferentes etapas do ciclo de infecção do vírus, as interações entre a proteína viral e membranas são interações de natureza eletrostática envolvendo regiões da proteína carregadas positivamente e fosfolipídios carregados negativamente, mais especificamente a fosfatidilserina (PS) (Carneiro *et al.*, 2002; Da Poian *et al.*, 2005; Carneiro *et al.*, 2006) (anexos A, B e C). Estudos prévios chegaram a especular que este fosfolipídio poderia ser o receptor celular para o VSV (Schlegel *et al.*, 1983). No entanto, já foi demonstrado que o VSV é capaz infectar células independente da presença de PS, mostrando que este fosfolipídio não é o receptor do VSV, podendo talvez funcionar como

co-receptor (Coil e Miller, 2004). Até o presente momento, o receptor específico para o VSV na membrana celular ainda não foi definido.

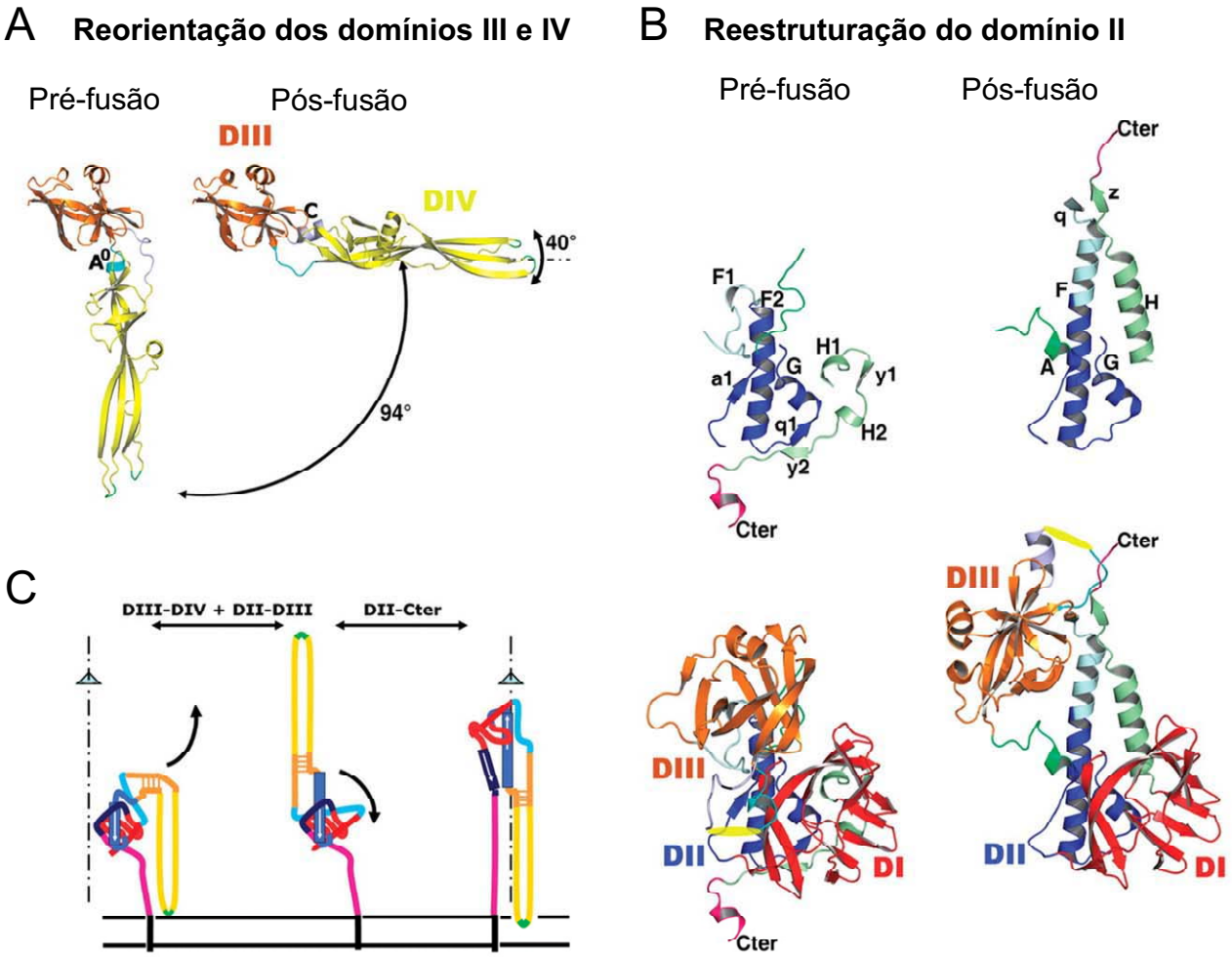

Figura 8: Mudanças estruturais da proteína G do VSV ocorridas na transição das conformações pré e pós-fusogênicas. (A) Rearranjo da orientação dos domínios III e IV. **(B)** Reestruturação do domínio II. **(C)** Representação esquemática da mudança conformacional. Domínio I em vermelho, domínio II em azul escuro e diferentes tonalidades de verde, domínio III em laranja, domínio IV em amarelo, *loops* de fusão em verde, porção C-terminal em rosa. Adaptado de Roche *et al.* (2007).

Vários estudos a respeito do efeito do pH sobre a proteína G do rabdovírus mostraram que as mudanças estruturais sofridas por esta glicoproteína durante a acidificação assim como a aquisição da capacidade de interagir com membranas negativamente carregadas ocorrem em uma faixa de pH bastante estreita, entre 6,2 e 5,8 (White *et al.*, 1981; Gaudin, 2000; Carneiro *et al.*, 2001). Esta é exatamente a faixa de pH na qual ocorre a protonação da cadeia lateral do aminoácido histidina (pK ~ 6,04). Isso nos sugeriu que a protonação de resíduos de histidina presentes na proteína G seria necessária para o desencadeamento do processo de fusão. Por esse motivo, a substância dietilpirocarbonato (DEPC), cujo mecanismo de modificação

específica de histidinas vem sendo estudado há anos, foi utilizada nos estudos apresentados nesta tese para descoberta de possíveis alvos de inativação viral durante a entrada do VSV nas células hospedeiras.

1.4 Modelo de estudo II: o vírus da dengue

O vírus da dengue é um membro da família Flaviviridae, na qual também se incluem os vírus da febre amarela, Saint Louis, Oeste do Nilo, Rio Bravo e outros vírus responsáveis por encefalites (Burke e Monath, 2001). Quatro sorotipos geneticamente distintos do vírus da dengue são conhecidos: DEN1, DEN2, DEN3 e DEN4, sendo DEN2 o de maior prevalência.

A infecção por este vírus possui um espectro de apresentação que varia desde a forma assintomática até quadros de hemorragia e choque, podendo evoluir, inclusive para o óbito (fig. 9) (Who, 1997; Figueiredo e Fonseca, 2002; Guzman e Kouri, 2002; Whitehead *et al.*, 2007). A dengue é uma doença febril aguda, com duração de 5 a 7 dias. A dengue clássica apresenta quadro clínico muito variável, geralmente com cefaléia, mialgia (dores no corpo), seguido de febre alta (39° a 40°) de início abrupto, acompanhada de prostração, artralgia, anorexia, astenia, dor retro-orbitária, náuseas, vômitos e rash cutâneo. Associada à síndrome febril, em alguns casos pode ocorrer hepatomegalia dolorosa e, principalmente, nas crianças, dor abdominal generalizada. Com o desaparecimento da febre, há regressão dos sinais e sintomas, podendo ainda persistir a fadiga (Figueiredo e Fonseca, 2002; Guzman e Kouri, 2002). Já nos casos da dengue hemorrágica, apesar dos sintomas iniciais serem semelhantes aos da dengue clássica, ocorre um rápido aparecimento de manifestações hemorrágicas, como petéquias, equimoses, epistaxe, gengivorragia, sangramento gastrintestinal, hematúria e metrorragia. Os casos típicos da dengue hemorrágica são caracterizados por febre alta, fenômenos hemorrágicos e hepatomegalia. Nos casos graves, conhecidos como síndrome do choque hemorrágico da dengue, ocorre insuficiência circulatória (choque) imediatamente após o desaparecimento da febre. Sua duração é curta, podendo levar ao óbito em 12 a 24 horas ou à recuperação rápida após terapia apropriada. Um achado laboratorial importante da dengue hemorrágica é a trombocitopenia com hemoconcentração concomitante. A gravidade deste quadro está relacionada à efusão do plasma, caracterizada por valores crescentes do hematócrito (Figueiredo e Fonseca, 2002; Guzman e Kouri, 2002).

O vírus da dengue é transmitido em um ciclo envolvendo humanos e mosquitos, sendo *Aedes aegypti* o vetor mais importante. Este se encontra principalmente em áreas temperadas e tropicais, em geral durante o verão (Wilder-Smith e Schwartz, 2005). Cerca de dois terços da população mundial vive em áreas onde a dengue é endêmica ou epidêmica, sendo estimado

que cerca de 50-100 milhões de pessoas sejam infectadas com o vírus todo o ano, 250-500 mil desenvolvam dengue hemorrágica e 12 mil morram em decorrência desta infecção (Rigau-Perez *et al.*, 1998; Gubler, 2002).

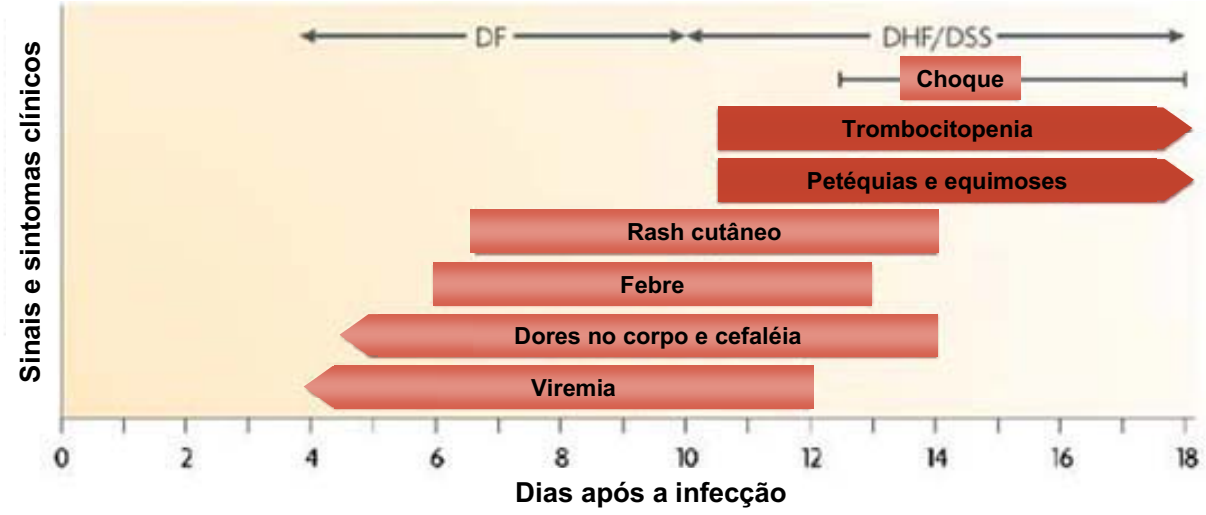

Figura 9: Representação esquemática do curso temporal de aparecimento dos sintomas e sinais clínicos da dengue. DF - dengue clássica, DHF - dengue hemorrágica, DSS - síndrome do choque da dengue hemorrágica. Adaptado de Whitehead *et al.* (2007).

No Brasil, a dengue encontra-se hoje presente em todos os 27 estados da federação, sendo responsável por cerca de 60-70% das notificações nas Américas (Siqueira *et al.*, 2005; Camara *et al.*, 2007). Em 1981, os sorotipos DEN1 e DEN4 foram os primeiros a serem isolados em uma epidemia de dengue ocorrida Boa Vista, Estado de Roraima (Osanai *et al.*, 1983). Após um silêncio epidemiológico, o sorotipo DEN1 invadiu o sudeste (Rio de Janeiro e Minas Gerais) e o nordeste (Alagoas, Ceará, Pernambuco, Bahia) em 1986-1987 (Schatzmayr *et al.*, 1986), espalhando-se pelo país desde então, com as entradas dos sorotipos DEN2 em 1990-1991 (Nogueira *et al.*, 1991), e o DEN3 em 2001-2002 (Nogueira *et al.*, 2001; Nogueira *et al.*, 2005).

Dois fatores estão diretamente relacionados com a incidência de dengue no Brasil e no mundo: distribuição ampla do vetor e taxa de transmissão rápida do vírus (Pinheiro e Corber, 1997; Figueroa e Ramos, 2000; Guzman e Kouri, 2002). O controle do vetor, que a princípio parecia ser a melhor solução, mostrou-se ineficiente no Brasil nos últimos anos, tanto pela interrupção dos programas de combate ao mosquito, quanto pelo aparecimento de mosquitos e larvas resistentes a diversos inseticidas e larvicidas. Além disso, tais programas para serem efetivos exigem financiamento contínuo ao longo dos anos, principalmente em um país de dimensões como a do Brasil (Teixeira *et al.*, 2005).

Sendo assim, a formulação de uma vacina tetravalente que seja eficaz contra os quatro sorotipos e produza uma imunidade duradoura é extremamente necessária. Já existem vacinas de vírus atenuado, inativado (partícula inteira e subunidade) e vacina de DNA que estão sendo desenvolvidas, algumas delas já em testes clínicos (Whitehead *et al.*, 2007).

1.4.1 A Estrutura dos Flavivírus

Os flavivírus são partículas esféricas de aproximadamente 50nm de diâmetro, formados por um capsídeo ribonucléico icosaédrico envolto por uma membrana lipídica. O nucleocapsídeo é composto pelo genoma viral, uma fita simples de RNA, polaridade positiva, fortemente associado à proteína C (capsídica). Envolvendo este conjunto temos o envelope lipídico, que está associado a duas proteínas: a glicoproteína E (envelope) e a proteína M (membrana) (fig. 10B) (Lindenbach e Rice, 2001; Kuhn *et al.*, 2002).

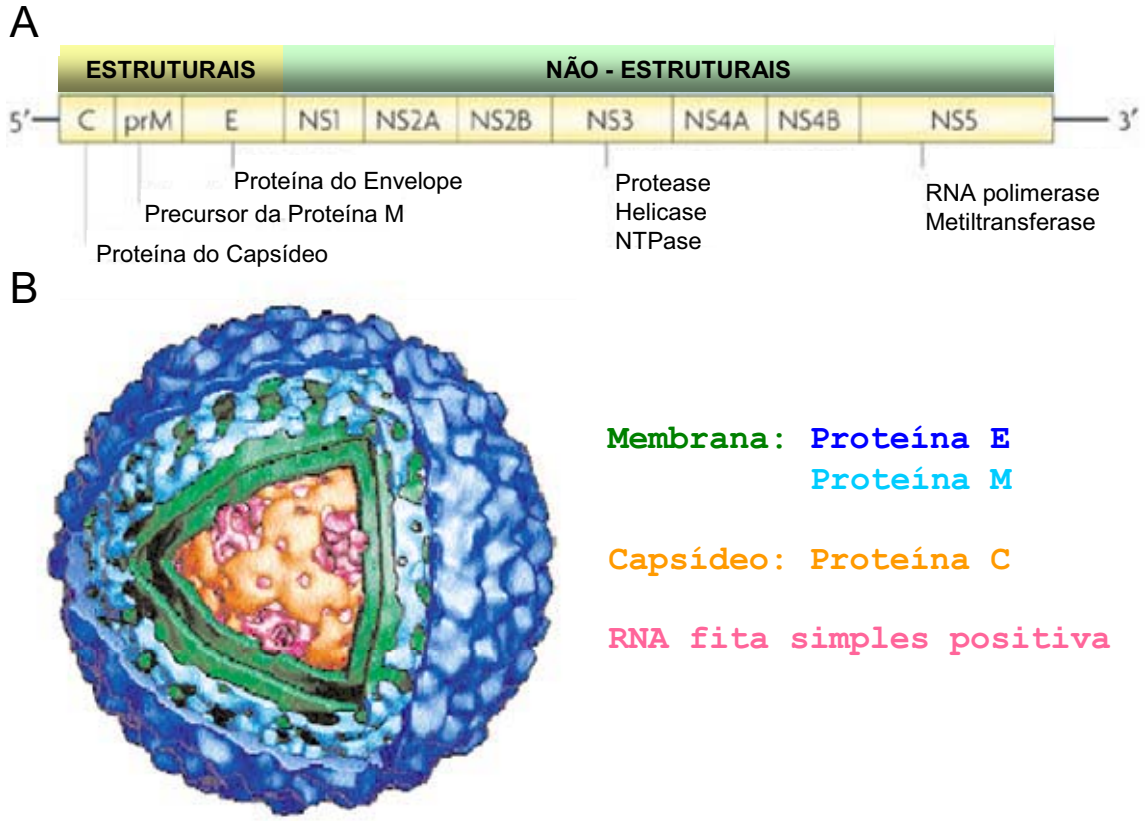

Figura 10: Representação esquemática da estrutura do vírus da dengue e do genoma viral. (A) Organização do genoma do vírus da dengue. **(B)** Estrutura da partícula viral obtida por crio-microscopia. Podem ser observadas duas camadas protéicas mais externas (azuis claro e escuro), compostas pelas proteínas E e M, uma bicamada lipídica (verde), um nucleocapsídeo (laranja), composto pela proteína C, e finalmente, o RNA genômico (vermelho) empacotado no centro do vírus. Adaptado de Kuhn *et al.* (2002); Smith (2002) e Whitehead *et al.* (2007).

1.4.2 Ciclo de replicação dos Flavivírus

Para que ocorra uma replicação viral bem sucedida, os flavivírus precisam liberar seu nucleocapsídeo no citoplasma (fig. 11). Para isso, o vírus da dengue se liga aos receptores presente na superfície celular através da proteína E. Existem estudos que sugerem o envolvimento direto do heparan sulfato (HS), um glicosaminoglicano (GAG) carregado negativamente, na ligação do vírus à membrana alvo (Chen *et al.*, 1997; Hung *et al.*, 1999; Hilgard e Stockert, 2000; Germi *et al.*, 2002). No entanto, outros autores acreditam que o HS é apenas um fator presente na superfície celular que agrega as partículas virais, facilitando sua interação com seus co-receptores protéicos (Martinez-Barragan e Del Angel, 2001; Thepparit e Smith, 2004). Além disso, dependendo do tipo celular estudado, o HS nem é necessário para infecção pelo vírus da dengue (Bielefeldt-Ohmann *et al.*, 2001). Na realidade, não se conhece o verdadeiro receptor do vírus da dengue e várias outras moléculas já foram envolvidas até o presente momento, como as "*heat shock proteins*" 90 e 70 (Reyes-Del Valle *et al.*, 2005), GRP78/BiP (glucose-regulating protein 78) (Jindadamrongwech *et al.*, 2004), CD-14 (Chen *et al.*, 1999), receptor de laminina (Thepparit e Smith, 2004) e, mais recentemente, o DC-SIGN (dendritic-cell-specific ICAM-grabbing non-integrin) (Navarro-Sanchez *et al.*, 2003; Tassaneetrithep *et al.*, 2003; Lozach *et al.*, 2005; Pokidysheva *et al.*, 2006).

Após a ligação ao receptor específico, ocorre a endocitose da partícula viral (Mukhopadhyay *et al.*, 2005). A acidificação do compartimento endossomal ocasiona a fusão do envelope viral com a membrana endossomal, liberando o capsídeo no citoplasma. A proteína do capsídeo se dissocia, iniciando o processo de tradução e replicação do genoma viral. O genoma do vírus da dengue (fig. 10A) codifica uma poliproteína processada pela combinação de serino-proteases virais e enzimas celulares. Como resultado desta clivagem, são obtidas três proteínas estruturais (C, prM, and E) e sete não-estruturais (NS1, NS2A, NS2B, NS3, NS4A, NS4B, NS5) (Lindenbach e Rice, 2001; Lindenbach e Rice, 2003). Assim são formadas as proteínas virais necessárias para a montagem viral.

O processo de montagem dos vírus acontece inicialmente no lúmen do retículo endoplasmático, onde primeiro são gerados vírus imaturos, compostos de nucleocapsídeo, envelope e proteínas E e pré-M formando um estável complexo de heterodímeros, que não é capaz de induzir fusão de membranas (Guirakhoo *et al.*, 1991). Acredita-se que a proteína pré-M protege a proteína E de adquirir precocemente uma conformação fusogênica durante o processo de secreção e também funcione como uma chaperona para a organização desta proteína (Heinz e Allison, 2003). Após a clivagem da proteína pré-M pela furina celular no

complexo de Golgi, as partículas virais se tornam maduras e infectantes (Stadler *et al.*, 1997; Elshuber *et al.*, 2003). Os vírus formados são liberados da célula infectada por exocitose.

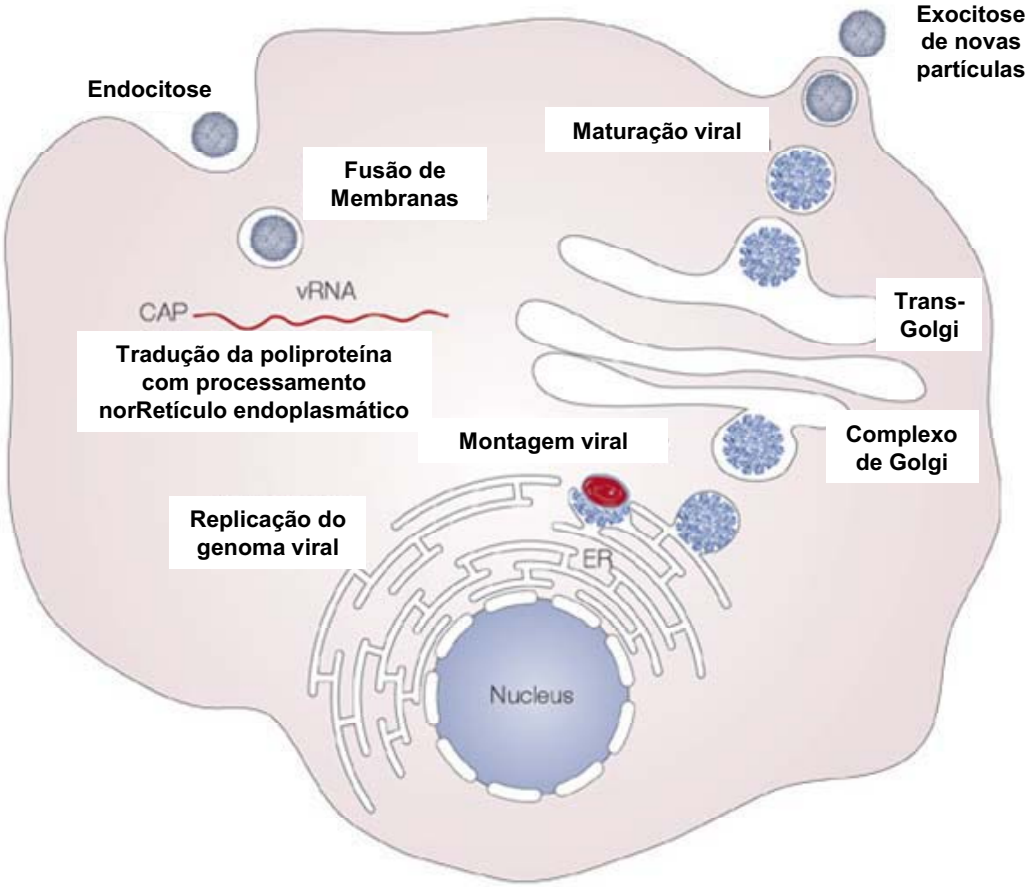

Figura 11: Ciclo de replicação do vírus da dengue. Estão representadas as principais etapas do ciclo de replicação: ligação do vírus à membrana celular através da ligação da proteína E do vírus com os receptores da superfície celular, endocitose das partículas virais mediada pelo receptor da célula do hospedeiro, acidificação do meio endossomal induzindo mudança conformacional irreversível da proteína do envelope viral e promovendo a fusão com a membrana endossomal, liberação do capsídeo no citoplasma da célula, tradução do RNA genômico e processamento da poliproteína, replicação do genoma viral originando fitas de RNA intermediárias negativas, morfogênese dos virions em vesículas intracelulares, transporte dos virions e maturação da glicoproteína do envelope, fusão da vesícula contendo os virions com a membrana da célula e liberação destes no meio extracelular. Adaptado de Lindenbach e Rice (2001) e Mukhopadhyay *et al.* (2005).

1.4.3 Proteína E e seu peptídeo de fusão

A proteína E é a maior proteína estrutural do vírus da dengue, sendo responsável pela ligação do vírus à célula hospedeira e pela fusão de membranas, etapa essencial para entrada do vírus na célula hospedeira (Mukhopadhyay *et al.*, 2005; Clyde *et al.*, 2006). Esta glicoproteína é composta de três "barris de folhas-β" (fig. 12): o domínio I contém a extremidade N-terminal; o domínio II contém uma região de dimerização e o peptídeo de

fusão em sua extremidade distal; e o domínio III contém os sítios de ligação ao receptor celular (Modis *et al.*, 2003). A proteína E encontra-se na forma de homodímeros dispostos paralelamente à superfície viral em pH neutro, com seu peptídeo de fusão inacessível ao meio externo (fig. 12A) (Modis *et al.*, 2003).

A proteína E é classificada como uma proteína de fusão de classe II, devido a sua estrutura ser formada principalmente por folhas-β e de seu peptídeo de fusão estar localizado no meio da seqüência da proteína (Modis *et al.*, 2004).

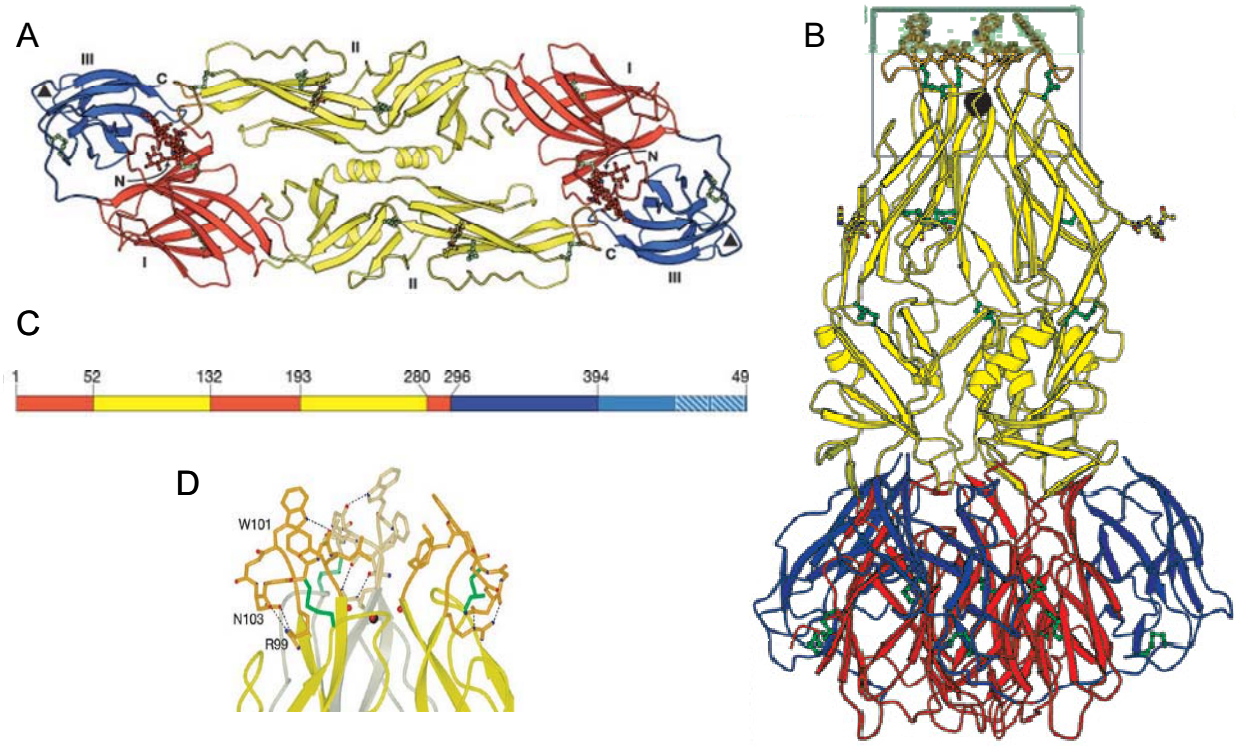

Figura 12: Estrutura cristalográfica da proteína E do vírus da dengue. (A) Conformação pré-fusogênica - Visão do homodímero. **(B)** Conformação pós fusogênica - Visão do trímero. **(C)** Diagrama linear mostrando os resíduos de aminoácidos correspondentes a cada domínio. **(D)** Maior detalhe da ponta do trímero, onde está localizado o *loop* de fusão, mostrando a presença dos aminoácidos hidrofóbicos. Domínio I em vermelho, domínio II em amarelo e domínio III em azul. O peptídeo de fusão (aa 98-110) está marcado pela letra C. A letra N marca o sítio de glicosilação. O triângulo marca o *loop* de ligação ao receptor cellular. Adaptado de Modis *et al.* (2004).

A reorganização estrutural necessária para aquisição da conformação fusogênica é desencadeada pela exposição da proteína E ao pH ácido e se inicia pelo rearranjo das orientações relativas dos domínios da proteína E (fig. 13) (Modis *et al.*, 2004). O domínio II gira aproximadamente 30° em relação ao domínio I. Já o domínio III sofre um maior deslocamento na transição de dímero para trímero, pois gira cerca de 70° e desloca seu centro

de massa 36 Å à frente do domínio II, fazendo com que ele não se encontre mais estendido linearmente junto com os domínios I e II. Estas reorientações são responsáveis pela formação dos trímeros, exposição do peptídeo de fusão e formação da haste de hemifusão (explicada anteriormente). O processo continua com a reestruturação do domínio III, que aproxima o peptídeo de fusão e a porção transmembrana, ou seja, as membranas viral e endossomal. Com isso é formado o poro de fusão, permitindo a liberação do nucleocapsídeo no citoplasma. Resumidamente, quando o pH é acidificado, ocorre a conversão irreversível dos homodímeros para homotrímeros (Allison *et al.*, 1995; Stiasny *et al.*, 1996; Kuhn *et al.*, 2002), com exposição do peptídeo de fusão no topo do trímero e conseqüente início da reação de fusão (Mukhopadhyay *et al.*, 2005). O peptídeo de fusão durante toda a reestruturação da proteína E se mantém com a mesma conformação (Modis *et al.*, 2004).

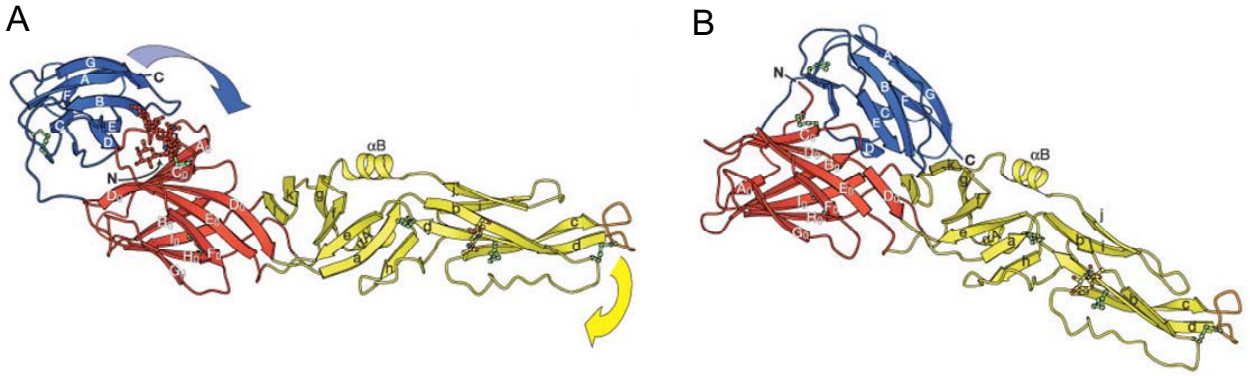

Figura 13: Rearranjo dos domínios da proteína E durante a transição para trímero. (A) Estrutura do monômero na conformação pré-fusogênica, encontrada nos dímeros de proteína E em pH neutro. **(B)** Estrutura do monômero na conformação pós-fusogênica, encontrada nos trímeros após exposição ao pH ácido. Ocorre um rearranjo dos domínios II e III (demonstrado pelas setas em A), que mudam sua orientação relativa, fazendo com que o C-terminal se aproxime do peptideo de fusão, ficando 39 Å mais perto. O peptídeo de fusão permanece essencialmente com a mesma conformação antes e depois da fusão. Adaptado de Modis *et al.* (2004).

Observa-se no alinhamento das seqüências de aminoácidos das proteínas E dos diferentes flavivírus uma homologia de 62 a 77% entre os quatro sorotipos de vírus da dengue e de 40 a 45% entre os diferentes flavivírus. A região entre os resíduos 98 e 110 é idêntica em todos os flavivírus, exceto por uma única substituição no vírus *tick born encephalitis* (TBE) (fig. 14). Esta região é considerada o peptídeo de fusão, visto que possui grande homologia entre os flavivírus e encontra-se exposta nos homotrímeros de proteína E (fig. 12C e D). Além disso, substituições de aminoácidos nesta região foram capazes de abolir a fusão de membranas mediada pela proteína E (Allison *et al.*, 2001).

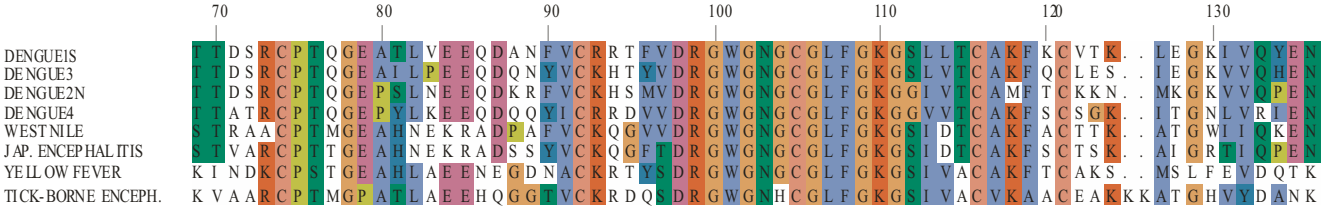

Figura 14: Alinhamento da região do peptídeo de fusão da glicoproteína E de alguns flavivírus. Dengue tipo 1 (cepa Singapura S275/90); dengue tipo 3; dengue tipo 2 (Nova Guiné C); dengue tipo 4; vírus do Nilo do Oeste; encefalite japonesa (cepa Nakayama); febre amarela (cepa 17D) e encefalite transmitida por carrapato (cepa Neudoerfl).

Através do uso de metodologias baseadas em espectroscopia de fluorescência, nesta tese foi realizado o primeiro estudo da interação do peptídeo de fusão do vírus da dengue com membranas.

1.5 Mecanismos de inativação viral

O desenvolvimento de novas estratégias para inativação viral representa uma importante linha de pesquisa na área da virologia, visto que a disponibilidade de medicamentos antivirais com eficácia clínica comprovada é reduzida (De Clercq, 2004) e que existe carência de vacinas seguras e eficazes contra diversas viroses.

A identificação de uma série de proteínas e enzimas virais essenciais para a replicação dos vírus e suficientemente diferentes das proteínas celulares viabilizou o desenvolvimento de drogas direcionadas exclusivamente a alvos virais que seriam, em princípio, inofensivas às proteínas celulares. A maioria destas drogas inibe enzimas envolvidas na replicação viral, como é o caso, por exemplo, do aciclovir, que após processamento intracelular se torna um potente inibidor da DNA polimerase do vírus do herpes (Crumpacker *et al.*, 1979); ou dos inibidores nucleosídicos e não-nucleosídicos da transcriptase reversa dos retrovírus (Autran *et al.*, 1997).

Embora a inibição das enzimas envolvidas na replicação viral seja uma abordagem muito eficaz para o desenvolvimento de drogas antivirais, esta estratégia não tem utilidade para a formulação de vacinas. Com este intuito, foram desenvolvidas técnicas de inativação viral que modificavam a partícula viral, bloqueando sua entrada nas células hospedeiras na etapa da adsorção. Os compostos mais utilizados eram a formalina (Bachmann *et al.*, 1993) e detergentes (Seitz *et al.*, 2002), sendo também usada a aplicação de radiação ultra-violeta (UV) (Bay e Reichmann, 1979). No entanto, estes procedimentos de inativação acarretam na desnaturação das proteínas de superfície viral, comprometendo a imunogenicidade da maioria

das partículas virais, ou seja, a indução de imunoglobulinas do tipo G (IgG) neutralizantes (Bachmann *et al.*, 1994). Por isso, nos últimos 50 anos foram realizados diversos estudos de inativação viral para formulação de vacinas, com a descoberta de novos compostos e procedimentos. Uma revisão mais detalhada destas abordagens foi recentemente publicada por nós e se encontra anexada ao final desta seção (artigo 1).

Dentre os compostos descobertos nos últimos anos, destacam-se aqueles inativadores virais que impedem a entrada dos vírus envelopados nas células hospedeiras pela inibição da fusão de membranas: cianovirina (Dey *et al.*, 2000), hipericina e rosa de bengala (Lenard *et al.*, 1993; Lenard e Vanderoef, 1993). O mecanismo de ação dos dois últimos compostos químicos está relacionado com a formação de cross-linking das proteínas virais de superfície. Já o mecanismo molecular de ação da cianovirina foi muito estudado para o HIV e envolve interações físicas com a proteína de membrana gp120 (Boyd *et al.*, 1997). Estudos demonstraram que esta molécula se liga aos oligossacarídeos com alta concentração de manose presentes na gp120 (Bewley e Otero-Quintero, 2001; Bolmstedt *et al.*, 2001; Shenoy *et al.*, 2001). Outros vírus envelopados que contém oligosacarídeos similares também foram inativados pela cianovirina (Dey *et al.*, 2000; Barrientos *et al.*, 2003; O'keefe *et al.*, 2003; Helle *et al.*, 2006). As propriedades antigênicas e imunogênicas das partículas virais inativadas por estes compostos ainda não foram avaliadas.

1.5.1 Inativação do VSV

O VSV pode ser inativado por tratamento com formalina, com β-propiolactona ou com luz UV (Bachmann *et al.*, 1993; Bachmann *et al.*, 1994). Nestes casos, o vírus inativado não foi capaz de induzir a produção de IgG em animais imunizados, embora a resposta de IgM tenha se mantido inalterada. Em relação à reposta citotóxica, apenas o vírus inativado por luz UV foi capaz suscitar resposta de linfócitos T citotóxicos (Bachmann *et al.*, 1994).

Além desses métodos usuais, já foram utilizados detergentes (Seitz *et al.*, 2002), bis-ANS (Bonafe *et al.*, 2000), hipericina e rosa de bengala (Lenard *et al.*, 1993). Também podem ser citados os métodos físicos, como pressão hidrostática (Silva *et al.*, 1992). A fotoinativação ainda é utilizada frequentemente associada com diversos compostos químicos (Hirayama *et al.*, 1997; Kasermann e Kempf, 1997; Kasermann e Kempf, 1998; Hirayama *et al.*, 1999; Lim *et al.*, 2002). No entanto, nestes estudos de inativação do VSV não foram avaliadas as capacidades antigênica e imunogênica das partículas virais inativadas, visto que muitas destas metodologias são utilizadas principalmente para inativação em produtos sanguíneos e processos de desinfecção, não visando a obtenção de antígenos para formulação de vacinas.

Técnicas mais sofisticadas como o rearranjo genético do VSV já foram apontadas como uma forma eficiente de atenuação viral (Wertz *et al.*, 1998; Flanagan *et al.*, 2001). O afastamento do gene da proteína N da região promotora reduziu os níveis de transcrição e da síntese da proteína N com conseqüente atenuação da replicação do vírus e de sua letalidade para camundongos, preservando sua capacidade imunogênica (Wertz *et al.*, 1998).

1.5.2 Dietilpirocarbonato

O dietilpirocarbonato (DEPC) é um composto químico muito utilizado em estudos com proteínas devido a sua grande especificidade de reação com resíduos de histidina (Lundblad e Noyes, 1984). Este composto reage com resíduos de histidina em sistemas modelo e em proteínas, e resulta na substituição de uma das posições de nitrogênio do anel imidazol, gerando N-carbetoxihistidina (Miles, 1977), como mostrado na equação (1). A formação do N-carbetoxihistidina pode ser acompanhada espectrofotometricamente, com um máximo de absorção entre 230 e 250 nm (Ovadi *et al.*, 1967).

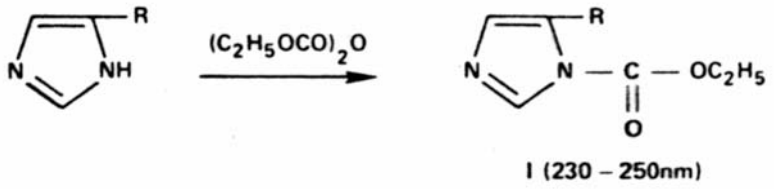

Eq. (1)

.

Existem descritos na literatura vários exemplos do uso de DEPC para estudar a função de resíduos de histidina em diversas proteínas (Lundblad e Noyes, 1984). A modificação de proteínas com DEPC foi utilizada com sucesso para estudos de inativação de enzimas, como peroxidases, heparinases e ATPases (Bhattacharyya *et al.*, 1992; Shriver *et al.*, 1998; Dzhandzhugazyan e Plesner, 2000). Nesta tese, descreveremos pela primeira vez a utilização do DEPC para a inativação viral.

1.6 Artigo 1

Advances in the Development of Inactivated Virus Vaccines

Fausto Stauffer, Tatiana El-Bacha e Andrea T. Da Poian

Publicado em 2006 no periódico

Recent Patents on Anti-Infective Drug Discovery

Recent Patents on Anti-Infective Drug Discovery, 2006, *1*, 000-000

Advances in the Development of Inactivated Virus Vaccines

Fausto Stauffer, Tatiana El-Bacha and Andrea T. Da Poian*

Instituto de Bioquímica Médica, Programa de Biologia Molecular e Biotecnologia, Universidade Federal do Rio de Janeiro, Rio de Janeiro, RJ 21941-590, Brazil

Received: ???? ??, 2005; Accepted: ???? ??, 2006; Revised: March 24, 2006

Abstract: Vaccine discovery stands out as one of the public health interventions that has achieved the greatest impact in world's health. Vaccination is the most effective means of disease prevention, especially for viral infections. Starting with the use of smallpox vaccine by Jenner in the late 1700s, the technology for vaccine development has seen numerous advances. Currently, vaccines available for human viral illness are based on live attenuated (e.g. measles, mumps, and rubella), inactivated (e.g. hepatitis A) and recombinant (e.g. hepatitis B) viruses. Among these, inactivated vaccines are known for their easy production and safety. The present article reviews the literature and patents related to the mechanisms used for viral inactivation, mainly chemical and physical procedures, including the novel strategies that are currently being explored and that have been recently patent protected.

Keywords: Virus, viral inactivation, chemical methods, physical methods, vaccines.

INTRODUCTION

Vaccination is a valuable public health tool, being a safe and cost-effective strategy for controlling infectious diseases [1]. Progress in development and use of vaccines has led to the decline and, in some cases, eradication of important infectious diseases, such as smallpox [2]. Traditionally, vaccines against viruses are classified as attenuated or inactivated. Live attenuated vaccines are based on the attenuation of the pathogen until its virulence is greatly decreased but its immunogenicity is retained. Alternatively, inactivated vaccines consist of either whole killed virus or specific viral proteins. In the case of whole-virus inactivated vaccines, the inactivation treatment through different processes (for review, see [3]) must ensure that all virus particles are inactivated in order for the vaccine to be safe. Because such vaccines, also called dead vaccines, may contain certain viral proteins or cellular components which could lead to undesirable immune responses in the host, the production of subunit vaccines, which contain specific viral proteins and retain immunogenicity properties, was of great importance in this field. Because only individual antigens are used in subunit vaccines, their immunogenicity is often reduced and the use of split vaccines, which contain a combination of viral proteins with preserved integrity, may be more effective. More recently, new strategies for vaccine development have emerged, such as recombinant viral proteins [4] and DNA vaccines [5].

Despite the advances in immunology, molecular biology and genetics, viral inactivation remains an important procedure in basic research, since it is an easy and relatively cheap approach to producing new and safe vaccines. Moreover, this procedure can also be used for other purposes, such as treatment of viral infections and clearance of viruses from plasma and plasma products, equipment and biotechnology products. Since no inactivation method is effective for all viruses and all purposes, a number of different inactivation treatments are being studied and developed. In this review, we will focus on the procedures available and their effectiveness in vaccine development against viruses.

There are several inactivation techniques that use chemical or physical procedures and have been cited in patents (Table **1**). However, only six whole-virus inactivated vaccines are currently available for use in humans (Table **2**) [3]. In these cases, the viruses are inactivated by chemical methods, using formalin or β-propiolactone. In addition to the chemical treatments used for these established vaccines, other compounds are used for virus inactivation, including anilinonaphthalene sulfonate compounds, urea, detergent, psoralens, aziridines, sodium periodate and diethylpyrocarbonate. The physical methods used for virus inactivation, such as UV irradiation, heat and high pressure, will also be reviewed.

CHEMICAL INACTIVATION OF VIRUSES

Concerning the chemical processes for virus inactivation, several compounds are used. Although aldehydes, such as formaldehyde, are the most common, there is a growing list of patented compounds and patented combinations of treatments which have proved to be effective in virus inactivation and thus may be suitable for vaccine development.

Inactivation using formalin (a saturated solution of formaldehyde) is usually performed by placing the virus suspension in contact with a formalin solution, at 37ºC, the concentration depending on the type of virus. The inactivation of viruses with formaldehyde involves a number of reactions with amino, imino, amido, sulphydryl and hydroxy groups and with peptide linkages within proteins [6]. One of its principal advantages is that, as a result of cross-linking, the gross three-dimensional architecture of

*Address correspondence to this author at the Instituto de Bioquímica Médica, Programa de Biologia Molecular e Biotecnologia, Universidade Federal do Rio de Janeiro, Rio de Janeiro, RJ 21941-590, Brazil; Tel: +55-21-22706264; Fax: +55-21-22708647; E-mail: dapoian@bioqmed.ufrj.br

1574-891X/06 $100.00+.00

Table 1. Inactivation Methods Used for Producing Virus Inactivated Vaccines

Chemical	Physical	Combined
Ascorbic Acid Beta Propiolactone Beta-aminophenylketone Non Ionic Detergents Diethylpyrocarbonate Ethylenimine Formalin / Formaldehyde Phenol	Heat Pressure UV Light	Ascorbic Acid + UV Light Beta Propiolactone + UV Light Formalin + Heat Formalin + UV Heat + Low Pressure Pressure + Heat or Cold Psoralen + UV

Table 2. Inactivated Virus Vaccines Currently Available Against Human Diseases

Disease	Inactivation Method
Flu	β-propiolactone or formalin
Hepatitis A	Formaldehyde/formalin
Japanese Encephalitis	Formaldehyde/formalin
Poliomyelitis	Formaldehyde/formalin
Rabies	β-propiolactone or phenol
Tick-Borne Encephalitis	Formaldehyde/formalin

proteins is conserved. This chemical compound has proved effective for production of vaccines against hepatitis A [7, 8], polio [9, 10], influenza [11], rabies [12], measles [13], Japanese encephalitis [14, 15] and immunodeficiency [16, 17] viruses. A practical disadvantage of this method is the long period of incubation required for successful virus inactivation. One solution to this problem is to increase the concentration of formalin in the solution to reduce incubation time, although it may increase the toxicity of the vaccine. Another problem concerning this compound is that formalin has proven to be reactogenic and it may be responsible for the side effects experienced by some people after vaccination. With respect to the preservation of immunogenicity, there is a clear association between the concentration needed to inactivate the viruses and the complexity of the process of virus inactivation. Some viruses (e.g. SARS coronavirus and human immunodeficiency virus type 1, HIV-1) need lower concentrations of formaldehyde to be inactivated, preserving their immunogenicity [18] and their neutralizing epitopes [19]. Conversely, it has been shown that formalin strongly affects antigenic structure in concentrations necessary to inactivate HIV-1 [20], poliovirus [21] and foot-and-mouth disease virus [22], making the vaccine not only hazardous but ineffective in protecting against infection, since dead vaccines are only effective if the structure of viral proteins is intact.

Another inactivating agent widely used in the production of both human and animal virus vaccines is β-propiolactone (BPL). This chemical compound acts on the nucleic acid of the virus, with little or no effect on the immunogenic properties of the viral protein coat [23]. One of the major advantages of this alkylating agent is that it undergoes complete hydrolysis in an aqueous medium, forming non-toxic products [24]. It was shown that low concentrations of BPL completely inactivate influenza [25] and rabies [12, 24, 26] viruses without destroying their antigenic properties. The currently available human vaccines using this compound protect against flu [27] and rabies [28] (Table **2**). The disadvantages of this inactivating method are the elevated cost of BPL and the risk of adverse reactions. These reactions have been associated with the presence of _-propiolactone-altered human albumin in vaccine preparations (e.g. human diploid cell rabies vaccine) and the development of immunoglobulin E (IgE) antibodies to this allergen [29, 30].

Ethylenimine and related derivatives, such as binary ethylenimine (BEI) and acethylethylenimine, are also used for virus inactivation and have proven to be efficient for the development of vaccines against foot-and-mouth disease [31-33], polio [34], influenza [34] and rabies [35] viruses. Moreover, these compounds have also been shown to efficiently inactivate several RNA and DNA viruses [36]. The aziridine BEI inactivates viruses by a mechanism similar to BPL, reacting with nucleic acids [31]. As with BPL, there is no evidence that BEI reacts with viral proteins, and thus it preserves the antigenic regions of the viruses [37, 38]. In contrast to BPL, BEI has the advantage of low cost, and it is less hazardous to manipulate [31]. Moreover, the vaccine inactivated with BEI is very stable [35].

Although higher concentrations may decrease the time required for complete inactivation, this choice of conditions can also compromise the safety of the invention. Additionally, aggressive treatment may also affect virus structure and decrease vaccine efficiency. On the other hand, inactivation under mild conditions may favor vaccine safety. In this case, treatment of the viruses with psoralens, such as 4'-aminomethyl 4,5'-8-trimethylpsoralen, in a non-oxidizing atmosphere (such as argon gas) along with UV irradiation, has proven effective in inactivating some viruses, such as bluetongue virus [39], HIV-1 and other immunodeficiency viruses [40-43], rotavirus [44] and other single and double-stranded DNA or RNA viruses [45, 46]. The antigenic structure of viral proteins is preserved after inactivation and this compound leaves no harmful residue [47]. The mechanism of action is based on intercalation of the psoralen between the base pairs of double-stranded nucleic acids, forming covalent adducts to pyrimidine bases upon

absorption of long-wave ultraviolet light [48, 49]. The covalently bonded psoralens act as inhibitors of DNA replication and thus have the potential to stop the viral replication process. Although this method seems suitable for vaccine preparation, it is still only used in viral inactivation of plasma products [50-52]. A great disadvantage of this methodology is the requirement for special equipment where the inactivation process is performed.

Experiments with vaccinia virus revealed that ascorbic acid is a viral-inactivating agent when it undergoes auto-oxidation catalyzed by Cu^{++} [53]. Other studies have shown that its main target may be nucleic acids, since RNA infectivity is lost after ascorbic acid treatment [54]. Viruses that have been inactivated by this compound include parainfluenza-3 virus, transmissible gastroenteritis virus [55], poliovirus, coxsackie, echovirus [54], herpes simplex virus types 1 and 2, cytomegalovirus, parainfluenza-2 virus [56], HIV-1 [57] and rabies virus [58]. This agent is less hazardous than other commonly used chemicals, and it is inexpensive and effective for viral inactivation, allowing the virus particles to retain their antigenicity [56].

Compounds such as β-aminophenylketones has been shown to be effective in inactivating enveloped viruses [59]. When several phenylketone compounds were tested over a wide range of concentrations, dyclonine was most effective. As with formalin treatment, viral inactivation was achieved by placing the viruses in contact with the compound at 37ºC. Herpes simplex virus types 1 and 2 were readily inactivated by this kind of treatment although picornaviruses and vaccinia viruses were more resistant in cell culture testing. *In vivo* protection from herpes simplex virus type 1 was also observed.

A new approach to viral inactivation is the use of diethylpyrocarbonate (DEPC). This compound is a widely used tool in chemical modification of proteins because of the high selectivity of the reagent for histidyl residues [60]. Modification with DEPC was successfully used in inactivation studies of various groups of enzymes, e.g. peroxidases, heparinases and ATPases [61-63]. It has been used for inactivation of measles, smallpox, polio and type A influenza viruses [64]. More recently, our group demonstrated inactivation of vesicular stomatitis virus by DEPC, suggesting that this procedure can be used for other enveloped viruses [65]. We were able to show that histidine residues play a critical role in membrane fusion catalyzed by viral glycoproteins, and since DEPC modifies His residues, its mechanism of action seems to be based on inhibition of the fusion event, an essential step for the entry of enveloped viruses into host cells [66]. Besides providing an easy approach to inactivation of enveloped viruses, DEPC-inactivated viruses retain their immunogenicity [65].

PHYSICAL INACTIVATION OF VIRUSES

Virus inactivation by heat must almost always be combined with another treatment, usually chemical, for successful results [8, 9, 20, 59, 67]. The use of a chemical compound, although ensuring complete virus inactivation, may increase the toxicity of the vaccine. The temperature used for heat inactivation is around 37ºC. Higher temperatures have also been used to eliminate the need for the combined use of heat and an aggressive chemical treat-ment. When influenza virus was submitted to temperatures ranging from 45 to 59ºC for 25-180 minutes, it became at least 99% inactive [68]. The residual infectivity was inacti-vated with a small dose of a non-carcinogenic compound such as thiomersal in combination with ethyl ester. These two chemicals can also be combined with the virus during heat inactivation. Such treatment was said to be safe because it abolishes the use of formalin or other aggressive compounds and still evokes humoral responses. One advantage of this invention in comparison with formalin treatment is the reduced incubation period required for inactivation. In addition, there was also an increase in interferon levels in mice, which may indicate the increased immunogenicity induced by such treatment. This vaccine proved to be effective for the immunization of mice when administered intranasally or intraperitoneally.

Another commonly used procedure is ultra-violet (UV) irradiation. UV action is considered a physico-chemical process, wherein covalent bonds of the cyclic molecules of the purine and pyrimidine bases are disrupted by the excitation energy of the UV radiation, damaging the nucleic acids of viruses and other microorganisms. When the virus is exposed to effective UVC (100 to 280 nm) radiation, the inactivation process occurs within seconds [69]. However, this method changes protein structure by affecting disulfide bonds, thus destroying antigenic regions. Therefore, it is usually used in combination with other methods, as previously mentioned for heat treatment. Successful treatments were achieved in association with psoralens [40-42, 45, 46], formalin [69] and β-propiolactone [70]. One study with hepatitis A virus showed that UV treatment alone was able to inactivate the virus, maintaining the antigenic regions, since the action of UV was predominantly on the nucleic acid [71]. According to the authors, the protocol used was simple, rapid, inexpensive and safe.

Another method used for virus inactivation is to treat the virus with a mixture of a solvent (e.g. tri-n-butyl phosphate, TNBP) and a non-ionic detergent, such as sodium desoxycholate, Tween™ 80 or Triton-X-100, for hours at temperatures between 6 and 37ºC. This solvent/detergent treatment [72] is widely used for virus inactivation during the manufacture of plasma-derived medicinal products. The procedure has been used for inactivation of HIV, hepatitis B and C viruses [73], influenza virus [74] and other enveloped viruses [75]. Moreover, it is effective in producing influenza split vaccines [76]. Besides the ability of non-ionic detergents to disintegrate viral particles, it has been shown that they solubilize membrane proteins under mild conditions, preserving the native structure of the protein and creating a lipid-like environment that stabilizes the solubilized proteins. The use of a detergent from the group of polysorbates, such as Tween™ at concentrations of 10-20%, promoted the inactivation of several enveloped viruses, such as HIV-1 and HIV-2, tick-borne encephalitis, hepatitis C, influenza and herpes [20] viruses. A complete inactivation of HIV-1 was achieved in only 10 minutes of incubation at 20-40ºC. Much longer incubation times (10 hours) were necessary to inactivate only 0.03-0.1% of the same virus with formalin, indicating the special advantage of the

combined treatment with detergent and relatively low temperature.

The latest physical approach used for viral inactivation is hydrostatic pressure (HP). A study with vesicular stomatitis virus was the first demonstration that HP is able to inactivate a membrane-enveloped virus [77]. Following this study, other viruses were shown to be inactivated by HP, such as herpes simplex virus, human cytomegalovirus [78], foot-and-mouth disease virus [79], parvovirus [80], influenza virus [81], HIV-1 [82], simian immunodeficiency virus [83] and rotavirus [84]. Pressurization induces the dissociation of viral protein subunits, followed by complete or partial re-association on decompression, without substantial loss of protein function or structure [77, 80]. The reassembled particle is non-infectious and immunogenic [77]. One disadvantage of this method is the long time necessary to inactivate viruses and the requirement for a high-pressure bomb. Another concern is the temperature of inactivation which can interfere with the inactivation process [80].

CONCLUSION

In this work, we reviewed the patents related to procedures of whole-virus inactivation for development of vaccines. The technique most used for viral inactivation is the mild treatment of viruses with formalin or β-propiolactone. However, these methods have disadvantages such as long periods of incubation for successful virus inactivation, toxicity of the compound to the host and interference with virus structure that modifies the immunogenic regions. Moreover, there have been reports of failure to inactivate associated with both of these methodologies even in the recent past, predominantly with formaldehyde [85-88]. Thus, after 50 years of research, new procedures and substances have been discovered, including psoralens, ethylenimine and non-ionic detergents. Unfortunately, all of them show disadvantages similar to those of formalin and beta-propiolactone.

Nowadays, the main goal in the viral inactivation field is to improve the existing methods. On reviewing the patents and work from the last five years, it is clear that most of them tend to make alterations in procedure during the inactivation process, since the sequence of events while inactivating a virus is extremely important for the preparation of a safe and effective vaccine. For example, it has been shown that influenza virus obtained from a serum- and protein-free cell culture and inactivated before the purification step exhibits significantly greater antigen purity. Because virus antigens lack specific proteins that could trigger an allergic reaction, this kind of invention may be helpful for vaccines used for the prophylaxis of influenza virus infection [11].

The combination of different procedures is another strategy used for virus inactivation. Usually, a physical method is combined with a chemical compound. It was shown that formalin with UV [69] or heat [8] was a successful combination. Since formalin induces cross-linking of viral proteins [89], it protects the structure from being destroyed by the physical methods. Another significant advance was the application of pressure in different temperatures [80], which substantially reduces both the pressure and the time necessary for inactivation.

In conclusion, both physical and chemical treatments are used for the production of effective inactivated-virus vaccines. Moreover, whole killed vaccine is safer than live attenuated vaccines and they are easier and cheaper to produce than subunit and split vaccines. Despite the advances in this field, mild treatment of the most resistant viruses still induces changes in the antigenic structure of viral particles, thus compromising the safety of the procedure and delaying the production of successful vaccines. Consequently, the vaccines currently in use for humans are still inactivated by aggressive chemical compounds, such as formalin and β-propiolactone. Judging from the growing list of patents for new compounds, one can expect that in the near future novel technologies will allow the production of inactivated vaccines against other viral diseases.

ACKNOWLEDGMENTS

We thank Dr. Martha Sorenson for the critical reading of the manuscript. This work was supported by grants from Conselho Nacional de Desenvolvimento Científico e Tecnológico (CNPq), Coordenação de Aperfeiçoamento de Pessoal de Nível Superior (CAPES) and Fundação Carlos Chagas Filho de Amparo à Pesquisa do Estado do Rio de Janeiro (FAPERJ).

REFERENCES

[1] Ada GL, Ramsay AJ. In: Vaccines, vaccination, and the immune response. Philadelphia, Lippincott-Raven. 1997.
[2] Fenner F. Smallpox and its eradication. Geneve, WHO. 1988.
[3] Ada G. Vaccines and vaccination. N Engl J Med 2001; 345(14): 1042-53.
[4] Arnon R, Ben-Yedidia T. Old and new vaccine approaches. Int Immunopharmacol 2003; 3(8): 1195-204.
[5] Fynan EF, Webster RG, Fuller DH, Haynes JR, Santoro JC, Robinson HL. DNA vaccines: a novel approach to immunization. Int J Immunopharmacol 1995; 17(2): 79-83.
[6] Gard S. Theoretical considerations in the inactivation of viruses by chemical means. Ann N Y Acad Sci 1960; 83: 638-48.
[7] Schmidtke P, Habermehl P, Knuf M, Meyer CU, Sanger R, Zepp F. Cell mediated and antibody immune response to inactivated hepatitis A vaccine. Vaccine 2005; 23(44): 5127-32.
*[8] Chitamber, S.D., Kalanidhi, A.P.: WO2005070454 (**2005**).
[9] Montagnon, B.J., Fanget, B.J.C.: US4525349 (**1985**).
[10] Behringwerke, A.G.: GB949684 (**1964**).
*[11] Barrett, N., Kistner, O., Gerencer, M., Dorner, F.: US2005196413 (**2005**).
[12] Merieux, I.: GB1212363 (**1970**).
[13] Behringwerke, A.G.: GB1161414 (**1969**).
[14] Sugawara K, Nishiyama K, Ishikawa Y, Abe M, Sonoda K, Komatsu K, *et al*. Development of Vero cell-derived inactivated Japanese encephalitis vaccine. Biologicals 2002; 30(4): 303-14.
[15] Appaiahgari MB, Vrati S. Immunogenicity and protective efficacy in mice of a formaldehyde-inactivated Indian strain of Japanese encephalitis virus grown in Vero cells. Vaccine 2004; 22(27-28): 3669-75.
[16] Rossio JL, Esser MT, Suryanarayana K, Schneider DK, Bess JW, Jr., Vasquez GM, *et al*. Inactivation of human immunodeficiency virus type 1 infectivity with preservation of conformational and functional integrity of virion surface proteins. J Virol 1998; 72(10): 7992-8001.
[17] Murphey-Corb M, Martin LN, Davison-Fairburn B, Montelaro RC, Miller M, West M, *et al*. A formalin-inactivated whole SIV vaccine confers protection in macaques. Science 1989; 246(4935): 1293-7.

[18] Xiong S, Wang YF, Zhang MY, Liu XJ, Zhang CH, Liu SS, *et al*. Immunogenicity of SARS inactivated vaccine in BALB/c mice. Immunol Lett 2004; 95(2): 139-43.
[19] Sattentau QJ. Conservation of HIV-1 gp120 neutralizing epitopes after formalin inactivation. Aids 1995; 9(12): 1383-5.
[20] Barrett, N., Kistner, O., Dorner, F.: US6136321 (**2000**).
[21] Ferguson M, Wood DJ, Minor PD. Antigenic structure of poliovirus in inactivated vaccines. J Gen Virol 1993; 74(Pt 4): 685-90.
[22] Nair SP, Sen AK. A study on the immune response of sheep to foot and mouth disease virus vaccine type 'O' prepared with different inactivants and adjuvants. Acta Virol 1992; 36(5): 473-8.
[23] Logrippo GA, Hartman FW. Antigenicity of beta-propiolactone-inactivated virus vaccines. J Immunol 1955; 75(2): 123-8.
[24] Wiktor TJ, Sokol F, Kuwert E, Koprowski H. Immunogenicity of concentrated and purified rabies vaccine of tissue culture origin. Proc Soc Exp Biol Med 1969; 131(3): 799-805.
[25] Philips, N.V.: GB811099 (**1959**).
[26] Frazatti-Gallina NM, Mourao-Fuches RM, Paoli RL, Silva ML, Miyaki C, Valentini EJ, *et al*. Vero-cell rabies vaccine produced using serum-free medium. Vaccine 2004; 23(4): 511-7.
[27] Cox RJ, Brokstad KA, Ogra P. Influenza virus: immunity and vaccination strategies. Comparison of the immune response to inactivated and live, attenuated influenza vaccines. Scand J Immunol 2004; 59(1): 1-15.
[28] Perez O, Paolazzi CC. Production methods for rabies vaccine. J Ind Microbiol Biotechnol 1997; 18(5): 340-7.
[29] Swanson MC, Rosanoff E, Gurwith M, Deitch M, Schnurrenberger P, Reed CE. IgE and IgG antibodies to beta-propiolactone and human serum albumin associated with urticarial reactions to rabies vaccine. J Infect Dis 1987; 155(5): 909-13.
[30] Anderson MC, Baer H, Frazier DJ, Quinnan GV. The role of specific IgE and beta-propiolactone in reactions resulting from booster doses of human diploid cell rabies vaccine. J Allergy Clin Immunol 1987; 80(6): 861-8.
[31] Bahnemann HG. Binary ethylenimine as an inactivant for foot-and-mouth disease virus and its application for vaccine production. Arch Virol 1975; 47(1): 47-56.
[32] Cunliffe HR. Inactivation of foot-and-mouth disease virus with ethylenimine. Appl Microbiol 1973; 26(5): 747-50.
[33] Bauer, K., Mussgay, M., Wittman, G.: US3636196 (**1972**).
[34] Melvin, P.A., Pryce, J.M.G.: US3318775 (**1967**).
[35] Larghi OP, Nebel AE. Rabies virus inactivation by binary ethylenimine: new method for inactivated vaccine production. J Clin Microbiol 1980; 11(2): 120-2.
[36] Bahnemann HG. Inactivation of viral antigens for vaccine preparation with particular reference to the application of binary ethylenimine. Vaccine 1990; 8(4): 299-303.
[37] Brown F, Meyer RF, Law M, Kramer E, Newman JF. A universal virus inactivant for decontaminating blood and biopharmaceutical products. Biologicals 1998; 26(1): 39-47.
[38] Burrage T, Kramer E, Brown F. Structural differences between foot-and-mouth disease and poliomyelitis viruses influence their inactivation by aziridines. Vaccine 2000; 18(22): 2454-61.
[39] Giles, R.E., Stevens, D.R., Wiesehahn, G.P.: US4545987 (**1985**).
[40] Rios, A.: US6383806 (**2002**).
[41] Rios, A.: US6503753 (**2003**).
[42] Karp, N.M.: WO2005040353 (**2005**).
[43] Carlson JR, McGraw TP, Keddie E, Yee JL, Rosenthal A, Langlois AJ, *et al*. Vaccine protection of rhesus macaques against simian immunodeficiency virus infection. AIDS Res Hum Retroviruses 1990; 6(11): 1239-46.
[44] Groene WS, Shaw RD. Psoralen preparation of antigenically intact noninfectious rotavirus particles. J Virol Methods 1992; 38(1): 93-102.
[45] Wiesehahn, G.P., Creagan, R.P., Stevens, D.R., Giles, R.: US5106619 (**1992**).
[46] Wiesehahn, G.P., Creagan, R.P., Stevens, D.R., Giles, R.: US4693981 (**1987**).
[47] Hanson CV. Photochemical inactivation of viruses with psoralens: an overview. Blood Cells 1992; 18(1): 7-25.
[48] Cimino GD, Gamper HB, Isaacs ST, Hearst JE. Psoralens as photoactive probes of nucleic acid structure and function: organic chemistry, photochemistry, and biochemistry. Annu Rev Biochem 1985; 54: 1151-93.
[49] Hearst JE, Isaacs ST, Kanne D, Rapoport H, Straub K. The reaction of the psoralens with deoxyribonucleic acid. Q Rev Biophys 1984; 17(1): 1-44.
[50] Park, S.C., Goodrich, R.P.J., Yerram, N.S., Sowemimo-Coker, S.O., Platz, M.S., Aquila, B.M. US5516629. (**1996**).
[51] Alter HJ, Creagan RP, Morel PA, Wiesehahn GP, Dorman BP, Corash L, *et al.* Photochemical decontamination of blood components containing hepatitis B and non-A, non-B virus. Lancet 1988; 2(8626-8627): 1446-50.
[52] Snyder EL, Dodd RY. Reducing the risk of blood transfusion. Hematology (Am Soc Hematol Educ Program) 2001: 433-42.
[53] Turner GS. Inactivation of Vaccinia Virus by Ascorbic Acid. J Gen Microbiol 1964; 35: 75-80.
[54] Salo RJ, Cliver DO. Inactivation of enteroviruses by ascorbic acid and sodium bisulfite. Appl Environ Microbiol 1978; 36(1): 68-75.
[55] Bordt, D., Draayer, H. EP0310317. (**1989**).
[56] White LA, Freeman CY, Forrester BD, Chappell WA. *In vitro* effect of ascorbic acid on infectivity of herpesviruses and paramyxoviruses. J Clin Microbiol 1986; 24(4): 527-31.
[57] Rawal BD, Bartolini F, Vyas GN. *In vitro* inactivation of human immunodeficiency virus by ascorbic acid. Biologicals 1995; 23(1): 75-81.
[58] Madhusudana SN, Shamsundar R, Seetharaman S. *In vitro* inactivation of the rabies virus by ascorbic acid. Int J Infect Dis 2004; 8(1): 21-5.
[59] Baratz, B.S., Phillips, R.A., Steward, D.L.: US4333941 (**1982**).
[60] Miles EW. Modification of histidyl residues in proteins by diethylpyrocarbonate. Methods Enzymol 1977; 47: 431-42.
[61] Bhattacharyya DK, Bandyopadhyay U, Banerjee RK. Chemical and kinetic evidence for an essential histidine in horseradish peroxidase for iodide oxidation. J Biol Chem 1992; 267(14): 9800-4.
[62] Dzhandzhugazyan KN, Plesner L. Diethyl pyrocarbonate inactivates CD39/ecto-ATPDase by modifying His-59. Biochim Biophys Acta 2000; 1466(1-2): 267-77.
[63] Shriver Z, Hu Y, Sasisekharan R. Heparinase II from Flavobacterium heparinum. Role of histidine residues in enzymatic activity as probed by chemical modification and site-directed mutagenesis. J Biol Chem 1998; 273(17): 10160-7.
[64] Pfizer. GB986046. (**1965**).
*[65] Stauffer, F., Miranda, J.M., Carneiro, F.A., Machado, G., Da Poian, A.T. BR0401466. (**2005**).
[66] Carneiro FA, Stauffer F, Lima CS, Juliano MA, Juliano L, Da Poian AT. Membrane fusion induced by vesicular stomatitis virus depends on histidine protonation. J Biol Chem 2003; 278(16): 13789-94.
[67] Mellencamp, M.W.: US2005084502 (**2005**).
[68] Zakay-Rones, Z., Levy, R.: WO9714434 (**1997**).
*[69] Reiter, M., Mundt, W., Barrett, N., Kistner, O.: WO2005118000 (**2005**).
[70] Lo Grippo, G.A., Timm, E.A., Taylor, A.R.: US3076748 (**1963**).
[71] Wang CH, Tschen SY, Flehmig B. Antigenicity of hepatitis A virus after ultra-violet inactivation. Vaccine 1995; 13(9): 835-40.
[72] Horowitz B, Wiebe ME, Lippin A, Vandersande J, Stryker MH. Inactivation of viruses in labile blood derivatives. II. Physical methods. Transfusion 1985; 25(6): 523-7.
[73] Piet MP, Chin S, Prince AM, Brotman B, Cundell AM, Horowitz B. The use of tri(n-butyl)phosphate detergent mixtures to inactivate hepatitis viruses and human immunodeficiency virus in plasma and plasma's subsequent fractionation. Transfusion 1990; 30(7): 591-8.
[74] Danihelkova H, Zavadova H. Disruption of influenza virus A by diethylether-Tween and tri-N-butyl phosphate-Tween mixtures. Acta Virol 1984; 28(1): 26-32.
[75] Seitz H, Blumel J, Schmidt I, Willkommen H, Lower J. Comparable virus inactivation by bovine or vegetable derived Tween 80 during solvent/detergent treatment. Biologicals 2002; 30(3): 197-205.
[76] Gross PA, Ennis FA, Gaerlan PF, Denning CR, Setia U, Davis WJ, *et al*. Comparison of new triton X-100- and tween-ether-treated split-treated vaccines in children. J Clin Microbiol 1981; 14(5): 534-8.
[77] Silva JL, Luan P, Glaser M, Voss EW, Weber G. Effects of hydrostatic pressure on a membrane-enveloped virus: high immunogenicity of the pressure-inactivated virus. J Virol 1992; 66(4): 2111-7.

[78] Nakagami T, Shigehisa T, Ohmori T, Taji S, Hase A, Kimura T, *et al*. Inactivation of herpes viruses by high hydrostatic pressure. J Virol Methods 1992; 38(2): 255-61.

[79] Ishimaru D, Sa-Carvalho D, Silva JL. Pressure-inactivated FMDV: a potential vaccine. Vaccine 2004; 22(17-18): 2334-9.

*[80] Hess, R.A., Manak, M.M., Dusing, S.K.: WO2002056824 (**2002**).

[81] Gou, S., Gou, H., Wang, C.: CN1269245 (**2000**).

[82] Otake T, Kawahata T, Mori H, Kojima Y, Hayakawa K. Novel method of inactivation of human immunodeficiency virus type 1 by the freeze pressure generation method. Appl Microbiol Biotechnol 2005; 67(6): 746-51.

[83] Jurkiewicz E, Villas-Boas M, Silva JL, Weber G, Hunsmann G, Clegg RM. Inactivation of simian immunodeficiency virus by hydrostatic pressure. Proc Natl Acad Sci U S A 1995; 92(15): 6935-7.

[84] Pontes L, Cordeiro Y, Giongo V, Villas-Boas M, Barreto A, Araujo JR, *et al*. Pressure-induced formation of inactive triple-shelled rotavirus particles is associated with changes in the spike protein Vp4. J Mol Biol 2001; 307(5): 1171-9.

[85] Smith DG, Mamay HK, Marshall RG, Wagner JC. Venezulean equine encephalomyelitis; laboratory aspects of fourteen human cases following vaccination and attempts to isolate the virus from the vaccine. Am J Hyg 1956; 63(2): 150-64.

[86] Nathanson N, Langmuir AD. The Cutter Incident. Poliomyelitis Following Formaldehyde- Inactivated Poliovirus Vaccination in the United States During the Spring of 1955. Ii. Relationship of Poliomyelitis to Cutter Vaccine. Am J Hyg 1963; 78: 29-60.

[87] Beck E, Strohmaier K. Subtyping of European foot-and-mouth disease virus strains by nucleotide sequence determination. J Virol 1987; 61(5): 1621-9.

[88] Brown F. Review of accidents caused by incomplete inactivation of viruses. Dev Biol Stand 1993; 81: 103-7.

[89] Bachmann MF, Bast C, Hengartner H, Zinkernagel RM. Immunogenicity of a viral model vaccine after different inactivation procedures. Med Microbiol Immunol (Berl) 1994; 183(2): 95-104.

RESULTADOS

2 Resultados

2.1 Parte I

Elucidação dos mecanismos da fusão de membranas mediada pelo VSV e pelo vírus da dengue

A entrada dos vírus envelopados na célula hospedeira sempre envolve uma etapa de fusão com membranas celulares (plasmática ou endossomal). Este processo é catalisado pelas glicoproteínas do envelope viral, que sofrem uma mudança conformacional desencadeada pela interação do vírus com seu receptor celular específico ou exposição ao pH ácido do meio endossomal. Nesta reestruturação da proteína de superfície viral, ocorre a exposição do peptídeo de fusão, que desestabiliza a membrana alvo, iniciando a reação de fusão.

Na parte I desta tese, tivemos como objetivo desvendar os mecanismos moleculares da fusão de membranas mediada pelo VSV e pelo vírus da dengue, permitindo o reconhecimento de possíveis alvos para inibição da entrada dos vírus nas células. Para isso, realizamos estudos de interação tanto da partícula viral inteira quanto de seu peptídeo de fusão com vesículas lipídicas, simulando as membranas biológicas. O resumo dos resultados obtidos encontra-se a seguir, e os resultados completos serão apresentados na forma de artigos científicos já publicados (artigos 2 e 3).

A fusão de membranas mediada pelo VSV é catalisada pela proteína G, que sofre mudanças conformacionais no pH ácido do meio endossomal. A faixa de pH em que o vírus adquire a capacidade fusogênica é muito estreita, entre 6.2 e 5.8, sugerindo que a protonação de resíduos de histidina é requerida para este processo. Para investigar tal hipótese, nós modificamos quimicamente os resíduos de histidina da proteína G com DEPC, um composto que reage covalentemente com um dos nitrogênios do anel imidazol da histidina, impedindo sua protonação. Observamos através de espectrofluorimetria que o tratamento viral com DEPC acarretou na inibição tanto da fusão de membranas quanto da reestruturação da glicoproteína do VSV, indicando que a protonação de histidinas está envolvida na aquisição da conformação fusogênica. Análise de espectrometria de massas dos fragmentos trípticos da proteína G modificada permitiram a identificação dos resíduos de histidina quimicamente modificados pelo DEPC. Utilizando peptídeos sintéticos, demonstramos que o segmento localizado entre os resíduos 145 e 168 da glicoproteína viral, conhecido como peptídeo p2-like, era capaz de mediar a fusão de forma tão eficiente quanto a partícula viral inteira e que sua atividade fusogênica dependia da protonação das histidinas 148 e 149. Estes resultados compõem o artigo 2 desta tese, que foi publicado em 2003 no periódico *Journal of Biological*

Chemistry, sendo o primeiro artigo na literatura científica a evidenciar que a protonação de resíduos de histidina está envolvida com a aquisição da conformação fusogênica de glicoproteínas virais.

Já no caso do vírus da dengue, a proteína E é a responsável pelo processo de fusão entre o envelope viral e a membrana endossomal. O alinhamento da seqüência de aminoácidos da glicoproteína E de diferentes flavivírus evidenciou que havia grande homologia no segmento localizado entre os resíduos 98 e 110. Estudos prévios de substituições de aminoácidos nesta região foram capazes de abolir a fusão de membranas mediada pela proteína E de outros flavivírus (ex. TBE vírus), sugerindo que talvez esta seqüência representasse o peptídeo de fusão. A análise da estrutura tridimensional da proteína E do vírus da dengue reforçou tal hipótese, mostrando que este segmento corresponde a um *loop*, no meio de folhas beta, e se encontra exposto no topo da molécula durante a interação com membranas. No entanto, nenhum destes estudos apresentou evidência direta de que este segmento interagia com membranas. Com este intuito, sintetizamos esta seqüência com parte das folhas beta adjacentes e realizamos um estudo de interação com vesículas lipídicas através de técnicas de espectrofluorimetria. Os dados obtidos mostraram que o peptídeo interage com membranas e é capaz de induzir fusão de lipossomas, indicando que realmente esta seqüência pode estar catalisando a fusão de membranas mediada pelo vírus da dengue. Tanto a partição quanto a reação de fusão foram mais intensas na presença de fosfolipídios negativos e são dependentes do pH e da força iônica do meio, demonstrando a importância de interações eletrostáticas entre o peptídeo e componentes carregados negativamente das membranas alvo. Também observamos que na presença destes componentes negativos provavelmente ocorre oligomerização do peptídeo, sendo esta etapa importante para o processo de fusão catalisado pela proteína E. Estes resultados foram obtidos durante meu doutorado *sandwich* realizado na Universidade de Lisboa e compõem o artigo 3 desta tese, que foi recentemente aceito para a publicação no periódico *Molecular Membrane Biology*.

2.1.1 Artigo 2

Membrane Fusion Induced by Vesicular Stomatitis Virus Depends on Histidine Protonation

Fabiana A. Carneiro*, Fausto Stauffer*, Carla S. Lima, Maria A. Juliano, Luiz Juliano e Andrea T. Da Poian

Publicado em 2003 no periódico

Journal of Biological Chemistry

* Contribuíram igualmente para este trabalho

THE JOURNAL OF BIOLOGICAL CHEMISTRY
Vol. 278, No. 16, Issue of April 18, pp. 13789–13794, 2003
Printed in U.S.A.

Membrane Fusion Induced by Vesicular Stomatitis Virus Depends on Histidine Protonation*

Received for publication, October 17, 2002, and in revised form, January 27, 2003
Published, JBC Papers in Press, February 4, 2003, DOI 10.1074/jbc.M210615200

Fabiana A. Carneiro‡§, Fausto Stauffer‡§, Carla S. Lima‡, Maria A. Juliano¶, Luiz Juliano¶, and Andrea T. Da Poian‡‖

From the ‡Departamento de Bioquímica Médica, Instituto de Ciências Biomédicas, Universidade Federal do Rio de Janeiro, Rio de Janeiro RJ 21941-590 and ¶Departamento de Biofísica, Escola Paulista de Medicina, Universidad Federal de São Paulo, Rua Três de Maio, 100, São Paulo 04044-020, Brazil

Entry of enveloped animal viruses into their host cells always depends on a step of membrane fusion triggered by conformational changes in viral envelope glycoproteins. Vesicular stomatitis virus (VSV) infection is mediated by virus spike glycoprotein G, which induces membrane fusion at the acidic environment of the endosomal compartment. VSV-induced membrane fusion occurs at a very narrow pH range, between 6.2 and 5.8, suggesting that His protonation is required for this process. To investigate the role of His in VSV fusion, we chemically modified these residues using diethylpyrocarbonate (DEPC). We found that DEPC treatment inhibited membrane fusion mediated by VSV in a concentration-dependent manner and that the complete inhibition of fusion was fully reversed by incubation of modified virus with hydroxylamine. Fluorescence measurements showed that VSV modification with DEPC abolished pH-induced conformational changes in G protein, suggesting that His protonation drives G protein interaction with the target membrane at acidic pH. Mass spectrometry analysis of tryptic fragments of modified G protein allowed the identification of the putative active His residues. Using synthetic peptides, we showed that the modification of His-148 and His-149 by DEPC, as well as the substitution of these residues by Ala, completely inhibited peptide-induced fusion, suggesting the direct participation of these His in VSV fusion.

Membrane fusion is an essential step in the entry of enveloped viruses into their host cells (1–3). Virus-induced fusion is always mediated by viral surface glycoprotein and may occur through two different general mechanisms: (i) surface fusion between viral envelope and host cell plasma membrane after virus interaction with its cellular receptor, and (ii) fusion of endosomal membrane with viral envelope after virus particle internalization by receptor-mediated endocytosis. In the latter case, fusion is triggered by conformational changes in viral glycoproteins induced by the decrease in the pH of the endosomal medium.

Vesicular stomatitis virus (VSV)[1] is a member of *Rhabdoviridae* family, genus *Vesiculovirus*. Rhabdoviruses contain helically wound ribonucleocapisid surrounded by a lipid bilayer through which spikes project. These spikes are formed by trimers of a single type of glycoprotein, named G protein. VSV enters into the cell by endocytosis followed by low pH-induced membrane fusion in the endosome (4, 5), which is catalyzed by VSV G protein (6). A common feature of viral fusion proteins is that they bear a highly conserved hydrophobic fusion domain, which is most often located at the N terminus of the polypeptide chain (7). However, VSV G protein does not contain an apolar amino acid sequence similar to the fusion peptides found in other viruses, suggesting alternative mechanisms involved in VSV-induced membrane fusion.

We have shown recently (8) that VSV-induced fusion depends on a dramatic structure reorganization of G protein, which occurs within a very narrow pH range, close to 6.0. In addition, we have found that VSV binding to membranes, as well as the fusion reaction, were highly dependent on electrostatic interactions between negative charges on membrane surface and positively charged amino acids in G protein at the fusion pH (9). These results suggest the involvement of histidyl residue(s) in G protein conformational changes required for fusion, because the protonation of imidazole ring occurs at the fusion pH range (pK = 6.0).

Hydrophobic photolabeling experiments allowed the identification of a G protein segment comprising amino acids 59 to 221, which interacts with membranes at low pH (10). Furthermore, studies using site-directed mutagenesis in the region spanning amino acids 117 to 137 have shown a reduction of G protein-induced fusion efficiency (11–13). However, there is no conclusive evidence that this sequence participates directly in the fusion reaction. Another region of rhabdovirus G protein has been implicated in its interaction with anionic phospholipids. This segment was better characterized for viral hemorrhagic septicemia virus, a rhabdovirus of salmonids, and it was named p2 peptide (14, 15). Viral hemorrhagic septicemia virus p2 peptide mediates phospholipid vesicle fusion, lipid mixing, and leakage of liposome contents and inserts itself into liposome membranes by adopting a β–sheet conformation (16). p2-like peptide was found among all rhabdoviruses and contains two histidyl residues in VSV G protein (17).

To evaluate the role of G protein His residues in VSV-in-

* This work was supported by grants from Conselho Nacional de Desenvolvimento Científico e Tecnológico, Fundação Carlos Chagas Filho de Amparo à Pesquisa do Estado do Rio de Janeiro, Fundação de Amparo Pesquisa do Estado de São Paulo, and Human Frontiers for Science Progress (RG 00043/2000-M). The costs of publication of this article were defrayed in part by the payment of page charges. This article must therefore be hereby marked "*advertisement*" in accordance with 18 U.S.C. Section 1734 solely to indicate this fact.

§ Contributed equally to this work.

‖ To whom correspondence should be addressed. Tel.: 55-21-22706264; Fax: 55-21-22708647; E-mail: dapoian@bioqmed.ufrj.br.

[1] The abbreviations used are: VSV, vesicular stomatitis virus; DEPC, diethylpyrocarbonate; PS, phosphatidylserine; PC, phosphotidylcholine; 10-PyPC, 1-hexadecanoyl-2-(1-pyrenedecanoyl)-*sn*-glycero-3-phosphocholine; MALDI-TOF, matrix-assisted laser desorption ionization time-of-flight; HIV-1, human immunodeficiency virus, type 1; MES, 4-morpholineethanesulfonic acid; HPLC, high pressure liquid chromatography.

duced membrane fusion we modified these residues using diethylpyrocarbonate (DEPC). We showed that His protonation was essential both for low pH-induced conformational changes of VSV G protein and for the fusion reaction itself. Mass spectrometry analysis of G protein fragments obtained by limited proteolysis allowed the identification of the putative active His residues. Using synthetic peptides, we found that VSV p2-like peptide (sequence between amino acids 145 and 168) was as efficient as the virus in catalyzing membrane fusion at pH 6.0 and that the modification of His-148 and His-149 by DEPC completely abolished fusion activity. Substitution of the His by Ala residues inhibits peptide-mediated fusion, confirming the requirement of His protonation in VSV-induced membrane fusion.

MATERIALS AND METHODS

Chemicals—DEPC, phosphatidylserine (PS) and phosphotidylcholine (PC) from bovine brain, trypsin from bovine pancreas, and phenylmethylsulfonyl fluoride were purchased from Sigma. 1-Hexadecanoyl-2-(1-pyrenedecanoyl)-*sn*-glycero-3-phosphocholine (10-PyPC) was purchased from Molecular Probes Inc., Eugene, OR. All other reagents were of analytical grade.

Virus Propagation and Purification—VSV Indiana was propagated in monolayer cultures of BHK-21 cells. The cells were grown at 37 °C in roller bottles containing 150 ml of Dulbecco's modified Eagle's medium supplemented with 10% fetal bovine serum, 100 μg/ml ampicillin, 5 μg/ml gentamicin. When the cells reached confluence, the medium was removed, and the cell monolayer was infected with VSV at a multiplicity of 0.1 plaque-forming unit/ml. The cultures were kept at 37 °C for 16–20 h, and the virus were harvested and purified by differential centrifugation followed by equilibrium sedimentation in a sucrose gradient as described elsewhere (18). Purified virions were stored at −70 °C.

Preparation of Liposomes—Phospholipids were dissolved in chloroform and evaporated under nitrogen. The lipid film formed was resuspended in 20 mM MES, 30 mM Tris buffer, pH 7.5 or 6.0, at a final concentration of 1 mM. The suspension was vortexed vigorously for 5 min. Small unilamellar vesicles were obtained by sonicating the turbid suspension using a Branson Sonifier (Sonic Power Company, Danbury, CT) equipped with a titanium microtip probe. Sonication was performed in an ice bath, alternating cycles of 30 s at 20% full power with 60-s resting intervals until a transparent solution was obtained (~10 cycles). The vesicles used in this study were composed of PC and PS at a 1:3 ratio. For fusion assays, 1% 10-PyPC was incorporated in PC:PS vesicles by vortexing for 10 min.

Sample Modification with DEPC—DEPC solutions were freshly prepared by dilution of the reagent in cold ethanol. The concentration of stock DEPC solution was determined by reaction with 10 mM imidazole (19). For modification with DEPC, VSV was diluted in 20 mM MES, 30 mM Tris buffer, pH 7.5. At fixed time intervals, aliquots of DEPC were added to the mixture, and the reaction was monitored by the increase of absorbance at 240 nm because of the formation of *N*-carbethoxyhistidine using a Hitachi U-2001 spectrophotometer. The final concentration of DEPC ranged from 0.005 to 0.05 mM.

To study the kinetics of modification, VSV was diluted in 20 mM MES, 30 mM Tris buffer, pH 7.5, and the reaction was initiated by the addition of 0.02 mM DEPC at 25 °C. The time course of the reaction was monitored by an increase of absorbance at 240 nm.

Reversal of DEPC Inactivation—VSV was reacted with 0.02 mM DEPC at 25 °C. After 3 min, the mixture was incubated with 400 mM hydroxylamine (from a 3 M stock solution of hydroxylamine in 20 mM MES, 30 mM Tris buffer, adjusted to pH 7.5) for 15 min at 25 °C. For demodification of peptides, the experiment was carried out at the same conditions except that the concentrations of DEPC and hydroxylamine used were 0.2 and 500 mM, respectively. For the control, a solution that contained the same concentration of hydroxylamine without DEPC was used.

Liposome Fusion Assay—A suspension of liposomes of different phospholipid composition containing equal amounts of unlabeled vesicles and vesicles labeled with 10-PyPC were prepared in 20 mM MES, 30 mM Tris buffer, pH 6.0 or 7.5, with a final phospholipid concentration of 0.1 mM. The emission spectrum of pyrene-labeled vesicles exhibited a broad excimer fluorescence peak with maximal intensity at 480 nm and two sharp peaks at 376 and 385 nm because of monomer fluorescence emission (not shown). The fusion reaction was initiated by addition of purified VSV preincubated with different concentrations of DEPC for 3 min at 25 °C, ranging from 0.005 to 0.02 mM. Fusion was followed by the decrease in the 10-PyPC excimer/monomer fluorescence intensity ratio, which was measured by exciting the sample at 340 nm and collecting the fluorescence intensities of excimer and monomer at 480 and 376 nm, respectively. A control experiment using equivalent volumes of ethanol (without DEPC) was performed under comparable conditions. For peptide-induced fusion, the concentration of DEPC used was 0.02 and 0.2 mM.

Intrinsic Fluorescence Measurements—G protein conformational changes during VSV interaction with membranes of different phospholipid composition were monitored by the changes in virus intrinsic fluorescence. VSV (final protein concentration of 15 μg/ml) was incubated with a liposome suspension containing 1 mM phospholipid in 20 mM MES, 30 mM Tris buffer, pH 6.0. Intrinsic fluorescence data were recorded using a Hitachi F-4500 fluorescence spectrometer, exciting the samples at 280 nm, and collecting emission between 300 and 420 nm.

MALDI-TOF Mass Spectrometry of Modified VSV G Protein—VSV (0.3 mg/ml) was reacted with 0.02 mM DEPC for 15 min at 25 °C. After modification, G protein was denatured by virus incubation with 8 M urea for 1 h. Then, the sample was diluted 4-fold in 10 mM Tris buffer, pH 7.4, and incubated with trypsin (final concentration of 11 mg/ml) for 4 h at 37 °C. The reaction was stopped by addition of 0.1 mM phenylmethylsulfonyl fluoride. The tryptic peptides were separated from the remaining virus by filtration. For mass spectrometry analysis, aliquots of 1 μl of the digested sample mixed with 1 μl of the matrix solution (a saturated solution of α-cyano-4-hydroxycinnamic acid in 50% acetonitrile, 0.1% trifluoroacetic acid) were applied on the plate and allowed to dry at room temperature. Mass profiles of digested G protein were obtained on a Voyager-DE PRO (Applied Biosystems) equipped with a nitrogen laser (λ = 337 nm). Fifty laser shots were summed per sample spectrum, and an average of five spectra was used. The masses obtained were searched against a protein data base containing the sequence of bovine trypsin and VSV G protein using the ExPASy Molecular Biology Server (www.expasy.org). Searches were also done with the DEPC modification option turned on.

Peptides Synthesis—All peptides were synthesized by solid phase using the Fmoc (*N*-(9-fluorenyl)methoxycarbonyl) methodology, and all protected amino acids were purchased from Calbiochem-Novabiochem or from Neosystem (Strasbourg, France). The syntheses were done in an automated bench-top simultaneous multiple solid-phase peptide synthesizer (PSSM 8 system from Shimadzu). The final deprotected peptides were purified by semipreparative HPLC using an Econosil C-18 column (10 μm, 22.5 × 250 mm) and a two-solvent system, Solvent A (trifluoroacetic acid/H_2O) (1:1000) (v/v) and Solvent B (trifluoroacetic acid/acetonitrile/H_2O) (1:900:100) (v/v/v). The column was eluted at a flow rate of 5 ml·min^{-1} with a 10 or 30 to 50 or 60% gradient of Solvent B over 30 or 45 min. Analytical HPLC was performed using a binary HPLC system from Shimadzu with a SPD-10AV Shimadzu UV-visible detector, coupled to an Ultrasphere C-18 column (5 μm, 4.6 × 150 mm), which was eluted with a two-solvent system, Solvent A1 (H_3PO_4/H_2O) (1:1000) (v/v) and Solvent B1 (acetonitrile/H_2O/H_3PO_4) (900:100:1) (v/v/v) at a flow rate of 1.7 ml·min^{-1} and a 10–80% gradient of B1 over 15 min. The HPLC column-eluted materials were monitored by their absorbance at 220 nm. The molecular mass and purity of synthesized peptides were checked by MALDI-TOF mass spectrometry (TofSpec-E; Micromass) and/or peptide sequencing using a protein sequencer PPSQ-23 (Shimadzu, Tokyo, Japan).

RESULTS

Role of G Protein His Residues in VSV-induced Membrane Fusion—VSV was incubated with increasing concentrations of DEPC, which reacts with His-forming *N*-carbethoxyhistidyl derivatives (19), and the virus-mediated membrane fusion was quantified by measuring the decrease in pyrene phospholipid excimer/monomer fluorescence ratio (9, 20) (Fig. 1). Incubation of 0.02 mM DEPC with VSV (15 μg/ml) completely abolished virus ability to mediate membrane fusion, whereas lower concentrations of DEPC partially inhibits it. The formation of *N*-carbethoxyhistidine was followed spectrophotometrically by the absorbance increase in 240 nm (19). The major changes observed in absorbance occurred when the virus was incubated with DEPC in final concentrations up to 0.03 mM (Fig. 2*A*). Kinetics of VSV modification with 0.02 mM DEPC revealed that the reaction was completed after 3 min (Fig. 2*B*). To further

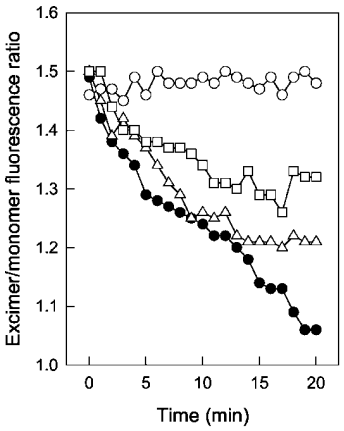

FIG. 1. **His modification by DEPC impairs VSV-induced membrane fusion.** Equal amounts of unlabeled vesicles and vesicles labeled with 10-PyPC were incubated with purified VSV (●) or VSV pre-incubated with 0.005 (△), 0.01 (□), and 0.02 (○) mM DEPC. The vesicles were composed of PC:PS (1:3) and were prepared in 20 mM MES, 30 mM Tris buffer, pH 6.0, in a final phospholipid concentration of 0.1 mM. VSV-induced membrane fusion was measured by the decrease in the 10-PyPC excimer/monomer fluorescence ratio. 10-PyPC was excited at 340 nm, and the intensities were collected at 376 and 480 nm for monomer and excimer, respectively. The final protein concentration was 15 μg/ml.

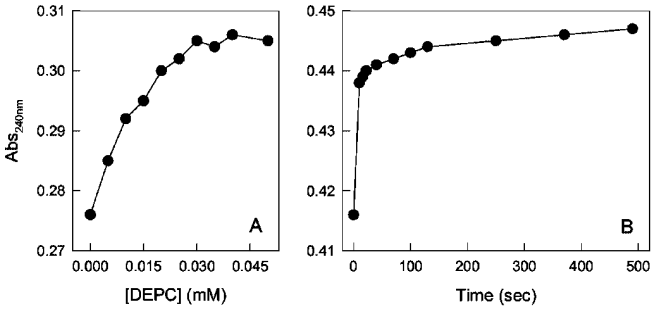

FIG. 2. **VSV modification with DEPC.** *A*, purified VSV was diluted in 20 mM MES, 30 mM Tris buffer, pH 7.5, and incubated with different concentrations of DEPC. The formation of carbethoxyhistidyl residues was followed by the increase in the absorbance at 240 nm. The final protein concentration was 35 μg/ml. *B*, kinetics of VSV His modification with 0.02 mM DEPC. The final protein concentration was 140 μg/ml.

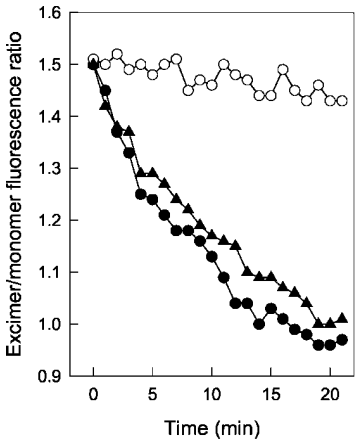

FIG. 3. **Reversal of DEPC-induced modification in VSV G protein His residues with hydroxylamine.** Equal amounts of unlabeled vesicles and vesicles labeled with 10-PyPC were incubated with purified VSV (●), VSV pre-incubated with DEPC 0.02 mM (○), or VSV pre-incubated with DEPC 0.02 mM for 3 min and then incubated with hydroxylamine 400 mM for 15 min (▲). The final protein concentration was 15 μg/ml. Other experimental conditions were as in Fig. 1.

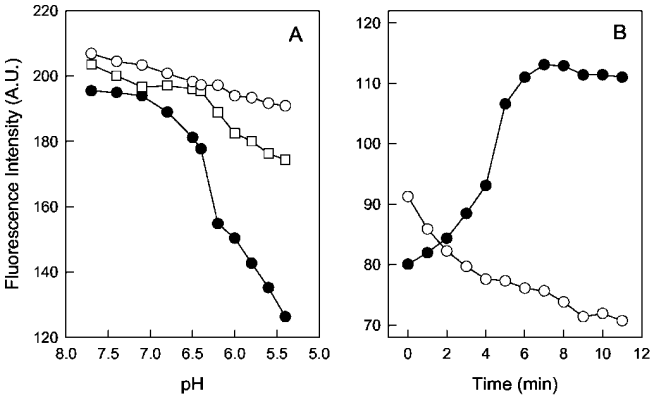

FIG. 4. **pH-induced conformational changes on VSV G protein involve His protonation.** *A*, purified VSV (●) or VSV pre-incubated with 0.002 mM DEPC (□) or 0.02 mM DEPC (○) were diluted in 20 mM MES, 30 mM Tris buffer, pH 7.5, to a final protein concentration of 25 μg/ml. Tryptophan fluorescence emission at 334 nm was recorded whereas pH was gradually acidified by addition of HCl. The excitation wavelength was 280 nm. *B*, kinetics of G protein interaction with liposomes at low pH was measured by intrinsic fluorescence of purified VSV (●) or VSV pre-incubated with 0.02 mM DEPC (○). Vesicles composed of PC:PS (1:3) were prepared in 20 mM MES, 30 mM Tris buffer, pH 6.0, in a final phospholipid concentration of 0.1 mM. The excitation wavelength was 280 nm, and the emission was collected at 334 nm. The final protein concentration was 25 μg/ml.

test whether modification of His residues was responsible for inhibition of virus fusion activity, hydroxylamine, which removes the carbethoxy group from imidazole group (19), was added 3 min after VSV incubation with 0.02 mM DEPC. Virus incubation with hydroxylamine after modification with 0.02 mM DEPC completely restored its ability to catalyze membrane fusion (Fig. 3). This set of results indicates that His protonation is required for membrane fusion catalyzed by VSV, suggesting a central role of His in pH-induced conformational changes in VSV G protein.

His Protonation Is Involved in pH-induced Conformational Changes on G Protein—We have shown recently (8) that G protein interaction with liposomes at pH 6.0 resulted in dramatic protein conformational changes, which can be followed by intrinsic fluorescence. In the presence of vesicles composed of PC and PS, a great increase in tryptophan fluorescence of G protein occurred upon acidification of the medium, whereas pH decrease led to intrinsic fluorescence quenching in the absence of liposomes (8). VSV incubation with DEPC inhibited intrinsic fluorescence quenching during acidification, suggesting the involvement of His protonation in G protein conformational changes (Fig. 4*A*). Time course of fluorescence increase after VSV incubation with liposomes, at pH 6.0, is shown in Fig. 4*B*. The increase in fluorescence was completely inhibited when the virus was incubated with 0.02 mM DEPC. These results indicate that the G protein conformational changes that take place during protein-lipid interaction are mediated by His protonation at pH 6.0.

Mass Spectrometry Analysis of Modified G Protein—VSV G protein contains a total of 16 His residues. Previous investigations have revealed that a specific domain spanning residues 59 to 221, which contains 6 His residues, interacted with the target membrane at low pH (10). To determine whether DEPC treatment modified the His residues within this sequence, the peptides obtained after limited proteolysis of modified G protein were analyzed by MALDI-TOF mass spectrometry. Seven fragments could be identified as VSV G protein peptides (Table I). These peptides cover 64% of G protein (329/511 amino acids). We also analyzed the data considering the increase in mass because of DEPC modification, and four modified peptides could be identified (Table II). Two of these peptides are in-

TABLE I
MALDI-TOF mass spectrometry analysis of peptides from VSV G protein

Fragment	Expected mass	Measured mass	Δ mass	Sequence
3–66	7375.704	7375.351	0.353	CLLYLAFLFIGVNCKFTIVFPHNQKGNWKNVPSNYHYCPSSSDLNWHNDLIGTALQVK MPKSHK
18–87	8084.867	8085.424	−0.557	FTIVFPHNQKGNWKNVPSNYHYCPSSSDLNWHNDLIGTALQVKMPKSHKAIQADGWM CHASKWVTTCDFR
217–236	2185.997	2185.850	0.147	EGTGFRSNYFAYETGGKACK
294–370	8486.476	8486.161	0.314	ILDYSLCQETWSKIRAGLPISPVDLSYLAPKNPGTGPAFTIINGTLKYFETRYIRVDIAAPI LSRMVGMISGTTTER
341–417	8766.324	8766.349	−0.024	YFETRYIRVDIAAPILSRMVGMISGTTTERELWDDWAPYEDVEIGPNGVLRTSSGYKFPL YMIGHGMLDSDLHLSSK
449–493	5103.903	5103.627	0.275	NPIELVEGWFSSWKSSIASFFFIIGLIIGLFLVLRVGIHLCIKLK
463–483	2326.394	2326.737	−0.343	SSIASFFFIIGLIIGLFLVLR

TABLE II
MALDI-TOF mass spectrometry analysis of DEPC-modified peptides from VSV G protein

Fragment	Expected mass	Measured mass	Δ mass	Number of modified His	Sequence
3–63	7239.582	7239.194	0.387	3	CLLYLAFLFIGVNCKFTIVFPHNQKGNWKNVPSNYHYCPSSSD LNWHNDLIGTALQVKMPK
32–87	6460.004	6459.685	0.319	1	NVPSNYHYCPSSSDLNWHNDLIGTALQVKMPKSHKAIQADGW MCHASKWVTTCDFR
110–168	6588.162	6588.522	−0.360	1	ESIEQTKQGTWLNPGFPPQSCGYATVTDAEAVIVQVTPHHVL VDEYTGEWVDSQFINGK
392–417	3028.443	3028.409	0.033	2	TSSGYKFPLYMIGHGMLDSDLHLSSK

[a] Underlined letters indicate possible sites of modifications.

cluded in the membrane-interacting domain (32–87 and 110–168), suggesting that the active His are located within this segment.

Role of p2-like Peptide in VSV-induced Membrane Fusion— The putative fusion peptide (region 117–137) and the p2-like peptide (region 145–168) are located within one of the modified segments of G protein identified by mass spectrometry. To evaluate the ability of both the p2-like peptide and the putative fusion peptide in catalyzing fusion *in vitro*, we synthesized a number of peptides (Fig. 5). Besides the putative fusion peptide and the p2-like peptide, we synthesized three other His-containing sequences to be used as controls. The peptides corresponding to the sequences between amino acids 65–85 and 170–190 contain two His residues and are located within the sequence that was identified as the membrane-interacting segment by photolabeling experiments (10). The peptide between amino acids 395–418 was also chosen, because it was found to be modified by DEPC treatment by mass spectrometry analysis (Table II).

Fig. 6 shows that the p2-like peptide was as efficient as the whole virus to catalyze fusion of PC:PS vesicles. Using p2-like peptide in a 50-fold lower concentration, which gives a peptide molar concentration similar to G protein concentration used in virus-induced fusion, we obtained a very similar profile (Fig. 6*B*). In addition, peptide-induced fusion presented the same requirements of VSV-mediated fusion. It occurs at pH 6.0 but not at pH 7.5 and depends on the presence of PS on the target membrane (Fig. 6*B*). These data suggest a direct participation of p2-like peptide in VSV-induced membrane fusion. On the other hand, when the synthetic peptide corresponding to the VSV putative fusion peptide was assayed for liposome fusion, it failed to induce a decrease in pyrene excimer/monomer fluorescence ratio (Fig. 6*C*). This result shows that this sequence alone is not able to catalyze fusion reaction and reinforces the involvement of p2-like peptide in VSV fusion.

The pH dependence of membrane fusion mediated by p2-like peptide suggests the participation of His in the process. To evaluate whether His protonation was also necessary for peptide-induced fusion, as observed for the virus, the effect of peptide incubation with DEPC on the membrane fusion was analyzed. As shown on the Fig. 7*A*, His modification by DEPC abolished peptide activity, suggesting that His residues are crucial for membrane recognition and fusion. Hydroxylamine treatment reversed fusion inhibition by DEPC modification (Fig. 7*A*). In addition, substitution of both His-148 and His-149 for Ala residues on the peptide sequence completely abolished fusion, whereas removing one of the His residues led to a less efficient fusion (Fig. 7*B*). All other G protein amino acid sequences containing two His residues used as controls did not present fusion activity (Fig. 7*C*). These results together suggest that VSV p2-like peptide directly participates in membrane fusion mediated by G protein and that protonation of His is necessary for peptide fusion activity.

```
117-137     117 Q G T W L D P G F P Q S S G Y A T V T D

p2-like wt  145 V T P H H V L V D E Y T G E W V D S Q F
H148A           . . . A . . . . . . . . . . . . . . .
H149A           . . . . A . . . . . . . . . . . . . .
H148,149A       . . . A A . . . . . . . . . . . . . .

65-85       85  H K A I Q A D G W M C H A S K W V T T C D
170-190     170 S N Y I C P T V H N S T T W H S D Y K V K
395-418     395 G Y K F P L W M I G H G M L D S D L H L S S K A
```

FIG. 5. **Amino acid sequences of the peptides used in this study.** The putative VSV fusion peptide corresponds to the G protein sequence between residues 117 and 137. VSV p2-like peptides used in this study correspond to VSV G protein residues between 145 and 168. His-148 or His-149 or both were substituted for Ala residues. *Dots* represent wild-type residues. Peptides corresponding to other G protein sequences between residues 65 and 85, 170 and 190, and 395 and 418 were used as control peptides containing two histidines.

DISCUSSION

In this work, we describe two main findings concerning VSV-induced membrane fusion. First, we showed that fusion is driven by His protonation at the pH range of endosomal medium. Although several residues have already been implicated in G protein fusion ability, to our knowledge His has never been considered. Second, we found that VSV p2-like peptide was as efficient as the whole virus in catalyzing fusion, whereas the

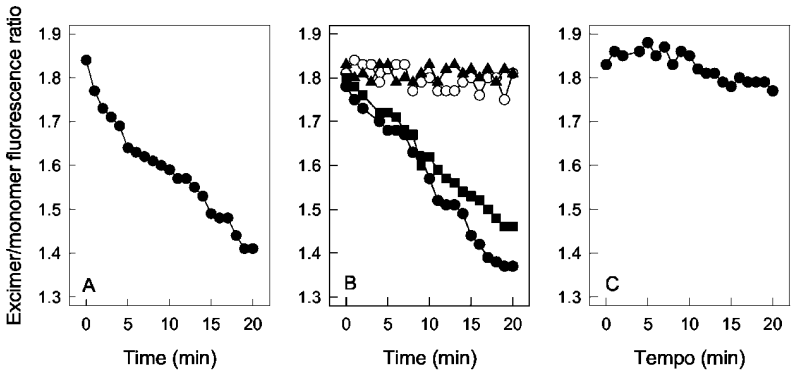

FIG. 6. **Role of p2-like peptide in VSV-induced membrane fusion.** Equal amounts of unlabeled vesicles and vesicles labeled with 10-PyPC were incubated with purified VSV (*A*), VSV p2-like peptide (*B*), or VSV peptide 117–137 (*C*). The vesicles were prepared in 20 mM MES, 30 mM Tris buffer in a final phospholipid concentration of 0.1 mM. Membrane fusion was measured by the decrease in the 10-PyPC excimer/monomer fluorescence ratio. 10-PyPC was excited at 340 nm, and the intensities were collected at 376 and 480 nm for monomer and excimer, respectively. The vesicles used were composed of PC:PS (1:3) at pH 6.0 (●), PC:PS (1:3) at pH 7.5(○), and PC only at pH 6.0 (▲). The final viral protein concentration was 15 μg/ml, and peptide concentration was 10 μg/ml (●, ○, ▲) or 0.2 μg/ml (■).

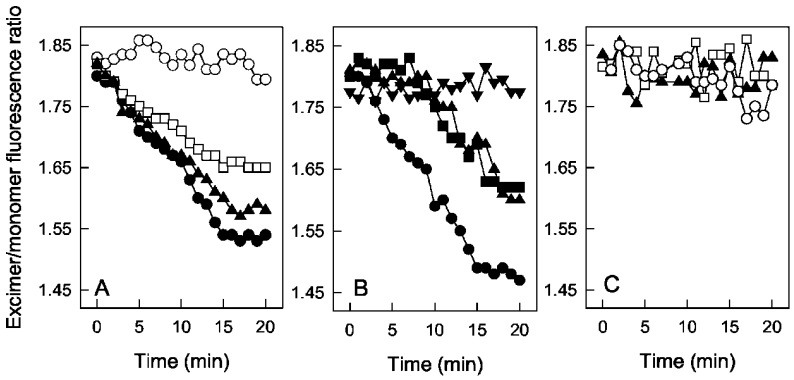

FIG. 7. **His-148 and His-149 are important for peptide-induced membrane fusion.** *A*, membrane fusion induced by p2-like peptide (●), peptide pre-incubated with 0.02 mM DEPC (□) or 0.2 mM DEPC (○), or peptide pre-incubated with 0.2 mM DEPC for 3 min and then incubated with 500 mM hydroxylamine for 15 min (▲). *B*, effect of His substitution on p2-like peptide-induced fusion. Membrane fusion activity was evaluated for wild-type p2-like peptide (●), H148A (▲), H149A (■), and H148A,H149A double-mutant peptide (▼). *C*, membrane fusion activity of VSV peptide 65–85 (○), 170–190 (□), and 395–418 (▲). The final peptide concentrations was 10 μg/ml. Other experimental conditions were as in Fig. 1.

putative fusion peptide failed to induce fusion. VSV p2-like peptide contains two His residues, whose protonation are required for its fusion activity.

The identification of the amino acid residues essential for membrane fusion mediated by viral glycoproteins might contribute to the elucidation of the molecular mechanisms underlying the fusion event. In the case of VSV, mutational analysis have shown that substitution of conserved Gly, Pro, or Asp present in the region between amino acids 117 and 137 either abolished fusion ability of G protein or shifted the optimum pH of fusion (11–13). Based on these results, the authors proposed that this segment was the putative fusion domain of VSV G protein. However, direct evidence that this particular region interacts with the target membrane is still lacking. VSV-induced membrane fusion occurs in a very narrow pH range, between 5.8 and 6.2 (4, 8). This indicates that the protonation of a small number of ionizable groups is required for G protein structural changes. His is the only amino acid whose ionization pK_a is in the range of VSV fusion, suggesting that fusion is driven by His protonation. Using DEPC, we showed that His modification abolished pH-induced conformational changes on G protein and the fusion reaction catalyzed by the virus. VSV putative fusion peptide contains no His, and thus it cannot be modified by DEPC. In addition, we found that a synthetic peptide corresponding to the VSV putative fusion sequence failed to induced phospholipid vesicle fusion, although several studies have reported that synthetic fusion peptides of different viruses promote fusion independent of the remainder protein (21–25). Further investigation will be necessary to answer whether the segment between amino acids 117 and 137 of G protein directly participates in VSV fusion or whether the substitution of its conserved amino acids affects the conformation or the exposure of other membrane-interacting sequences in G protein.

Another question to be answered is how general is the requirement of His protonation for pH-dependent viral membrane fusion. In the case of influenza virus, for example, the participation of hemagglutinin N-terminal peptide in fusion is very well established, although this peptide does not contain His residues. In this case, however, the fusion occurs at pH 5.0, in which protonation of acidic amino acids could take place. Another possibility that could not be discarded so far is that the protonation of His residues in other regions of the fusion protein could affect the overall protein structure leading to the exposure of the fusion peptide.

We have shown recently (9) that G protein-membrane interaction is highly dependent on the presence of PS, a negatively charged phospholipid, in the target membrane. In addition, we have found that G protein conformational changes, as well as VSV-mediated fusion, are driven by electrostatic interactions. Based on the results showed here, we believe that the protonation of His residues could generate positive charges on G protein, which might contribute to the electrostatic interactions required for protein insertion in membrane during fusion.

Heptad repeats play an important role in many viral membrane fusion processes. Three-dimensional structures of frag-

ments from several viral fusion proteins, including influenza hemagglutinin, Moloney leukemia virus transmembrane (TM) subunit, HIV-1 glycoprotein 41, Ebola virus GP2, and simian immunodeficiency virus glycoprotein 41, have been determined (26–30). The results obtained revealed that these proteins adopt a post-fusion hairpin structure formed by the interaction of N-terminal and C-terminal heptad-repeat segments, which generate a trimeric coiled-coil (31). For Sendai virus, heptad repeats were shown to bind phospholipid membranes with high affinity, probably assisting in bringing viral and cellular membranes closer (32, 33). Indeed, studies using synthetic peptides supported a direct role of the N-terminal heptad repeat in Sendai virus fusion event (34). The G protein from all rhabdoviruses also presents heptad repeats (14), which were mapped as the PS binding domain of this protein (17). We showed here that a synthetic peptide corresponding to VSV G protein heptad repeat, the p2-like peptide, was very efficient in mediating pH-dependent fusion of PS-containing vesicles, which, as found for the whole virus, was inhibited by treatment of the peptide with DEPC. p2-like peptide from viral hemorrhagic septicemia virus, another rhabdovirus, was also able to induce membrane fusion (16). These results together suggest that p2-like peptides play an active role in the rhabdoviral fusogenic process. Whether they can be considered the actual rhabdovirus fusion peptides depends on further investigation.

A common feature of several viral fusion glycoproteins is that they are synthesized as a fusion-incompetent precursor that is cleaved to generate the fusogenic protein. The fusion machinery from rhabdovirus is completely different. The fusion occurs through reversible conformational changes that do not require activation by proteolytic cleavage (35, 36). Our previous results showed that VSV G protein underwent a dramatic loss of secondary structure at the fusogenic pH, which was shown to be necessary for fusion (8). The loss of secondary structure during fusion seems to be another particular feature of rhabdovirus fusion, because most of viral fusion peptides adopt an α-helical structure when inserted in the lipid bilayer, which is necessary for their fusogenic activity (21–24, 37). In the case of HIV-1, however, it is hypothesized that the fusion peptide underwent conformational transitions from α-helix to β-structures when bound to the target membrane (38–40), suggesting that fusion may require conformational flexibility of the fusion peptide itself. The results described here suggests that, at least in the case of VSV, the structural transitions that drive fusion reaction depend on His protonation.

Acknowledgments—We thank Dr. Gonzalo de Prat-Gay for encouragement, Dr. Ronaldo Mohana-Borges for critical reading of the manuscript, Dr. Russolina B. Zingali for helpful suggestions, and Simone C. L. Leão and Denis L. S. Dutra for technical assistance. We also thank Dr. Adalberto R. Vieyra for use of the fluorometer and the "Rede Proteômica do Estado do Rio de Janeiro" for use of the mass spectrometry facility.

REFERENCES

1. Gaudin, Y., Ruigrok, R. W. H., and Brunner, J. (1995) *J. Gen. Virol.* **76,** 1541–1556
2. Hernandez, L. D., Hoffman, L. R., Wolfsberg, T. G., and White, J. M. (1996) *Annu. Rev. Cell Dev. Biol.* **12,** 627–661
3. Eckert, D. M., and Kim, P. S. (2001) *Annu. Rev. Biochem.* **70,** 777–810
4. White, J., Matlin, K., and Helenius, A. (1981) *J. Cell Biol.* **89,** 674–679
5. Da Poian, A. T., Gomes, A. M. O., and Coelho-Sampaio, T. (1998) *J. Virol. Meth.* **70,** 45–58
6. Florkiewicz, R. Z., and Rose, J. K. (1984) *Science* **225,** 721–723
7. Durell, S. R., Martin, I., Ruisschaert, J.-M., Shai, Y., and Blumenthal, R. (1997) *Mol. Membr. Biol.* **14,** 97–112
8. Carneiro, F. A., Ferradosa, A. S., and Da Poian, A. T. (2001) *J. Biol. Chem.* **276,** 62–67
9. Carneiro, F. A., Bianconi, M. L., Weissmuller, G., Stauffer, F., and Da Poian, A. T. (2002) *J. Virol.* **76,** 3756–3764
10. Durrer, P., Gaudin, Y., Ruigrok, W. H., Graf, R., and Brunner, J. (1995) *J. Biol. Chem.* **270,** 17575–17581
11. Li, Y., Drone, C., Sat, E., and Ghosh, H. P. (1993) *J. Virol.* **67,** 4070–4077
12. Zhang, L., and Ghosh, H. P. (1994) *J. Virol.* **68,** 2186–2193
13. Fredericksen, B. L., and Whitt, M. (1995) *J. Virol.* **69,** 1435–1443
14. Coll, J. M. (1995) *Virus Genes* **10,** 107–114
15. Estepa, A., and Coll, J. M. (1996) *J. Virol. Meth.* **61,** 37–45
16. Nuñez, E., Fernandez, A. M., Estepa, A., Gonzalez-Ros, J. M., Gavilanes, F., and Coll, J. M. (1998) *Virology* **243,** 322–330
17. Coll, J. M. (1997) *Arch. Virol.* **142,** 2089–2097
18. Da Poian, A. T., Gomes, A. M. O., Oliveira, R. J. N., and Silva, J. L. (1996) *Proc. Natl. Acad. Sci. U. S. A.* **93,** 8268–8273
19. Miles, E. W. (1977) *Methods Enzymol.* **47,** 431–442
20. Pal, R., Barenholz, Y., and Wagner, R. R. (1988) *Biochemistry* **27,** 30–36
21. Lear, J. D., and DeGrado, W. F. (1987) *J. Biol. Chem.* **262,** 6500–6505
22. Takahashi, S. (1990) *Biochemistry* **29,** 6257–6264
23. Rafalski, M., Lear, J. D., and DeGrado, W. F. (1990) *Biochemistry* **29,** 7917–7922
24. Martin, I., Dubois, M. C., Defrise-Quertain, F., Saermark, T., Burny, A., Brasseur, R., and Ruysschaert, J. M. (1994) *J. Virol.* **68,** 1139–1148
25. Martin, I., Ruysschaert, J. M., and Epand, R. M. (1999) *Adv. Drug Deliv. Rev.* **38,** 233–255
26. Bullough, P. A., Hughson, F. M., Skehel, J. J., and Wiley, D. C. (1994) *Nature* **371,** 37–43
27. Fass, D., Harrison, S. C., and Kim, P. S. (1996) *Nat. Struct. Biol.* **3,** 465–469
28. Chan, D. C., Fass, D., Berger, J. M., and Kim, P. S. (1997) *Cell* **89,** 263–273
29. Weissenhorn, W., Carfi, A., Lee, K. H., Skehel, J. J., and Wiley, D. C. (1998) *Mol. Cell.* **2,** 605–616
30. Caffrey, M., Cai, M., Kaufman, J., Stahl, S. J., Wingfield, P. T., Covell, D. G., Gronenborn, A. M., and Clore, G. M. (1998) *EMBO J.* **17,** 4572–4584
31. Skehel, J. J., and Wiley, D. C. (1998) *Cell* **95,** 871–874
32. Ghosh, J. K., Peisajovich, S. G., Ovadia, M., and Shai, Y. (1998) *J. Biol. Chem.* **273,** 27182–27190
33. Ben-Efraim, I., Kliger, Y., Hermesh, C., and Shai, Y. (1999) *J. Mol. Biol.* **285,** 609–625
34. Ghosh, J. K., and Shai, Y. (1999) *J. Mol. Biol.* **292,** 531–546
35. Gaudin, Y., Ruigrok, R. W., Knossow, M., and Flamand, A. (1993) *J. Virol.* **67,** 1365–1372
36. Gaudin, Y., Tuffereau, C., Durrer, P., Brunner, J., Flamand, A., and Ruigrok, R. (1999) *Mol. Membr. Biol.* **16,** 21–31
37. Rafalski, M., Ortiz, A., Rockwell, A., van Ginkel, L. C., Lear, J. D., DeGrado, W. F., and Wilschut, J. (1991) *Biochemistry* **30,** 10211–10220
38. Nieva, J. L., Nir, S., Muga, A., Goni, F. M., and Wilschut, J. (1994) *Biochemistry* **33,** 3201–3209
39. Yang, J., Gabrys, C. M., and Weliky, D. P. (2001) *Biochemistry* **40,** 8126–8137
40. Saéz-Cirión, A., and Nieva, J. L. (2002) *Biochim. Biophys. Acta* **1564,** 57–65

2.1.2 Artigo 3

Interaction between dengue virus fusion peptide and lipid bilayers depends on peptide clustering

Fausto Stauffer, Manuel N. Melo, Fabiana A. Carneiro, Francisco J. R. Sousa, Maria A. Juliano, Ronaldo Mohana-Borges, Andrea T. Da Poian e Miguel A.R.B. Castanho

Aceito para publicação em 2007 no periódico

Molecular Membrane Biology

Molecular Membrane Biology, March–April 2008; 25(2): 1–11

informa healthcare

Interaction between dengue virus fusion peptide and lipid bilayers depends on peptide clustering

FAUSTO STAUFFER[1,2], MANUEL NUNO MELO[2], FABIANA A. CARNEIRO[1], FRANCISCO J. R. SOUSA[3], MARIA A. JULIANO[4], LUIZ JULIANO[4], RONALDO MOHANA-BORGES[3], ANDREA T. DA POIAN[1], & MIGUEL A. R. B. CASTANHO[2]

[1]*Instituto de Bioquímica Médica, Universidade Federal do Rio de Janeiro, Rio de Janeiro, Brazil,* [2]*Centro de Química e Bioquímica, Faculdade de Ciências da UL, Lisboa, Portugal,* [3]*Laboratório de Genômica Estrutural, Instituto de Biofísica Carlos Chagas Filho, Universidade Federal do Rio de Janeiro, Rio de Janeiro, Brazil and* [4]*Departamento de Biofísica, Escola Paulista de Medicina, UNIFESP, São Paulo, Brazil*

(Received 10 May 2007; and in revised form 5 July 2007)

Abstract

Dengue fever is one of the most widespread tropical diseases in the world. The disease is caused by a virus member of the *Flaviviridae* family, a group of enveloped positive sense single-stranded RNA virus. Dengue virus infection is mediated by virus glycoprotein E, which binds to the cell surface. After uptake by endocytosis, this protein induces the fusion between viral envelope and endosomal membrane at the acidic environment of the endosomal compartment. In this work, we evaluated by steady-state and time-resolved fluorescence spectroscopy the interaction between the peptide believed to be the dengue virus fusion peptide and large unilamellar vesicles, studying the extent of partition, fusion capacity and depth of insertion in membranes. The role of the bilayer composition (neutral and anionic phospholipids), ionic strength and pH of the medium were also studied. Our results indicate that dengue virus fusion peptide has a high affinity to vesicles composed of anionic lipids and that the interaction is mainly electrostatic. Both partition coefficient and fusion index are enhanced by negatively charged phospholipids. The location determined by differential fluorescence quenching using lipophilic probes demonstrated that the peptide is in an intermediate depth in the bilayers, in-between the bilayer core and its surface. Ultimately, these data provide novel insights on the interaction between dengue virus fusion peptide and its target membranes, namely, the role of oligomerization and specific types of membranes.

Keywords: *Dengue virus fusion peptide, oligomerization, partition, membrane fusion, lipid membrane*

Introduction

Membrane fusion is the central molecular event during the entry of enveloped viruses into cells. The critical agents of this process are viral surface proteins, primed to facilitate bilayer fusion and triggered to do so by the conditions of viral interaction with the target cell. Dengue virus, an enveloped virus, belongs to the *Flaviviridae* family, together with other pathogenic viruses such as Yellow Fever, Saint Louis, West Nile and Tick-Borne Encephalitis (TBE) [1]. The viral genomic material is composed of a positive sense single-stranded RNA molecule, which encodes a polyprotein that is processed co- and post-translationally by proteases into at least ten discrete products. Three of them are associated with the virions: the E (envelope), M (membrane), and C (capsid) proteins [1]. Dengue virus enters into a host cell when the E glycoprotein binds to a receptor [2] and undergoes conformational rearrangement due to the reduced pH of the endosomal medium.

In the mature virions, E protein forms dimers that lie on the viral membrane [3]. The determination of E protein structure at the postfusion conformation revealed that the dimers are converted to a trimers after the fusion, with the fusion peptide located at the tip of the trimer [4]. It has been proposed that the conversion from the dimers to the trimers is a two step process [5]. The first step is a reversible dissociation of the ectodomains, which is important to make the tip of domain-II (putative fusion peptide) accessible for the interactions with the target membrane and the second one is the irreversible

Correspondence: Miguel A. R. B. Castanho, Centro de Química e Bioquímica, Faculdade de Ciências da UL, Campo Grande, C8, 1749-016 Lisboa, Portugal. Tel: +351 21 7500931. Fax: +351 21 7500088. E-mail: castanho@fc.ul.pt

ISSN 0968-7688 print/ISSN 1464-5203 online
DOI: 10.1080/09687680701633091

trimerization. The self-associated proteins bear three'fusion loops' at the tip of the trimers to insert them into the host-cell membrane. After that, viral nucleocapsid can be released into the host cell cytoplasm.

The purpose of the present work is to study dengue virus fusion peptide in aqueous solution and its interaction with different membrane model systems. Steady-state and time-resolved fluorescence spectroscopy were used to obtain structural information and to evaluate the fundamental principles that govern DEN Fpep incorporation in the membrane model systems and its location in the phospholipid bilayer. Ultimately, these data provide novel insights on the mechanism of action of dengue virus fusion peptide, namely, the role of oligomerization and specific types of membranes.

Materials and methods

Buffer 10 mM MES, 20 mM Tris buffer, pH 5.5, was used throughout this study, unless otherwise stated.

Chemicals

POPC (1-palmitoyl-2-oleyl-*sn*-glycero-3-phosphocholine) and POPG (1-palmitoyl-2-oleyl-*sn*-glycero-3-[phosphor-rac-(1-glycerol)]) were purchased from Avanti Polar-Lipids (Alabaster, AL). Cholesterol was from Sigma (St. Louis, MO) and 5NS (5-doxyl-stearic acid) and 16NS (16-doxyl-stearic acid) were from Aldrich Chem. Co. (Milwaukee, WT). All other reagents were of analytical grade.

Peptides synthesis

The putative dengue virus fusion peptide (amino acid sequence between 98 and 112) and the peptide fragment of dengue E protein corresponding to the amino acid sequence between 88 and 123, KRFVCKHSMVDRGWGNGCGLFGKGGIVTCAMFTCKK (named DEN Fpep), which contains the putative fusion loop (underlined amino acids), were synthesized by solid phase with the substitution of the cysteine residues (92, 116 and 121) for serine residues. Fmoc methodology was used and all protected amino acids were purchased from Calbiochem–Novabiochem (San Diego, USA) or from Neosystem (Strasbourg, France). The syntheses were carried out in an automated bench-top simultaneous multiple solid-phase peptide synthesizer (PSSM 8 system from Shimadzu). The final deprotected peptides were purified by semipreparative HPLC using an Econosil C-18 column (10 μm, 22.5 × 250 mm) and a two-solvent system: (A) trifluoroacetic acid/H_2O (1:1000, v/v) and (B) trifluoroacetic acid/acetonitrile/H_2O (1:900:100, v/v/v). The column was eluted at a flow rate of 5 ml/min with a 10 or 30 to 50 or 60% gradient of solvent B over 30 or 45 min. Analytical HPLC was performed using a binary HPLC system from Shimadzu with a SPD-10AV Shimadzu UV/VIS detector, coupled to an Ultrasphere C-18 column (5 μm, 4.6 × 150 mm), which was eluted with solvent systems A1 (H_3PO_4/H_2O, 1:1000, v/v) and B1 (acetonitrile/H_2O/H_3PO_4, 900:100:1, v/v/v) at a flow rate of 1.7 ml/min and a 10–80% gradient of B1 over 15 min. The HPLC column eluted materials were monitored by their absorbance at 220 nm. The molecular mass and purity of synthesized peptides were checked by MALDI-TOF mass spectrometry (TofSpec-E, Micromass) and/or peptide sequencing using a protein sequencer PPSQ-23 (Shimadzu Tokyo, Japan).

Preparation of lipid vesicles

Large unilamellar vesicles (LUVs), with typical 100 nm diameter [6] were prepared by the extrusion method described elsewhere [7] and used as models of biological membranes.

Steady-state fluorescence studies

All fluorescence measurements were performed with a Fluorolog-3 Spectrofluorimeter from Jobin-Yvon/Horiba, and acquired with DataMax v2.20 software programmme. Samples were excited at 280 nm (unless stated otherwise) and emission spectra were collected from 300 to 450 nm and were blank corrected. All spectra were also corrected with the instrumental correction function. Excitation and emission slits with 4-nm bandpass were used for all measurements.

Time-resolved fluorescence studies

Fluorescence lifetimes acquisitions were monitored using the time-correlated single photon counting, TCSPC, technique with a 280-nm LED laser source (IBH, UK). Lifetimes were calculated from time-resolved fluorescence intensity decays using 10 Kcounts in the peak channel. Fluorescence intensity decay curves were deconvoluted with the instrument software package DAS6 (IBH, UK) and analyzed as a sum of three exponential terms. The mean average lifetime, $<\tau>$, is:

$$\langle\tau\rangle = \frac{\sum a_i \tau_i^2}{\sum a_i \tau_i} \quad (1)$$

where a_i is the pre-exponential factor and τ_i is the fluorescence lifetime of each i component [8].The

goodness of the fit was judged from the global chi-square value and weighted residuals distribution.

Extent of partition in LUV

The extent and kinetics of partition assays of DEN Fpep (18 uM) were carried out with LUVs of POPC, POPC:POPG (4:1) and POPC:cholesterol (18, 25 and 33% molar of cholesterol). Titrations of DEN Fpep with lipidic suspensions (up to 4.5 mM) were used to evaluate the extent of partition. Samples were incubated for 10 min after each addition of lipid suspension. The partition coefficient, K_p, is calculated from the experimental data fitting with equation 2 as described elsewhere [9], unless critical concentration-dependent phenomena is observed at low global lipid:peptide ratios in the samples [10].

$$\frac{I}{I_W} = \frac{1 + K_p \gamma_L \frac{I_L}{I_W}[L]}{1 + K_p \gamma_L [L]} \qquad (2)$$

where I_W and I_L are the fluorescence intensities in aqueous solution and in lipid solution, respectively, γ_L is the molar volume of lipid, and [L] is the lipidic concentration [9]. (γ_L used was 7.63×10^{-1} $dm^3 .mol^{-1}$ for vesicles containing POPC [11].

Determination of extent of partition when concentration-dependent phenomena occur

Titration curves of 9, 18 and 36 μM DEN Fpep were carried out with LUVs of POPC:POPG (4:1). Critical points were taken as the maximum value in each curve and were used to determine the K_p from the experimental data fitting with equation 3 as described by [10]. This equation describes the dependence of peptide concentration at which a critical point occurs as a linear function of the phospholipid concentration in the system at that point.

$$[P] = \frac{\sigma}{K_p \gamma_L} + \sigma [L] \qquad (3)$$

where σ is the constant local P:L proportion in a saturated membrane, γ_L is the molar volume of lipid, [L] is the lipid concentration, and [P] is the peptide concentration at the saturation point when the lipid concentration is [L]. γ_L used was 7.63×10^{-1} dm^3 $.mol^{-1}$ for vesicles containing POPC [11].

Location in lipidic membranes

Quenching assays were followed by fluorescence intensity and lifetime with excitation at 280 nm and emission at 340 nm unless stated otherwise. Fluorescence quenching by acrylamide was carried out using wavelength $\lambda_{exc} = 290$ nm to minimize the relative quencher/fluorophore light absorption ratio. Nevertheless, the quenching data were corrected for the simultaneous light absorption of fluorophore and quencher [12]. Quenching assays data were analyzed by the Stern–Volmer equation (Equation 4),

$$\frac{I_0}{I} = 1 + K_{SV}[Q] \qquad (4)$$

where I and I_0 are the fluorescence intensity or lifetime of the sample in the presence and absence of quencher, respectively, K_{SV} is the Stern–Volmer constant, and [Q] the concentration of quencher [8,13].

Acrylamide is unable to efficiently quench the fluorescence of Trp residues deeply buried in the bilayer; titration of peptide in the presence of LUVs with this quencher gives initial insight on peptide in-depth location [14]. Fluorescence emission quenching ($\lambda_{exc} = 290$ nm, $\lambda_{em} = 340$ nm) with acrylamide was carried out with LUVs composed of POPC: POPG (4:1), both below (0.77 mM lipid in buffer) and above (3.5 mM lipid in buffer) the critical global lipid:peptide ratio in the sample.

To further evaluate the membrane in-depth location of the DEN Fpep Trp residue, differential quenching methodologies were used. 5NS and 16NS are quenchers of Trp fluorescence, which have different locations in the lipidic bilayer. 5NS is located near the interface whereas 16NS buries more deeply into the bilayer core [15]. Titration of peptide samples (18 μM), in the presence of LUVs composed of POPC:POPG (4:1), both below (0.77 mM lipid in buffer) and above (3.5 mM lipid in buffer) the critical global lipid:peptide ratio in the sample, was carried out with small aliquots of ethanolic solution of 5NS and 16NS (70 mM stock); final ethanol concentration was kept below 2%). The assays were followed by fluorescence emission intensity ($\lambda_{exc} = 280$ nm, $\lambda_{em} = 340$ nm). Data were corrected for simultaneous absorption of fluorophore and quencher [12]. The effective quencher concentration in the lipidic bilayer matrix, $[Q]_L$, was used in the Stern–Volmer plots (equation 5);

$$[Q]_L \approx \frac{K_{p,q}[Q]_T}{1 + K_{p,q} Y_L [L]} \qquad \gamma_L [L] << 1 \qquad (5)$$

where $[Q]_T$ is the quencher concentration in total sample volume and $K_{p,q}$ is the quencher partition coefficient [16]. For gel phase vesicles, $K_{p,Q}$ equals 12570 and 3340 for 5 NS and 16 NS, respectively. In crystal-liquid-like phase, the values used for 5 NS and 16 NS were 89000 and 9730, respectively [17].

Membrane fusion induced by Dengue virus fusion peptide

Fusion was tracked using the Forster's resonance energy transfer (FRET)-based methodology [18–20]. Briefly, vesicles doped with both 1% N-NBD-PE (donor) and 1% N-Rh-PE (acceptor) and unlabeled vesicles were mixed; after that, 18 μM of the peptides was added. If fusion between unlabeled vesicles and donor/acceptor-labeled vesicles occurs, the average distance between donors and acceptors increases, that is, FRET efficiency decreases. POPC, POPC:POPI (4:1), POPC:POPS (4:1) and POPC:POPG (4:1) were used, both below (0.77 mM lipid in buffer) and above (3.5 mM lipid in buffer) the critical global lipid:peptide ratio in the sample. Fluorescence intensity was followed with $\lambda_{exc} = 470$ nm (NBD absorption) and $\lambda_{em} = 590$ nm (Rh emission). Control experiments (peptide absence for spontaneous background fusion and 0.2% triton X-100 for total fusion) were carried out in all cases.

Results

Amino acid sequence alignment of E proteins indicates 62–77% homology among the four dengue virus serotypes and 40–50% homology among the different flaviviruses. The segment between residues 98 and 110 of E glycoprotein forms a loop in domain II of dengue E glycoprotein [5] and has been considered to be the fusion peptide of the flaviviruses because:(i) it presents a very high homology among all the members of the *Flaviviridae* family (it is identical in all of them, except for a single residue in the TBE virus), and (ii) site-directed mutagenesis in that region prevents the virus fusion (Allison et al. 2001). However, when we tested the fusion activity of a synthetic peptide corresponding to this segment, a very low peptide-induced fusion was obtained (Figure 1A). This occurred probably because this putative fusion peptide has only 13 residues and, therefore, it is very flexible to maintain the active structure. Thus, to stabilize the fusion peptide loop we decided to flank each side of the sequence with amino acids forming part of the β-strand structure, according to the crystallographic data [5]. The larger peptide was much more efficient in promoting fusion (Figure 1A), and so it was used throughout this study referred as DEN Fpep (Figure 1B).

Photophysical characterization of DEN Fpep interaction with membrane model systems

The interaction of DEN Fpep with LUV was followed by the changes in several spectroscopic parameters of Trp residues, namely, fluorescence intensity, fluorescence spectral shifts, and fluorescence lifetime. A significant blue-shift is observed in the emission spectra of the DEN Fpep in the presence of phospholipids vesicles (Figure 2A). The effect is more pronounced for vesicles containing negatively charged phospholipids. This spectral shift is known to be due to the incorporation of Trp residues in a more hydrophobic environment. This result is supported by the fluorescence quenching experiments using the hydrophilic quencher acrylamide (Figure 2B). These experiments were carried out with 18 μM peptide in aqueous solution and in the presence of 0.77 or 3.45 mM POPC:POPG

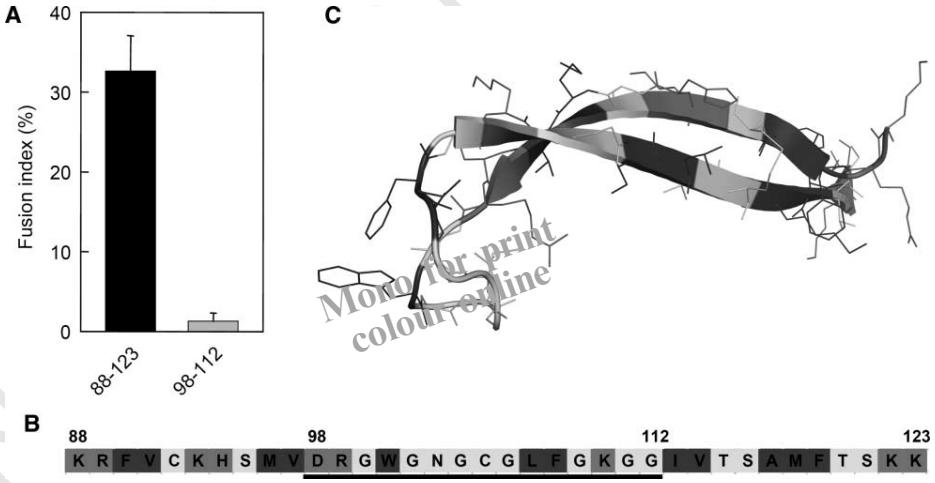

Figure 1. Fusion activity (A) and amino acid sequence (B) of two peptides fragments of dengue E glycoprotein corresponding to the putative fusion peptide alone (amino acids between 98 and 112, underlined in B) or with part of two flanking β-strands, named DEN Fpep (amino acids between 88 and 123). DEN Fpep arrangement as it appears in the structure of E glycoprotein (C) solved by Modis et al. [5]. Hydrophobic (blue), non-charged polar (green) and charged polar (red) residues are represented. This figure is reproduced in colour in *Molecular Membrane Biology* online.

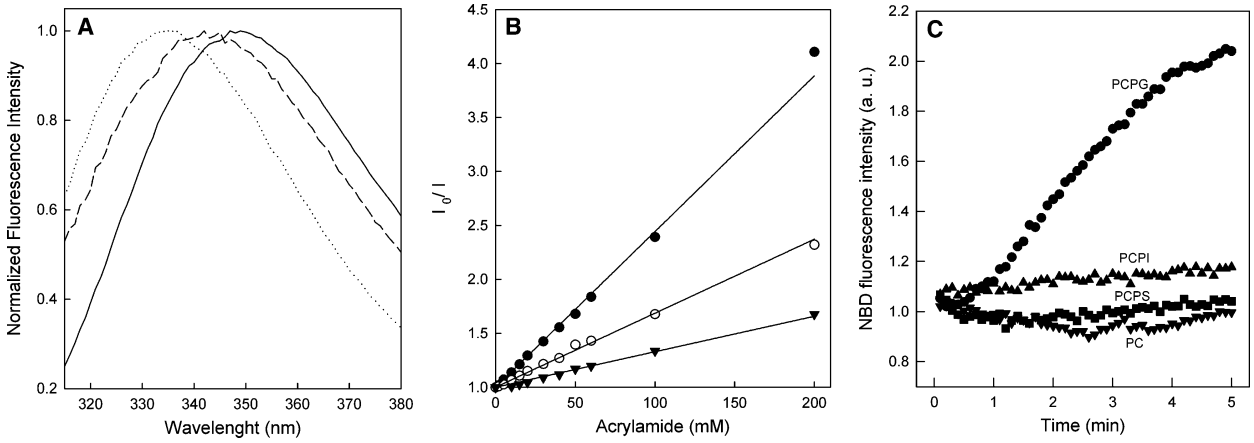

Figure 2. Interaction of DEN Fpep with LUVs. (A) Normalized fluorescence emission spectra of DEN Fpep in buffer pH 5.5 (black solid line) or in the presence of 3.45 mM LUVs of POPC:POPG (4:1) (dotted line) or POPC (long dashes). (B) Quenching of fluorescence emission of fusion peptide by acrylamide in aqueous solution (closed circle), in the presence of 0.77 (open circle) or 3.45 mM (closed triangle) POPC:POPG 4:1 (LUVs). (C) LUV fusion induced by DEN virus fusion peptide. Fusion reaction was tracked using the Forster resonance energy transfer-based methodology described elsewhere. We used 0.77mM POPC:POPG (4:1) (closed circle), POPC:POPI (4:1) (closed up triangle), POPC:POPS (4:1) (closed square) and POPC 100% (closed down triangle) unlabeled vesicles or labeled with N-NBD-PE and N-Rh-PE. The final peptide concentration was 18 mM in 20 mM MES, 30 mM Tris buffer, pH 5.5.

(4:1) LUVs. Results from the linear Stern–Volmer plots showed lower K_{SV} values in the presence of lipids than in aqueous solution, meaning that the fluorescence emission of DEN Fpep Trp in the presence of LUVs is not so efficiently quenched by acrylamide. Thus, the Trp residue is at least partially inserted in the lipid bilayer.

POPC:POPG was chosen as the anionic phospholipid-containing liposomes because peptide-induced fusion activity was evident only when this anionic vesicles were used (Figure 2C), although the peptide was able to interact with other liposomes systems tested (as followed by the blue shift in Trp fluorescence spectra).

Upon the partitioning of DEN Fpep to vesicles (Figure 3A), there was a decrease in fluorescence intensity for the neutral POPC LUV, with or without cholesterol. For the anionic system, the fluorescence intensity of DEN Fpep initially increases until reaching a maximum at about 1 mM lipid concentration. Then, a decrease at higher lipid concentrations occurs (Figure 3A; closed squares). On the other hand, average fluorescence excited state lifetime, $<\tau>$, shows a regular increase (Figure 3A;

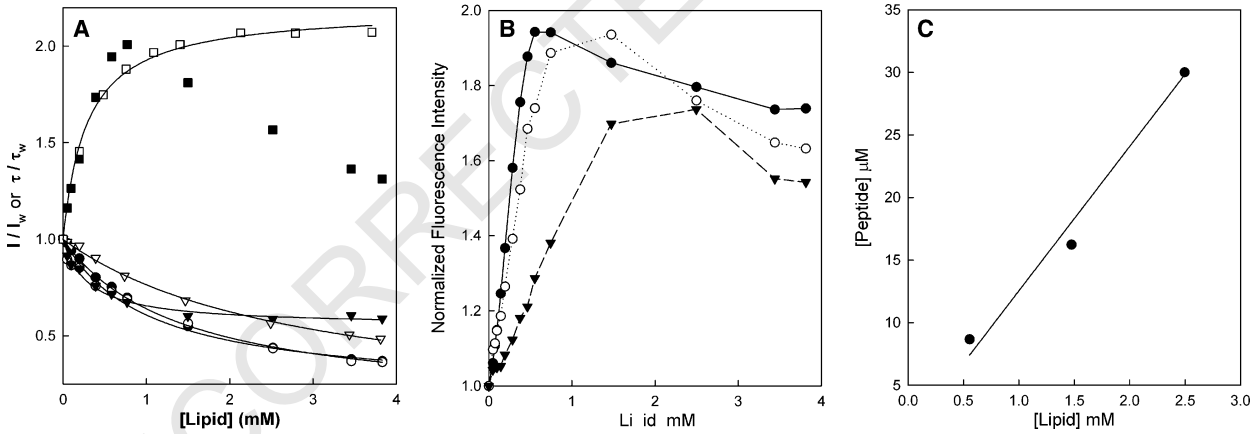

Figure 3. Partition of DEN Fpep into LUVs (A) and extent of partition into POPC:POPG LUVs (B and C). (A) Fluorescence emission intensity of DEN Fpep normalized to [L] = 0 (I/Iw) upon titration with LUVs of POPC (open triangles), POPC:POPG (4:1) (filled squares), or POPC:Cholesterol 18% (filled triangle), 25% (open circle) and 33% (filled circle) – Equation 2 was used to fit the data. Fluorescence lifetimes upon titration with LUVs of POPC:POPG (4:1) are shown in open squares.(B) Fluorescence emission intensity of DEN Fpep at concentration of 9 (closed circle), 18 (open circle) and 36 mM (closed triangle) DEN Fpep normalized to [L] = 0 (I/Iw) upon titration with LUVs of POPC:POPG (4:1) in 20 mM MES, 30 mM Tris buffer, pH 5.5. (C) Linear relationship between [peptide] and [lipid] at the critical point. Total peptide and phospholipid concentrations at critical points for the POPG:POPC system, together with the corresponding fitting by Equation 3 (solid lines). Saturation points were obtained from the partition curves at different peptide concentrations (Figure 3B).

open squares). Lifetimes gradually increase upon POPG-containing vesicles addition, even after overcoming 1 mM lipid concentration. $<\tau>$ for other LUV compositions (POPC, POPC with cholesterol) were determined with no significant changes compared to DEN Fpep in aqueous buffer (data not show).

The fluorescence intensity recorded in the titration of aqueous suspensions of the DEN Fpep (18 μM) with lipid vesicles of different lipid mixtures (Figure 3A) was used to calculate the partition coefficient (Table I) by fitting the data with equation 2. In case of anionic lipid system, application use is not possible due to the concentration-dependent critical phenomena occurring at about 1 mM lipid; equation 3 was used instead. This equation results from a model in which two regimes are considered [10]: (1) a 'saturation' regime, at high global peptide:lipid ratios in the sample, where the local concentration of the peptide in the membrane is constant and not dependent on the concentration of the peptide in the aqueous phase (the constant parameter that describes the system is the local membrane peptide:-lipid ratio, σ), and (2) an 'excess lipid' regime, at high global lipid: peptide ratios in the sample, where the system is described by the constant Nernst-like partition coefficient, $K_p = [\text{peptide}]_L/[\text{peptide}]_W$ [9]; $[\text{peptide}]_L$ and $[\text{peptide}]_W$ are the peptide concentrations in the local lipidic and 'bulk' aqueous environment, respectively. The critical points in the curves represent the exact condition where both σ and K_p are valid to describe the system, i.e., the exact condition where the local concentration of the peptide in the membrane and in aqueous phase are predicted by σ and K_p simultaneously. Critical points are the border lines between both regimes.

Table I. Partition constants for different lipid compositions.

Vesicle composition	Kρ (× 10^{-3})	σ	Equation used
POPC	0.4	–	2
POPC:Cholesterol (2:1)	0.5	–	2
POPC:POPG (4:1)**	8.7	0.011	3

The critical points (Figure 3C) were obtained from the partition curves with different peptide concentrations (Figure 3B) and were fitted using Equation 3. The σ value of 0.011 means a local concentration in the membrane of ~90 lipids per peptide. This value is quite large and very different from those values obtained with antimicrobial peptides and cannot be assigned to spatial saturation of the membrane surface or charge equivalence (18 negatively charged lipids per peptide inserted in the membrane). The results are indicative of oligomerization driven by the high local concentration of the peptide in the membrane but not strictly motivated by saturation phenomena.

In order to investigate the role of electrostatic interactions on the partition of DEN Fpep to vesicles, the effect of high ionic strength on its interaction with POPC:POPG vesicles was evaluated. Titration of aqueous suspensions of the DEN Fpep (18 μM) in the presence of 200 mM NaCl with lipidic vesicles was carried out (Figure 4A). At this salt concentration, the increase of fluorescence intensity at lower peptide/lipid ratios was abolished. In addition, we studied the partition curves at low (5.5) and slightly alkaline (8.0) pH. The contour of the curve is the same at both pH, but the maximum fluorescence intensity is higher at pH 5.5 (Figure 4B).

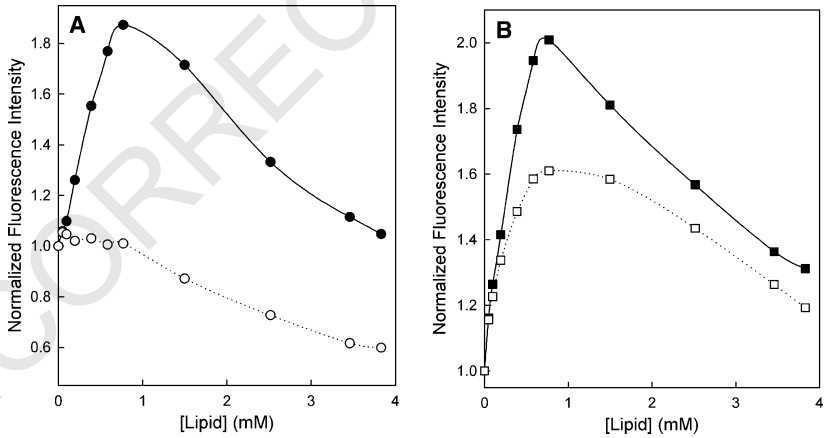

Figure 4. Effect of high ionic strength and pH on DEN Fpep partition into lipidic vesicles. Fluorescence emission intensity of DEN Fpep normalized to [L] = 0 (I/I_w) upon titration with LUVs of POPC:POPG (4:1): (A) in the presence of low (filled circles; no added NaCl) and high (200 mM NaCl, open circles) ionic strength; (B) at pH 5.5 (filled square) and pH 8.0 (open square). The final peptide concentration was 18 μM in 20 mM MES, 30 mM Tris buffer. 200 mM NaCl (A) leads to an intermediate situation, between the one obtained with POPC and POPC:POPG 4:1 without NaCl.

DEN Fpep location in the lipid bilayer

The previous results obtained from fluorescence quenching experiments using the hydrophilic quencher acrylamide (Figure 2B) showed that the Trp residue is at least partially located inside the lipid bilayer. To further evaluate the in-depth location of the DEN Fpep Trp residue when it is interacting with the POPC:POPG vesicles, fluorescence quenching by the lipophilic probes 5NS and 16NS was used. These two derivatized fatty acids differ in the position of the quencher moiety (doxyl) in the hydrocarbon chain. They are used to evaluate the depth of the fluorophore in the membrane, by comparing the quenching results obtained with each of them. The closer the Trp residues are to the quencher group, the more efficient quenching is. Thus, 5NS probes the bilayer interface whereas 16NS probes its core. Initial experiments using steady-state fluorescence intensities showed a pronounced static quenching between the fluorophore and the quencher. This prompted us to use the parallax method [21] to find the depth of the Trp residues in the membranes. The quenching experiments were performed with fixed concentrations of peptide and lipid (0.77 or 3.45 mM), and increasing concentration of quencher. The Stern-Volmer plots with the effective local concentration of 5NS and 16NS in the lipid bilayers are presented in Figure 5A and 5B.

DEN Fpep induced vesicle fusion

Vesicle fusion implies that (1) the inner content of two or more vesicles is mixed and (2) lipids from previously separated bilayers coexist in the same bilayer after fusion [22]. Fusion may result from a variety of stimuli. The FRET-based methodology described elsewhere was used to study vesicle fusion [18–20]. The results obtained in the saturated and non-saturated conditions are presented in Figure 6. Fusion is more efficient using a high [peptide]/[lipid] ratio (membrane 'saturation' range).

Discussion

Interaction with membrane model systems

The different fluorescence spectroscopy methodologies clearly show that DEN Fpep is incorporated into the membrane model systems studied, independently of the phospholipids composition. However, there is more extensive peptide incorporation in LUV containing negatively charged phospholipids. Besides, there is more pronounced blue-shift of the emission spectra of DEN Fpep in the presence of vesicles containing POPG (negatively charged phospholipid headgroup) (Figure 2A). Moreover, the partition coefficients are approximately 18 fold larger when negatively charged vesicles are present (Table I). In this situation, partition is influenced by ionic strength and pH (Figure 4), due to the positive net formal charge of the peptide at neutral pH (eight positively and only one negatively charged residues) (Figure 1B). The use of POPG increases the electrostatic component of the peptide partition constant and might stabilize its structure upon membrane incorporation [23]. Although the negatively-charged phospholipids are usually segregated in the inner side of the cellular membranes, cell surface contains many other negatively-charged molecules, as, for example, the heparan sulfate (HS). HS, the most ubiquitous member of the glycosaminoglycans (GAGs), is used by many viruses to bind to target cells [24–26], including the dengue virus. Studies have shown that dengue

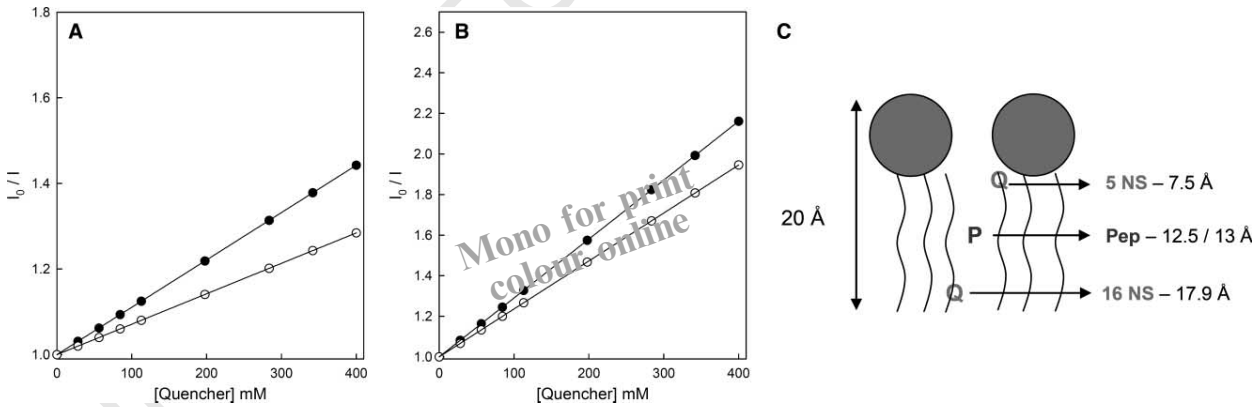

Figure 5. In-depth location of DEN Fpep in LUVs using Stern-Volmer Plots. Quenching by the derivatized lipophilic molecules 5NS (closed circles) and 16NS (open circles) in the presence of 0.77 mM (A) or 3.45 mM (B) POPC:POPG (4:1) vesicles. (C) Schematic representation of DEN fusion peptide location in membranes, using Parallax method [21]. P represents the location of fusion peptide Trp in the external monolayer. The final peptide concentration was 18 μM in 20 mM MES, 30 mM Tris buffer. This figure is reproduced in colour in *Molecular Membrane Biology* online.

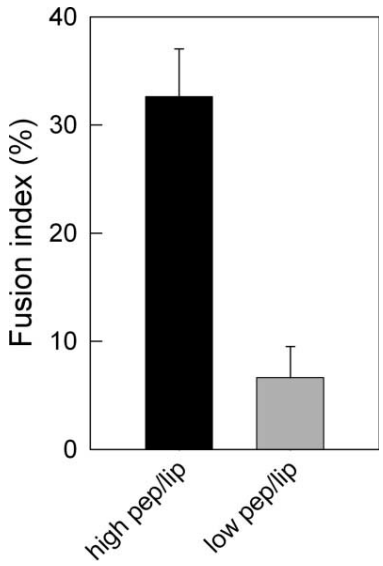

Figure 6. LUV fusion induced by DEN virus fusion peptide. Fusion reaction was tracked using the Forster resonance energy transfer-based methodology described elsewhere. We used POPC:POPG (4:1) unlabeled vesicles or labeled with N-NBD-PE and N-Rh-PE, in the 'saturated' (high pep/lip) or non-saturated (low pep/lip) condition. The process was initiated by addition of the peptide and the FRET efficiency was accompanied for 10 min. The fusion index of 100% was calculated by adding 0.2% Triton final concentration. The final peptide concentration was 18 uM peptide in 10 mM MES, 20 mM TRIS buffer, pH 5.5.

glycoprotein bound to highly sulfated GAGs on the surface of Vero cells and that infection of these cells could be prevented by heparin and by high-sulfate HS [27]. This negatively-charged GAG might act directly as a receptor or help to concentrate these viruses on the cell surface, facilitating the interaction with the specific high-affinity receptors. Thus, the presence of negative phospholipids might be mimicking these molecules, being important for enhancing the interaction between the peptide and membranes.

Electrostaic interaction with the inner side of the cellular membrane surface cannot be discarded. Crystallographic data obtained with the dengue virus fusion protein [5] show that clustered fusion loops form a nonpolar apex with a hydrophobic core, suggested to penetrate the hydrophobic region of the lipid bilayers. The fluid and dynamic nature of the cell membrane, favours interaction of the fusion peptide with the inner layer of (negatively) charged lipids. Once the lipid bilayer structure is perturbed due to the challenge imposed by the charged peptide at its surface, it is possible that the peptide comes in direct contact with the inner layer of lipids. This interaction has been the subject of intense study and is quite well demonstrated for other classes of membrane-active peptides, such as antimicrobial and cell-penetrating peptides [28,29]. Fusion peptides are short hydrophobic but frequently cationic sequences, which are characteristics found in most membrane-active peptides. Upon contact of this kind of peptides with one surface of the lipid bilayer, a local charge and concentration gradient is created. These gradients may be driving forces for lipid flip-flop and/or peptide. Gibbons et al. [30] showed for the Semliki Forest virus that the glycine-rich main chain interacts tightly with the lipid heads, projecting aromatic side chains into the aliphatic region of the lipid bilayer. Therefore, perturbation of the bilayer may reach its core and extend to the other leaflet through electrostatic interactions.

Combined analysis of steady state and time resolved fluorescence partition curves indicate that partition into vesicles without negatively charged phospholipids induces a static intramolecular (conformational) quenching of DEN Fpep, whereas POPG-containing vesicles cause an increase on fluorescence intensity first (lipid up to 1 mM) and a pronounced static intramolecular quenching afterwards. This data suggest that there is probably a great peptide conformational flexibility that may be facilitated by the high content of glycines. Other fusion peptides, such as avian sarcoma leukosis virus [31] and influenza virus [32] fusion peptides, reveal similar conformational flexibility that is critical for membrane fusion [33]. For Semliki Forest Virus, the fusion loops show considerable plasticity and is a gly-rich flexible sequence [30]. Moreover, fusion loop clustering modulates interaction with lipid bilayers, which is in agreement with our findings (see end of this section).

It is noteworthy the saturation-like phenomenon (Figure 3) that usually occurs when the interaction with lipids is very strong, like those between antimicrobial peptide and membranes [10], for instance. In a titration of DEN Fpep with vesicles, at low lipid concentrations, the incorporation of peptide into the vesicles containing POPG seems to be regulated by the constant lipid:peptide ratio, since a linear relationship between fluorescence intensity and lipid concentration was observed at low lipid concentrations. The overall titration curve is not hyperbolic-like, in contrast to expectation from simple partition without membrane saturation [9]. After the maximal fluorescence intensity critical point, which was dependent on the peptide concentration, a non-linear relationship resulted. This new regime is assigned to far-from-saturating conditions due to the increased lipid concentration. In this regime, partition is regulated by K_p. Membrane saturation may occur at low lipid concentrations and high K_p values. Combination of both conditions leads to membrane saturation because the bound peptide concentration hypothetically dictated by K_p

is higher than what the membrane can accommodate. In the case of DEN Fpep, however, a membrane saturation due to complete crowding of the membrane or peptide:lipid charge equivalence in the membrane surface is not compatible with a local 90 lipid:peptide ratio in the membrane containing 20% anionic lipid. Oligomerization precedes complete saturation, triggering a conformational change that improves membranetropism (see below).

Localization in the membrane

Fluorescence quenching data showed that the DEN Fpep is equally quenched (similar K_{SV} values) by the doxyl group in 5NS and in 16NS (Figure 5A and 5B), independently of the peptide:phospholipid ratio. Thus, it can be reasoned that the fluorophore is located in an intermediate depth of the hemilayer, in between the positions 5 and 16 of the acyl chains. The quenching data was used for the measurement of the depth of insertion of the Trp side chain by PARALAX method developed by [21], indicating that the Trp is located approximately 12.5Å from membrane surface (Figure 5C).

Membrane fusion induced by DEN Fpep

During dengue virus infection, the pH induced membrane fusion is a crucial step for the viral RNA evasion from the endosome into the cytoplasm. This process is catalyzed by E glycoprotein, more specifically its fusion peptide. In this study, fusion induced by DEN Fpep was more efficient using anionic phospholipids (POPG) and a high macroscopic peptide:lipid ratio (Figure 6). Anionic lipids may not have a direct role in fusion. POPG interference with fusion may result from enhanced partition into the membrane as showed in Table I. The fusion index is greater in the saturated-like membrane concentration range, indicating that self-associated fusion peptides are more membranotropic. This may help to explain why fusion occurs with oligomerized E protein. At the local microscopic level, at the point of insertion of the fusion peptides during fusion, a high peptide:lipid ratio is created, similar to the one that occurs in nearly saturated membranes. It is worth mentioning that, at high local peptide concentration in the membrane, the depth of the peptide in the lipid bilayers does not change significantly. Peptide-peptide interaction (such as forced by crowding effects in vesicles or protein oligomerization during virus-cell fusion) probably triggers conformational changes responsible for distinct photophysical parameters (e.g., fluorescence quantum yield).

Conclusion

DEN Fpep is the putative fusion peptide in the middle of two beta sheets (Figure 1). In this work, we used fluorescence spectroscopy-based methodologies to study the interaction of the peptide with

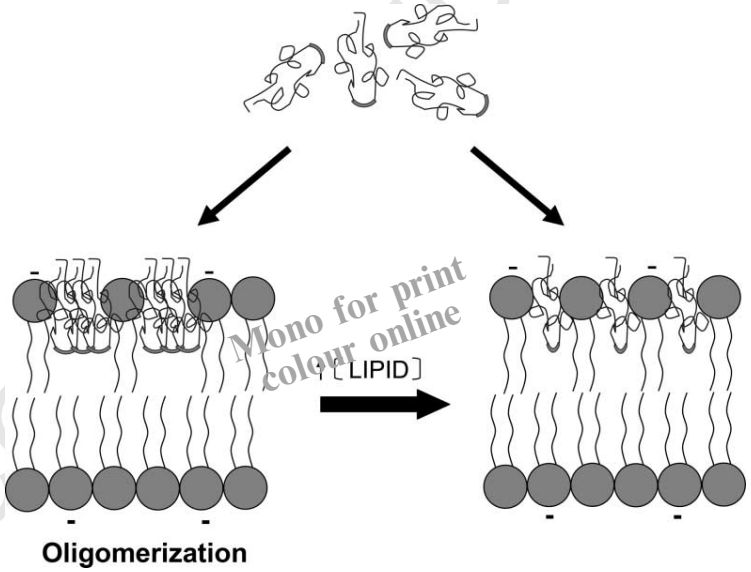

Figure 7. Schematic representation of the proposed mechanism of interaction between DEN Fpep and lipidic vesicles. DEN Fpep clearly interacts more extensively with anionic lipid containing vesicles. The mechanism of interaction depends on the macroscopic peptide:lipid ratio in the sample. At high ratio, oligomerization occurs due to quasi-complete crowding and is buried in an intermediate position of the outer hemilayer, in a compact (closely packed) conformation. Upon addition of lipid, at low peptide:lipid ratio, the peptide suffers a conformational change, probably small, leading to static quenching of Trp fluorescence, without changing its in-depth location. This figure is reproduced in colour in *Molecular Membrane Biology* online.

model membranes. Analysis of our results shows: (i) the peptide interacts with model membranes, independently of its lipid composition, as supported by changes in fluorescence intensity and blue shifts occurring upon addition of vesicles, but the presence of anionic lipids leads to a more extensive partition; (ii) partition curves with vesicles containing negatively charged phospholipids show that the fluorescence intensity reaches a maximum at $\sim$1 mM of lipids, followed by a progressive decrease, which is not accompanied by lifetimes. Lifetimes reach a plateau. This suggests that the interaction depends on the global peptide:lipid ratio in the sample. Moreover, that result indirectly suggests that the peptide undergoes structural changes, probably small, dependent of that ratio, leading to a static quenching of Trp fluorescence; (iii) quenching studies indicate that the DEN Fpep Trp residue is buried in the middle of the outer hemilayer, independently of the peptide:lipid ratio (5NS and 16NS have similar quenching efficiency); (iv) DEN Fpep is able to induce membrane fusion, but the process is more efficient using vesicles containing anionic lipids and at high macroscopic peptide:lipid ratio.

Based on the data described above, one can hypothesize in general terms what might be the mechanism of interaction between DEN Fpep and membranes at the molecular level. As depicted in Figure 7, the interaction depends on the global peptide:lipid ratio in the sample. At high ratio, it is possible to detect oligomerization. Until a certain critical ratio, oligomerized peptides will be buried in an intermediate depth in the outer hemilayer in a conformation constrained by packing. This stage of interaction only occurs with vesicles containing anionic phospholipids, since quasi-saturation results from the high affinity between the peptide and the lipid. Upon addition of excess lipid, at low peptide: lipid ratios, the peptide is conformationally unrestricted because crowding disappears and undergoes structural changes, probably small, without changing its in-depth location. The oligomerized, quasi-saturated situation seems to be a suitable model for studying the interaction of viral particles and cell membranes. The micro-environment composed of the cell membrane phospholipids and the viral surface proteins has a high local peptide:lipid ratio. We believe this may be the reason behind protein E oligomerization for viral fusion, the fusion peptides forming the tip of a trimer. Our results indicate that membrane fusion is more efficient in this situation. Moreover, a preferential interaction of the fusion peptides of the E protein with anionic lipids may drive the depth of insertion further to the interior of the membrane, closer to the negatively charged inner (cytoplasmatic) lipid hemilayer, which further perturbs membranes and favors fusion.

Altogether, these data provide novel insights on the mechanism of dengue virus fusion peptide, namely the frequently overlooked role of viral proteins oligomerization.

Acknowledgements

We thank Sónia Troeira Henriques from Lisbon University (Portugal) for valuable help.

This work was supported by grants from Conselho Nacional de Desenvolvimento Científico e Tecnológico (CNPq), Fundação Carlos Chagas Filho de Amparo à Pesquisa do Estado do Rio de Janeiro (FAPERJ), Fundação de Amparo à Pesquisa do Estado de São Paulo (FAPESP), Coordenação de Aperfeiçoamento de Pessoal de Nível Superior (CAPES), Gabinete de Relações Internacionais da Ciência e do Ensino Superior (GRICES), Special Programme for Research and Training in Tropical Diseases (TDR) of World health Organization (WHO), Third World Academy of Sciences (TWAS) and Fundação para a Ciência e Tecnologia (Portugal), including a grant to M. Melo (SFRH/BD/24778/2005). F. Stauffer was recipient of a fellowship from CAPES (BEX 1279/05).

References

[1] Lindenbach BD, Rice CM. 2001. Flaviviridae: The viruses and their replication. In: Fields BN, Howley PM, Griffin DE, Lamb RA, Martin MA, Roizman B, Straus SE, Knipe DM, editors. Fields' virology, 4th ed. Philadelphia: Lippincott Williams & Wilkins. p. 991–1041.

[2] Crill WD, Roehrig JT. 2001. Monoclonal antibodies that bind to domain III of dengue virus E glycoprotein are the most efficient blockers of virus adsorption to Vero cells. J Virol 75:7769–7773.

[3] Kuhn RJ, Zhang W, Rossmann MG, Pletnev SV, Corver J, Lenches E, Jones CT, Mukhopadhyay S, Chipman PR, Strauss EG, Baker TS, Strauss JH. 2002. Structure of dengue virus: implications for flavivirus organization, maturation, and fusion. Cell 108:717–725.

[4] Modis Y, Ogata S, Clements D, Harrison SC. 2003. A ligand-binding pocket in the dengue virus envelope glycoprotein. Proc Natl Acad Sci USA 100:6986–6991.

[5] Modis Y, Ogata S, Clements D, Harrison SC. 2004. Structure of the dengue virus envelope protein after membrane fusion. Nature 427:313–319.

[6] Wieprecht T, Beyermann M, Seelig J. 2002. Thermodynamics of the coil-alpha-helix transition of amphipathic peptides in a membrane environment: the role of vesicle curvature. Biophys Chem 96:191–201.

[7] Mayer LD, Hope MJ, Cullis PR. 1986. Vesicles of variable sizes produced by a rapid extrusion procedure. Biochim Biophys Acta 858:161–168.

[8] Lakowicz JR, editor. 1999. Principles of fluorescence spectroscopy. 2nd ed. New York: Kluwer Academic/Plenum. 725 pp.

[9] Santos NC, Prieto M, Castanho MA. 2003. Quantifying molecular partition into model systems of biomembranes: an

emphasis on optical spectroscopic methods. Biochim Biophys Acta 1612:123–135.

AQ2 [10] Melo MN, Castanho MARB. 2007. Omiganan interaction with bacterial membranes and cell wall models. Assigning a biological role to saturation. Biochim Biophys Acta DOI:10.1016/j.bbamem.2007.02.005.

[11] Chiu SW, Jakobsson E, Subramaniam S, Scott HL. 1999. Combined monte carlo and molecular dynamics simulation of fully hydrated dioleyl and palmitoyl-oleyl phosphatidylcholine lipid bilayers. Biophys J 77:2462–2469.

[12] Coutinho A, Prieto M. 1993. Ribonuclease T1 and alcohol dehydrogenase fluorescence quenching by acrylamide. J Chem Educ 70:425–428.

[13] Santos NC, Castanho MA. 2002. Fluorescence spectroscopy methodologies on the study of proteins and peptides. Trends Appl Spectrosc 4:113–125.

[14] Caputo GA, London E. 2003. Cumulative effects of amino acid substitutions and hydrophobic mismatch upon the transmembrane stability and conformation of hydrophobic alpha-helices. Biochemistry 42:3275–3285.

[15] Fernandes MX, Garcia de la Torre J, Castanho MA. 2002. Joint determination by Brownian dynamics and fluorescence quenching of the in-depth location profile of biomolecules in membranes. Anal Biochem 307:1–12.

[16] Santos NC, Prieto M, Castanho MA. 1998. Interaction of the major epitope region of HIV protein gp41 with membrane model systems. A fluorescence spectroscopy study. Biochemistry 37:8674–8682.

[17] Wardlaw JR, Sawyer WH, Ghiggino KP. 1987. Vertical fluctuations of phospholipid acyl chains in bilayers. FEBS Lett 223:20–24.

[18] Maier O, Oberle V, Hoekstra D. 2002. Fluorescent lipid probes: some properties and applications (a review). Chem Phys Lipids 116:3–18.

[19] Haugland RP, editor. 2002. Handbook of fluorescent probes and research products. 9th ed. New York: Molecular Probes.

[20] Pecheur EI, Martin I, Ruysschaert JM, Bienvenue A, Hoekstra D. 1998. Membrane fusion induced by 11-mer anionic and cationic peptides: a structure-function study. Biochemistry 37:2361–2371.

[21] Chattopadhyay A, London E. 1987. Parallax method for direct measurement of membrane penetration depth utilizing fluorescence quenching by spin-labeled phospholipids. Biochemistry 26:39–45.

[22] Basanez G. 2002. Membrane fusion: the process and its energy suppliers. Cell Mol Life Sci 59:1478–1490.

[23] Murray D, Arbuzova A, Honig B, McLaughlin S. 2002. The role of electrostatic and nonpolar interactions in the association of peripheral proteins with membranes. Curr Topics Membr 52:271–302.

[24] Feldman SA, Audet S, Beeler JA. 2000. The fusion glycoprotein of human respiratory syncytial virus facilitates virus attachment and infectivity via an interaction with cellular heparan sulfate. J Virol 74:6442–6447.

[25] Fry EE, Lea SM, Jackson T, Newman JW, Ellard FM, Blakemore WE, Abu-Ghazaleh R, Samuel A, King AM, Stuart DI. 1999. The structure and function of a foot-and-mouth disease virus-oligosaccharide receptor complex. Embo J 18:543–554.

[26] Shukla D, Liu J, Blaiklock P, Shworak NW, Bai X, Esko JD, Cohen GH, Eisenberg RJ, Rosenberg RD, Spear PG. 1999. A novel role for 3-O-sulfated heparan sulfate in herpes simplex virus 1 entry. Cell 99:13–22.

[27] Chen Y, Maguire T, Hileman RE, Fromm JR, Esko JD, Linhardt RJ, Marks RM. 1997. Dengue virus infectivity depends on envelope protein binding to target cell heparan sulfate. Nat Med 3:866–871.

[28] Ludtke S, He K, Huang H. 1995. Membrane thinning caused by magainin 2. Biochemistry 34:16764–16769.

[29] Magzoub M, Graslund A. 2004. Cell-penetrating peptides: small from inception to application. Q Rev Biophys 37: 147–195.

[30] Gibbons DL, Vaney MC, Roussel A, Vigouroux A, Reilly B, Lepault J, Kielian M, Rey FA. 2004. Conformational change and protein-protein interactions of the fusion protein of Semliki Forest virus. Nature 427:320–325.

[31] Cheng SF, Wu CW, Kantchev EA, Chang DK. 2004. Structure and membrane interaction of the internal fusion peptide of avian sarcoma leukosis virus. Eur J Biochem 271:4725–4736.

[32] Chang DK, Cheng SF, Deo Trivedi V, Yang SH. 2000. The amino-terminal region of the fusion peptide of influenza virus hemagglutinin HA2 inserts into sodium dodecyl sulfate micelle with residues 16–18 at the aqueous boundary at acidic pH. Oligomerization and the conformational flexibility. J Biol Chem 275:19150–19158.

[33] Pecheur EI, Sainte-Marie J, Bienven e A, Hoekstra D. 1999. Peptides and membrane fusion: towards an understanding of the molecular mechanism of protein-induced fusion. J Membr Biol 167:1–17.

2.2 Parte II

Descoberta de um novo composto inativador viral baseado na inibição de fusão de membranas e sua aplicação na formulação de uma vacina

A elucidação dos mecanismos moleculares envolvidos na reação de fusão de membranas catalisada pelas glicoproteínas virais pode contribuir para a decoberta de possíveis alvos para inibição da entrada dos vírus em suas células hospedeiras, auxiliando no desenvolvimento de novos antivirais e de vacinas.

Na parte II desta tese, tivemos como objetivo descobrir um novo composto inativador viral baseado em dados obtidos dos estudos básicos de elucidação do mecanismo de entrada dos vírus nas células, realizados na parte I. Todos os passos utilizados na caracterização da inativação viral baseada na inibição da fusão de membranas são resumidamente expostos a seguir. Os resultados completos se encontram apresentados na forma de artigos científicos (artigos 4 e 5).

Como citado na parte I dos resultados, nós descobrimos que o DEPC modifica especificamente os resíduos de histidina da proteína G do VSV, inibindo as mudanças conformacionais desta glicoproteína desencadeadas pelo pH ácido e consequentemente a fusão de membranas mediada pelo VSV (artigo 2). Isto nos indicou que provavelmente o tratamento viral com DEPC seria capaz de inativar o VSV. Para testar esta hipótese, fizemos experimentos em modelos celular e animal, mostrando que a modificação viral com DEPC abolia a infectividade e patogenicidade do VSV. Posteriormente, avaliamos por microscopia eletrônica e ELISA de competição que as regiões antigênicas da glicoproteína viral estavam preservadas. Estes resultados indicavam o potencial uso do DEPC na formulação de vacinas inativadas baseada na inibição da fusão de membranas. Esta foi a primeira vez que o DEPC foi utilizado como inativador viral, de forma que a partir dos resultados obtidos, depositamos uma patente no Instituto Nacional da Propriedade Industrial (INPI) em 2004 (patente 1). Os resultados foram posteriormente publicados no periódico *Antiviral Research* (artigo 4).

O próximo passo foi avaliar a imunogenicidade das partículas virais inativadas pelo DEPC em camundongos. Observamos que o animal imunizado por via intraperitoneal com três doses de VSV tratado com DEPC misturado com adjuvantes apresentava uma resposta humoral semelhante àquela induzida pelo vírus nativo. Os anticorpos gerados eram capazes de reconhecer e neutralizar o VSV não modificado, além de proteger de forma eficiente os animais do desafio com uma dose letal de vírus. Em suma, nossos dados sugerem que a inativação viral com DEPC pode ser utilizada para o desenvolvimento de vacinas. Estes dados compõem o artigo 5 desta tese, praticamente aceito para publicação no periódico *Vaccine.*

2.2.1 Patente 1

Composição para Inativação Viral, Processo de Inativação Viral, Vacina e Processo de Produção de Vacina

Fausto Stauffer, Joari M. de Miranda, Fabiana A. Carneiro, Gisele Machado e Andrea T. Da Poian

Depositada em 2004 no INPI

Publicada em 2005 na Revista da Propriedade Industrial

Relatório descritivo

Composição para Inativação Viral, Processo de Inativação Viral, Vacina e Processo de Produção de Vacina

Campo da Invenção

A presente invenção refere-se genericamente a uma composição para inativação viral, a um processo de inativação viral, a uma vacina contra o VSV e a um processo para a produção de vacina contra a VSV. Mais especificamente, refere-se a uma composição que inibe a infecção e a replicação viral, bem como o desenvolvimento da patologia estomatite vesicular em animais. A presente invenção refere-se adicionalmente a um processo de inativação viral através do contato do vírus da VSV com a substância DEPC. A inativação do VSV possibilita a obtenção de uma vacina contras as patologias causadas pelo mesmo.

Antecedentes da Invenção

A estomatite vesicular causada pelo VSV afeta bovinos, eqüinos e suínos, e suas manifestações clínicas incluem vesiculação e/ou ulceração severa na língua e nos tecidos orais, podendo, às vezes, provocar lesões nos pés e nas tetas dos animais acometidos, o que resulta em uma substancial perda de produtividade (Letchworth, G. J. *et al.* (1999) *Vet. J.* **157**, 239-260). Os sintomas desta doença são indistingüíveis daqueles observados na febre aftosa, exceto por afetar também eqüinos. A estomatite vesicular causada pelo VSV ocorre anualmente desde o sudeste dos Estados Unidos até o norte da América do Sul, passando pelo México e por toda a América Central. Nestas regiões, os sorotipos predominantes são VSV New Jersey (VSV-NJ) e VSV Indiana (VSV-IN). No Brasil, é endêmico o sorotipo Indiana 3, ou Alagoas (Federer, K. E. *et al.* (1967) *Res. Vet. Sci.* **8**, 103-117; Andrade, C. M. *et al.* (1980) *An. Microbiol. (Rio de Janeiro)* **25**, 81-87). Outros vesiculovírus são endêmicos na Índia e na África. Nos Estados Unidos os dois surtos mais recentes ocorreram em 1997 e 1998, afetando principalmente eqüinos (McCluskey, B. J. *et al.* (1999) *J. Am. Vet. Med.*

Assoc. **215**, 1259-1262). Em 1995, um grande surto atingiu rebanhos bovinos causando um impacto significativo na indústria de carne do Colorado (Bridges, V. E. *et al.* (1997) *J. Am. Vet. Med. Assoc.* **211**, 556-560).

Para infectar uma célula, os vírus devem aderir à superfície celular, penetrar na célula e tornar seu genoma suficientemente exposto às maquinarias enzimáticas virais e celulares para sua transcrição e tradução. A identificação de uma série de proteínas e enzimas virais essenciais para a replicação dos vírus e suficientemente diferentes das proteínas celulares viabilizou o desenvolvimento de drogas direcionadas exclusivamente a alvos virais que seriam, em princípio, inofensivas às proteínas celulares. A maioria destas drogas inibe enzimas envolvidas na replicação viral, como é o caso, por exemplo, do aciclovir, que após processamento intracelular se torna um potente inibidor da DNA polimerase do vírus do herpes (Crumpacker *et al.* (1979) Antimicrob. Agents Chemother. 15, 642-645); ou dos inibidores nucleosídicos e não-nucleosídicos da transcriptase reversa dos retrovírus (Autran, B. *et al.* (1997) Science 277, 112-116). Recentemente, o impedimento da entrada dos vírus nas células hospedeiras também vem se mostrando um alvo importante em terapias anti-virais.

A fusão de membranas no processo de infecção viral

Na classificação dos vírus um dos critérios de separação dos mesmos ocorre em função da presença ou ausência de envelopes. Para efeitos da presente invenção, serão abordados os aspectos envolvendo somente os vírus envelopados.

A internalização dos vírus envelopados sempre envolve uma etapa de fusão de membranas, que pode ser a fusão direta de seu envelope com a membrana plasmática da célula, ou sua fusão com a membrana do compartimento endossomal após a acidificação (Lanzrein, M. *et al*. (1994) Biochem. J. 302, 313-320; Hernandez, L. D. et al. (1996) Annu. Rev. Cell Dev. Biol. 12, 627-661; Weissnhorn, W. et al. (1999) Mol. Membr. Biol. 16, 3-9). A fusão de membranas mediada pelos vírus envelopados é sempre catalisada

por glicoproteínas presentes no envelope viral, que sofrem mudanças conformacionais seja pela interação com o receptor na membrana plasmática, seja em decorrência da diminuição do pH no interior do endossoma, causando a exposição de regiões hidrofóbicas que interagem com a membrana alvo (Gaudin, Y. *et al*. (1995) J. Gen. Virol. 76, 1541-1556; Hernandez, L. D. *et al.* (1996) Annu. Rev. Cell Dev. Biol. 12, 627-661; Weissnhorn, W. *et al*. (1999) Mol. Membr. Biol. 16, 3-9).

No primeiro caso, o mecanismo de fusão melhor caracterizado é aquele mediado pelas glicoproteínas gp120/gp41 do HIV-1 (Chan, D. C. & Kim, P. S. (1998) Cell 93, 681-684). A interação entre a gp120 e o receptor celular para o vírus (a molécula de CD4 e uma proteína co-receptora, CCR5 ou CXCR4) resulta em uma série de mudanças conformacionais no complexo gp120/gp41 culminando com a inserção do peptídeo hidrofóbico presente na gp41 na membrana da célula hospedeira. A proteína gp41 se dobra, formando uma estrutura conhecida como hairpin (grampo de cabelo) (Chan, D. C. et al. (1997) Cell 89, 263-273). Peptídeos derivados da região C-terminal da gp41 interferem na formação desta estrutura e inibem de forma bastante efetiva a infecção do HIV-1 (Wild, C. T. *et al*. (1994) Proc. Natl. Acad. Sci. USA. 91, 9770-9774). Um destes peptídeos, denominado T-20, está atualmente em testes clínicos em humanos, apresentando excelentes resultados (Kilby, J. M. *et al.* (1998) Nat. Med. 4, 1302-1307).

No caso da fusão endossomal, a glicoproteína de fusão mais bem estudada é a do vírus influenza, a hemaglutinina (HA), cuja estrutura foi resolvida com resolução atômica tanto em pH neutro como em pH ácido (Wilson, I. A. *et a*l. (1981) Nature 289, 366-372, Bullough, P. A. *et al.* (1994) Nature 371, 37-43). Em resposta à diminuição do pH, a HA sofre uma grande mudança conformacional, expondo um peptídeo hidrofóbico que se liga à membrana-alvo.

O vírus da estomatite vesicular

O vírus da estomatite vesicular (VSV) é o membro mais estudado da família Rhabdoviridae, um grupo de vírus com grande abrangência de hospedeiros (plantas, animais invertebrados e vertebrados). Os rabdovírus são formados por um capsídeo ribonucleico helicoidal envolto por uma membrana lipídica (Wagner, R. R. (1987) Em "The rhabdoviruses". R. R. Wagner, ed. Plenum Press, New York, pp 9-74). O capsídeo ribonucleico é composto por uma fita simples de RNA fortemente associado a uma proteína principal - a proteína N - e a duas outras proteínas - L e P - que juntas constituem a RNA polimerase viral. O envelope lipídico está associado a duas proteínas: a glicoproteína G, integral à membrana, cujos trímeros formam as espículas virais, e a proteína M, que interage com a face interna da membrana e com o capsídeo ribonucleico. O VSV se liga aos receptores celulares através da proteína G, sendo esta, então, responsável pela adsorção e infectividade viral. A entrada do vírus na célula se dá por endocitose mediada por receptor e sua replicação depende da acidificação endossomal (Matlin, K. S. *et al*. (1982) J. Mol. Biol. 156, 609-631).

A fusão de membranas mediada pelo vírus da estomatite vesicular

A membrana do VSV possui aproximadamente 1.200 moléculas da proteína G, a glicoproteína de superfície deste vírus, sendo essa proteína envolvida em pelo menos dois passos importantes do processo de infecção do VSV: o reconhecimento da célula com conseqüente adsorção à superfície desta, e o processo de fusão de membranas, fundamental à liberação do genoma viral no citoplasma.

A fusão de membranas mediada pela proteína G depende da diminuição do pH (White, J. *et* al. (1981) J. Cell Biol. 89, 674-679). As mudanças conformacionais necessárias para a fusão têm sido motivo de vários estudos. Até o presente mostrou-se que em pH ácido ocorre a estabilização do trímero da proteína G (Doms, R. W. *et al*. (1987) J. Cell Biol. 105, 1957-1969). Os trímeros da proteína G apresentam estabilidade diferencial na presença de

octilglicosídeo e Triton X-100, sugerindo que o ambiente que circunda a seqüência de ancoramento na membrana também influencia a interação entre as subunidades da proteína G (Wilcox, M. D. *et al*. (1992) *Biochemistry* 31, 10458-10464). A proteína G não apresenta nem um domínio de fusão típico, nem uma outra seqüência hidrofóbica óbvia além da sua porção transmembrana. Desta forma, o que se acredita é que haja a formação de um domínio cuja estrutura terciária gere um ambiente hidrofóbico capaz de interagir com a membrana e mediar a fusão. Durrer e colaboradores mostraram que durante as transições conformacionais decorrentes da acidificação, um segmento do ectodomínio tornava-se capaz de interagir com membranas (Durrer, P. *et al*. (1995) *J. Biol. Chem*. 29, 17575-17581). A fragmentação da proteína com brometo de cianogênio revelou que este segmento estava contido entre os aminoácidos 59-221.

Substituições de aminoácidos em regiões do ectodomínio da proteína G vêm sendo usadas como outra estratégia de localização do peptídeo de fusão do VSV. Mutações em resíduos presentes na região 117-137, que são altamente conservadas nos vesiculovírus, sugeriram que esta região continha o domínio de fusão (Zhang, L. & Ghosh, H. P. (1994) J. Virol. 68, 2186-2193; Fredericksen, B. e Whitt, M. A. (1995) *J. Virol*. 69, 1435-1443). A substituição dos resíduos de glicina, prolina e ácido aspártico conservados ou aboliram a fusão de membranas mediada pela proteína ou modificaram o pH ótimo da reação. Mutações em outra região conservada, entre os aminoácidos 395-418, também aboliu ou diminui a atividade de fusão (Shokralla, S. *et al*. (1998) *Virology* 256, 119-129). A importância do domínio transmembrana na fusão de membranas mediada pelo VSV também foi estudada (Odell, D. *et al.* (1997) *J. Virol*. 71, 7996-8000; Cleverley, P. Z. & Lenard, J. (1998) Proc. Natl. Acad. Sci. USA 95, 3425-3430). Estes trabalhos mostraram a importância de 6 resíduos presentes nestes domínio (GLIIGL) e levaram à proposição de que seria necessária a dobra deste segmento em uma das glicinas para que ocorresse a formação do poro de fusão e a hemifusão propriamente dita.

Recentemente, as mudanças estruturais sofridas por esta proteína em função da diminuição do pH e de sua interação com vesículas lipídicas foram caracterizadas, simulando o processo de endocitose do vírus e a fusão de membranas (Carneiro, F. A. *et al*. (2001) *J. Biol. Chem*. 276, 62-67). Nesse trabalho, à medida que o pH diminui, uma dramática mudança conformacional na proteína ocorre. Primeiramente, há a exposição de um domínio hidrofóbico que interage com a membrana alvo, e em seguida ocorre perda de estruturas secundária e terciária, que, em pHs mais baixos ainda, se reorganizam em uma nova estrutura (Carneiro, F. A. *et al*. (2001) *J. Biol. Chem*. 276, 62-67). As características e a termodinâmica da interação entre a proteína G e vesículas de diferentes composições lipídicas também foram estudadas através do uso da microscopia de força atômica, calorimetria e espectroscopia de fluorescência (Carneiro, F. A. *et al.* (2002) *J. Virol*. 76, 3756-3764). Em diferentes etapas do ciclo de infecção do vírus independente do reconhecimento da membrana, da interação com esta membrana em pH baixo, e da catálise da fusão de membranas propriamente dita, as interações determinantes são interações eletrostáticas entre regiões da proteína positivamente carregadas e fosfolipídeos negativamente carregados.

Esses resultados sugerem que as mudanças estruturais sofridas pela proteína G durante a acidificação, assim como a aquisição da capacidade de interagir com membranas negativamente carregadas ocorrem em uma faixa de pH bastante estreita, entre 6,2 e 5,8. Esta é exatamente a faixa de pH na qual ocorre a protonação da cadeia lateral do aminoácido histidina (pK ~ 6,04). Isso sugeriu que a protonação de resíduos de histidina presentes na proteína G seria necessária para o desencadeamento do processo de fusão. Por esse motivo para efeitos da presente invenção, a substância Dietilpirocarbonato (DEPC), cujo mecanismo de modificação específica de histidinas vem sendo estudado há anos, foi utilizada no desenvolvimento da presente invenção.

Na faixa de pH entre 5.5 e 7.5, DEPC é razoavelmente específico para reação com resíduos de histidina (Lundblad, R. L. & Noyes, C. M. (1984) em “Chemical reagents for protein modification”, CRC Press, Boca Raton, Florida).

DEPC reage com resíduos de histidina em sistemas modelo e em proteínas, e resulta na substituição de uma das posições de nitrogênio do anel imidazol, gerando N-carbetoxihistidina (Miles, E. W. (1977) Meth. Enzymol. **47**, 431-442), como mostrado na equação 1:

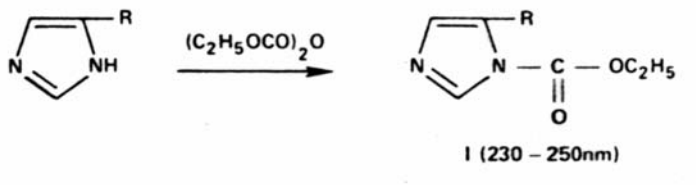

A formação do N-carbetoxihistidina pode ser acompanhada espectrofotometricamente, com um máximo de absorção entre 230 e 250 nm (Ovádi, J. et al. (1967) Biochim. Biophys. Acta **2**, 455-500).

Existem descritos na literatura vários exemplos do uso de DEPC para estudar a função de resíduos de histidina em diversas proteínas (Lundblad, R. L. & Noyes, C. M. (1984) em “Chemical reagents for protein modification”, CRC Press, Boca Raton, Florida).

A partir de experimentos envolvendo vírus VSV e DEPC foi possível mostrar que o vírus modificado perdia a capacidade de mediar a fusão de membranas devido à inibição das mudanças conformacionais na proteína G. Além disso, as seqüências modificadas pelo DEPC foram identificadas através de experimentos de espectrometria de massa, o que permitiu, a partir do uso de peptídeos sintéticos, identificar o peptídeo de fusão do VSV e caracterizar os requerimentos necessários à sua participação na fusão de membranas mediada pelo vírus (Carneiro, F. A. *et al*. (2003) *J. Biol. Chem*. 278, 13789-13794).

O único relato encontrado na literatura patentária utilizando o DEPC como um agente inativador viral foi descrito na patente norte americana US 986,046, de 1963. Esta patente descreve um processo detalhado para produção de vacinas utilizando solução aquosa de DEPC, de modo que os vírus inativados por este processo sejam imunogênicos, mas não patogênicos. Foram utilizados como exemplos quatro tipos de vírus: sarampo (vírus

envelopado), varíola (vírus envelopado), pólio (vírus não envelopado) e influenza A. A eficácia das vacinas foi avaliada por meio de titulação por TCID (dose infecciosa em cultura de tecido) e dosagem de anticorpos no soro de animais vacinados. Entretanto, a presente invenção propõe uma composição para inativação viral capaz de adicionalmente inibir a infecção e a replicação do vírus VSV.

Dentre as patentes relacionadas com a inativação do VSV, a patente norte americana US 4,556,556, de 1985, refere-se a um composto químico que atua sobre partícula viral, tornando-a inativa ou atenuada, e possibilitando sua utilização em formulação de vacinas. Neste caso, o autor descreve uma vacina contra o VSV contendo partículas virais inativadas pela associação psoraleno e luz ultravioleta. Por intermédio da análise dos resultados de titulação viral, dosagem de anticorpos em modelos animais e sobrevivência dos animais vacinados expostos ao vírus selvagem, foi demonstrado que o VSV inativado desta forma mantém sua imunogenicidade e é completamente não infeccioso, podendo por isso ser administrado com segurança como vacina. Por outro lado, a presente invenção produz efeito semelhante através da manipulação de uma única substância.

A patente européia EP 0822819 propõe uma emulsão formada por um solvente e um carreador de óleo para aplicação tópica a fim de inibir a infecção causada particularmente pelos vírus envelopados de uma maneira geral. Essa emulsão possui a capacidade de inibir a infecção viral e a replicação. Contudo, a presente invenção produz efeito idêntico a partir da manipulação somente do solvente orgânico DEPC (dietilpirocarbonato).

O pedido norte americano US 2004/0047844 propõe compostos alquil-aminos capazes de inativar bactérias, fungos, leveduras, micoplasmas, células de mamíferos ou de outros animais, vírus ou vírus envelopados como Flaviviridae, Retroviridae, Togaviridae, Rhabdoviridae, Herpesviridae, VSV, SFV, HIV, MuLV, BVDV, e CMV. Particularmente os ingredientes ativos são aminas anfipáticas carregadas e/ ou óxidos de amina anfipáticos carregados.

Ao contrário da presente invenção, para que os compostos ativos funcionem de forma eficaz, a solução deve estar dentro de uma faixa de pH específica (5,0 a 8,0), sendo preferencialmente 7,2, o que acarreta em maiores cuidados na confecção do composto de inativação biológica da US 2004/0047844A1.

Um outro exemplo de inativação viral está descrito na patente norte americana US 6369048. Nesse trabalho a inativação é realizada através do contato, em condições específicas, da composição biológica com um solvente orgânico pertencente ao grupo dos triacilfosfatos. Essa metodologia é útil na inativação dos vírus não envelopados e dessa forma, diminui a capacidade, bem como inibe a infecção e a replicação viral. Entretanto, a presente invenção atua inativando o vírus VSV, que compreende um vírus envelopado.

O VSV também pode ser inativado por tratamento com formalina, com β-propiolactona ou com luz UV (Bachmann M. F. *et al.* (1993) *J. Virol*. 67, 3917-3922; Bachmann M. F. *et al*. (1994) *Med. Microbiol. Immunol*. 183, 95-104). Nestes casos, o vírus inativado não foi capaz de induzir a produção de IgG, embora a resposta de IgM tenha se mantido inalterada. Apenas o vírus inativado por luz UV foi capaz suscitar resposta de linfócitos T citotóxicos (Bachmann M. F. *et al*. (1994) *Med. Microbiol. Immunol*. 183, 95-104). Porém, a presente invenção supera os resultados acima, ao impedir o aparecimento do infiltrado inflamatório nos cortes histológicos de animais infectados e tratados com a presente invenção, característico da reação inflamatória.

Mais recentemente, o rearranjo genético do VSV vem sendo apontado como uma forma eficiente de atenuação viral (Wertz, G. W. *et al*. (1998) *Proc. Natl. Acad. Sci*. USA 95, 3501-3506; Flanagan, E. B. *et al*. (2001) *J. Virol*. 75, 6107-6114). O afastamento do gene da proteína N da região promotora reduziu os níveis de transcrição e da síntese da proteína N com conseqüente uma atenuação da replicação do vírus e de sua letalidade para camundongos (Wertz , G. W. *et al.* (1998) *Proc. Natl. Acad. Sci*. USA 95, 3501-3506). A literatura patentária inclui o pedido de patente US2003/0124146, que propõe a construção de um vetor recombinante Rhabdovírus expressando um

polipeptídeo antigênico do vírus da estomatite vesicular, por exemplo, a fim resultar em uma resposta imune pelo hospedeiro. Pelo fato da presente invenção não utilizar a tecnologia do DNA recombinante, a mesma permite o barateamento das etapas da produção o que economicamente permite um volume maior de produção e conseqüentemente, um beneficiamento para mais animais.

Outras patentes referem-se a compostos químicos que interferem no ciclo de vida dos vírus, ou seja, poderiam ser utilizados para o tratamento de infecções virais (drogas antivirais). É o caso da patente norte americana US 4,396,628, de 1983, que demonstra que a dansilcadaverina é mais eficaz que a amantadina e outros agentes antivirais no bloqueio da entrada do VSV em células de camundongo. Outros compostos químicos, como compostos que contêm hipericina ou pseudohipericina (US 4,898,891, de 1990); 3-deazoadenosina (US 4,148,888, de 1979); e bases fracas parcialmente solúveis em água (EP 0095833, de 1983), também foram patenteados como antivirais. Contudo, tais mecanismos apenas atuam na diminuição da taxa de replicação viral e não propõem o desenvolvimento de uma composição de inativação viral capaz de inativar o vírus, ou seja, inibindo a infecção e a replicação do vírus VSV, bem como impedindo o desenvolvimento patológico da estomatite vesicular.

A presente invenção propõe a inativação do vírus VSV (vírus da estomatite vesicular) através da utilização de uma substância orgânica, o DEPC (dietilpirocarbonato). A eficiência dessa metodologia é dose dependente de DEPC, porém a dose ideal não apresenta efeito citotóxico para as células infectadas pelo vírus. Dessa forma, a presente invenção resolve o problema da inativação do vírus VSV de forma simples, menos custosa e eficaz.

Sumário da invenção

É objeto da presente invenção uma composição para inativação viral, mais especificamente a inativação do vírus VSV causador da doença estomatite vesicular. Essa composição possui uma solução aquosa contendo o

solvente orgânico DEPC (dietilpirocarbonato) e o vírus VSV. Ao inativar o vírus VSV, a presente invenção impede a infecção e a replicação do vírus VSV, bem como o desenvolvimento patológico da estomatite vesicular.

É um adicional objeto da presente invenção o processo de inativação viral através da contactação do mesmo com uma solução aquosa contendo o composto orgânico DEPC (dietilpirocarbonato).

Em um aspecto, os vírus inativados pelo processo da presente invenção são úteis na preparação de vacinas contra as doenças que os referidos vírus acarretam. É, portanto, um adicional objeto da presente invenção uma vacina contra as patologias causadas pelo VSV.

Em ainda outro aspecto, sendo, por tanto ainda outro objeto da presente invenção, é provido um processo para a preparação de vacinas.

Breve Descrição das Figuras

Figura 1: Microscopia ótica das células BHK21 tratadas ou não com DEPC após 20 horas pós-infecção com o VSV. Tratamento com DEPC inibe o efeito citopático induzido pelo VSV. Células BHK_{21} foram infectadas com VSV tratado ou não com DEPC em diferentes concentrações. As células foram examinadas por microscopia ótica 20 horas pós-infecção. (A) Célula não infectada; (B) célula infectada com VSV tratado com DEPC 0,5 mM; (C) 0,1 mM; (D) 0,05 mM; (E) 0,01 mM; e (F) célula infectada com VSV não tratado (F). Foi utilizada uma multiplicidade de infecção (m.o.i.) de 0,1.

Figura 2: Gráfico representativo da taxa de mortalidade de camundongos BALB/c infectados com VSV tratado ou não com DEPC acompanhados diariamente por 5 semanas. Sobrevivência de camundongos BALB/c infectados com VSV não tratado ou tratado com DEPC. Camundongos BALB/c foram inoculados por via intranasal com $2,0 \times 10^6$ $TCID_{50}$ de VSV não tratado (●) ou tratado com 0.5 mM de DEPC (○). A taxa de mortalidade dos camundongos foi acompanhada diariamente por 5 semanas. Como grupo controle, camundongos foram infectados somente com PBS contendo 0,5 mM de DEPC (▲).

Figura 3: Cortes histológicos longitudinais passando pelo ventrículo lateral de camundongos inoculados com VSV ou com VSV tratado com DEPC. A e B - Cortes longitudinais passando pelo ventrículo lateral de camundongos inoculados com VSV (A) ou com VSV tratado com DEPC (B). Observa-se presença de infiltrado inflamatório caracterizando ventriculite (*) em A, o que não foi observado em B (*).HC – hipocampo (A e B barra = 50μm). C e D - Cortes longitudinais na região do bulbo olfatório corados por hematoxilina e eosina mostram a presença de infiltrado inflamatório subpial em C (seta), o que não foi observado em D (seta). CG - camada glomerular (C e D barra = 12,5μm).

Descrição Detalhada da Invenção

De acordo com a presente invenção, a composição de inativação viral proposta impede a fusão de membranas mediada pelo vírus da estomatite vesicular, inibindo sua replicação nas células-alvo e desenvolvimento da patologia característica em modelo animal. Estes efeitos se devem à modificação de resíduos de histidina presentes na glicoproteína, localizados na superfície viral, a proteína G, pelo tratamento do vírus com dietilpirocarbonato (DEPC). A fim de potencializar o resultado da presente invenção, outros componentes podem ser usados em combinação com a composição da presente invenção. Para efeitos da mesma, os componentes podem ser químicos compreendendo substâncias orgânicas ou inorgânicas e/ ou outros componentes tais como, a irradiação ultra-violeta, a irradiação ultra-sônica, radiação iônica como a X, gama e beta ou radiação eletrônica. Adicionalmente, para efeitos da presente invenção o termo “inativação” compreende inibir a infecção e a replicação viral, bem como o desenvolvimento da patologia característica da estomatite vesicular.

Os exemplos descritos a seguir ilustram, mas não limitam a presente invenção.

EXEMPLOS

EXEMPLO 1- Efeitos do vírus VSV tratado com DEPC em amostras biológicas

A. Inibição do efeito citopático induzido pelo VSV pelo tratamento viral com DEPC

Muitos vírus são capazes de induzir morte celular, levando a lise das células infectadas (Levine *et al*. (1993) *Nature* 361, 739-742; Agol, V. I. *et al.* (1998) Virology 252, 343-353). Nos últimos estágios da infecção pelo VSV, mudanças morfológicas que antecedem a morte celular causada pelo vírus, conhecidas como efeito citopático, podem ser observadas microscopicamente. O efeito citopático induzido pelo VSV é caracterizado por células arredondadas e encolhidas, núcleo deformado e cromatina condensada.

Durante a infecção de células BHK_{21}, o efeito citopático clássico ocorre 16-20 horas pós-infecção. Sendo assim, as alterações morfológicas destas células foram observadas por microscopia após 20 horas de infecção com VSV controle e modificado com concentrações crescentes de DEPC (figura 1).

As imagens mostram uma inibição progressiva do efeito citopático induzido pelo VSV a medida que a concentração de DEPC utilizada para modificação viral aumenta. Estes resultados mostram ainda que o DEPC não é citotóxico nestas concentrações.

B. Inativação do VSV modificado com DEPC

Para determinar o número de partículas infectantes remanescentes nas amostras de VSV modificadas com DEPC, o VSV modificado por 15 minutos com concentrações crescentes de DEPC (0.01, 0.05, 0.1 e 0.5 mM) foi titulado pelo método de $TCID_{50}$ (tabela I).

Tabela I: Titulação das amostras de VSV modificadas com DEPC.

[DEPC] (mM)	Título (pfu/ml)
0	1.80×10^7
0.01	1.40×10^7
0.05	1.60×10^6
0.1	4.56×10^4
0.5	0

Comparando os títulos obtidos para as amostras modificadas com aquele obtido para o VSV controle, observamos que o tratamento com DEPC inativa o vírus de forma dose dependente. A pré-incubação do VSV com DEPC 0.5 mM inibiu completamente a infecção, havendo uma perda completa do título viral.

C. Inibição da replicação do VSV modificado com DEPC

Para avaliar a replicação do VSV, os sobrenadantes de células BHK_{21} infectadas com uma amostra de vírus controle e com uma amostra de vírus modificado com 0.5 mM de DEPC foram coletados em 4, 8, 12, 16, 20 e 24 horas após a infecção. A replicação viral foi estimada pela presença de partículas virais infectantes nos sobrenadantes coletados quantificadas pelo método de $TCID_{50}$ (tabela II).

Tabela II: Titulação dos sobrenadantes das culturas infectadas com VSV e VSV modificado com 0.5 mM DEPC.

Tempo pós-infecção (horas)	Título ($TCID_{50}$/ml)	
	VSV	VSV-DEPC
4	$4,52 \times 10^2$	0
8	$4,65 \times 10^2$	0
12	$8,00 \times 10^2$	0
16	$2,56 \times 10^4$	0
20	$3,03 \times 10^4$	0
24	$6,40 \times 10^3$	0

Os resultados obtidos mostram claramente que o tratamento com DEPC 0.5 mM inibe completamente a replicação do VSV.

D. Efeito da modificação do VSV com DEPC sobre a taxa de mortalidade de camundongos infectados

A inativação do vírus in vivo foi analisada através de curvas de sobrevivência de camundongos BALB/c inoculados com VSV controle e VSV modificado por pré-incubação com DEPC 0.5 mM (figura 2). Os camundongos controles foram inoculados somente com uma solução de DEPC 0.5 mM.

O percentual de sobrevivência de camundongos infectados com VSV controle foi de aproximadamente 40%. Já no grupo que foi inoculado com VSV tratado com DEPC, o perfil da curva de sobrevivência foi semelhante ao do grupo controle, com percentual maior que 85% 35 dias após a inoculação.

E. Efeito do tratamento do VSV com DEPC na resposta inflamatória no SNC

O VSV, quando inoculado intranasal, inicialmente se replica nos receptores olfatórios, sendo propagado para o SNC através do nervo olfatório em menos de 12 horas. No bulbo olfatório, o vírus se replica de forma invasiva, alcançando o ventrículo após 4-5 dias de infecção (Reiss e cols. (1998) Ann N Y Acad Sci. 855, 751-761). Como resposta à replicação viral, ocorre uma reação inflamatória nestas regiões do SNC. A fim de confirmar a inativação viral *in vivo*, cortes histopatológicos do encéfalo corados pela H-E foram examinados. Nos cortes de camundongos infectados com VSV não tratado, observamos infiltrado inflamatório em resposta a infecção viral (figuras 3A e C). No entanto, os cortes histológicos de camundongos infectados com VSV tratado com DEPC 0,5 mM mostram que houve uma inibição completa da resposta inflamatória (figuras 3B e D).

F. Efeitos da presente invenção nos vírus envelopados

A presente invenção compreende também a inativação dos vírus pertencentes às famílas: Herpesviridae, Togaviridae, Flaviviridae, Coronaviridae, Hepadnavirida, Filoviridae, Arenaviridae, Retroviridae, e Rhabdoviridae, sendo preferencialmente o VSV.

G. Amostras Biológicas

As amostras biológicas cujo vírus presente na mesma possa ser inativado compreendem os animais, mais especificamente os mamíferos e as suspensões celulares, mais especificamente as de animais.

EXEMPLO 2: Ensaios realizados

A. Ensaios para propagação do vírus

VSV indiana foi propagado em monocamadas de células BHK_{21}. As células foram crescidas em placas, a 37^0C, em estufa de CO_2, usando 10 mL de meio de cultura "Dulbecco's modified Eagle's medium" (DMEM) suplementado com 10% de soro fetal bovino (FBS), antibióticos - gentamicina (5mg/mL), ampicilina (10mg/mL) - e anfotericina B (5mg/mL), tamponado com bicarbonato de sódio. Após ficarem confluentes, o meio foi removido e a monocamada de células foi infectada com VSV em uma multiplicidade de infecção (m.o.i.) de 0,1. Após 30 minutos de infecção com o vírus na presença de 9 mL de DMEM não suplementado, adicionamos 1 mL de FBS, e mantivemos a cultura por 16-20 horas. Após a observação do efeito citopático, coletamos o meio de cultura e centrifugamos em uma centrífuga Sorvall a 5.000 rpm, por 10 minutos, em rotor GSA.

B. Ensaios para a purificação do vírus

O sobrenadante clarificado foi centrifugado em rotor Beckman Ti45 a 30.000rpm, por 2,5 horas. O sobrenadante foi descartado e o precipitado foi

ressuspenso em tampão 3E (Tris 0,12M; acetado de sódio 0,06M; EDTA 3 mM; pH 7,4) e centrifugado em gradiente contínuo de 5-40 % de sacarose (em tampão 3E) por 1 hora a 39.000 rpm, em rotor Beckman SW-41. A banda referente ao vírus foi coletada, dialisada contra tampão Tris-HCl 10mM pH 7,5. O estoque de vírus foi mantido em freezer -70^{0}C. O título viral foi determinado por método de $TCID_{50}$ (Reed, L. J. & Muench, H. (1938) Am. J. Hyg. 27, 493-497) em monocamadas de células BHK_{21} com 80% de confluência em placas de 96 poços.

C.Ensaios em células BHK21 do vírus VSV tratado com DEPC

Soluções de DEPC foram preparadas antes do experimento pela diluição do reagente em etanol e posteriormente em PBS 1x. A concentração do estoque de DEPC era determinada pela reação com imidazol 10mM (Miles, E. W. (1977) Meth. Enzymol. 47, 431-442. Para inativação viral, VSV foi pré-incubado com diferentes concentrações de DEPC por 15 minutos a 25^{0}C, variando de 0,01 a 0,5 mM. A pré-incubação do VSV com volume equivalente de etanol foi realizado como controle do experimento. A quantidade de etanol na solução final de incubação era menor que 1%.

Para estudo da inibição de infecção *in vitro*, foi determinado o $TCID_{50}$ do VSV controle e modificado com DEPC 0,01; 0,05; 0,1; e 0,5 mM. Além disso, monocamadas de células BHK_{21} em placas de 6 poços foram infectadas com VSV controle e modificado com DEPC 0,005; 0,01; 0,05; e 0,1 mM numa m.o.i. de 0,1. Após 20 horas de infecção, fotos foram tiradas em microscópio de contraste de fase, acoplado a uma câmera fotográfica (aumento de 10x).

Para estudo da inibição de replicação, infectamos monocamadas de células BHK_{21} em placas de 6 poços com VSV controle e modificado com 0,5 mM em uma m.o.i. de 0,1. Após 4, 8, 12, 16, 20 e 24 horas, os sobrenadantes foram coletados para determinação do $TCID_{50}$.

D.Ensaios em camundongos BALB/c do vírus VSV tratado com DEPC

Foram selecionados camundongos BALB/c do sexo masculino com seis a oito semanas de idade. Para realização da curva de sobrevivência, estes camundongos foram divididos em três grupos: controle, VSV e VSV-DEPC. No grupo VSV, os camundongos foram infectados com dose de 2,0 x 10^6 $TCID_{50}$ de VSV. No grupo VSV-DEPC, antes da inoculação o VSV foi tratado com DEPC 0,5 mM como descrito acima. No controle, foram inoculados somente DEPC 0,5 mM diluído em PBS. Em todos os grupos, a inoculação foi feita por via intranasal e com mesmo volume. Os camundongos foram acompanhados diariamente por 45 dias.

E. Efeitos no sistema nervoso central (SNC)

Para avaliar a inibição da infecção do VSV tratado com DEPC no SNC, camundongos infectados com VSV controle e que apresentavam sinais e sintomas da doença foram sacrificados e seus encéfalos fixados com formalina 10% e incluídos em parafina. Cortes histológicos longitudinais com 5μ e foram corados por hematoxilina e eosina para observação de alterações morfológicas. O mesmo foi feito com os encéfalos de camundongos infectados com VSV tratado com 0,5 mM de DEPC. Os cortes foram analisados e fotografados em microscópio Olympus BX50.

Os versados na arte apreciarão que a aplicação, a um animal, de uma composição compreendendo o VSV inativado conforme a presente invenção pode proporcionar a obtenção de resposta imune protetiva no referido animal. Conseqüentemente, está compreendida no escopo da presente invenção uma vacina contra as patologias causadas pelo VSV e também um processo de produção da referida vacina.

Reivindicações

Composição para Inativação Viral, Processo de Inativação Viral, Vacina e Processo de Produção de Vacina

1. Composição para inativação viral caracterizada pelo fato de compreender o solvente orgânico DEPC (dietilpirocarbonato) em solução aquosa.

2. Composição, de acordo com a reivindicação 1, caracterizada pelo fato de adicionalmente compreende anidrido etoxifórmico, dietiloxidiformato e dietildicarbonato.

3. Composição, de acordo com a reivindicação 1, caracterizada pelo fato de adicionalmente compreender outras substâncias úteis para a inativação viral.

4. Composição, de acordo com a reivindicação 1, caracterizada pelo fato de ser destinada à inativação de vírus envelopados selecionados das famílias virais: Rhabdoviridae, Togaviridae, Flaviviridae, Orthomyxoviridae, Coronaviridae, Bunyaviridae, Arenaviridae, Hepadnavirida, Paramyxoviridae, Herpesviridae, Filoviridae, e Retroviridae.

5. Processo de inativação viral caracterizado por compreender a contactação do vírus com uma solução aquosa contendo DEPC (dietilpirocarbonato).

6. Processo de produção de vacina caracterizado pelo fato de compreender a inativação do vírus VSV com um solvente orgânico DEPC (dietilpirocarbonato) em solução aquosa.

7. Vacina caracterizada pelo fato de compreender o vírus VSV inativado com um solvente orgânico DEPC (dietilpirocarbonato) em solução aquosa.

Resumo

Composição para Inativação Viral, Processo de Inativação Viral, Vacina e Processo de Produção de Vacina

A presente invenção refere-se a uma composição para inativação viral que compreende solução aquosa de DEPC (dietilpirocarbonato); a referida composição é útil para a inativação do vírus VSV em um processo de inativação viral, que por sua vez é útil para a preparação de vacinas.

Figura 1

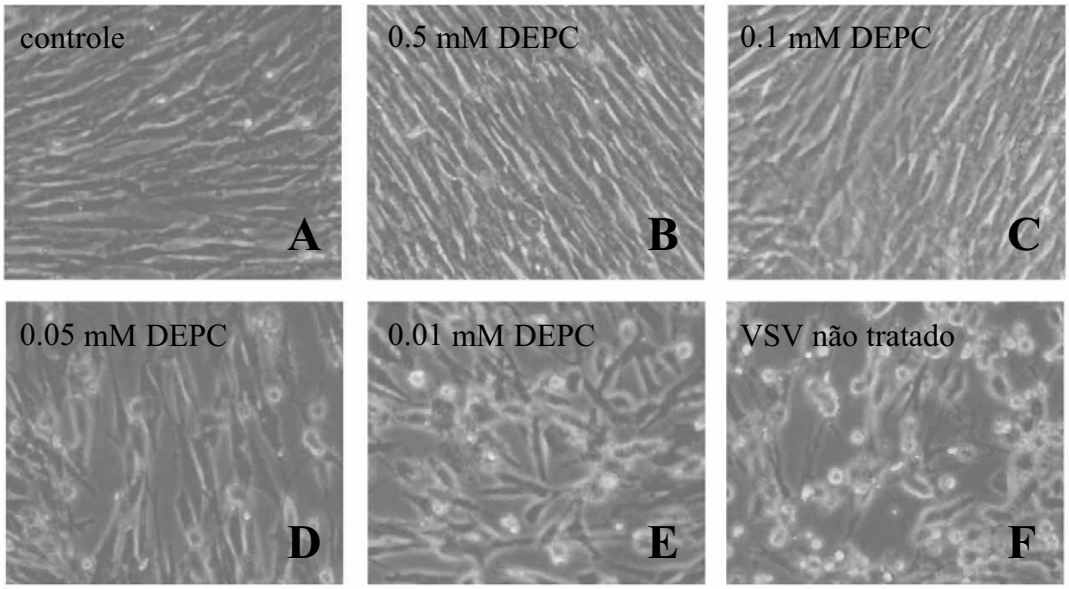

Figura 2

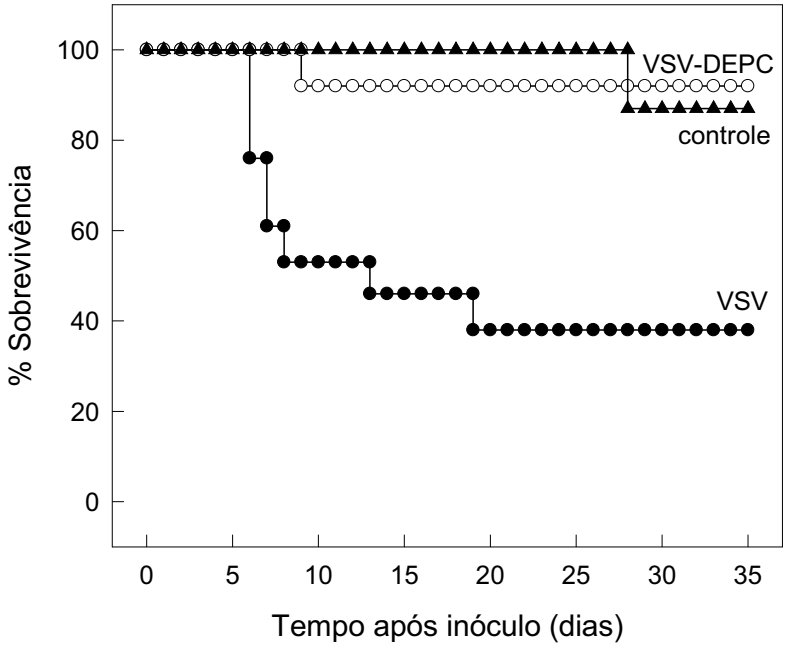

Figura 3

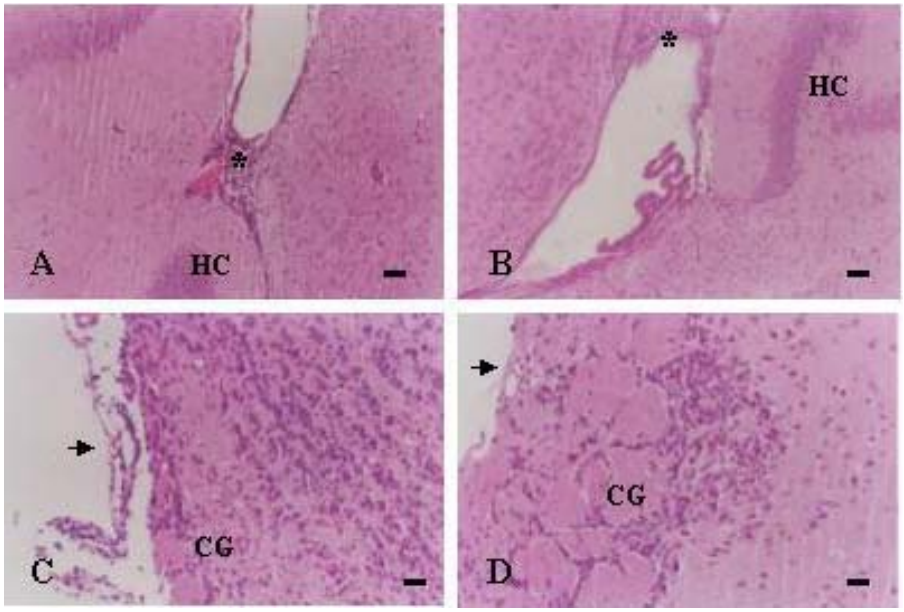

2.2.2 Artigo 4

Inactivation of vesicular stomatitis virus through inhibition of membrane fusion by chemical modification of the viral glycoprotein

Fausto Stauffer, Joari De Miranda, Marcos C. Schechter, Fabiana A. Carneiro, Leonardo T. Salgado, Gisele F. Machado e Andrea T. Da Poian

Publicado em 2007 no periódico

Antiviral Research

Available online at www.sciencedirect.com
ScienceDirect
Antiviral Research 73 (2007) 31–39
Antiviral Research
www.elsevier.com/locate/antiviral

Inactivation of vesicular stomatitis virus through inhibition of membrane fusion by chemical modification of the viral glycoprotein

Fausto Stauffer[a,1], Joari De Miranda[a,1], Marcos C. Schechter[a], Fabiana A. Carneiro[a], Leonardo T. Salgado[b], Gisele F. Machado[c], Andrea T. Da Poian[a,*]

[a] *Instituto de Bioquímica Médica, Programa de Biologia Molecular e Biotecnologia, Universidade Federal do Rio de Janeiro, Rio de Janeiro, RJ 21941-590, Brazil*
[b] *Laboratório de Biomineralização, Instituto de Ciências Biomédicas, Universidade Federal do Rio de Janeiro, Rio de Janeiro, RJ 21941-590, Brazil*
[c] *Departamento de Cirurgia Clínica e Reprodução Animal, Escola de Medicina Veterinária, Universidade Estadual Paulista, Araçatuba, SP 16050-680, Brazil*

Received 18 January 2006; accepted 11 July 2006

Abstract

Membrane fusion is an essential step in the entry of enveloped viruses into their host cells triggered by conformational changes in viral glycoproteins. We have demonstrated previously that modification of vesicular stomatitis virus (VSV) with diethylpyrocarbonate (DEPC) abolished conformational changes on VSV glycoprotein and the fusion reaction catalyzed by the virus. In the present study, we evaluated whether treatment with DEPC was able to inactivate the virus. Infectivity and viral replication were abolished by viral treatment with 0.5 mM DEPC. Mortality profile and inflammatory response in the central nervous system indicated that G protein modification with DEPC eliminates the ability of the virus to cause disease. In addition, DEPC treatment did not alter the conformational integrity of surface proteins of inactivated VSV as demonstrated by transmission electron microscopy and competitive ELISA. Taken together, our results suggest a potential use of histidine (His) modification to the development of a new process of viral inactivation based on fusion inhibition.

Keywords: Viral inactivation; Vesicular stomatitis virus; Membrane fusion; Diethylpyrocarbonate

1. Introduction

The development of new strategies to achieve viral inactivation is an important aim in virus research. Despite the advances in the field of immunology, molecular biology and genetics, viral inactivation remains an important procedure in basic research, since it is an easy and relatively cheap approach for producing new effective and safe vaccines against several viruses. The entry of enveloped viruses into a target cell always requires virus-mediated membrane fusion catalyzed by viral surface glycoprotein (Eckert and Kim, 2001; Hernandez et al., 1996; Skehel and Wiley, 2000). Virus-induced fusion may occur through two different general mechanisms: (i) fusion between viral envelope and host cell plasma membrane after virus interaction with its cellular receptor, or (ii) fusion with the endosomal membrane, after virus internalization by receptor-mediated endocytosis. In the latter case, the decrease in the pH of the endosomal medium triggers conformational changes in viral glycoproteins. This mechanism seems to be conserved among several viral families, which makes the fusion process a potentially attractive target for viral inactivation approaches.

Vesicular stomatitis virus (VSV), a member of Rhabdoviridae family, is composed by a helical ribonucleocapsid surrounded by a lipid bilayer covered by trimers of a single type of an integral glycoprotein, named G protein. VSV causes an acute disease that primarily affects cattle, horses and pigs. The clinical presentation of the disease is the development of vesicles and ulcers in the oral cavity and, less frequently, in the teats and coronary bands (Letchworth et al., 1999). Mortality rates are typically very low, but production suffers because affected animal lose weight and may develop lameness and mastitis. VSV enters into the cell by endocytosis followed by low-pH-induced membrane fusion (Da Poian et al., 1998; White et al., 1981). Cell recognition and fusion are mediated by the surface glycoprotein G. We have been studying the conformational changes

* Corresponding author. Tel.: +55 21 22706264; fax: +55 21 22708647.
E-mail address: dapoian@bioqmed.ufrj.br (A.T. Da Poian).
[1] These authors contributed equally to this work.

0166-3542/$ – see front matter © 2006 Elsevier B.V. All rights reserved.
doi:10.1016/j.antiviral.2006.07.007

in VSV G protein and its interaction with the target membrane during cellular recognition and fusion events (Carneiro et al., 2001, 2002). The observation of a dramatic reorganization in G protein structure at a very narrow pH range led us to propose a crucial role for the histidine (His) residues of VSV G protein in membrane fusion mediated by the virus (Carneiro et al., 2003). Using diethylpyrocarbonate (DEPC) to modify His residues of G protein, we showed that VSV-induced fusion was driven by His protonation at the pH range of endosomal medium. DEPC is a widely used tool in chemical modification of proteins because of the high selectivity of the reagent to histidyl residues (Miles, 1977). This compound covalently modifies histidines and makes them unable to be protonated. Modification with DEPC was successfully used in inactivation studies of various groups of enzymes, e.g., peroxidases, heparinases and ATPases (Bhattacharyya et al., 1992; Dzhandzhugazyan and Plesner, 2000; Shriver et al., 1998). However, DEPC has not been previously evaluated as a potentially useful antiviral compound.

The main aim of the present study was to evaluate whether viral treatment with DEPC was able to inactivate the virus. For this purpose, we analyzed the VSV infectivity after His modification in vitro and using an animal model. We showed that virus treatment with DEPC abolished virus replication in cell culture and eliminated the ability of the virus to cause disease in mice. Moreover, although the modified virus was shown to be completely inactivated in all the systems tested, virus structure and the antigenic domains of modified G protein were preserved. These results suggest that modification of His residues of viral fusion proteins might be used as a new process of viral inactivation.

2. Material and methods

2.1. Virus propagation and purification

VSV Indiana was propagated in monolayer cultures of BHK_{21} cells grown at 37 °C in petri dishes containing Dulbecco's modified Eagle's medium supplemented with 10% fetal bovine serum, 100 μg/ml penicillin and 0.0085% streptomycin sulfate. When the cells reached confluence, the medium was removed, and the cell monolayer was infected with VSV at a multiplicity of infection (MOI) of 0.1. The cultures were kept at 37 °C for 16–20 h and the virus were harvested and purified by differential centrifugation followed by equilibrium sedimentation in a sucrose gradient, as described elsewhere (Da Poian et al., 1996). Purified virions were stored at −70 °C.

2.2. Virus modification with DEPC

Diethylpyrocarbonate solutions were freshly prepared by dilution of the reagent in cold ethanol. The concentration of stock DEPC solution was determined by reaction with 10 mM imidazole (Miles, 1977). VSV was diluted in PBS, pH 7.4, to a final protein concentration of 60 μg/ml and incubated for 15 min at room temperature. The final concentration of DEPC ranged from 0.01 to 0.5 mM.

2.3. Preparation of liposome and fusion assay

Phosphotidylcholine (PC) and phosphatidylserine (PS) from bovine brain (Sigma Chemical Co.) in a molar ratio of 1:3 were dissolved in chloroform and evaporated under nitrogen. The lipid film formed was resuspended in 20 mM MES, 30 mM Tris buffer (pH 6.0) at a final concentration of 1 mM. The suspension was vortexed vigorously for 5 min. Small unilamellar vesicles (SUV) were obtained by sonicating the turbid suspension using a Branson Sonifier (Sonic Power Company, Danbury, CT) equipped with a titanium microtip probe, in an ice bath, alternating cycles of 30 s at 20% full power, with 60 s resting intervals until a transparent solution was obtained (approximately 10 cycles). For fusion assays, equal amounts of unlabeled vesicles and vesicles labeled with 1 mol% of each *N*-(7-nitro-2,1,3-benzoxadiazol-4-yl) phosphatidylethanolamine (NBD-PE) and *N*-(lissamine Rhodamine B sulfonyl) phosphatidylethanolamine (Rh-PE) (Molecular Probes Inc., Eugene, OR) were prepared in 20 mM MES, 30 mM Tris buffer (pH 6.0), at a final phospholipid concentration of 0.1 mM. The fusion reaction was initiated by addition of the VSV (final concentration of 5 μg/ml). Fusion was followed by the fluorescence resonance energy transfer (FRET) assay as described in Struck et al. (1981). In this assay, vesicles labeled with a combination of fluorescence energy transfer donor and acceptor lipid probes, NBD-PE and Rh-PE, respectively, are mixed with unlabeled membranes. FRET, detected as rhodamine emission resulting from NBD excitation, decreases when the average spatial separation of the probes is increased upon fusion of labeled membranes with unlabeled membranes. In our experiments, the samples were excited at 465 nm and the fluorescence intensities were collected at 530 and 590 nm for NBD-PE and Rh-PE, respectively, using a Hitachi F-4500 Fluorescence Spectrophotometer. The fusion index was calculated using as the 100% value, the fluorescence ratio after addition of 0.2% Triton X-100 to the vesicles.

2.4. Infection of BHK_{21} cells with VSV

Monolayers of the BHK_{21} cells in 6- or 24-well plates were first adsorbed with unmodified VSV or VSV treated with DEPC at a MOI of 0.1 for 1 h at 37 °C. In the case of the treated samples, the inoculum was based on the titer of untreated virus, what means that all the samples contain the same number of virus particles although the number of infectious viruses was lower in the treated samples. After 1 h incubation, the unbound viruses were removed by three gentle washings with serum-free medium and fresh medium was added to each plate for further incubation at 37 °C.

2.5. Determination of virus titers by $TCID_{50}$

Infectious particles of VSV were quantified by $TCID_{50}$ on BHK_{21} cells for unmodified VSV and VSV treated with different concentrations of DEPC, or for supernatants of infected cultures of BHK_{21}. The cells were grown at 37 °C in 96-well plates until the confluence was reached. Samples were serially

diluted 10-fold in culture medium, and 100 μl was added to cells in quadruplicate. Cells were cultured at 37 °C in 5% CO_2 for 24 h and stained with 0.2% crystal violet in 20% ethanol. The $TCID_{50}$ was calculated by the method described by Reed and Muench (1938). To test the reversibility of inactivation, VSV modified with 0.5 mM DEPC was incubated with 400 or 1200 mM hydroxylamine (from a 3 M stock solution) for 30 min or 2 h, at room temperature before the quantification of the infectious particles by $TCID_{50}$.

2.6. Western blotting analysis

Cells were infected in 6-well plates and after 4, 12 and 20 h of infection, the medium was removed, the cells were washed with PBS and lysed with 100 μl of lysis buffer (20 mM Tris–HCl, 0.2 mM EDTA, pH 7.4, containing 1% Triton X-100, 2 μg/ml leupeptin, 2 μg/ml aprotinin and 1 mM phenylmethylsulfonyl fluoride). The lysates were diluted five-fold in 30 μl of SDS-PAGE buffer containing β-mercaptoethanol and boiled for 5 min. Proteins were separated on 10% SDS-PAGE and transferred to a polyvinylidene difluoride (PVDF) membrane according to standard protocols. Blots were blocked in 5% nonfat dry milk in PBS and incubated with a mouse monoclonal antibody against VSV G protein (Alpha Diagnostic Int, San Antonio, TX), at a 1:5,000 dilution in blocking buffer. PVDF blots were washed with PBS, incubated with goat anti-mouse antibody conjugated with peroxidase (1:10,000 dilution) and revealed with ECL kit reagents (Amersham Biosciences). Molecular sizes were determined using prestained molecular weight markers (Sigma Chemical Co.). Purified VSV (100 ng) was added as positive control.

2.7. Immunofluorescence

BHK_{21} cells were grown on sterile coverslips in 24-well tissue culture dishes. At 12 h after infection, they were fixed and permeabilized with 100% methanol for 20 min at −20 °C. Cells were blocked at room temperature using 4% goat serum in PBS for 2 h and incubated with mouse monoclonal anti-VSV G protein antibody (Alpha Diagnostic Int) diluted 1:200 in PBS containing 1% goat serum. As secondary antibody, Cy3-labeled goat anti-mouse immunoglobulin G conjugate was used at a 1:400 dilution (Sigma Chemical Co.). Finally, slides were mounted with *N*-propyl-galacto and examined with a Nikon epifluorescence microscope equipped for photomicroscopy.

2.8. Infection of mice

Four- to 5-weeks-old BALB/c male mice were slightly anesthesized and inoculated intranasally with 2×10^6 infectious units of unmodified VSV or VSV treated with different concentrations of DEPC in 5 μl of sterile PBS. In the case of the treated samples, the inoculum was based on the titer of untreated virus, which means that all the samples contain the same number of virus particles although the number of infectious viruses was lower in the treated samples. Control mice received only PBS. After infection, mice were caged, maintained with free access to food and observed daily for survival for at least 35 days. Animals were housed under pathogen-free conditions.

2.9. Intracerebral inflammatory response

BALB/c mice were inoculated intranasally with VSV or VSV treated with 0.5 mM DEPC as described above. At day 5, the animals were perfused with PBS followed by 4% paraformaldehyde solution in phosphate buffer. The brains were removed and post-fixed for 2 h in the same paraformaldehyde solution. After serial dehydration in ethanol and xylol solutions the whole brain was embedded in paraffin. Serial sections of each brain were mounted in glass slides for staining with hematoxylin and eosin.

2.10. Electron microscopy

Unmodified VSV or VSV treated with 0.5 mM DEPC were visualized by transmission electron microscopy (TEM) after negative staining. Briefly, a drop (5 μl) of each sample was placed to a copper 300 mesh grid coated with a thin formvar film (20 nm). The liquid was partially removed with a filter paper after 45 s. The wet grids were stained with 5% phosphotungstic acid solution during 45 s. The grids were completely dried and observed in a JEOL 1200 EX TEM, operated at 80 kV.

2.11. Competitive ELISA

The antigenic properties of VSV G protein after virus treatment with DEPC were evaluated by competitive ELISA. ELISA microplates were coated with 0.1 μg VSV overnight at 4 °C. The plates were washed with PBS/0.05% Tween-20 and blocked with 2% milk powder in PBS/0.05% Tween-20 for 2 h at room temperature. After blocking, the plates were washed as before. Subsequently, immune sera collected from mice 7 days after intranasal inoculation of 2×10^6 infectious units of unmodified VSV (at a fixed dilution) were incubated at 37 °C for 1 h together with serial dilutions of VSV modified with 0.5 mM DEPC or virus denatured by boiling for 5 min. As positive control, the immune serum was incubated with unmodified virus in the same dilutions of treated viruses, and as negative control albumin at the same protein concentrations was used. After incubation, the samples were transferred to coated ELISA plates and incubated for 1 h at room temperature. Plates were washed as before and bound IgG was detected by addition of an anti-mouse horseradish peroxidase conjugate (1:5,000 dilution) (Santa Cruz Biotechnology) followed by *o*-phenylenediamine (OPD) substrate as indicated by the manufacturer (Sigma Chemical Co.). The reaction was stopped with 3 M sulfuric acid, and the optical density at 492 nm was determined in an ELISA reader.

3. Results

3.1. Treatment with DEPC decreases VSV infectivity by inhibiting membrane fusion

During VSV infection, the pH-induced membrane fusion is a crucial step for the viral RNA evasion from the endosome

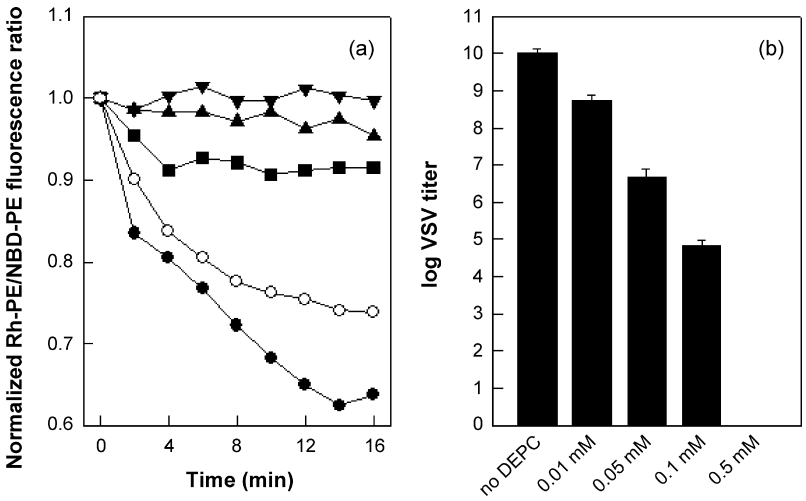

Fig. 1. DEPC treatment decreases the viral infectivity by inhibiting membrane fusion. (a) Equal amounts of unlabeled vesicles and vesicles labeled with NBD-PE and Rh-PE were incubated with purified VSV (●), or VSV pre-incubated with 0.01 mM (◯), 0.05 mM (■), 0.1 mM (▲) and 0.5 mM (▼) DEPC. The vesicles were composed of PC:PS (1:3) and were prepared in 20 mM MES, 30 mM Tris buffer, pH 6.0, at a final phospholipid concentration of 0.1 mM. VSV-induced membrane fusion was measured by the decrease in the Rh-PE/NBD-PE fluorescence ratio after addition of the virus in a final protein concentration of 5 μg/ml. The samples were excited at 465 nm and the fluorescence intensities were collected at 530 and 590 nm for NDB-PE and Rh-PE, respectively. (b) Titers of unmodified VSV or VSV treated with different concentrations of DEPC were measured in BHK_{21} cells by $TCID_{50}$. Data shown correspond to the results of four independent experiments.

into the cytoplasm. To quantify the VSV-induced membrane fusion after virus modification with DEPC, we used a liposome fusion assay based on NBD-PE/Rh-PE energy transfer (Struck et al., 1981). The addition of the untreated virus to the vesicles at pH 6.0 induced a decrease in the Rh-PE/NBD-PE fluorescence ratio that indicates an effective membrane fusion process (Fig. 1a). In contrast, DEPC treatment inhibited membrane fusion mediated by the virus in a concentration-dependent manner. To address whether DEPC treatment also decreases viral infectivity, we measured viral titers after treatment with different DEPC concentrations. Although the effect on viral titers was less pronounced than on membrane fusion after treatment with 0.05 and 0.1 mM DEPC, the treatment with 0.5 mM was sufficient to completely abolish VSV infectivity (Fig. 1b). Virus treated with the vehicle alone showed no change on the viral titer, excluding the possibility that the viral manipulation during the DEPC treatment decreased the viral titer (not shown).

To investigate the effect of DEPC treatment on viral replication, the viral protein synthesis and the viral titers recovered in the culture medium at different times after infection were measured (Fig. 2). When VSV was added to the culture medium at a MOI of 0.1, the release of viral progeny from BHK_{21} cells was maximal at 15–20 h after infection (Fig. 2a). Virus treatment with 0.1 and 0.5 mM DEPC abolished completely the production of virus progeny in the cultured cells, while treatment with 0.05 mM DEPC did not affect viral replication (Fig. 2b). Although virus growth was not observed for the sample treated with 0.1 mM DEPC, this sample did give an infectious titer of approximately 10^5 $TCID_{50}$/ml (Fig. 1b). This fact might be explained by the absence of infectious virus in the inoculum after the dilution required to normalize the number of total particles to that corresponding to the MOI of 0.1 used for the untreated sample inoculum (see Section 2). To monitor viral protein synthesis we performed an immunoblotting using anti-G protein antibody (Fig. 2c). G protein expression correlates to the appearance of viral progeny in the culture medium of the infected cells. It was maximal at 20 h after the infection and it was inhibited when the virus was treated with 0.1 and 0.5 mM DEPC. Treatment with 0.05 mM DEPC led to lower levels of G protein expression after 20 h of infection. The effect of VSV treatment with DEPC on the viral protein synthesis was confirmed by immunofluorescence (Fig. 2d). In cells incubated with the unmodified virus, G protein synthesis was clearly detected 12 h after infection, with the fluorescence staining particularly concentrated around the nucleus. On the other hand, when the virus was pretreated with 0.5 mM DEPC, no staining was observed in the cells.

3.2. *DEPC is a safe approach for inactivating viruses*

To be considered a safe method for viral inactivation, it is imperative that the infectivity is not restored in any condition. Hydroxylamine is a compound that specifically reverses DEPC modification of His residues by removing the carbethoxy group from imidazole group (Miles, 1977). Although the inhibition of VSV-induced fusion by virus treatment with 0.02 mM DEPC was reverted by incubation of the modified virus with hydroxylamine at a final concentration of 400 mM (Carneiro et al., 2003), fusion and infectivity were not restored after hydroxylamine treatment, even when higher concentrations of hydroxylamine or longer incubation periods were tested (Table 1).

Another concern is the possible cytotoxicity of DEPC. However, it is important to point out that free DEPC is very unstable in aqueous solution, being rapidly hydrolyzed (Berger, 1975; Miles, 1977), which suggests that no free DEPC would be present in the inactivated virus preparation. Indeed, time course of DEPC hydrolysis in PBS, pH 7.4, the buffer solution used to perform viral inactivation, revealed a half-time of 5 min (data not shown).

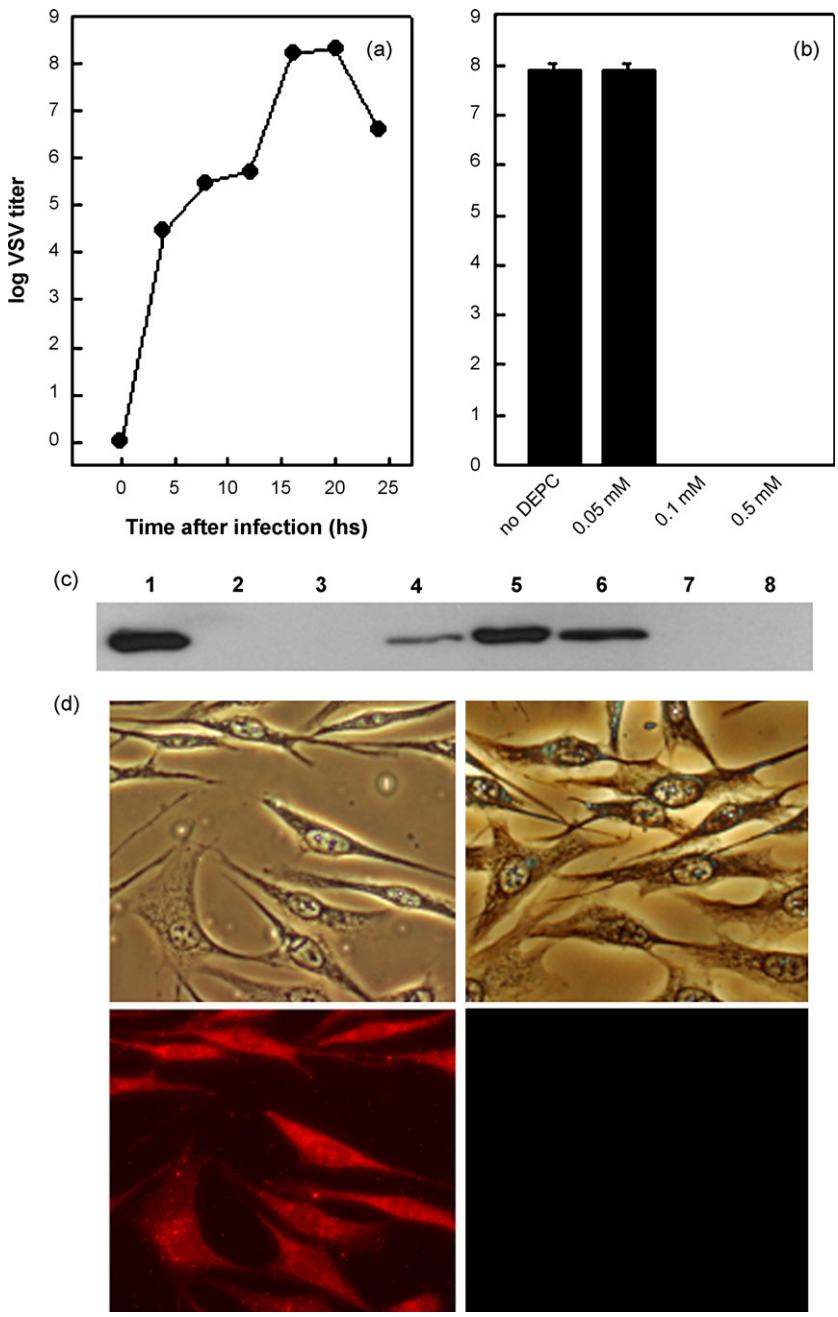

Fig. 2. Viral replication is inhibited by virus modification with DEPC. (a) Virus progeny released from BHK_{21} infected with unmodified VSV was followed by titrating the culture supernatants. (b) Virus release in supernatants of BHK_{21} cultures 20 h after incubation with control VSV or VSV treated with 0.05, 0.1 and 0.5 mM DEPC were compared. Data shown correspond to the results of four independent experiments. (c) Lysates from BHK_{21} cells were prepared for immunoblotting with monoclonal antibody against G protein. Purified VSV (100 ng) was used as positive control (lane 1). Lysates were prepared from non-infected cells (lane 2); from cells infected with unmodified VSV after 4 h (lane 3), 12 h (lane 4) and 20 h (lane 5); and from cells after 20 h of incubation with VSV treated with 0.05 mM DEPC (lane 6), 0.1 mM DEPC (lane 7) and 0.5 mM DEPC (lane 8). (d) BHK_{21} cells were infected with unmodified VSV (left) or VSV treated with 0.5 mM DEPC (right) and were visualized by phase-contrast (top) or by immunofluorescence using a VSV G protein monoclonal antibody (bottom) after 12 h. Magnification was 400×.

3.3. Treatment with DEPC abolishes VSV pathogenesis in mice

To determine the effect of treatment with DEPC on the pathogenesis of VSV, the survival rate of mice inoculated intranasally with VSV unmodified or treated with different concentrations of DEPC (Fig. 3) and the intracerebral inflammatory response to the virus (Fig. 4) were analyzed. It has been shown that when VSV is applied to the nasal neuroepithelium, it initially replicates in olfactory receptor neurons, and then it is transmitted along the olfactory nerve to the central nervous system (CNS) within 12 h (Reiss et al., 1998). In the olfactory bulb, the virus replicates invasively through the layers of the olfactory bulb, reaching the cerebral ventricles by days 4–5 post-infection, and the hindbrain by day 8 post-infection. In mice, infection causes encephalitis and may result in a 50% mortality rate when 2×10^6

Table 1
Effect of hydroxylamine on VSV inactivation and fusion

Treatment	Titer ($TCID_{50}$/ml)	Fusion index
Unmodified	1.70×10^{11}	17.2
DEPC 0.5 mM	$<10^{2}$ [a]	0.69
DEPC 0.5 mM + NH_2OH 0.4 M, 30 min	$<10^{2}$ [a]	0.89
DEPC 0.5 mM + NH_2OH 0.4 M, 2 h	$<10^{2}$ [a]	ND [b]
DEPC 0.5 mM + NH_2OH 1.2 M, 2 h	$<10^{2}$ [a]	ND [b]
Unmodified + NH_2OH 0.4 M	2.15×10^{9}	ND [b]
Unmodified + NH_2OH 1.2 M	$<10^{2}$ [a]	ND [b]

[a] 10^2 was the initial dilution required for avoiding hydroxylamine toxicity to cells.
[b] ND: not determined.

infectious units of VSV are inoculated intranasally (Reiss et al., 1998). Fig. 3 shows that we observed a survival rate of approximately 45% 7 days after mice inoculation with unmodified VSV, a result compatible with the literature. A similar survival profile was obtained when VSV was treated with 0.05 mM DEPC, while a mortality of 35% was observed for mice inoculated with the 0.1 mM treated sample. Such mortality rate shows that the mouse model is really sensitive to VSV infection since in this case the number of infectious particles inoculated was very low (the amount of infectious virus injected in the 0.1 mM treated sample was approximately 20 virions assuming an approximate 5log drop in titer due to treatment with this DEPC concentration, as shown in Fig. 1b). In contrast, for the groups inoculated with VSV treated with 0.2 and 0.5 mM DEPC the mortality rate was null. To confirm the viral inactivation in vivo, we performed pathological analysis of the brains of the infected animals with hematoxylin and eosin stain. In mice infected with

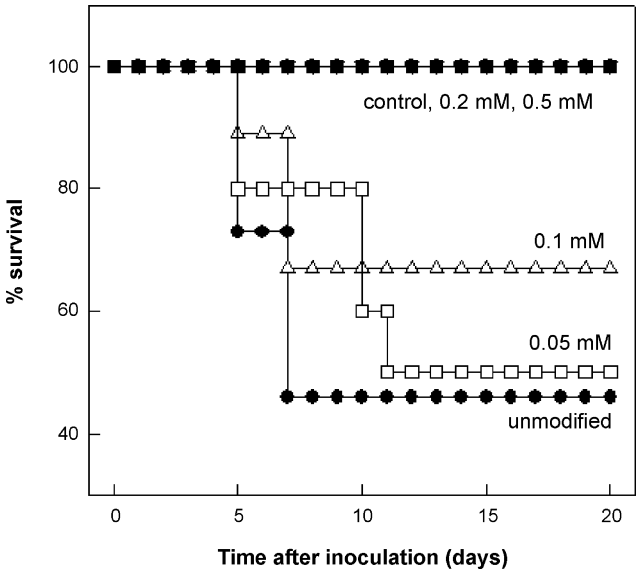

Fig. 3. Survival of BALB/c mice. BALB/c mice (10 per group) were inoculated intranasally with unmodified VSV (●) or VSV treated with 0.05 mM (□), 0.1 mM (△), 0.2 mM (▲) and 0.5 mM (▼) DEPC. The mortality rate was evaluated daily during 3 weeks. The control group was inoculated with PBS containing 0.5 mM DEPC (■).

unmodified VSV, we observed CNS inflammation, with complete destruction of the normal olfactory bulb parenchyma, and the presence of numerous neutrophiles at subpial region and in the lateral ventricles, characterizing viral meningitis and ventriculitis (Fig. 4a and c). However, brain from mice inoculated with VSV modified with 0.5 mM DEPC showed no inflammation (Fig. 4b and d).

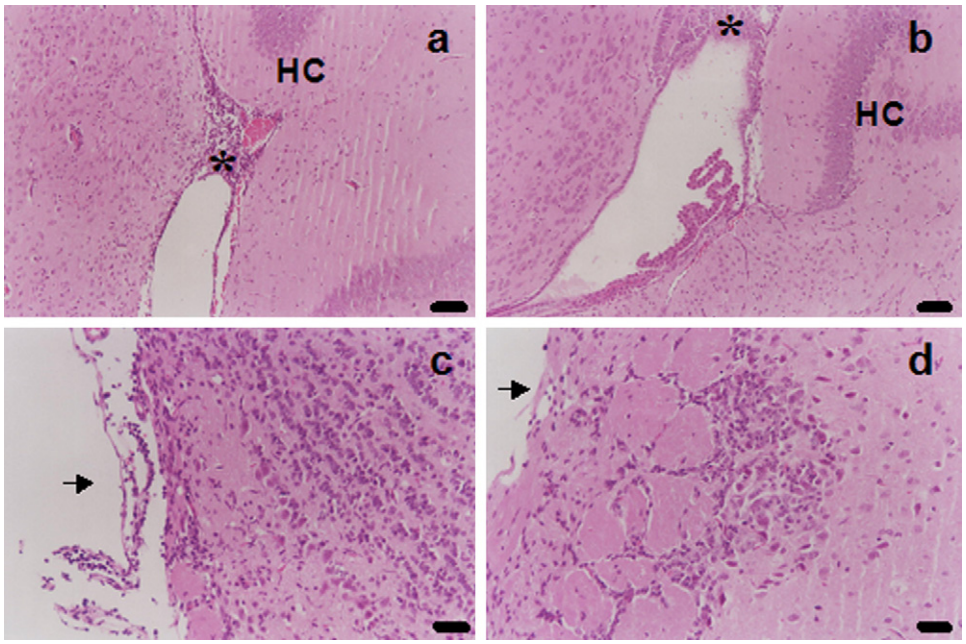

Fig. 4. DEPC-treated VSV does not cause viral encephalitis. Sections of brains showing the lateral ventricle (a and b) and the olfactory bulb (c and d) of mice infected with VSV (a and c) or VSV treated with 0.5 mM DEPC (b and d). In panels (a) and (c), there is a typical inflammatory infiltrate in the lateral ventricle, characterizing ventriculitis (*), and in subpial region of olfactory bulb (arrow), which is not observed in equivalent regions at panels (b) (*) and (d) (arrow). HC: hippocampus (A/B line = 50 mm); (C/D line = 12.5 mm).

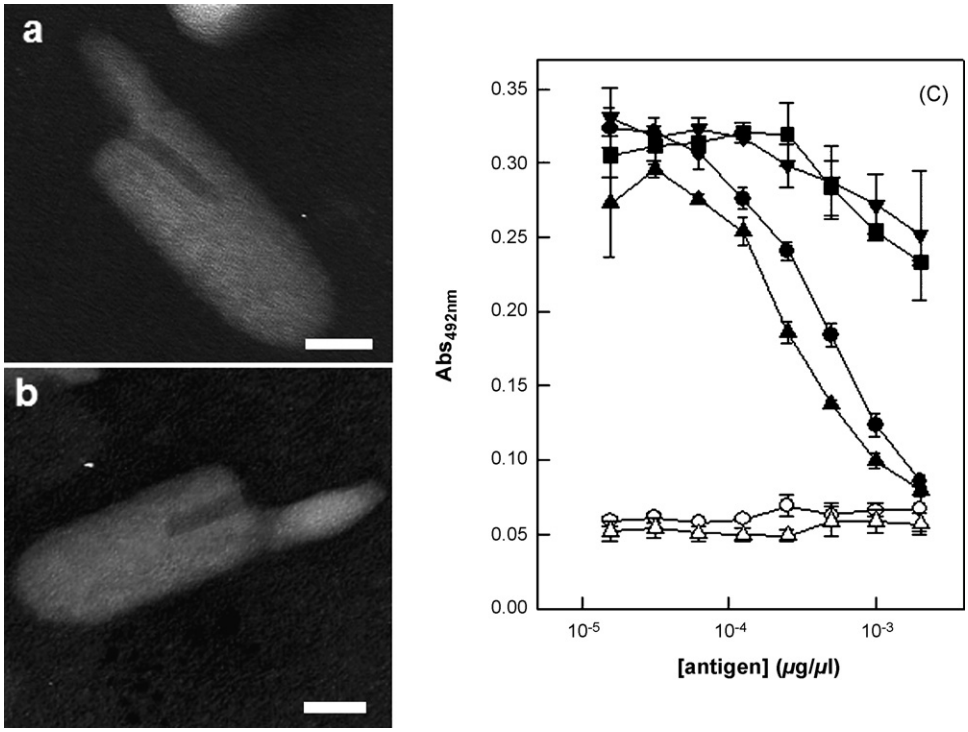

Fig. 5. Structural preservation of VSV after modification with DEPC. Transmission electron micrographs of (a) unmodified VSV, and (b) VSV treated with 0.5 mM of DEPC (bar = 50 nm). (c) Inhibition of binding of an immune serum against untreated VSV to plates coated with VSV by VSV modified with 0.5 mM DEPC (▲), or boiled (denaturated) VSV (■), assessed in a competitive ELISA. The maximal binding inhibition profile was determined using the untreated virus (●) as competition antigen, and bovine albumin (▼) was used as negative control. Unspecific binding of VSV (◯) or VSV treated with 0.5 mM DEPC (△) to sera was discarded using pre-immune sera.

3.4. Treatment with DEPC does not alter VSV structure

Transmission electron microscopy revealed that virus treated with 0.5 mM DEPC showed the same morphology of the unmodified VSV, suggesting that the structure of the inactivated virus was preserved (Fig. 5a and b). The preservation of G protein antigenic domains after DEPC treatment was analyzed by a competition ELISA (Fig. 5c). VSV modified with 0.5 mM DEPC bound to an immune serum against unmodified VSV with the same avidity as the unmodified virus. In contrast, virus denatured by boiling presented the same competitive activity as bovine albumin. These results show a clear difference between the antigenic properties of the DEPC-treated and heat-denatured viruses, although they are still preliminary to assure that the antigenic properties are completely preserved after DEPC treatment.

4. Discussion

In this study, we showed that treatment of VSV with DEPC results in a complete virus inactivation. We observed in cell culture that infectivity and viral replication were abolished by viral treatment with 0.5 mM DEPC and were partially inhibited at lower concentrations. Moreover, DEPC treatment also abolished VSV lethality in mice. The fact that DEPC is very hydrophilic (Miles, 1977) suggests that it should not be readily transported across the membrane. This was supported experimentally by Spires and Begenisich (1990), who showed different effects of DEPC on neurons when it was added to the intra- or to the extracellular media. Thus viral treatment with DEPC would not modify the enzymes located inside the virus particle, and the main mechanism of VSV inactivation by DEPC may reside in the reaction of this compound with the viral glycoprotein. In a previous study, we showed that 0.02 mM DEPC specifically modified G protein His residues, inhibiting pH-induced conformational changes on G protein and the fusion reaction catalyzed by the virus (Carneiro et al., 2003). However, we cannot exclude the possibility that other residues besides His could be modified after virus treatment with the higher DEPC concentration used here, since fusion and inactivation were not restored by incubation of the modified virus with hydroxylamine.

The membrane of some enveloped viruses fuses directly with the host cell plasma membrane through a pH-independent reaction, which is driven by virus binding to their cell receptor. On the other hand, many other enveloped viruses enter into the cells by the endocytic pathway and, for them, the membrane fusion reaction depends on the acidification of the endosomal medium. In this case, the low pH triggers conformational changes in the viral glycoproteins necessary for their conversion to the fusogenic state. For many viruses studied so far, the pH thresholds for fusion range between 5.0 and 6.5 (Chan and Kim, 1998; Gaudin et al., 1991; White et al., 1981), suggesting that His protonation (pKa ∼ 6.0) might be a more general requirement for the conversion of viral glycoprotein from the non-fusogenic to the fusogenic conformation. However, it could not be discarded that His residues of any viral protein (even from viruses that fuse directly to plasma membrane or non-enveloped viruses) may be

necessary for other events during the infection cycle, and then their modification with DEPC could inhibit infectivity through a mechanism different from fusion inhibition.

Other three compounds described previously promote viral inactivation by inhibiting membrane fusion: cyanovirin-N (Dey et al., 2000), hypericin and rose bengal (Lenard et al., 1993; Lenard and Vanderoef, 1993). Fusion inhibition due to the treatment of virus particles with hypericin or rose bengal results from the cross-linking of viral membrane proteins. The molecular mechanism of fusion inhibition promoted by cyanovirin-N involves physical interactions with gp120 envelope proteins (Boyd et al., 1997). Further studies on this mechanism revealed that cyanovirin-N binds to high-mannose oligosaccharides on gp120 (Bewley and Otero-Quintero, 2001; Bolmstedt et al., 2001; Shenoy et al., 2001). Cyanovirin-N was also shown to be potently active against other enveloped viruses containing similar oligosaccharides (Barrientos et al., 2003; Dey et al., 2000; O'Keefe et al., 2003). The immunogenic properties of virus inactivated by these compounds have not yet been evaluated.

In the past, the basic mechanism of enveloped viruses inactivation was to inhibit the virus entry in host cells at the adsorption stage, e.g., formalin (Bachmann et al., 1993), detergent (Seitz et al., 2002) and UV light (Bay and Reichmann, 1979). However, these inactivation procedures drastically impair induction of neutralizing IgG responses for most viruses (Bachmann et al., 1994), since these treatments led to the denaturation of viral surface proteins.

The use of DEPC for virus inactivation opens new possibilities for the development of safe vaccines. First, the inactivation by this compound is stable, since it covalently modifies histidines. Second, our present data indicate that DEPC treatment seems to preserve VSV structure. Ultrastructural morphology analyses showed that VSV treated with DEPC is similar to unmodified VSV. Furthermore, in marked contrast to virus inactivated by heat, DEPC-treated virus was recognized by antibodies against the unmodified VSV with the same avidity. However, although this data is suggestive that inactivated virus preserves the antigenic properties of the surface G proteins, further work is needed to unequivocally show that virus antigenicity is not altered, including studies on its reactivity against a panel of monoclonal antibodies. Nevertheless, the maintenance of conformation integrity in DEPC-inactivated virions suggests that such virions may be a useful in the pursuit of a potential vaccine antigen.

Acknowledgements

We thank Adriana Santos de Melo for technical assistance, Dr. Ada M.B. Alves and Maurício R.M.P. Luz for helpful suggestions and Dr. Sergio T. Ferreira for the use of the fluorescence microscope.

This work was supported by grants from Conselho Nacional de Desenvolvimento Científico e Tecnológico (CNPq), Centro Argentino-Brasileiro de Biotecnologia (CABBIO) and Fundação Carlos Chagas Filho de Amparo à Pesquisa do Estado do Rio de Janeiro (FAPERJ).

References

Bachmann, M.F., Kundig, T.M., Kalberer, C.P., Hengartner, H., Zinkernagel, R.M., 1993. Formalin inactivation of vesicular stomatitis virus impairs T-cell- but not T-help-independent B-cell responses. J. Virol. 67, 3917–3922.

Bachmann, M.F., Kundig, T.M., Hengartner, H., Zinkernagel, R.M., 1994. Regulation of IgG antibody titers by the amount persisting of immune-complexed antigen. Eur. J. Immunol. 24, 2567–2570.

Barrientos, L.G., O'Keefe, B.R., Bray, M., Sanchez, A., Gronenborn, A.M., Boyd, M.R., 2003. Cyanovirin-N binds to the viral surface glycoprotein, GP1,2 and inhibits infectivity of ebola virus. Antiviral Res. 58, 47–56.

Bay, P.H., Reichmann, M.E., 1979. UV inactivation of the biological activity of defective interfering particles generated by vesicular stomatitis virus. J. Virol. 32, 876–884.

Berger, S.L., 1975. Diethyl pyrocarbonate: an examination of its properties in buffered solutions with a new assay technique. Anal. Biochem. 67, 428–437.

Bewley, C.A., Otero-Quintero, S., 2001. The potent anti-HIV protein cyanovirin-N contains two novel carbohydrate binding sites that selectively bind to Man(8) D1D3 and Man(9) with nanomolar affinity: implications for binding to the HIV envelope protein gp120. J. Am. Chem. Soc. 123, 3892–3902.

Bhattacharyya, D.K., Bandyopadhyay, U., Banerjee, R.K., 1992. Chemical and kinetic evidence for an essential histidine in horseradish peroxidase for iodide oxidation. J. Biol. Chem. 267, 9800–9804.

Bolmstedt, A.J., O'Keefe, B.R., Shenoy, S.R., McMahon, J.B., Boyd, M.R., 2001. Cyanovirin-N defines a new class of antiviral agent targeting N-linked, high-mannose glycans in an oligosaccharide-specific manner. Mol. Pharmacol. 59, 949–954.

Boyd, M.R., Gustafson, K.R., McMahon, J.B., Shoemaker, R.H., O'Keefe, B.R., Mori, T., Gulakowski, R.J., Wu, L., Rivera, M.I., Laurencot, C.M., Currens, M.J., Cardellina, I.J.H., Buckheit, R.W., Nara, P.L., Pannell, L.K., Sowder, I.R.C., Henderson, L.E., 1997. Discovery of cyanovirin-N, a novel human immunodeficiency virus-inactivating protein that binds viral surface envelope glycoprotein gp120: potential applications to microbicide development. Antimicrob. Agents Chemother. 41, 1521–1530.

Carneiro, F.A., Ferradosa, A.S., Da Poian, A.T., 2001. Low pH-induced conformational changes in vesicular stomatitis virus glycoprotein involve dramatic structure reorganization. J. Biol. Chem. 276, 62–67.

Carneiro, F.A., Bianconi, M.L., Weissmuller, G., Stauffer, F., Da Poian, A.T., 2002. Membrane recognition by vesicular stomatitis virus involves enthalpy-driven protein–lipid interactions. J. Virol. 76, 3756–3764.

Carneiro, F.A., Stauffer, F., Lima, C.S., Juliano, M.A., Juliano, L., Da Poian, A.T., 2003. Membrane fusion induced by vesicular stomatitis virus depends on histidine protonation. J. Biol. Chem. 278, 13789–13794.

Chan, D.C., Kim, P.S., 1998. HIV entry and its inhibition. Cell 93, 681–684.

Da Poian, A.T., Gomes, A.M.O., Oliveira, R.J.N., Silva, J.L., 1996. Migration of vesicular stomatitis virus glycoprotein to the nucleus of infected cells. Proc. Natl. Acad. Sci. U.S.A. 93, 8268–8273.

Da Poian, A.T., Gomes, A.M.O., Coelho-Sampaio, T., 1998. Kinetics of intracellular viral disassembly and processing probed by Bodipy fluorescence dequenching. J. Virol. Methods 70, 45–58.

Dey, B., Lerner, D.L., Lusso, P., Boyd, M.R., Elder, J.H., Berger, E.A., 2000. Multiple antiviral activities of cyanovirin-N: blocking of human immunodeficiency virus type 1 gp120 interaction with CD4 and coreceptor and inhibition of diverse enveloped viruses. J. Virol. 74, 4562–4569.

Dzhandzhugazyan, K.N., Plesner, L., 2000. Diethyl pyrocarbonate inactivates CD39/ecto-ATPDase by modifying His-59. Biochim. Biophys. Acta 1466, 267–277.

Eckert, D.M., Kim, P.S., 2001. Mechanisms of viral membrane fusion and its inhibition. Annu. Rev. Biochem. 70, 777–810.

Gaudin, Y., Tuffereau, C., Segretain, D., Knossow, M., Flamand, A., 1991. Reversible conformational changes and fusion activity of rabies virus glycoprotein. J. Virol. 65, 4853–4859.

Hernandez, L.D., Hoffman, L.R., Wolfsberg, T.G., White, J.M., 1996. Virus–cell and cell–cell fusion. Annu. Rev. Cell Dev. Biol. 12, 627–661.

Lenard, J., Rabson, A., Vanderoef, R., 1993. Photodynamic inactivation of infectivity of human immunodeficiency virus and other enveloped viruses using hypericin and rose bengal: inhibition of fusion and syncytia formation. Proc. Natl. Acad. Sci. U.S.A. 90, 158–162.

Lenard, J., Vanderoef, R., 1993. Photoinactivation of influenza virus fusion and infectivity by rose bengal. Photochem. Photobiol. 58, 527–531.

Letchworth, G.J., Rodriguez, L.L., Del C. Barrera, J., 1999. Vesicular stomatitis. Vet. J. 157, 239–260.

Miles, E.W., 1977. Modification of histidyl residues in proteins by diethylpyrocarbonate. Methods Enzymol. 47, 431–442.

O'Keefe, B.R., Smee, D.F., Turpin, J.A., Saucedo, C.J., Gustafson, K.R., Mori, T., Blakeslee, D., Buckheit, R., Boyd, M.R., 2003. Potent anti-influenza activity of cyanovirin-N and interactions with viral hemagglutinin. Antimicrob. Agents Chemother. 47, 2518–2525.

Reed, L.J., Muench, H., 1938. A simple method of estimating fifty per cent endpoints. Am. J. Hyg. 27, 493–497.

Reiss, C.S., Plakhov, I.V., Komatsu, T., 1998. Viral replication in olfactory receptor neurons and entry into the olfactory bulb and brain. Ann. N. Y. Acad. Sci. 855, 751–761.

Seitz, H., Blumel, J., Schmidt, I., Willkommen, H., Lower, J., 2002. Comparable virus inactivation by bovine or vegetable derived Tween 80 during solvent/detergent treatment. Biologicals 30, 197–205.

Shenoy, S.R., O'Keefe, B.R., Bolmstedt, A.J., Cartner, L.K., Boyd, M.R., 2001. Selective interactions of the human immunodeficiency virus-inactivating protein cyanovirin-N with high-mannose oligosaccharides on gp120 and other glycoproteins. J. Pharmacol. Exp. Ther. 297, 704–710.

Shriver, Z., Hu, Y., Sasisekharan, R., 1998. Heparinase II from Flavobacterium heparinum. Role of histidine residues in enzymatic activity as probed by chemical modification and site-directed mutagenesis. J. Biol. Chem. 273, 10160–10167.

Skehel, J.J., Wiley, D.C., 2000. Receptor binding and membrane fusion in virus entry: the influenza hemagglutinin. Annu. Rev. Biochem. 69, 531–569.

Spires, S., Begenisich, T., 1990. Modification of potassium channel kinetics by histidine-specific reagents. J. Gen. Physiol. 96, 757–775.

Struck, D.K., Hoekstra, D., Pagano, R.E., 1981. Use of resonance energy transfer to monitor membrane fusion. Biochemistry 20, 4093–4099.

White, J., Matlin, K., Helenius, A., 1981. Cell fusion by Semliki Forest, influenza, and vesicular stomatitis viruses. J. Cell Biol. 89, 674–679.

2.2.3 Artigo 5

New chemical method of viral inactivation for vaccine development based on membrane fusion inhibition

Fausto Stauffer, Joari M. Miranda, Marcos C. Schechter, Fernando A. Queiroz, Nathalia O. Santos, Ada M.B. Alves e Andrea T. Da Poian

Submetido em 2007 ao periódico

Vaccine

Available online at www.sciencedirect.com
ScienceDirect
Vaccine 25 (2007) 7885–7892
Vaccine
www.elsevier.com/locate/vaccine

New chemical method of viral inactivation for vaccine development based on membrane fusion inhibition

Fausto Stauffer [a], Joari De Miranda [a], Marcos C. Schechter [a], Fernando A. Queiroz [a], Nathalia O. Santos [a], Ada M.B. Alves [b], Andrea T. Da Poian [a,*]

[a] *Instituto de Bioquímica Médica, Universidade Federal do Rio de Janeiro, Rio de Janeiro, RJ 21941-590, Brazil*
[b] *Laboratório de Imunopatologia, Instituto Oswaldo Cruz, Fundação Oswaldo Cruz, Rio de Janeiro, RJ 21040-900, Brazil*

Received 10 July 2007; received in revised form 30 August 2007; accepted 3 September 2007
Available online 29 September 2007

Abstract

Membrane fusion is an essential step in the entry of enveloped viruses into their host cells. This process is triggered by conformational changes in viral surface glycoproteins. We have demonstrated previously that modification of vesicular stomatitis virus (VSV) with diethylpyrocarbonate (DEPC) abolished the conformational changes on VSV glycoprotein and the fusion reaction induced by the virus. Moreover, we observed that viral treatment with DEPC inactivates the virus, preserving the conformational integrity of its surface proteins. In the present work, we evaluated the potential use of DEPC as a viral inactivating chemical agent for the development of useful vaccines. Pathogenicity and viral replication in Balb/c mice were abolished by viral treatment with 0.5 mM DEPC. In addition, antibodies elicited in mice after intraperitoneal immunization with DEPC-inactivated VSV mixed with adjuvants were able to recognize and neutralize the native virus and efficiently protected animals against the challenge with lethal doses of VSV. These results together suggest that viral inactivation with DEPC seems to be a suitable method for the development of safe vaccines.

Keywords: Viral inactivation; Diethylpyrocarbonate; Vesicular stomatitis virus

1. Introduction

Vaccination is a valuable public health tool, being a safe and cost-effective strategy for controlling infectious diseases [1]. The progress in development and use of vaccines resulted in the decline and, in some cases, eradication of important infectious diseases, as smallpox [2]. Traditionally, the vaccines developed against viruses consist of attenuated or inactivated pathogens or subunits vaccines. Live attenuated vaccines are based on the attenuation of the pathogen until its virulence is greatly decreased but its immunogenicity is retained. Alternatively, inactivated vaccines consist of whole killed virus, while subunit vaccines are based on only one or few virus proteins. In the case of whole virus inactivated vaccines, the inactivation treatment through different processes (for review, see [3,4]) must assure that all virus particles are inactivated in order for the vaccine to be safe. Despite the advances in the field of immunology, molecular biology and genetics, viral inactivation remains an important procedure in basic research, since it is an easy and relatively cheap approach to produce new and safe vaccines.

The entry of enveloped viruses into a target cell always requires virus-mediated membrane fusion catalyzed by viral surface glycoproteins [5–7]. Virus-induced fusion may occur through two different general mechanisms: (i) fusion between viral envelope and host cell plasma membrane after virus interaction with its cellular receptor, or (ii) fusion with the endosomal membrane, after virus internalization by receptor-mediated endocytosis. In the latter case, the decrease in the pH of the endosomal medium triggers conformational changes in viral glycoproteins. This mechanism seems to be conserved

* Corresponding author. Tel.: +55 21 22706264; fax: +55 21 22708647.
E-mail address: dapoian@bioqmed.ufrj.br (A.T. Da Poian).

0264-410X/$ – see front matter © 2007 Elsevier Ltd. All rights reserved.
doi:10.1016/j.vaccine.2007.09.025

among several viral families what makes the fusion process a potentially attractive target for viral inactivation approaches.

VSV, a member of *Rhabdoviridae* family, is composed by a helical ribonucleocapsid surrounded by a lipid bilayer covered with trimers of a single type of an integral glycoprotein, named G protein. VSV enters into the cell by endocytosis followed by low-pH-induced membrane fusion [8,9]. Cell recognition and fusion are mediated by the surface glycoprotein G. We have been studying the conformational changes in VSV G protein and its interaction with the target membrane during cellular recognition and fusion events [10,11]. The observation of a dramatic reorganization in G protein structure at a very narrow pH range (between pH 5.8 and 6.2) led us to propose a crucial role for the protonation of histidine residues ($pK_a \sim 6.0$) of VSV G protein in membrane fusion mediated by the virus [12]. Indeed, using diethylpyrocarbonate (DEPC) to modify His residues of G protein, we showed that VSV-induced fusion was driven by His protonation at the pH range of endosomal medium. DEPC is a widely used tool in chemical modification of proteins because of the high selectivity of the reagent to histidyl residues [13]. This compound covalently modifies His and makes them unable to be protonated. Recently, our group has shown that VSV treatment with DEPC inactivates the virus [14]. Moreover, the inactivated virus seemed to preserve the antigenic properties of the surface G proteins [14].

Based on these evidences, in the present work, we evaluated the potential use of DEPC as a viral inactivating chemical agent for the development of useful vaccine antigens. The results demonstrated that, in the viral model studied, virus treatment with DEPC was able to abolish viral infectivity and pathogenicity, to elicit neutralizing antibodies in mice and to confer protection in these animals against challenge using lethal doses of VSV.

2. Materials and methods

2.1. Virus propagation and purification

VSV Indiana was propagated in monolayer cultures of BHK21 cells grown at 37 °C in petri dishes containing Dulbecco's modified Eagle medium supplemented with 10% fetal bovine serum, 100 μg/mL penicillin, 0.0085% streptomycin sulfate. When the cells reached confluence, the medium was removed, and the cell monolayer was infected with VSV at a multiplicity of infection of 0.1. The cultures were kept at 37 °C for 16–20 h and the virus were harvested and purified by differential centrifugation followed by equilibrium sedimentation in a sucrose gradient as described elsewhere [15]. Purified virions were stored at −70 °C.

2.2. Virus modification with DEPC

Diethylpyrocarbonate (DEPC) solutions were freshly prepared by dilution of the reagent in cold ethanol. The concentration of stock DEPC solution was determined by reaction with 10 mM imidazole [13]. VSV (13.75 mg/mL) was diluted in PBS, pH 7.4 to a final protein concentration of 1.375 mg/mL and incubated with 0.5 mM DEPC for 15 min at room temperature. For mouse immunization, the modified virus was further diluted to a final protein concentration of 0.08 mg/mL, leading to a DEPC concentration in the inoculum lower than 0.03 mM.

2.3. Immunofluorescence and determination of virus titers in mouse brain

Groups of three Balb/c mice (4-week-old) were inoculated intranasally with VSV or DEPC-inactivated VSV. Five days after inoculation, mice were sacrificed and perfused with normal saline (PBS) and brains were removed. For immunofluorescence, whole brains were embedded in cryoprotetion solution (Tissue-Tek OCT compound, Sakura, USA) and frozen at −70 °C. Then, serial sections of each brain were incubated with mouse monoclonal anti-VSV G protein antibody (Alpha Diagnostic Int., San Antonio, TX) diluted 1:200 in PBS containing 1% goat serum. As secondary antibody, FITC-labeled goat anti-mouse immunoglobulin G conjugate was used at 1:400 dilution (Sigma Chemical Co.). Finally, slides were mounted with *N*-propil-galacto and examined with a Nikon epifluorescence microscope equipped for photomicroscopy. For determining viral titer, brains were homogenized and infectious particles of VSV in brain homogenates were quantified by $TCID_{50}$ on BHK21 cells. The cells were grown at 37 °C in 96-well plates until they reach the confluence. Samples were serially diluted 10-fold in culture medium, and 100 μL was added to cells in quadruplicate. Cells were cultured at 37 °C in 5% CO_2 for 24 h and stained with 0.2% crystal violet in 20% ethanol. The $TCID_{50}$ was calculated using the method described by Reed and Muench [16].

2.4. Breakdown of the blood brain barrier (BBB)

Groups of three Balb/c mice (4-week-old) were inoculated intranasally with VSV or DEPC-inactivated VSV. Five days after inoculation, mice were injected intraperitoneally with 200 μL of 2% Evans blue. One hour later, mice were sacrificed and perfused with normal saline (PBS). Brains were removed and photos were taken.

2.5. Mice immunization and challenge

Groups of 15 Balb/c mice (4-week-old) were inoculated by the intranasal (i.n.) or intraperitonial (i.p.) routes with VSV or DEPC-inactivated VSV, mixed or not with adjuvants. For i.n. immunization, mice were inoculated with 5 μL containing 4 μg of inactivated VSV diluted in PBS, mixed or not with 1 μg cholera toxin (CT). For i.p. immunization, mice were inoculated with 50 μL containing 4 μg of inactivated VSV diluted in PBS, mixed or not with 50 μL Freund's adjuvant.

Animals were separated in three groups, receiving one, two or three doses of the vaccine, 14 days apart. For i.n. or i.p. infection, mice were inoculated once with 2×10^6 $TCID_{50}$ VSV, diluted in 5 or 50 μL PBS, respectively. Blood was taken on day 4 after inoculation for measuring IgM response and on day 14 after each inoculation for measuring IgG response. Two weeks after the third i.p. dose, mice inoculated with DEPC-treated virus mixed with Freund's adjuvant were challenged with 2×10^4 $TCID_{50}$ of VSV. Survival rates and clinical signs of VSV infection (hyperexcitability, tremors, circling and paralysis) were recorded in the next 10 days. Animals were housed under pathogen-free conditions. For testing the durability of immune response, blood was taken once a month for the period of 1 year after the third i.p. immunization.

2.6. Antibody assays

The anti-VSV antibodies in mouse sera were detected by ELISA using VSV as solid-phase bound antigen. Briefly, ELISA microplates (Maxisorp, Nunc) were coated with 0.1 μg VSV at 4 °C. The plates were washed with PBS/0.05% Tween-20 and blocked with 2% milk powder in PBS/0.05% Tween-20 for 2 h at room temperature. After blocking, plates were washed as before, and incubated for 1 h at room temperature with serial dilutions (initial 1:50) of immune sera collected from immunized mice. Plates were then washed as before and bound IgG was detected by the addition of an anti-mouse horseradish peroxidase conjugate (1:5000 dilution) (Santa Cruz Biotechnology) followed by *o*-phenylenediamine (OPD) substrate as indicated by the manufacturer (Sigma Chemical Co.). The reaction was stopped with 3 M sulfuric acid and the optical density at 492 nm was determined in an ELISA reader. Titers were established as the reciprocal of serum dilution, which gave an absorbance above that of the respective pre-immune serum.

2.7. Serum neutralization test

The sera were initially heat inactivated for 30 min at 56 °C. Serial twofold dilutions in DMEM without FBS were mixed with equal volumes of unmodified VSV diluted to contain 10^3 infectious particles. The mixture was incubated for 90 min at 37 °C in an atmosphere with 5% CO_2. Then the serum–virus mixture was transferred onto BHK21 cell monolayers in 96-well plates. After incubation for 24 h at 37 °C, the monolayer was fixed and stained with 0.5% crystal violet. The 50% end-point dilution of each serum, corresponding to the dilution at which 50% of wells were completely protected from infection, was determined according to the Reed–Muench method [16].

2.8. Competition ELISA

ELISA microplates were coated with 0.1 μg VSV overnight at 4 °C. Plates were washed with PBS/0.05% Tween-20 and blocked with 2% milk powder in PBS/0.05% Tween-20 for 2 h at room temperature. After blocking, the plates were washed as before. Subsequently, immune serum collected from vaccinated mice (animals after three i.p. inoculation of 4 μg of DEPC-treated VSV mixed with adjuvant) was incubated at 37 °C for 1 h at a fixed dilution together with serial dilutions of unmodified VSV. As positive control, the immune serum collected from mice 7 days after i.n. inoculation of VSV was incubated with unmodified VSV in the same dilutions of the other incubation. Albumin at the same protein concentration was used with sera as a negative control. After incubation, samples were transferred to antigen-coated ELISA plates and incubated for 1 h at room temperature. Plates were washed as before and bound IgG was detected by addition of an anti-mouse horseradish peroxidase conjugate (1:5000 dilution) (Santa Cruz Biotechnology) followed by *o*-phenylenediamine (OPD) substrate as indicated by the manufacturer (Sigma Chemical Co.). The reaction was stopped with 3 M sulfuric acid and the optical density at 492 nm was determined in an ELISA reader.

3. Results

3.1. DEPC treatment abolishes VSV infectivity

To determine the effect of VSV treatment with DEPC in viral replication in mouse CNS, the viral protein synthesis in brain sections (Fig. 1a) and the viral titers in brain homogenates (Fig. 1b) from mice 5 days after nasal inoculation with unmodified or modified VSV were measured. Viral protein synthesis was followed by an immunofluorescence assay using an anti-G protein antibody (Fig. 1a). In brains from mice infected with unmodified VSV, we observed a great fluorescence staining, indicating the presence of G protein synthesis. On the other hand, when the virus was pretreated with 0.5 mM DEPC, no staining was observed in the brain. In addition, viral titer recovered from brains of mice inoculated with unmodified VSV was 10^5 $TCID_{50}$/mL, while no infectious particles were recovered from mice inoculated with treated VSV (Fig. 1b).

To further confirm that DEPC treatment abolishes VSV infectivity in mice, the integrity of blood brain barrier (Fig. 1c) and the survival rate (Fig. 1d) of mice inoculated intranasally with VSV unmodified or treated with DEPC were analyzed. We observed that VSV-infected mice showed disruption of the BBB, while mice inoculated with VSV treated with DEPC did not (Fig. 1c). Moreover, we observed a survival rate of approximately 45% 7 days after inoculation with unmodified VSV (Fig. 1d), which is in accordance to other reports [17]. In contrast, all animals inoculated with DEPC-treated VSV survived with no clinical signs of disease. Additionally, no death or clinical signs of chemical toxicity were recorded among the control group inoculated with PBS containing 0.5 mM DEPC.

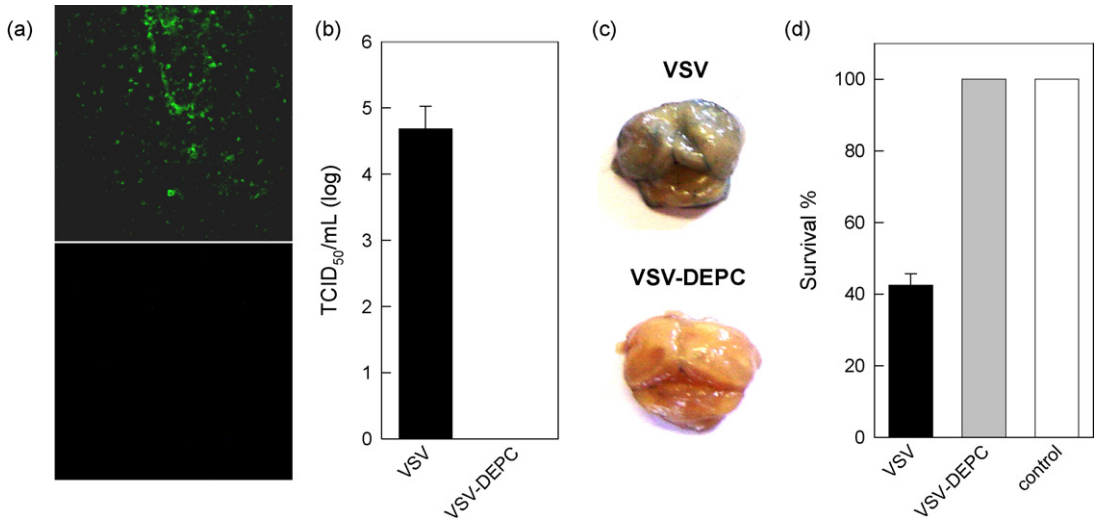

Fig. 1. Evaluation of the pathogenic potential of DEPC-treated VSV. (a) Mice were inoculated intranasally with unmodified VSV (top panel) or VSV treated with 0.5 mM DEPC (bottom panel) and after 5 days the brains were removed and an immunofluorescence using an anti-VSV G protein monoclonal antibody were performed in brain sections. Magnification was 200×. (b) Viral replication in mouse brain was determined by $TCID_{50}$ in brain homogenates on day 4 post-intranasal inoculation of VSV or DEPC-treated VSV. (c) Breakdown of the BBB following mouse inoculation with unmodified VSV (top panel) or DEPC-treated virus (bottom panel) was analyzed through whole brain staining with Evans blue after an i.p. inoculation of the dye. The brain was removed 1 h after dye inoculation from a mouse on day 5 post-inoculation. (d) BALB/c mice ($n = 10$ per group) were inoculated intranasally with unmodified VSV (black bar), VSV treated with 0.5 mM DEPC (gray bar) or PBS containing 0.5 mM DEPC (white bar) and mortality rates were evaluated 1 week after inoculation.

3.2. Inactivated VSV induces B-cell response

VSV is known to induce an antibody response with IgM peak around day 4, while specific IgG rises between days 6 and 8, peaking around day 14 [18,19]. To determine whether VSV inactivation with DEPC had an influence on the immunogenicity of viral antigens, the antibody response of BALB/c mice immunized with 4 μg of inactivated VSV was compared to that of mice infected with 2×10^6 $TCID_{50}$ VSV. Mice were inoculated intranasally or intraperitoneally. In the case of inactivated virus, animal groups received one, two or three doses given 2 weeks apart, combined or not with adjuvants. Blood samples were taken on day 4 after the first inoculation for the analysis of IgM response (Fig. 2) and 2 weeks after each immunization for the detection of IgG response (Fig. 3). DEPC inactivation led to a reduced IgM response, even in combination with adjuvants. Analysis of IgG response showed an induction of antibody titers. The IgG titers obtained after three doses of inactivated virus combined with adjuvant inoculated by the i.p. route were similar to that observed after i.n. inoculation of unmodified virus. This result confirmed that DEPC inactivation did not alter VSV immunogenicity. Time course of anti-VSV IgG response was analyzed after i.n and i.p. inoculation of DEPC-inactivated virus, revealing that antibody titers increased after each dose and remained stable in both cases (Fig. 4). IgG titers decreased approximately 50% 6 months after the third inoculation (30,573 ± 1643) and detectable titers were still observed after 1 year (14,629 ± 1360).

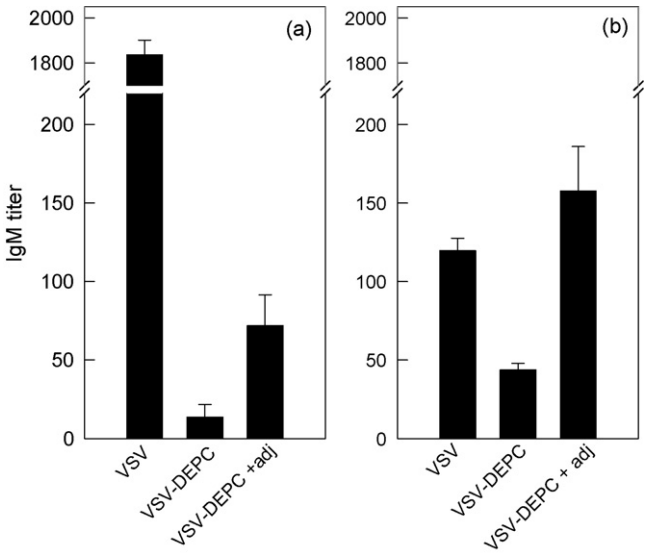

Fig. 2. Analysis of IgM response induced by DEPC-inactivated VSV. Mice were inoculated by the i.n. (a) or i.p. (b) routes with native or inactivated VSV, mixed or not with adjuvants ($n = 10$ per group). The cholera toxin (CT) and Freund's adjuvant were used as adjuvants for i.n. and i.p. administrations, respectively. IgM titers were determined by ELISA on day 4 after inoculation, using the native VSV as solid-phase bound antigen. Titers were established as the reciprocal serum dilutions that gave an absorbance above that of pre-immune sera.

3.3. VSV is efficiently recognized and neutralized by serum antibodies induced in vaccinated mice

In order to evaluate the effectiveness of the humoral immune response elicited in vaccinated mice, a neutralization assay (Fig. 5a) and a competition ELISA

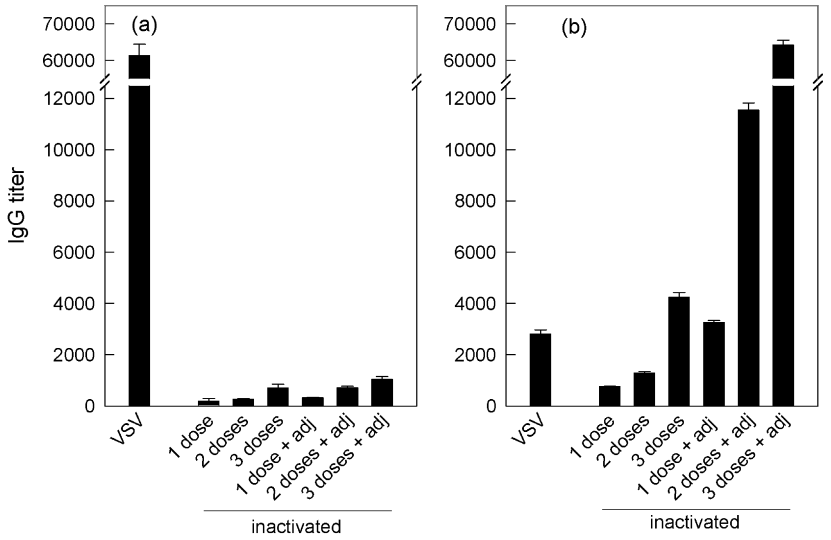

Fig. 3. Induction of IgG response induced by DEPC-inactivated VSV. Mice were inoculated by the i.n. (a) or i.p. (b) routes with native or inactivated VSV, mixed or not with adjuvants ($n = 10$ per group). The CT and Freund's adjuvant were used as adjuvants for i.n. and i.p. administrations, respectively. One, two or three doses were used in each group given 14 days apart, as shown in the figure. Sera were collected 14 days after each inoculation and IgG titers were determined by ELISA, using the native VSV as solid-phase bound antigen. Titers were established as the reciprocal serum dilutions that gave an absorbance above that of pre-immune sera.

(Fig. 5b) were performed. Fig. 5a shows that both sera obtained from mice inoculated with unmodified VSV (control) or inoculated with VSV treated with DEPC (vaccinated) presented similar neutralizing activity against unmodified VSV. Supporting this result, we observed in Fig. 5b that antibodies raised against VSV modified with 0.5 mM DEPC bound to VSV with the same avidity as the control serum, produced against the unmodified VSV. These results indicate that the antibodies elicited in vaccinated mice were able to recognize and neutralize VSV.

3.4. Immunized mice become protected against lethal VSV challenge

Mice immunized with three i.p. doses of DEPC-treated VSV mixed with Freund's adjuvant were challenged with a sub-lethal dose of VSV given by the intracerebral route and animals were monitored the next 10 days for mortality and clinical signs of disease (hyperexcitability, tremors, circling and paralysis). A 100% protection was observed in mice immunized with DEPC-inactivated VSV while only 30% of non-immunized animals survived after challenge

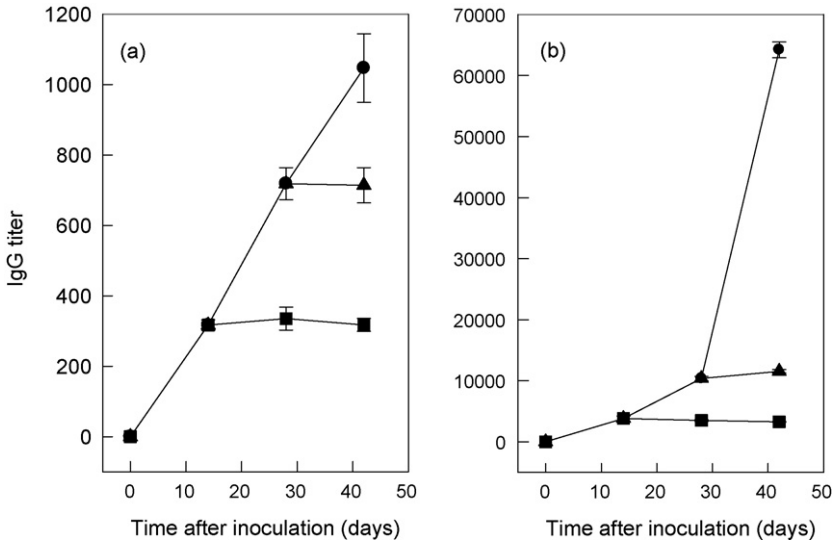

Fig. 4. Time course IgG response after intranasal or intraperitoneal immunization. Mice were inoculated intranasally (a) or intraperitoneally (b) with DEPC-inactivated VSV, mixed with the adjuvants cholera toxin (CT) and Freund's adjuvant, respectively ($n = 10$ per group). One (■), two (▲) or three (●) doses given 14 days apart were used for each group. Serum samples were collected 14 days after each inoculation and IgG titers were determined by ELISA, using the native VSV as solid-phase bound antigen. Titers were established as the reciprocal serum dilutions that gave an absorbance above that of pre-immune sera.

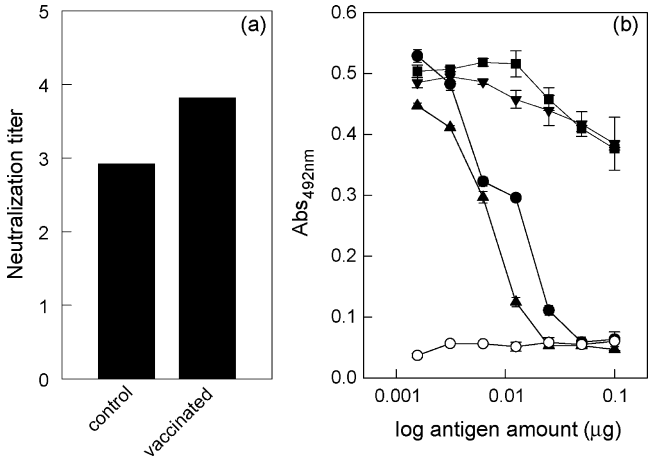

Fig. 5. Antibody recognition and neutralization of VSV. (a) Sera collected from mice inoculated with three i.p. doses of DEPC-treated VSV mixed with Freund's adjuvant (vaccinated) or from mice after i.n. inoculation of infectious VSV (control) were tested in a neutralization assay for VSV. Neutralizing titer, in a $\log_{10}$ scale, represent the highest serum dilution that reduced the number of virus plaques by 50%. (b) Competitive ELISA was used to compare the VSV binding avidity of antibodies elicited in mice immunized with native or DEPC-treated VSV. Immune sera collected from vaccinated mice (animals after three i.p. inoculation of DEPC-treated VSV mixed with adjuvant) (▲, ■) or mice inoculated intranasally with native VSV (●, ▼) were incubated at a fixed dilution together with serial dilutions of unmodified VSV (●, ▲) or bovine serum albumin as a control (▼, ■). As another control, pre-immune serum was incubated with serial dilutions of the native VSV (◯). Serum samples were then assayed in an IgG ELISA, using the native VSV as solid phase antigen.

(Fig. 6). Such results confirmed data presented above showing that the inactivation of VSV with DEPC maintained its immunogenicity and its capacity of inducing protection. Data collected from a group of challenge experiments suggest that protection was not achieved when the IgG titers were lower than 15,000 (not shown), suggesting that the three i.p. doses were necessary to generate immunity.

4. Discussion

Whole inactivated virions have been used successfully as vaccines for numerous viruses [20,21]. The technique mostly used for viral inactivation is the mild treatment of viruses with formalin or β-propiolactone. However, these methods have disadvantages as long periods of incubation for successful virus inactivation and toxicity of the compound to the host. Moreover, these inactivation procedures drastically impair induction of neutralizing IgG responses for most viruses [22], since these treatments led to the denaturation of viral surface proteins. Finally, there have been reports of failures on inactivation associated with both of these methodologies even in the recent past, predominantly with formaldehyde [23], which makes the discovery of new procedures and substances for the virus inactivation extremely relevant and important.

Recently, our group has shown that DEPC is a virus-inactivating compound that seemed to preserve the viral antigenic properties [14]. The mechanism of inactivation by DEPC may reside in the reaction of this compound with the viral glycoprotein, specifically modifying its His residues, since we have previously shown that His protonation is required for pH-induced conformational changes on VSV G protein necessary for the fusion reaction induced by the virus [12].

In the present report, we showed that the treatment of VSV with DEPC completely abolishes virus infectivity and pathogenicity in mice. When VSV is applied to the nasal neuroepithelium, it initially replicates in olfactory receptor neurons, and then it is transmitted along the olfactory nerve to the central nervous system (CNS) within 12 h [17]. In the olfactory bulb, the virus replicates invasively through the layers of the olfactory bulb, reaching the brain ventricles by day 4–5 post-infection, and the hindbrain by day 8 post-infection. In mice, infection causes encephalitis, usually due to the blood brain barrier (BBB) disruption, and may result in a 50% mortality rate when 2×10^6 infectious units of VSV are inoculated intranasally [17]. Thus, the absence of a pathogenic effect of DEPC-treated VSV inoculation was evaluated not only by its lethality in mice but also by the BBB integrity. All animals injected with DEPC-treated VSV survived after inoculation with no clinical signs. Furthermore, since dyes such as Evans blue, which are normally excluded from the brain by the intact BBB, are able to stain this organ when the integrity

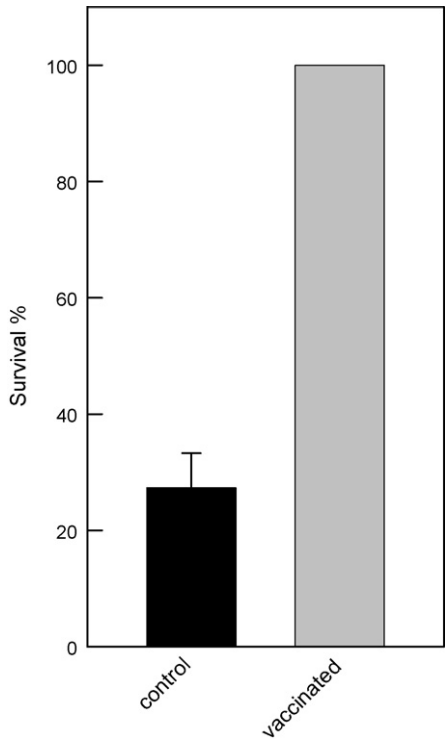

Fig. 6. Survival after challenge. Non-immunized mice (control) and animals inoculated with three i.p. doses of DEPC-treated VSV mixed with Freund's adjuvant (vaccinated) were challenged with an intracranial injection of 2×10^4 TCID50 of VSV, 2 weeks after the third dose. Survival rates were recorded 10 days after the challenge.

of the BBB is broken, native VSV or DEPC-treated VSV inoculated mice were injected with this dye and brain stainning was compared. Results revealed that the BBB integrity was maintained only in DEPC-treated VSV. Additionally, the presence of VSV in the central nervous system and virus antigens in brain sections were also investigated, showing that the treatment of VSV with DEPC completely abolished any replication of the virus in the brain of inoculated animals.

After the observation that DEPC-treated VSV had in fact became inactivated, the immunogenic characteristics of this virus were further evaluated. Mice inoculated only with DEPC-inactivated VSV presented low level of VSV-specific antibodies. Such results were already expected, since it is well known that inactivated vaccines, as well as subunit protein vaccines, usually induce a weak immune response when administered without adjuvants [24]. In order to increase the antibody response against DEPC-treated VSV, animals were immunized with a mixture of virus and adjuvants, the cholera toxin (CT) and Freund's adjuvant, for i.n. and i.p. immunizations, respectively. Both adjuvants enhanced the antibody response against inactivated VSV, although immunization with Freund's adjuvant induced higher levels of VSV-specific IgG. Cholera toxin was used in these experiments due to its high efficiency for the induction of systemic and mucosal immune responses [25,26]. However, the effect of such adjuvant was not as strong as the Freund's adjuvants for the systemic antibody response.

Although the differences in the magnitude of the humoral immune response induced with both adjuvants, in the two cases, the levels of specific-VSV antibodies were dose-dependent, with maximal IgG titers attained after the third virus dose. Furthermore, vaccination with three i.p. doses of DEPC-inactivated VSV mixed with Freund's adjuvant elicited specific antibody levels similar to those observed after the infection with non-inactivated VSV. Moreover, antibody titers remained high for the following 6 months, indicating that the administration of DEPC-inactivated VSV is able to induce a long-lasting immune response. Besides, these antibodies recognized the native VSV with the same avidity as antibodies raised against the unmodified virus and were able to efficiently neutralize the native virus in *in vitro* experiments. Such results indicated that the treatment of VSV with DEPC did not modify conformational structures of VSV proteins, preserving the immunogenic characteristics of native VSV. In order to confirm and extend these observations, the capacity of DEPC-inactivated VSV in providing protection against the challenge with infectious VSV was further analyzed. All the animals vaccinated with inactivated virus survived after challenge, while 75% of control animals died after inoculation with unmodified VSV.

All these results indicate that viral inactivation with DEPC seems to be a suitable method for the development of safe vaccines by multiples reasons: (a) the inactivation by this compound is stable, since it covalently modifies His residues in viral proteins [13]; (b) although DEPC is a cytotoxic agent, it is important to point out that free DEPC is very unstable in aqueous solution, being rapidly hydrolyzed [13,27], what assures that no free DEPC would be present in the inactivated virus preparation; (c) previous data indicated that DEPC treatment seems to preserve the structure of viral proteins [14]; (d) our present data indicate that the antibodies elicited by immunization with DEPC-inactivated VSV were able to recognize and neutralize the native virus and efficiently protect animals against the challenge with native virus.

However, it is important to point out that the proposed approach is limited because it should only work when (a) the uptake of virus involve the low pH-dependent endocytosis entry pathway and the reorganization of viral glycoproteins implies the protonation of histidine residues and (b) antibody response alone will be sufficient for inducing protection or long-term control of viral replication.

Acknowledgements

This work was supported by grants from Conselho Nacional de Desenvolvimento Científico e Tecnológico (CNPq), Fundação Carlos Chagas Filho de Amparo à Pesquisa do Estado do Rio de Janeiro (FAPERJ) and Coordenação de Aperfeiçoamento de Pessoal de Nível Superior (CAPES).

References

[1] Ada GL, Ramsay AJ. Vaccines, vaccination, and the immune response. Philadelphia: Lippincott-Raven; 1997.
[2] Fenner F. Smallpox and its eradication. Geneve: WHO; 1988.
[3] Ada G. Vaccines and vaccination. N Engl J Med 2001;345(14): 1042–53.
[4] Stauffer F, El-Bacha T, Da Poian AT. Advances in the development of inactivated virus vaccines. Recent Patents Anti-Infect Drug Discov 2006;1(3):291–6.
[5] Eckert DM, Kim PS. Mechanisms of viral membrane fusion and its inhibition. Annu Rev Biochem 2001;70:777–810.
[6] Hernandez LD, Hoffman LR, Wolfsberg TG, White JM. Virus–cell and cell–cell fusion. Annu Rev Cell Dev Biol 1996;12:627–61.
[7] Skehel JJ, Wiley DC. Receptor binding and membrane fusion in virus entry: the influenza hemagglutinin. Annu Rev Biochem 2000;69:531–69.
[8] Da Poian AT, Gomes AM, Coelho-Sampaio T. Kinetics of intracellular viral disassembly and processing probed by Bodipy fluorescence dequenching. J Virol Methods 1998;70(1):45–58.
[9] White J, Matlin K, Helenius A. Cell fusion by Semliki Forest, influenza, and vesicular stomatitis viruses. J Cell Biol 1981;89(3):674–9.
[10] Carneiro FA, Ferradosa AS, Da Poian AT. Low pH-induced conformational changes in vesicular stomatitis virus glycoprotein involve dramatic structure reorganization. J Biol Chem 2001;276(1): 62–7.
[11] Carneiro FA, Bianconi ML, Weissmuller G, Stauffer F, Da Poian AT. Membrane recognition by vesicular stomatitis virus involves enthalpy-driven protein–lipid interactions. J Virol 2002;76(8):3756–64.
[12] Carneiro FA, Stauffer F, Lima CS, Juliano MA, Juliano L, Da Poian AT. Membrane fusion induced by vesicular stomatitis virus depends on histidine protonation. J Biol Chem 2003;278(16):13789–94.
[13] Miles EW. Modification of histidyl residues in proteins by diethylpyrocarbonate. Methods Enzymol 1977;47:431–42.

[14] Stauffer F, De Miranda J, Schechter MC, Carneiro FA, Salgado LT, Machado GF, et al. Inactivation of vesicular stomatitis virus through inhibition of membrane fusion by chemical modification of the viral glycoprotein. Antiviral Res 2007;73(1):31–9.
[15] Da Poian AT, Gomes AM, Oliveira RJ, Silva JL. Migration of vesicular stomatitis virus glycoprotein to the nucleus of infected cells. Proc Natl Acad Sci USA 1996;93(16):8268–73.
[16] Reed LJ, Muench H. A simple method of estimating fifty percent endpoints. Am J Hyg 1938;27:493–7.
[17] Reiss CS, Plakhov IV, Komatsu T. Viral replication in olfactory receptor neurons and entry into the olfactory bulb and brain. Ann N Y Acad Sci 1998;855:751–61.
[18] Charan S, Zinkernagel RM. Antibody mediated suppression of secondary IgM response in nude mice against vesicular stomatitis virus. J Immunol 1986;136(8):3057–61.
[19] Leist TP, Cobbold SP, Waldmann H, Aguet M, Zinkernagel RM. Functional analysis of T lymphocyte subsets in antiviral host defense. J Immunol 1987;138(7):2278–81.
[20] Clemens R, Safary A, Hepburn A, Roche C, Stanbury WJ, Andre FE. Clinical experience with an inactivated hepatitis A vaccine. J Infect Dis 1995;171(1):S44–9.
[21] Murdin AD, Barreto L, Plotkin S. Inactivated poliovirus vaccine: past and present experience. Vaccine 1996;14(8):735–46.
[22] Bachmann MF, Bast C, Hengartner H, Zinkernagel RM. Immunogenicity of a viral model vaccine after different inactivation procedures. Med Microbiol Immunol 1994;183(2):95–104.
[23] Brown F. Review of accidents caused by incomplete inactivation of viruses. Dev Biol Stand 1993;81:103–7.
[24] O'Hagan DT, MacKichan ML, Singh M. Recent developments in adjuvants for vaccines against infectious diseases. Biomol Eng 2001;18(3):69–85.
[25] Lycke N, Holmgren J. Strong adjuvant properties of cholera toxin on gut mucosal immune responses to orally presented antigens. Immunology 1986;59(2):301–8.
[26] Elson CO, Ealding W. Generalized systemic and mucosal immunity in mice after mucosal stimulation with cholera toxin. J Immunol 1984;132(6):2736–41.
[27] Berger SL. Diethyl pyrocarbonate: an examination of its properties in buffered solutions with a new assay technique. Anal Biochem 1975;67:428–37.

DISCUSSÃO

3 Discussão

3.1 Parte I

Elucidação dos mecanismos da fusão de membranas mediada pelo VSV e pelo dengue

A entrada dos vírus na célula hospedeira é essencial para infecção viral. No caso dos vírus envelopados, o mecanismo de entrada envolve uma etapa de fusão com membranas celulares (plasmática ou endossomal). Este processo é mediado pelas proteínas de fusão que estão presentes no envelope viral e desencadeado após a interação do vírus com seu receptor celular específico ou exposição ao pH ácido do meio endossomal. Estes gatilhos acarretam na mudança conformacional das proteínas de fusão, com a subsequente exposição do peptídeo de fusão. Este segmento das glicoproteínas virais desestabiliza a membrana alvo, iniciando a reação de fusão. Sendo assim, o conhecimento das mudanças conformacionais das proteínas de fusão virais e de seus respectivos peptídeos de fusão e a identificação de resíduos de aminoácidos essenciais para a fusão de membranas são etapas básicas para a elucidação dos mecanismos moleculares do processo de fusão, permitindo o reconhecimento de possíveis alvos para inibição da entrada dos vírus nas células. Nesta tese, acreditamos ter contribuído para o avanço na elucidação do processo de fusão de membranas induzido pelo VSV e pelo vírus da dengue.

3.1.1 VSV

As mudanças estruturais sofridas pela proteína G durante a acidificação, assim como a aquisição da capacidade de interagir com membranas negativamente carregadas ocorrem em uma faixa de pH bastante estreita, entre 6,2 e 5,8 (White *et al.*, 1981; Carneiro *et al.*, 2001). Esta é exatamente a faixa de pH na qual ocorre a protonação da cadeia lateral do aminoácido histidina (pK ~ 6,04). Isso nos sugeriu que a protonação de resíduos de histidina presentes na proteína G seria necessária para o desencadeamento do processo de fusão.

Através de modificação das histidinas da proteína G com DEPC, demonstramos que tanto a mudança conformacional quanto a fusão de membranas catalisadas pelo VSV são dependentes da protonação de histidinas que ocorre durante a acidificação do meio endossomal (artigo 2). Antes da publicação deste artigo, o envolvimento de resíduos de histidina não havia sido avaliado como importante no processo de fusão mediado pelas glicoproteínas virais.

Após a publicação do artigo 2 em 2003, outros grupos mostraram a importância de resíduos de histidina, tanto na aquisição da conformação fusogênica (Stevens *et al.*, 2004;

Roussel *et al.*, 2006), quanto na infectividade e atividade fusogênica viral (Chanel-Vos e Kielian, 2004). Em 2005, publicamos uma revisão sobre proteínas de fusão viral, ressaltando a importância da protonação de resíduos de histidina para a aquisição da conformação fusogênica e interação com a membrana alvo (anexo 2) (Da Poian *et al.*, 2005). Mais recentemente, foi proposto um mecanismo para a mudança conformacional das proteínas de fusão desencadeada pelo pH ácido do meio endossomal, que envolve diretamente a protonação das histidinas (fig. 15). Segundo este modelo, que foi em parte baseado no artigo 2 e na revisão de 2005 publicados por nós, a protonação de resíduos de histidina específicos, localizados adjacentes a aminoácidos carregados positivamente, acarretaria no deslocamento das histidinas com a subseqüente formação de pontes salinas que estabilizariam a nova conformação adquirida (Kampmann *et al.*, 2006).

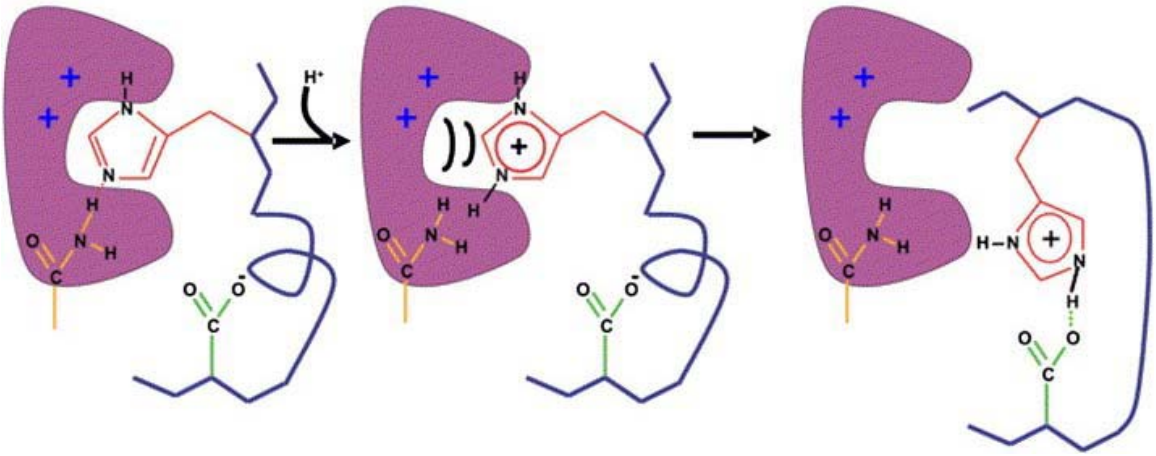

Figura 15: Diagrama esquemático do mecanismo proposto para mudança conformacional induzida pelo pH ácido. Nesta figura, estão representadas as interações dos resíduos de histidina nas proteínas de fusão viral nas conformações pré e pós-fusogênicas. No estado pré-fusão, os resíduos de histidina (em vermelho) estão localizados próximo a um domínio (em vinho) composto de aminoácidos carregados positivamente (representados pelo símbolo + em azul). No pH ácido, estes resíduos de histidina se tornam protonados e carregados positivamente. Isto favorece interações eletrostáticas com cadeias laterais de aminoácidos carregados negativamente (em verde), acarretando na movimentação dos resíduos de histidina com a formação de novas pontes salinas. Desta forma, a nova conformação adquirida torna-se mais estável. As pontes de hidrogênio envolvendo resíduos de histidina como aceptores também são "pertubadas" pela protonação. Extraído de Kampmann *et al.* (2006).

A formação das pontes salinas envolveria interações eletrostáticas entre os resíduos de histidina carregados positivamente e cadeias laterais de aminoácidos carregados negativamente, como os ácidos aspárticos e glutâmicos. Recentemente, nosso grupo identificou que os resíduos D^{153} e E^{158} da proteína G do VSV são importantes para o processo de fusão (Carneiro *et al.*, 2006b). Foi sugerido que estes aminoácidos participariam de interações eletrostáticas intermoleculares, estabilizando a conformação fusogênica adquirida no pH ácido do meio endossomal (Carneiro *et al.*, 2006b). Estas observações também sustentam o modelo proposto por Kampmann *et al.*, (2006).

Especificamente na proteína G do VSV, foram identificados resíduos de histidina, conservados nos rabdovírus (H^{423}, H^{178}, H^{76}), que estão associados na conformação pré-fusogênica (Roche *et al.*, 2007). A protonação destes resíduos provavelmente desestabiliza a interação entre o segmento C-terminal e o domínio de fusão, sendo o gatilho para o movimento inicial que dirige o *loop* de fusão para o topo da molécula, em direção a membrana alvo (Roche *et al.*, 2007). A conformação pós-fusogênica é estabilizada por novas pontes de hidrogênio e pontes salinas, como a interação entre os resíduos H^{423} e D^{153} (Roche *et al.*, 2007). Nós já havíamos identificado estes aminoácidos como importantes para o processo de fusão (artigo 2 e (Carneiro *et al.*, 2006b)).

Ainda no artigo 2, propusemos um novo peptídeo relacionado com a fusão do VSV. A identificação deste segmento da proteína G se iniciou com base nos dados de espectrometria de massa, onde foram observados quatro fragmentos trípticos que tiveram pelo menos uma de suas histidinas modificadas pelo DEPC: os segmentos entre os resíduos 3-63, 32-87, 110-168 e 392-417 (artigo 2, Tabela II).

O fragmento 110-168 apresenta, em sua seqüência, uma região de aminoácidos conservada entre os rabdovírus, denominada peptídeo *p2-like* (Coll, 1995). No caso do VSV, o peptídeo *p2-like* compreende os resíduos de aminoácidos 145-168 da proteína G. Existiam evidências do envolvimento deste peptídeo no processo de fusão mediado pelo VSV. Primeiro, neste segmento estão contidos os resíduos H^{148} e H^{149}, que foram modificadas pelo DEPC nos nossos experimentos. Além disso, havia sido demonstrado que este peptídeo apresentava capacidade de ligar-se seletivamente a fosfatidilserina (PS) (Coll, 1997), um fosfolipídio carregado negativamente que possui papel importante tanto na ligação do VSV à membrana da célula hospedeira (Carneiro *et al.*, 2006a) (anexo C) quanto no processo de fusão mediado por este vírus (Carneiro *et al.*, 2002) (anexo A).

O primeiro trabalho a identificar que esta seqüência da proteína G dos rabdovírus estava envolvida na interação com membranas foi realizado com o vírus da septicemia hemorrágica viral (VHSV). Este rabdovírus que infecta salmonídeos possuía um segmento localizado entre os resíduos 82 e 109 da proteína G capaz de se ligar a PS e que foi relacionado por evidências indiretas ao processo de fusão membranas (Estepa e Coll, 1996). Este peptídeo foi denominado p2 e é homólogo ao segmento 145 a 168 da proteína G do VSV (Coll, 1995). Posteriormente, esses autores demonstraram que um fragmento maior, contendo o peptídeo p2, possuía atividade fusogênica e por isso estaria implicado na fusão mediada pelo VHSV (Estepa *et al.*, 2001).

No caso do VSV, o peptídeo *p2-like* foi definitivamente relacionado com a fusão de membranas após a realização de experimento de fusão de lipossomas com diferentes peptídeos sintéticos (artigo 2, fig. 6). Este segmento da proteína G foi tão eficiente quanto o vírus inteiro em mediar a fusão de lipossomas. A reação de fusão catalisada pelo peptídeo p2-like possuía as mesmas características daquela catalisada pelo VSV: dependência de pH ácido e da presença de fosfolipídio negativo (PS). Já o suposto peptídeo de fusão do VSV (segmento 117-137) (ver seção 1.3.3) (Zhang e Ghosh, 1994; Fredericksen e Whitt, 1995) não era capaz de promover a fusão de membranas.

Tanto o segmento 145-168 (*p2-like*) quanto o 117-137 estão inseridos na porção da proteína G (59-221) capaz de interagir com membranas durante as transições conformacionais decorrentes da acidificação (Durrer *et al.*, 1995). Com a determinação da estrutura cristalográfica da proteína G, sugeriu-se a existência de um domínio de fusão (resíduos 69-188) (fig. 16), uma estrutura composta de folhas beta, que contém dois *loops* onde são encontrados resíduos aromáticos (W88, Y89, Y132, A133) (Roche *et al.*, 2006). Estes aminoácidos estão no topo da molécula e seriam responsáveis pela desestabilização inicial da membrana alvo. Sendo assim, as seqüências de aminoácidos 145-168 e 117-137 (assinaladas na fig. 16) podem não representar especificamente o peptídeo de fusão da proteína G do VSV, apesar de provavelmente possuírem papéis importantes durante o processo de fusão.

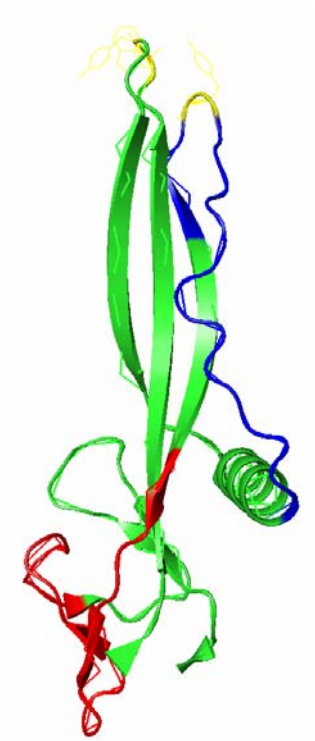

Figura 16: Estrutura cristalográfica do domínio de fusão da proteína G do VSV nas conformação pós fusogênica. Segmentos 145-168 (*p2-like*) em vermelho, 117-137 em azul e aminoácidos aromáricos em amarelo.

3.1.2 Vírus da Dengue

Apesar dos estudos estruturais realizados com a glicoproteína E do vírus da dengue, até o presente momento não existem trabalhos publicados com seu peptídeo de fusão. Este segmento da proteína E, que compreende os aminoácidos 98-110, apresenta grande homologia entre os flavivírus. Corresponde a um *loop*, no meio de folhas beta, localizado no domínio II, que contém aminoácidos hidrofóbicos (W^{101}, L^{107} e F^{108}). Este peptídeo se encontra

"escondido" nos homodímeros de proteína E em pH neutro e exposto no topo da molécula nos homotrímeros em pH ácido, iniciando o processo de fusão através da desestabilização da membrana alvo. Estudos prévios de substituições de aminoácidos nesta região foram capazes de abolir a fusão de membranas mediada pela proteína E de outros flavivírus (ex. TBE vírus) (Allison *et al.*, 2001).

Através do uso de metodologias baseadas em espectroscopia de fluorescência, estudamos a interação do peptídeo de fusão do vírus da dengue com modelos de membranas (artigo 3). Neste artigo, mostramos que o peptídeo interage com membranas e é capaz de induzir fusão de lipossomas, indicando que realmente esta seqüência pode estar catalisando a fusão de membranas mediada pelo vírus da dengue. Tanto a partição para membranas quanto a reação de fusão foram mais intensas na presença de fosfolipídios negativos e são dependentes do pH e da força iônica do meio, mostrando a importância de interações eletrostáticas entre o peptídeo e componentes carregados negativamente das membranas alvo, como já havíamos mostrado para o VSV (Carneiro *et al.*, 2002; Carneiro *et al.*, 2006b). Adicionalmente, mostramos que provavelmente ocorre oligomerização do peptídeo da dengue na presença de fosfolipídios negativos. Os peptídeos oligomerizados adquirem uma nova conformação que supostamente favorece a desestabilização da membrana com subseqüente reação de fusão mais eficiente, como foi observado.

A importância da oligomerização das glicoproteínas virais para o processo de fusão é inquestionável (Harrison, 2005; Weissenhorn *et al.*, 2007). Estudos prévios já demonstraram que peptídeos de fusão oligomerizados são mais fusogênicos do que monômeros ou grandes agregados (Lau *et al.*, 2004; Yang *et al.*, 2004) e que, geralmente, a oligomerização desses peptídeos é desencadeada por mudanças na sua estrutura secundária (Han e Tamm, 2000; Yang e Weliky, 2003; Li *et al.*, 2004).

No caso da proteína E do vírus da dengue, ocorre a formação de trímeros e exposição dos peptídeos de fusão no topo da molécula desencadeadas pela exposição ao pH ácido do meio endossomal. Apesar da glicoproteína viral sofrer uma mudança estrutural durante este processo, seu peptídeo de fusão mantém a mesma conformação em pH neutro e ácido (Modis *et al.*, 2004). Sendo assim, a oligomerização deste peptídeo não se deve a mudanças em sua estrutura secundária. O processo parece ser desencadeado por interações eletrostáticas entre o peptídeo (carga global +7, pois possui oito resíduos carregados positivamente e somente um negativo) e componentes carregados negativamente nas membranas, sendo por isso somente observado quando utilizamos fosfolipídios carregados negativamente.

Isso sugere que o mecanismo de interação e desestabilização de membranas do peptídeo de fusão da proteína E é semelhante ao desempenhado pelos peptídeos antimicrobianos, conhecido como modelo *carpet* (Pouny *et al.*, 1992; Shai, 1999). Segundo este modelo, acontece inicialmente uma interação entre a porção hidrofílica (carregada positivamente) dos peptídeos com componentes negativamente carregados na membrana alvo através de interações eletrostáticas. Posteriormente, ocorre a associação desses peptídeos na superfície da membrana, ou seja, a oligomerização dos peptídeos. Isto acarreta na formação de domínios hidrofóbicos, permitindo então o surgimento de interações hidrofóbicas que são requeridas para a desestabilização da membrana (Jenssen *et al.*, 2006).

O componente negativo das membranas alvo pode ser representado por qualquer molécula carregada negativamente presente na membrana celular, como o heparan sulfato (HS). Já foi demonstrado que este glicosaminoglicano (GAG) carregado negativamente pode agir diretamente como um receptor celular para o vírus da dengue (Chen *et al.*, 1997; Hung *et al.*, 1999; Hilgard e Stockert, 2000; Germi *et al.*, 2002) ou ser apenas um fator presente na superfície celular que agrega as partículas virais (Martinez-Barragan e Del Angel, 2001; Thepparit e Smith, 2004).

Em face dos dados apresentados, foi proposto um mecanismo molecular de interação entre o peptídeo de fusão do vírus da dengue e membranas (artigo 3, fig. 7). Na presença de elevada razão [peptídeo]/[lipídio], ocorre oligomerização dos peptídeos e a fusão de membranas é mais eficiente. A formação de oligômeros foi observada somente na presença de fosfolipídios negativos, demonstrando a necessidade de interações eletrostáticas entre o peptídeo e componentes carregados negativamente nas membranas alvo, como sugerido no modelo *carpet*. Ao imaginarmos a interação vírus-célula, podemos especular que o microambiente formado pelos fosfolipídios da membrana endossomal e os peptídeos de fusão presentes no topo dos trímeros de proteína E possui uma elevada razão [peptídeo]/[lipídio], justificando então a oligomerização desta glicoproteína para o processo de fusão mediado pelo vírus da dengue.

3.2 Parte II

Descoberta de um novo composto inativador viral baseado na inibição de fusão de membranas e sua aplicação na formulação de uma vacina

O desenvolvimento de novas estratégias de inativação viral é uma importante vertente na área da virologia. Apesar dos avanços no campo da imunologia, biologia molecular e genética, os mecanismos de inativação viral ainda são muito utilizados para produção de vacinas, visto que são métodos eficazes, simples e mais econômicos. Além disso, o uso de vírus inativados como antígenos de vacinas já foi utilizado com sucesso para diversas doenças (Clemens *et al.*, 1995; Murdin *et al.*, 1996). Por último, as técnicas de inativação viral podem ser utilizadas para o tratamento de doenças virais e também para a depuração viral de produtos sanguíneos e de equipamentos.

As técnicas de inativação viral mais utilizadas até o dia de hoje para formulação de vacinas de vírus inativados são baseadas no uso de compostos químicos, mais especificamente a formalina e o beta proprionato (artigo 1, tabela 2). Estes métodos inibem a entrada dos vírus nas células impedindo a ligação das partículas virais às células hospedeiras. No entanto, acarretam na desnaturação das proteínas de superfície viral, modificando tanto a capacidade antigênica quanto a imunogênica dos vírus (Bachmann *et al.*, 1994). Outras desvantagens incluem a necessidade de longos períodos de incubação para uma inativação eficaz, a toxicidade do composto para o organismo, além de relatos na literatura de inativação incompleta com estes compostos (Nathanson e Langmuir, 1963; Brown, 1993). Sendo assim, a busca de novos compostos inativadores virais é de grande importância e relevância na área da virologia.

Nos últimos cinco anos, grande destaque tem sido concedido aos agentes que atuam na entrada dos vírus nas células hospedeiras, tanto na adsorção quanto na fusão de membranas (Irurzun e Carrasco, 2001; Moore e Doms, 2003; Altmeyer, 2004; Moscona, 2005; Meanwell, 2006; Yeung *et al.*, 2006; Este e Telenti, 2007; Yeung e Meanwell, 2007). Ao desvendar os mecanismos de entrada do HIV-1 nas suas células alvo, foram descobertos importantes passos da fusão da membrana viral com a celular, mediada pelas glicoproteínas gp120/gp41 do HIV (Chan *et al.*, 1997; Chan e Kim, 1998). Isto possibilitou o desenvolvimento de uma nova classe de medicamentos anti-HIV, os inibidores de entrada viral, que são medicamentos inibidores de fusão ou antagonistas de co-receptores (Este e Telenti, 2007).

Dentre os inibidores de fusão do HIV, um peptídeo de 36 resíduos de aminoácidos construído com base na seqüência de aminoácidos da região helicoidal C-terminal da gp41, conhecido como T20, enfuvirtida ou fuzeon®, foi o primeiro inibidor de entrada a ser

aprovado para uso clínico (Fletcher, 2003; Matthews *et al.*, 2004; Morse e Maldarelli, 2007). Outros peptídeos que interferem com o processo de fusão de diferentes vírus já foram descritos (Cianci *et al.*, 2005; Liao e Kielian, 2005; Kirschner *et al.*, 2007). A descoberta e caracterização destes novos inibidores é um exemplo de como estudos básicos utilizados para elucidação do mecanismo de entrada dos vírus nas células hospedeiras podem levar ao desenvolvimento de novos antivirais e auxiliar na formulação de vacinas.

Nesta tese, nós descobrimos que o DEPC modifica especificamente os resíduos de histidina da proteína G do VSV, inibindo as mudanças conformacionais desta glicoproteína desencadeadas pelo pH ácido e consequentemente a fusão de membranas mediada pelo VSV (artigo 2). Posteriormente, mostramos que o tratamento do VSV com DEPC resulta na completa inativação viral, tanto no modelo celular quanto no animal (artigos 4 e 5). Esta foi a primeira vez que este composto foi utilizado como inativador viral, sendo por isso protegido por patente depositada no INPI (Patente 1). Com base nesses dados, foi sugerido que o mecanismo de inativação viral com DEPC se deve na modificação da glicoproteína viral com a inibição da fusão de membranas mediada pelo VSV. Reforçando esta hipótese, temos o fato do DEPC ser um composto muito hidrofílico (Miles, 1977), sugerindo que ele não atravessa a membrana viral, o que impossibilitaria a modificação de enzima no interior da partícula viral.

Adicionalmente, mostramos que o vírus tratado com DEPC mantinha sua capacidade antigênica (artigo 4) e imunogênica (artigo 5). A resposta imunológica foi avaliada através da dosagem de anticorpos no soro de animais inoculados por via intranasal ou intraperitoneal com VSV inativado. A produção de anticorpos era dependente da via e número de inoculações. Também observamos a necessidade do uso de adjuvantes, visto que vacinas inativadas geralmente induzem uma fraca resposta imune (O'hagan *et al.*, 2001). Dos diversos esquemas de imunização utilizados, a inoculação intraperitoneal de três doses de VSV inativado com DEPC misturado com adjuvante desencadeou níveis de anticorpos equivalentes ao induzido pela infecção ocasionada VSV. Estes anticorpos eram capazes de reconhecer e neutralizar o vírus nativo (artigo 5, figura 5). Além disso, os títulos de anticorpos se mantiveram estáveis durante seis meses, indicando que houve a indução de resposta imune de longa duração. Por último, demonstramos que os animais vacinados, ou seja, inoculados com o VSV inativado com DEPC, sobreviveram ao desafio com uma inoculação intracraniana do vírus, enquanto que 75% dos animais controle morreram (artigo 5, figura 6).

Todos estes resultados indicam que o uso de DEPC para inativação viral é adequado para o desenvolvimento de vacinas. Também podemos dizer que é um método seguro devido a duas razões: primeiro, a inativação por este composto é estável, pois ele modifica

covalentemente os resíduos de histidina (Miles, 1977); segundo, esta substância livre é instável em solução aquosa, sendo rapidamente hidrolisada (Berger, 1975; Miles, 1977), o que assegura que não existe DEPC livre na preparação de vírus inativado.

Nossa hipótese é que o DEPC pode ser utilizado para formulação de vacinas para diferentes vírus envelopados inativados (patente 1, artigo 5). No caso desses vírus cujo mecanismo de entrada nas células hospedeiras se dá através de endocitose mediado por receptor, a reação de fusão de membranas depende da acidificação do meio endossomal. Nesta situação, o pH ácido desencadeia mudanças conformacionais nas glicoproteínas virais que são necessárias para aquisição do estado fusogênico. A faixa de pH para a fusão de diversos vírus envelopados estudados até então varia de 5.0 a 6.5 (fig. 17) (White *et al.*, 1981; Gaudin *et al.*, 1995; Chan e Kim, 1998), indicando que a protonação de resíduos de histidina (pKa ~ 6.0) nas glicoproteínas virais deve ser requerida para a obtenção da conformação fusogênica de todos esses vírus, como já foi abordado na parte I desta discussão.

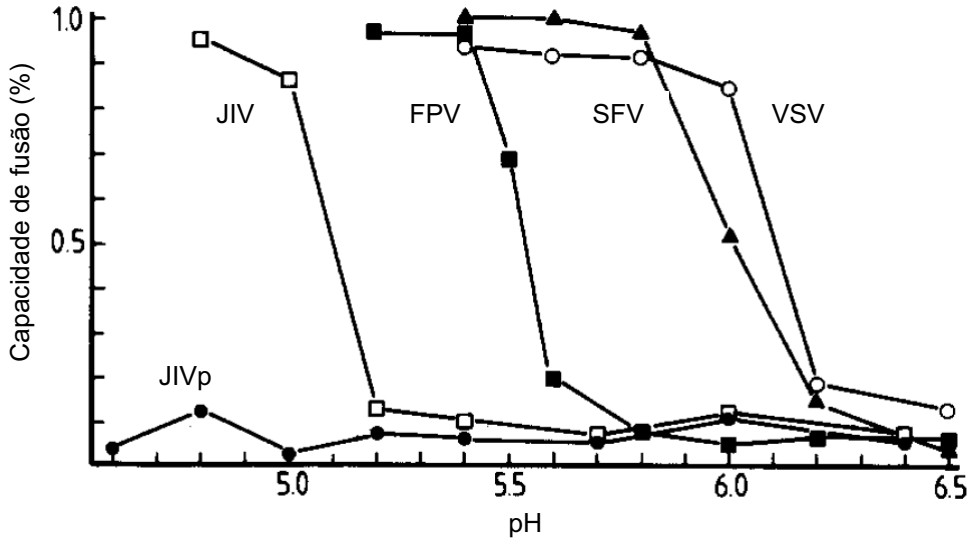

Figura 17: Dependência do pH para a aquisição da conformação fusogênica de diferentes vírus envelopados. Capacidade de fusão ao longo do pH para os vírus indicados na figura. SFV - *semliki forrest virus*, VSV - vírus da estomatite vesicular, JIV - vírus influenza japonês, FPV - *fowl plaque virus*, JIVp - precursor do vírus influenza japonês. Adaptado de (White *et al.*, 1981).

Sendo assim, é sugerido nesta tese que o tratamento com DEPC poderá ser utilizado para a inativação de vírus envelopados através da inibição da fusão de membranas catalisada pelas proteínas de superfície virais. Estes vírus inativados servem de antígenos para o desenvolvimento de novas vacinas.

REFERÊNCIAS

REFERÊNCIAS

Allende, R. e P. M. Germano. Comparison of virus neutralisation and enzyme-linked immunosorbent assay for the identification of antibodies against vesicular stomatitis (Indiana 3) virus. Rev Sci Tech, v.12, n.3, Set, p.849-55. 1993.

Allison, S. L., J. Schalich, *et al.* Mutational evidence for an internal fusion peptide in flavivirus envelope protein E. J Virol, v.75, n.9, Maio, p.4268-75. 2001.

Allison, S. L., J. Schalich, *et al.*. Oligomeric rearrangement of tick-borne encephalitis virus envelope proteins induced by an acidic pH. J Virol, v.69, n.2, Fev, p.695-700. 1995.

Altmeyer, R. Virus attachment and entry offer numerous targets for antiviral therapy. Curr Pharm Des, v.10, n.30, p.3701-12. 2004.

Autran, B., G. Carcelain, *et al.* Positive effects of combined antiretroviral therapy on CD4+ T cell homeostasis and function in advanced HIV disease. Science, v.277, n.5322, Jul 4, p.112-6. 1997.

Bachmann, M. F., C. Bast, *et al.* Immunogenicity of a viral model vaccine after different inactivation procedures. Med Microbiol Immunol, v.183, n.2, Maio, p.95-104. 1994.

Bachmann, M. F., T. M. Kundig, *et al.* Formalin inactivation of vesicular stomatitis virus impairs T-cell- but not T-help-independent B-cell responses. J Virol, v.67, n.7, Jul, p.3917-22. 1993.

Barrientos, L. G., B. R. O'keefe, *et al.* Cyanovirin-N binds to the viral surface glycoprotein, GP1,2 and inhibits infectivity of Ebola virus. Antiviral Res, v.58, n.1, Mar, p.47-56. 2003.

Bay, P. H. e M. E. Reichmann. UV inactivation of the biological activity of defective interfering particles generated by vesicular stomatitis virus. J Virol, v.32, n.3, Dez, p.876-84. 1979.

Berger, S. L. Diethyl pyrocarbonate: an examination of its properties in buffered solutions with a new assay technique. Anal. Biochem., v.67, p.428-437. 1975.

Bewley, C. A. e S. Otero-Quintero. The potent anti-HIV protein cyanovirin-N contains two novel carbohydrate binding sites that selectively bind to Man(8) D1D3 and Man(9) with nanomolar affinity: implications for binding to the HIV envelope protein gp120. J Am Chem Soc, v.123, n.17, Maio 2, p.3892-902. 2001.

Bhattacharyya, D. K., U. Bandyopadhyay, *et al.* Chemical and kinetic evidence for an essential histidine in horseradish peroxidase for iodide oxidation. J Biol Chem, v.267, n.14, Maio 15, p.9800-4. 1992.

Bielefeldt-Ohmann, H., M. Meyer, *et al.* Dengue virus binding to human leukocyte cell lines: receptor usage differs between cell types and virus strains. Virus Res, v.73, n.1, Jan, p.81-9. 2001.

Bolmstedt, A. J., B. R. O'keefe, *et al.* Cyanovirin-N defines a new class of antiviral agent targeting N-linked, high-mannose glycans in an oligosaccharide-specific manner. Mol Pharmacol, v.59, n.5, Maio, p.949-54. 2001.

Bonafe, C. F., M. Glaser, *et al.* Virus inactivation by anilinonaphthalene sulfonate compounds and comparison with other ligands. Biochem Biophys Res Commun, v.275, n.3, Set 7, p.955-61. 2000.

Boyd, M. R., K. R. Gustafson, *et al.* Discovery of cyanovirin-N, a novel human immunodeficiency virus-inactivating protein that binds viral surface envelope glycoprotein gp120: potential applications to microbicide development. Antimicrob Agents Chemother, v.41, n.7, Jul, p.1521-30. 1997.

Bressanelli, S., K. Stiasny, *et al.* Structure of a flavivirus envelope glycoprotein in its low-pH-induced membrane fusion conformation. Embo J, v.23, n.4, Fev 25, p.728-38. 2004.

Bridges, V. E., B. J. Mccluskey, *et al.* Review of the 1995 vesicular stomatitis outbreak in the western United States. J Am Vet Med Assoc, v.211, n.5, Set 1, p.556-60. 1997.

Brown, F. Review of accidents caused by incomplete inactivation of viruses. Dev Biol Stand, v.81, p.103-7. 1993.

Bullough, P. A., F. M. Hughson, *et al.* Structure of influenza haemagglutinin at the pH of membrane fusion. Nature, v.371, n.6492, Set 1, p.37-43. 1994.

Burke, D. S. e T. P. Monath. Flaviviruses. In: D. M. Knipe e P. M. Howley (Ed.). Fields virology. Philadelphia: Lippincott/The Williams & Wilkins Co., 2001. Flaviviruses, p.1043-1125

Camara, F. P., R. L. Theophilo, *et al.* [Regional and dynamics characteristics of dengue in Brazil: a retrospective study]. Rev Soc Bras Med Trop, v.40, n.2, Mar-Abr, p.192-6. 2007.

Carneiro, F. A., M. L. Bianconi, *et al.* Membrane recognition by vesicular stomatitis virus involves enthalpy-driven protein-lipid interactions. J Virol, v.76, n.8, Abr, p.3756-64. 2002.

Carneiro, F. A., A. S. Ferradosa, *et al.* Low pH-induced conformational changes in vesicular stomatitis virus glycoprotein involve dramatic structure reorganization. J Biol Chem, v.276, n.1, Jan 5, p.62-7. 2001.

Carneiro, F. A., P. A. Lapido-Loureiro, *et al.* Probing the interaction between vesicular stomatitis virus and phosphatidylserine. Eur Biophys J, v.35, n.2, Jan, p.145-54. 2006a.

Carneiro, F. A., G. Vandenbussche, *et al.* Charged residues are involved in membrane fusion mediated by a hydrophilic peptide located in vesicular stomatitis virus G protein. Mol Membr Biol, v.23, n.5, Sep-Oct, p.396-406. 2006b.

Carr, C. M., C. Chaudhry, *et al.* Influenza hemagglutinin is spring-loaded by a metastable native conformation. Proc Natl Acad Sci U S A, v.94, n.26, Dez 23, p.14306-13. 1997.

Chan, D. C., D. Fass, *et al.* Core structure of gp41 from the HIV envelope glycoprotein. Cell, v.89, n.2, Abr 18, p.263-73. 1997.

Chan, D. C. e P. S. Kim. HIV entry and its inhibition. Cell, v.93, n.5, Maio 29, p.681-4. 1998.

Chandran, K., N. J. Sullivan, *et al.* Endosomal proteolysis of the Ebola virus glycoprotein is necessary for infection. Science, v.308, n.5728, Jun 10, p.1643-5. 2005.

Chanel-Vos, C. e M. Kielian. A conserved histidine in the ij loop of the Semliki Forest virus E1 protein plays an important role in membrane fusion. J Virol, v.78, n.24, Dez, p.13543-52. 2004.

Chen, L., J. J. Gorman, *et al.* The structure of the fusion glycoprotein of Newcastle disease virus suggests a novel paradigm for the molecular mechanism of membrane fusion. Structure, v.9, n.3, Mar 7, p.255-66. 2001.

Chen, Y., T. Maguire, *et al.* Dengue virus infectivity depends on envelope protein binding to target cell heparan sulfate. Nat Med, v.3, n.8, Ago, p.866-71. 1997.

Chen, Y. C., S. Y. Wang, *et al.* Bacterial lipopolysaccharide inhibits dengue virus infection of primary human monocytes/macrophages by blockade of virus entry via a CD14-dependent mechanism. J Virol, v.73, n.4, Abr, p.2650-7. 1999.

Cianci, C., N. Meanwell, *et al.* Antiviral activity and molecular mechanism of an orally active respiratory syncytial virus fusion inhibitor. J Antimicrob Chemother, v.55, n.3, Mar, p.289-92. 2005.

Clemens, R., A. Safary, *et al.* Clinical experience with an inactivated hepatitis A vaccine. J Infect Dis, v.171 Suppl 1, Mar, p.S44-9. 1995.

Cleverley, D. Z. e J. Lenard. The transmembrane domain in viral fusion: essential role for a conserved glycine residue in vesicular stomatitis virus G protein. Proc Natl Acad Sci U S A, v.95, n.7, Mar 31, p.3425-30. 1998.

Clyde, K., J. L. Kyle, *et al.* Recent advances in deciphering viral and host determinants of dengue virus replication and pathogenesis. J Virol, v.80, n.23, Dez, p.11418-31. 2006.

Coil, D. A. e A. D. Miller. Phosphatidylserine is not the cell surface receptor for vesicular stomatitis virus. J Virol, v.78, n.20, Out, p.10920-6. 2004.

Coll, J. M. Synthetic peptides reveal a phospholipid binding domain in the glycoprotein of VHSV, a salmonid rhabdovirus. Vet Res, v.26, n.5-6, p.399-407. 1995.

Coll, J. M. Synthetic peptides from the heptad repeats of the glycoproteins of rabies, vesicular stomatitis and fish rhabdoviruses bind phosphatidylserine. Arch Virol, v.142, n.10, p.2089-97. 1997.

Cotton, W. E. Vesicular stomatitis in its relation to the diagnosis of foot-and-mouth disease. J. Am. Vet. Med. Assoc., v.69, p.313-332. 1926.

Cotton, W. E. Vesicular stomatitis. Vet. Med., v.22, p.169-175. 1927.

Crumpacker, C. S., L. E. Schnipper, *et al.* Growth inhibition by acycloguanosine of herpesviruses isolated from human infections. Antimicrob Agents Chemother, v.15, n.5, Maio, p.642-5. 1979.

Da Poian, A. T., F. A. Carneiro, *et al.* Viral membrane fusion: is glycoprotein G of rhabdoviruses a representative of a new class of viral fusion proteins? Braz J Med Biol Res, v.38, n.6, Jun, p.813-23. 2005.

De Clercq, E. Antiviral drugs in current clinical use. J Clin Virol, v.30, n.2, Jun, p.115-33. 2004.

Dey, B., D. L. Lerner, *et al.* Multiple antiviral activities of cyanovirin-N: blocking of human immunodeficiency virus type 1 gp120 interaction with CD4 and coreceptor and inhibition of diverse enveloped viruses. J Virol, v.74, n.10, Maio, p.4562-9. 2000.

Dimitrov, D. S. Virus entry: molecular mechanisms and biomedical applications. Nat Rev Microbiol, v.2, n.2, Fev, p.109-22. 2004.

Durrer, P., Y. Gaudin, *et al.* Photolabeling identifies a putative fusion domain in the envelope glycoprotein of rabies and vesicular stomatitis viruses. J Biol Chem, v.270, n.29, Jul 21, p.17575-81. 1995.

Dzhandzhugazyan, K. N. e L. Plesner. Diethyl pyrocarbonate inactivates CD39/ecto-ATPDase by modifying His-59. Biochim Biophys Acta, v.1466, n.1-2, Jun 1, p.267-77. 2000.

Earp, L. J., S. E. Delos, *et al.* The many mechanisms of viral membrane fusion proteins. Curr Top Microbiol Immunol, v.285, p.25-66. 2005.

Eckert, D. M. e P. S. Kim. Mechanisms of viral membrane fusion and its inhibition. Annu Rev Biochem, v.70, p.777-810. 2001.

Eidelman, O., R. Schlegel, *et al.* pH-dependent fusion induced by vesicular stomatitis virus glycoprotein reconstituted into phospholipid vesicles. J Biol Chem, v.259, n.7, Abr 10, p.4622-8. 1984.

Elshuber, S., S. L. Allison, *et al.* Cleavage of protein prM is necessary for infection of BHK-21 cells by tick-borne encephalitis virus. J Gen Virol, v.84, n.Pt 1, Jan, p.183-91. 2003.

Epand, R. M. Fusion peptides and the mechanism of viral fusion. Biochim Biophys Acta, v.1614, n.1, Jul 11, p.116-21. 2003.

Este, J. A. e A. Telenti. HIV entry inhibitors. Lancet, v.370, n.9581, Jul 7, p.81-8. 2007.

Estepa, A. e J. M. Coll. Pepscan mapping and fusion-related properties of the major phosphatidylserine-binding domain of the glycoprotein of viral hemorrhagic septicemia virus, a salmonid rhabdovirus. Virology, v.216, n.1, Fev 1, p.60-70. 1996.

Estepa, A. M., A. I. Rocha, *et al.* A protein G fragment from the salmonid viral hemorrhagic septicemia rhabdovirus induces cell-to-cell fusion and membrane phosphatidylserine translocation at low pH. J Biol Chem, v.276, n.49, Dez 7, p.46268-75. 2001.

Fass, D., S. C. Harrison, *et al.* Retrovirus envelope domain at 1.7 angstrom resolution. Nat Struct Biol, v.3, n.5, Maio, p.465-9. 1996.

Federer, K. E., R. Burrows, *et al.* Vesicular stomatitis virus--the relationship between some strains of the Indiana serotype. Res Vet Sci, v.8, n.1, Jan, p.103-17. 1967.

Fields, B. N. e K. Hawkins. Human infection with the virus of vesicular stomatitis during an epizootic. N Engl J Med, v.277, n.19, Nov 9, p.989-94. 1967.

Figueiredo, L. T. M. e B. A. L. Fonseca. Dengue. In: R. Veronesi e R. Focaccia (Ed.). Tratado de Infectologia. Rio de Janeiro: Atheneu, 2002. Dengue, p.204-217

Figueroa, R. e C. Ramos. Dengue virus (serotype 3) circulation in endemic countries and its reappearance in America. Arch Med Res, v.31, n.4, Jul-Ago, p.429-30. 2000.

Flanagan, E. B., J. M. Zamparo, *et al.* Rearrangement of the genes of vesicular stomatitis virus eliminates clinical disease in the natural host: new strategy for vaccine development. J Virol, v.75, n.13, Jul, p.6107-14. 2001.

Fletcher, C. V. Enfuvirtide, a new drug for HIV infection. Lancet, v.361, n.9369, Maio 10, p.1577-8. 2003.

Fredericksen, B. L. e M. A. Whitt. Vesicular stomatitis virus glycoprotein mutations that affect membrane fusion activity and abolish virus infectivity. J Virol, v.69, n.3, Mar, p.1435-43. 1995.

Gaudin, Y. Rabies virus-induced membrane fusion pathway. J Cell Biol, v.150, n.3, Ago 7, p.601-12. 2000.

Gaudin, Y., R. W. Ruigrok, *et al.* Low-pH induced conformational changes in viral fusion proteins: implications for the fusion mechanism. J Gen Virol, v.76 (Pt 7), Jul, p.1541-56. 1995.

Germi, R., J. M. Crance, *et al.* Heparan sulfate-mediated binding of infectious dengue virus type 2 and yellow fever virus. Virology, v.292, n.1, Jan 5, p.162-8. 2002.

Gibbons, D. L., M. C. Vaney, *et al.* Conformational change and protein-protein interactions of the fusion protein of Semliki Forest virus. Nature, v.427, n.6972, Jan 22, p.320-5. 2004.

Gubler, D. J. Epidemic dengue/dengue hemorrhagic fever as a public health, social and economic problem in the 21st century. Trends Microbiol, v.10, n.2, Fev, p.100-3. 2002.

Guirakhoo, F., F. X. Heinz, *et al.* Fusion activity of flaviviruses: comparison of mature and immature (prM-containing) tick-borne encephalitis virions. J Gen Virol, v.72 (Pt 6), Jun, p.1323-9. 1991.

Guzman, M. G. e G. Kouri. Dengue: an update. Lancet Infect Dis, v.2, n.1, Jan, p.33-42. 2002.

Han, X. e L. K. Tamm. pH-dependent self-association of influenza hemagglutinin fusion peptides in lipid bilayers. J Mol Biol, v.304, n.5, Dez 15, p.953-65. 2000.

Hanson, R. P. Discussion of the natural history of vesicular stomatitis. Am J Epidemiol, v.87, n.2, Mar, p.264-6. 1968.

Harrison, S. C. Mechanism of membrane fusion by viral envelope proteins. Adv Virus Res, v.64, p.231-61. 2005.

Heinz, F. X. e S. L. Allison. The machinery for flavivirus fusion with host cell membranes. Curr Opin Microbiol, v.4, n.4, Ago, p.450-5. 2001.

Heinz, F. X. e S. L. Allison. Flavivirus structure and membrane fusion. Adv Virus Res, v.59, p.63-97. 2003.

Heldwein, E. E., H. Lou, *et al.* Crystal structure of glycoprotein B from herpes simplex virus 1. Science, v.313, n.5784, Jul 14, p.217-20. 2006.

Helle, F., C. Wychowski, *et al.* Cyanovirin-N inhibits hepatitis C virus entry by binding to envelope protein glycans. J Biol Chem, v.281, n.35, Set 1, p.25177-83. 2006.

Hernandez, L. D., L. R. Hoffman, *et al.* Virus-cell and cell-cell fusion. Annu Rev Cell Dev Biol, v.12, p.627-61. 1996.

Hilgard, P. e R. Stockert. Heparan sulfate proteoglycans initiate dengue virus infection of hepatocytes. Hepatology, v.32, n.5, Nov, p.1069-77. 2000.

Hirayama, J., H. Abe, *et al.* Photoinactivation of vesicular stomatitis virus with fullerene conjugated with methoxy polyethylene glycol amine. Biol Pharm Bull, v.22, n.10, Out, p.1106-9. 1999.

Hirayama, J., K. Ikebuchi, *et al.* Photoinactivation of virus infectivity by hypocrellin A. Photochem Photobiol, v.66, n.5, Nov, p.697-700. 1997.

Hofner, M. C., W. C. Carpenter, *et al.* A hemi-nested PCR assay for the detection and identification of vesicular stomatitis virus nucleic acid. J Virol Methods, v.50, n.1-3, Dez, p.11-20. 1994.

Hung, S. L., P. L. Lee, *et al.* Analysis of the steps involved in Dengue virus entry into host cells. Virology, v.257, n.1, Abr 25, p.156-67. 1999.

Irurzun, A. e L. Carrasco. Entry of poliovirus into cells is blocked by valinomycin and concanamycin A. Biochemistry, v.40, n.12, Mar 27, p.3589-600. 2001.

Jahn, R., T. Lang, *et al.* Membrane fusion. Cell, v.112, n.4, Fev 21, p.519-33. 2003.

Jeetendra, E., K. Ghosh, *et al.* The membrane-proximal region of vesicular stomatitis virus glycoprotein G ectodomain is critical for fusion and virus infectivity. J Virol, v.77, n.23, Dez, p.12807-18. 2003.

Jenssen, H., P. Hamill, *et al.* Peptide antimicrobial agents. Clin Microbiol Rev, v.19, n.3, Jul, p.491-511. 2006.

Jindadamrongwech, S., C. Thepparit, *et al.* Identification of GRP 78 (BiP) as a liver cell expressed receptor element for dengue virus serotype 2. Arch Virol, v.149, n.5, Maio, p.915-27. 2004.

Johnson, K. M., J. E. Vogel, *et al.* Clinical and serological response to laboratory-acquired human infection by Indiana type vesicular stomatitis virus (VSV). Am J Trop Med Hyg, v.15, n.2, Mar, p.244-6. 1966.

Kampmann, T., D. S. Mueller, *et al.* The Role of histidine residues in low-pH-mediated viral membrane fusion. Structure, v.14, n.10, Out, p.1481-7. 2006.

Kasermann, F. e C. Kempf. Photodynamic inactivation of enveloped viruses by buckminsterfullerene. Antiviral Res, v.34, n.1, Mar, p.65-70. 1997.

Kasermann, F. e C. Kempf. Inactivation of enveloped viruses by singlet oxygen thermally generated from a polymeric naphthalene derivative. Antiviral Res, v.38, n.1, Abr, p.55-62. 1998.

Kielian, M. e F. A. Rey. Virus membrane-fusion proteins: more than one way to make a hairpin. Nat Rev Microbiol, v.4, n.1, Jan, p.67-76. 2006.

Kirschner, A. N., A. S. Lowrey, *et al.* Binding site interactions between Epstein-Barr virus fusion proteins gp42 and gH/gL reveal a peptide that inhibits both epithelial and B-cell membrane fusion. J Virol, Jun 20. 2007.

Kuhn, R. J., W. Zhang, *et al.* Structure of dengue virus: implications for flavivirus organization, maturation, and fusion. Cell, v.108, n.5, Mar 8, p.717-25. 2002.

Lau, W. L., D. S. Ege, *et al.* Oligomerization of fusogenic peptides promotes membrane fusion by enhancing membrane destabilization. Biophys J, v.86, n.1 Pt 1, Jan, p.272-84. 2004.

Lenard, J., A. Rabson, *et al.* Photodynamic inactivation of infectivity of human immunodeficiency virus and other enveloped viruses using hypericin and rose bengal: inhibition of fusion and syncytia formation. Proc Natl Acad Sci U S A, v.90, n.1, Jan 1, p.158-62. 1993.

Lenard, J. e R. Vanderoef. Photoinactivation of influenza virus fusion and infectivity by rose bengal. Photochem Photobiol, v.58, n.4, Out, p.527-31. 1993.

Lescar, J., A. Roussel, *et al.* The Fusion glycoprotein shell of Semliki Forest virus: an icosahedral assembly primed for fusogenic activation at endosomal pH. Cell, v.105, n.1, Abr 6, p.137-48. 2001.

Letchworth, G. J., L. L. Rodriguez, *et al.* Vesicular stomatitis. Vet J, v.157, n.3, Maio, p.239-60. 1999.

Li, W., F. Nicol, *et al.* GALA: a designed synthetic pH-responsive amphipathic peptide with applications in drug and gene delivery. Adv Drug Deliv Rev, v.56, n.7, Abr 23, p.967-85. 2004.

Liao, M. e M. Kielian. Domain III from class II fusion proteins functions as a dominant-negative inhibitor of virus membrane fusion. J Cell Biol, v.171, n.1, Out 10, p.111-20. 2005.

Lim, D. S., S. H. Ko, *et al.* Photoinactivation of vesicular stomatitis virus by a photodynamic agent, chlorophyll derivatives from silkworm excreta. J Photochem Photobiol B, v.67, n.3, Jul, p.149-56. 2002.

Lindenbach, B. D. e C. M. Rice. Flaviviridae: the viruses and their replication. In: D. M. Knipe e P. M. Howley (Ed.). Fields virology. Philadelphia: Lippincott/The Williams & Wilkins Co., 2001. Flaviviridae: the viruses and their replication, p.991-1042

Lindenbach, B. D. e C. M. Rice. Molecular biology of flaviviruses. Adv Virus Res, v.59, p.23-61. 2003.

Lozach, P. Y., L. Burleigh, *et al.* Dendritic cell-specific intercellular adhesion molecule 3-grabbing non-integrin (DC-SIGN)-mediated enhancement of dengue virus infection is independent of DC-SIGN internalization signals. J Biol Chem, v.280, n.25, Jun 24, p.23698-708. 2005.

Lundblad, R. L. e C. M. Noyes. Chemical reagents for protein modification. Boca Raton, Fla.: CRC Press. 1984

Marsh, M. e A. Helenius. Virus entry: open sesame. Cell, v.124, n.4, Fev 24, p.729-40. 2006.

Martinez-Barragan, J. J. e R. M. Del Angel. Identification of a putative coreceptor on Vero cells that participates in dengue 4 virus infection. J Virol, v.75, n.17, Set, p.7818-27. 2001.

Matlin, K. S., H. Reggio, *et al.* Pathway of vesicular stomatitis virus entry leading to infection. J Mol Biol, v.156, n.3, Abr 15, p.609-31. 1982.

Matsuyama, S., S. E. Delos, *et al.* Sequential roles of receptor binding and low pH in forming prehairpin and hairpin conformations of a retroviral envelope glycoprotein. J Virol, v.78, n.15, Ago, p.8201-9. 2004.

Matthews, T., M. Salgo, *et al.* Enfuvirtide: the first therapy to inhibit the entry of HIV-1 into host CD4 lymphocytes. Nat Rev Drug Discov, v.3, n.3, Mar, p.215-25. 2004.

Mccluskey, B. J., H. S. Hurd, *et al.* Review of the 1997 outbreak of vesicular stomatitis in the western United States. J Am Vet Med Assoc, v.215, n.9, Nov 1, p.1259-62. 1999.

Meanwell, N. A. Hepatitis C virus entry: an intriguing challenge for drug discovery. Curr Opin Investig Drugs, v.7, n.8, Ago, p.727-32. 2006.

Miles, E. W. Modification of histidyl residues in proteins by diethylpyrocarbonate. Methods Enzymol, v.47, p.431-42. 1977.

Modis, Y., S. Ogata, *et al.* A ligand-binding pocket in the dengue virus envelope glycoprotein. Proc Natl Acad Sci U S A, v.100, n.12, Jun 10, p.6986-91. 2003.

Modis, Y., S. Ogata, *et al.* Structure of the dengue virus envelope protein after membrane fusion. Nature, v.427, n.6972, Jan 22, p.313-9. 2004.

Moore, J. P. e R. W. Doms. The entry of entry inhibitors: a fusion of science and medicine. Proc Natl Acad Sci U S A, v.100, n.19, Set 16, p.10598-602. 2003.

Morse, C. e F. Maldarelli. Enfuvirtide antiviral activity despite rebound viremia and resistance mutations: fitness tampering or a case of persistent braking on entering? J Infect Dis, v.195, n.3, Fev 1, p.318-21. 2007.

Moscona, A. Entry of parainfluenza virus into cells as a target for interrupting childhood respiratory disease. J Clin Invest, v.115, n.7, Jul, p.1688-98. 2005.

Mothes, W., A. L. Boerger, *et al.* Retroviral entry mediated by receptor priming and low pH triggering of an envelope glycoprotein. Cell, v.103, n.4, Nov 10, p.679-89. 2000.

Mukhopadhyay, S., R. J. Kuhn, *et al.* A structural perspective of the flavivirus life cycle. Nat Rev Microbiol, v.3, n.1, Jan, p.13-22. 2005.

Murdin, A. D., L. Barreto, *et al.* Inactivated poliovirus vaccine: past and present experience. Vaccine, v.14, n.8, Jun, p.735-46. 1996.

Nathanson, N. e A. D. Langmuir. The Cutter Incident. Poliomyelitis Following Formaldehyde- Inactivated Poliovirus Vaccination in the United States During the Spring of 1955. Am J Hyg, v.78, Jul, p.16-60. 1963.

Navarro-Sanchez, E., R. Altmeyer, *et al.* Dendritic-cell-specific ICAM3-grabbing non-integrin is essential for the productive infection of human dendritic cells by mosquito-cell-derived dengue viruses. EMBO Rep, v.4, n.7, Jul, p.723-8. 2003.

Nogueira, R. M., M. P. Miagostovich, *et al.* Dengue virus type 3 in Rio de Janeiro, Brazil. Mem Inst Oswaldo Cruz, v.96, n.7, Out, p.925-6. 2001.

Nogueira, R. M., H. G. Schatzmayr, *et al.* Dengue virus type 3, Brazil, 2002. Emerg Infect Dis, v.11, n.9, Set, p.1376-81. 2005.

Nogueira, R. M., S. M. Zagner, *et al.* Dengue haemorrhagic fever/dengue shock syndrome (DHF/DSS) caused by serotype 2 in Brazil. Mem Inst Oswaldo Cruz, v.86, n.2, Abr-Jun, p.269. 1991.

O'hagan, D. T., M. L. Mackichan, *et al.* Recent developments in adjuvants for vaccines against infectious diseases. Biomol Eng, v.18, n.3, Out 15, p.69-85. 2001.

O'keefe, B. R., D. F. Smee, *et al.* Potent anti-influenza activity of cyanovirin-N and interactions with viral hemagglutinin. Antimicrob Agents Chemother, v.47, n.8, Ago, p.2518-25. 2003.

Odell, D., E. Wanas, *et al.* Influence of membrane anchoring and cytoplasmic domains on the fusogenic activity of vesicular stomatitis virus glycoprotein G. J Virol, v.71, n.10, Out, p.7996-8000. 1997.

Osanai, C. H., A. P. Travassos Da Rosa, *et al.* [Dengue outbreak in Boa Vista, Roraima. Preliminary report]. Rev Inst Med Trop Sao Paulo, v.25, n.1, Jan-Fev, p.53-4. 1983.

Ovadi, J., S. Libor, *et al.* Spectrophotometric determination of histidine in proteins with diethylpyrocarbonate. Acta Biochim. Biophys. Acad. Sci. Hung., v.2, p.455-458. 1967.

Pak, C. C., A. Puri, *et al.* Conformational changes and fusion activity of vesicular stomatitis virus glycoprotein: [125I]iodonaphthyl azide photolabeling studies in biological membranes. Biochemistry, v.36, n.29, Jul 22, p.8890-6. 1997.

Pinheiro, F. P. e S. J. Corber. Global situation of dengue and dengue haemorrhagic fever, and its emergence in the Americas. World Health Stat Q, v.50, n.3-4, p.161-9. 1997.

Pokidysheva, E., Y. Zhang, *et al.* Cryo-EM reconstruction of dengue virus in complex with the carbohydrate recognition domain of DC-SIGN. Cell, v.124, n.3, Fev 10, p.485-93. 2006.

Pouny, Y., D. Rapaport, *et al.* Interaction of antimicrobial dermaseptin and its fluorescently labeled analogues with phospholipid membranes. Biochemistry, v.31, n.49, Dez 15, p.12416-23. 1992.

Puri, A., J. Winick, *et al.* Activation of vesicular stomatitis virus fusion with cells by pretreatment at low pH. J Biol Chem, v.263, n.10, Abr 5, p.4749-53. 1988.

Quiroz, E., N. Moreno, *et al.* A human case of encephalitis associated with vesicular stomatitis virus (Indiana serotype) infection. Am J Trop Med Hyg, v.39, n.3, Set, p.312-4. 1988.

Rey, F. A., F. X. Heinz, *et al.* The envelope glycoprotein from tick-borne encephalitis virus at 2 A resolution. Nature, v.375, n.6529, Maio 25, p.291-8. 1995.

Reyes-Del Valle, J., S. Chavez-Salinas, *et al.* Heat shock protein 90 and heat shock protein 70 are components of dengue virus receptor complex in human cells. J Virol, v.79, n.8, Abr, p.4557-67. 2005.

Rigau-Perez, J. G., G. G. Clark, *et al.* Dengue and dengue haemorrhagic fever. Lancet, v.352, n.9132, Set 19, p.971-7. 1998.

Roche, S., S. Bressanelli, *et al.* Crystal structure of the low-pH form of the vesicular stomatitis virus glycoprotein G. Science, v.313, n.5784, Jul 14, p.187-91. 2006.

Roche, S. e Y. Gaudin. Characterization of the equilibrium between the native and fusion-inactive conformation of rabies virus glycoprotein indicates that the fusion complex is made of several trimers. Virology, v.297, n.1, Maio 25, p.128-35. 2002.

Roche, S., F. A. Rey, *et al.* Structure of the prefusion form of the vesicular stomatitis virus glycoprotein G. Science, v.315, n.5813, Fev 9, p.843-8. 2007.

Rodriguez, L. L. Emergence and re-emergence of vesicular stomatitis in the United States. Virus Res, v.85, n.2, Maio 10, p.211-9. 2002.

Rodriguez, L. L., G. J. Letchworth, *et al.* Rapid detection of vesicular stomatitis virus New Jersey serotype in clinical samples by using polymerase chain reaction. J Clin Microbiol, v.31, n.8, Ago, p.2016-20. 1993.

Rose, J. K. e M. A. Whitt. Rhabdoviridae: the viruses and their replication. In: D. M. Knipe e P. M. Howley (Ed.). Fields virology. Philadelphia: Lippincott/The Williams & Wilkins Co., 2001. Rhabdoviridae: the viruses and their replication, p.1221-1244

Roussel, A., J. Lescar, *et al.* Structure and interactions at the viral surface of the envelope protein E1 of Semliki Forest virus. Structure, v.14, n.1, Jan, p.75-86. 2006.

Schatzmayr, H. G., R. M. Nogueira, *et al.* An outbreak of dengue virus at Rio de Janeiro--1986. Mem Inst Oswaldo Cruz, v.81, n.2, Abr-Jun, p.245-6. 1986.

Schlegel, R., T. S. Tralka, *et al.* Inhibition of VSV binding and infectivity by phosphatidylserine: is phosphatidylserine a VSV-binding site? Cell, v.32, n.2, Fev, p.639-46. 1983.

Seitz, H., J. Blumel, *et al.* Comparable virus inactivation by bovine or vegetable derived Tween 80 during solvent/detergent treatment. Biologicals, v.30, n.3, Set, p.197-205. 2002.

Shai, Y. Mechanism of the binding, insertion and destabilization of phospholipid bilayer membranes by alpha-helical antimicrobial and cell non-selective membrane-lytic peptides. Biochim Biophys Acta, v.1462, n.1-2, Dez 15, p.55-70. 1999.

Shenoy, S. R., B. R. O'keefe, *et al.* Selective interactions of the human immunodeficiency virus-inactivating protein cyanovirin-N with high-mannose oligosaccharides on gp120 and other glycoproteins. J Pharmacol Exp Ther, v.297, n.2, Maio, p.704-10. 2001.

Shokralla, S., Y. He, *et al.* Mutations in a carboxy-terminal region of vesicular stomatitis virus glycoprotein G that affect membrane fusion activity. Virology, v.242, n.1, Mar 1, p.39-50. 1998.

Shriver, Z., Y. Hu, *et al.* Heparinase II from Flavobacterium heparinum. Role of histidine residues in enzymatic activity as probed by chemical modification and site-directed mutagenesis. J Biol Chem, v.273, n.17, Abr 24, p.10160-7. 1998.

Sieczkarski, S. B. e G. R. Whittaker. Dissecting virus entry via endocytosis. J Gen Virol, v.83, n.Pt 7, Jul, p.1535-45. 2002.

Sieczkarski, S. B. e G. R. Whittaker. Viral entry. Curr Top Microbiol Immunol, v.285, p.1-23. 2005.

Silva, J. L., P. Luan, *et al.* Effects of hydrostatic pressure on a membrane-enveloped virus: high immunogenicity of the pressure-inactivated virus. J Virol, v.66, n.4, Abr, p.2111-7. 1992.

Siqueira, J. B., Jr., C. M. Martelli, *et al.* Dengue and dengue hemorrhagic fever, Brazil, 1981-2002. Emerg Infect Dis, v.11, n.1, Jan, p.48-53. 2005.

Skehel, J. J. e D. C. Wiley. Receptor binding and membrane fusion in virus entry: the influenza hemagglutinin. Annu Rev Biochem, v.69, p.531-69. 2000.

Smith, A. E. e A. Helenius. How viruses enter animal cells. Science, v.304, n.5668, Abr 9, p.237-42. 2004.

Smith, T. Picture story. Does Dengue virus fuse using beta-barrels? Nat Struct Biol, v.9, n.4, Abr, p.244. 2002.

Stadler, K., S. L. Allison, *et al.* Proteolytic activation of tick-borne encephalitis virus by furin. J Virol, v.71, n.11, Nov, p.8475-81. 1997.

Stauffer, F., T. El-Bacha, *et al.* Advances in the Development of Inactivated Virus Vaccines Recent Patents on Anti-Infective Drug Discovery, v.1, n.3, p.291-296. 2006.

Stevens, J., A. L. Corper, *et al.* Structure of the uncleaved human H1 hemagglutinin from the extinct 1918 influenza virus. Science, v.303, n.5665, Mar 19, p.1866-70. 2004.

Stiasny, K., S. L. Allison, *et al.* Role of metastability and acidic pH in membrane fusion by tick-borne encephalitis virus. J Virol, v.75, n.16, Ago, p.7392-8. 2001.

Stiasny, K., S. L. Allison, *et al.* Structural requirements for low-pH-induced rearrangements in the envelope glycoprotein of tick-borne encephalitis virus. J Virol, v.70, n.11, Nov, p.8142-7. 1996.

Tassaneetrithep, B., T. H. Burgess, *et al.* DC-SIGN (CD209) mediates dengue virus infection of human dendritic cells. J Exp Med, v.197, n.7, Abr 7, p.823-9. 2003.

Teixeira, M. G., M. C. Costa, *et al.* Dengue and dengue hemorrhagic fever epidemics in Brazil: what research is needed based on trends, surveillance, and control experiences? Cad Saude Publica, v.21, n.5, Set-Out, p.1307-15. 2005.

Tesh, R. B., J. Boshell, *et al.* Natural infection of humans, animals, and phlebotomine sand flies with the Alagoas serotype of vesicular stomatitis virus in Colombia. Am J Trop Med Hyg, v.36, n.3, Maio, p.653-61. 1987.

Thepparit, C. e D. R. Smith. Serotype-specific entry of dengue virus into liver cells: identification of the 37-kilodalton/67-kilodalton high-affinity laminin receptor as a dengue virus serotype 1 receptor. J Virol, v.78, n.22, Nov, p.12647-56. 2004.

Wagner, R. R. Rhabdovirus biology and infection: an overview. In: R. R. Wagner (Ed.). The rhabdoviruses. New York: Plenum, 1987. Rhabdovirus biology and infection: an overview., p.9-74

Weissenhorn, W., A. Carfi, *et al.* Crystal structure of the Ebola virus membrane fusion subunit, GP2, from the envelope glycoprotein ectodomain. Mol Cell, v.2, n.5, Nov, p.605-16. 1998.

Weissenhorn, W., A. Dessen, *et al.* Structural basis for membrane fusion by enveloped viruses. Mol Membr Biol, v.16, n.1, Jan-Mar, p.3-9. 1999.

Weissenhorn, W., A. Hinz, *et al.* Virus membrane fusion. FEBS Lett, v.581, n.11, Maio 22, p.2150-5. 2007.

Wertz, G. W., V. P. Perepelitsa, *et al.* Gene rearrangement attenuates expression and lethality of a nonsegmented negative strand RNA virus. Proc Natl Acad Sci U S A, v.95, n.7, Mar 31, p.3501-6. 1998.

White, J., M. Kielian, *et al.* Membrane fusion proteins of enveloped animal viruses. Q Rev Biophys, v.16, n.2, Maio, p.151-95. 1983.

White, J., K. Matlin, *et al.* Cell fusion by Semliki Forest, influenza, and vesicular stomatitis viruses. J Cell Biol, v.89, n.3, Jun, p.674-9. 1981.

Whitehead, S. S., J. E. Blaney, *et al.* Prospects for a dengue virus vaccine. Nat Rev Microbiol, v.5, n.7, Jul, p.518-28. 2007.

Who. Dengue haemorrhagic fever: diagnosis, treatment prevention and control. WHO. Geneva, 1997. p.

Wilder-Smith, A. e E. Schwartz. Dengue in travelers. N Engl J Med, v.353, n.9, Set 1, p.924-32. 2005.

Wilks, C. R. Vesicular stomatitis and other vesiculovirus infections. In: J. A. W. Coetzer, G. R. Thomson, *et al* (Ed.). Infectious diseases of livestock with special reference to Southern Africa. Oxford: Oxford University Press, v.1, 1994. Vesicular stomatitis and other vesiculovirus infections., p.563-566

Wilson, I. A., J. J. Skehel, *et al.* Structure of the haemagglutinin membrane glycoprotein of influenza virus at 3 A resolution. Nature, v.289, n.5796, Jan 29, p.366-73. 1981.

Xu, Y., Y. Liu, *et al.* Structural basis for coronavirus-mediated membrane fusion. Crystal structure of mouse hepatitis virus spike protein fusion core. J Biol Chem, v.279, n.29, Jul 16, p.30514-22. 2004.

Xu, Y., Z. Lou, *et al.* Crystal structure of severe acute respiratory syndrome coronavirus spike protein fusion core. J Biol Chem, v.279, n.47, Nov 19, p.49414-9. 2004.

Yang, J., M. Prorok, *et al.* Oligomeric beta-structure of the membrane-bound HIV-1 fusion peptide formed from soluble monomers. Biophys J, v.87, n.3, Set, p.1951-63. 2004.

Yang, J. e D. P. Weliky. Solid-state nuclear magnetic resonance evidence for parallel and antiparallel strand arrangements in the membrane-associated HIV-1 fusion peptide. Biochemistry, v.42, n.40, Out 14, p.11879-90. 2003.

Yeung, K. S. e N. A. Meanwell. Recent developments in the virology and antiviral research of severe acute respiratory syndrome coronavirus. Infect Disord Drug Targets, v.7, n.1, Mar, p.29-41. 2007.

Yeung, K. S., G. A. Yamanaka, *et al.* Severe acute respiratory syndrome coronavirus entry into host cells: Opportunities for therapeutic intervention. Med Res Rev, v.26, n.4, Jul, p.414-33. 2006.

Yin, H. S., R. G. Paterson, *et al.* Structure of the uncleaved ectodomain of the paramyxovirus (hPIV3) fusion protein. Proc Natl Acad Sci U S A, v.102, n.26, Jun 28, p.9288-93. 2005.

Yin, H. S., X. Wen, *et al.* Structure of the parainfluenza virus 5 F protein in its metastable, prefusion conformation. Nature, v.439, n.7072, Jan 5, p.38-44. 2006.

Zhang, L. e H. P. Ghosh. Characterization of the putative fusogenic domain in vesicular stomatitis virus glycoprotein G. J Virol, v.68, n.4, Abr, p.2186-93. 1994.

ANEXOS

ANEXO A

Membrane Recognition by Vesicular Stomatitis Virus Involves Enthalpy-Driven Protein-Lipid Interactions

Fabiana A. Carneiro, M. Lucia Bianconi, Gilberto Weissmüller, Fausto Stauffer e Andrea T. Da Poian

Publicado em 2002 no periódico

Journal of Virology

JOURNAL OF VIROLOGY, Apr. 2002, p. 3756–3764 Vol. 76, No. 8
0022-538X/02/$04.00+0 DOI: 10.1128/JVI.76.8.3756–3764.2002

Membrane Recognition by Vesicular Stomatitis Virus Involves Enthalpy-Driven Protein-Lipid Interactions

Fabiana A. Carneiro,[1] M. Lucia Bianconi,[1] Gilberto Weissmüller,[2] Fausto Stauffer,[1] and Andrea T. Da Poian[1]*

Departamento de Bioquímica Médica, Instituto de Ciências Biomédicas,[1] and Instituto de Biofísica Carlos Chagas Filho,[2] Universidade Federal do Rio de Janeiro, Rio de Janeiro, RJ 21941-590, Brazil

Received 26 October 2001/Accepted 16 January 2002

Vesicular stomatitis virus (VSV) infection depends on the fusion of viral and cellular membranes, which is mediated by virus spike glycoprotein G at the acidic environment of the endosomal compartment. VSV G protein does not contain a hydrophobic amino acid sequence similar to the fusion peptides found among other viral glycoproteins, suggesting that membrane recognition occurs through an alternative mechanism. Here we studied the interaction between VSV G protein and liposomes of different phospholipid composition by force spectroscopy, isothermal titration calorimetry (ITC), and fluorescence spectroscopy. Force spectroscopy experiments revealed the requirement for negatively charged phospholipids for VSV binding to membranes, suggesting that this interaction is electrostatic in nature. In addition, ITC experiments showed that VSV binding to liposomes is an enthalpically driven process. Fluorescence data also showed the lack of VSV interaction with the vesicles as well as inhibition of VSV-induced membrane fusion at high ionic strength. Intrinsic fluorescence measurements showed that the extent of G protein conformational changes depends on the presence of phosphatidylserine (PS) on the target membrane. Although the increase in PS content did not change the binding profile, the rate of the fusion reaction was remarkably increased when the PS content was increased from 25 to 75%. On the basis of these data, we suggest that G protein binding to the target membrane essentially depends on electrostatic interactions, probably between positive charges on the protein surface and negatively charged phospholipids in the cellular membrane. In addition, the fusion is exothermic, indicating no entropic constraints to this process.

Entry of enveloped animal viruses into their host cells always involves a step of membrane fusion, which is mediated by viral envelope glycoproteins (20, 23, 51). Two general mechanisms have been defined for the fusion reaction: (i) surface fusion between the viral envelope and host cell plasma membrane and (ii) fusion of the endosomal membrane with the viral envelope after virus particle internalization by receptor-mediated endocytosis. In the first case, a well-characterized fusion mechanism is that mediated by the human immunodeficiency virus (HIV) gp120 and gp41 glycoproteins (7). Interaction between gp120, the cellular CD4 molecule, and a coreceptor protein leads to the insertion of the gp41 hydrophobic fusion peptide into the plasma membrane. gp41 forms a trimeric coiled-coil containing two interacting α-helical peptides that acquire a six-helix bundle structure (8, 28).

Fusion at the endosome is triggered by conformational changes in viral glycoproteins induced by the low pH of this cellular compartment. The best-studied low-pH-activated viral fusion protein is the influenza virus glycoprotein hemagglutinin (HA). The X-ray structure of influenza virus HA was determined at both neutral and fusogenic pHs (5, 53). The conformational changes observed suggest that the hydrophobic fusion peptide moves to the tip of the molecule and is delivered toward the target membrane (5). The conformational transition occurs within a narrow pH range, corresponding to the optimal pH of fusion, in which the protein acquires the ability to interact with detergent micelles and lipid vesicles (46). This interaction leads to the insertion of the fusion peptide into the membrane, where a pore is formed (4, 48).

Vesicular stomatitis virus (VSV) enters the cell by endocytosis, followed by low-pH-induced membrane fusion mediated by its spike glycoprotein, named the G protein (12, 30). This protein is a trimeric type I glycoprotein of 67 kDa, which is anchored in the viral membrane via a single transmembrane anchor sequence close to the C terminus (39). Unlike most viral fusion proteins, VSV G protein does not contain an apolar amino acid sequence similar to the fusion peptides (23). Most of the studies on G protein-mediated fusion have focused on the description of the amino acids important for the low-pH-induced conformational change (9, 19, 45, 56). We have recently shown that, at the fusogenic pH, a dramatic conformational change on VSV G protein takes place, including loss and reorganization of its secondary and tertiary structures (6). Our results also indicated that the G protein interacts with target membranes through the formation and/or exposure of a hydrophobic domain at pHs close to 6.0, although the mechanism and the nature of protein-lipid interactions during fusion still remain unclear.

Here we describe a study of VSV-membrane interaction by force spectroscopy, isothermal titration calorimetry (ITC), and fluorescence spectroscopy. We show that VSV-membrane interactions as well as the fusion reaction mediated by the virus are highly dependent on the presence of negative charges on the vesicle surface. In addition, both VSV binding to phospho-

* Corresponding author. Mailing address: Departamento de Bioquímica Médica, Instituto de Ciências Biomédicas, Universidade Federal do Rio de Janeiro, Rio de Janeiro, RJ 21941-590, Brazil. Phone: 55-21-2270 6264. Fax: 55-21-2270 8647. E-mail: dapoian@bioqmed.ufrj.br.

lipid vesicles and the VSV-induced membrane fusion are enthalpy-driven reactions, suggesting the involvement of electrostatic interactions. This was confirmed by the lack of binding and fusion reaction at high ionic strength. Our results show that, although we cannot discard hydrophobic contributions in both processes, VSV interaction with the target membrane is probably driven by electrostatic interactions and H-bond formation.

MATERIALS AND METHODS

Virus propagation and purification. VSV strain Indiana was propagated in monolayer cultures of BHK-21 cells. The cells were grown at 37°C in roller bottles containing 150 ml of Dulbecco's modified Eagle's medium supplemented with 10% fetal bovine serum (Cultilab, Campinas, SP, Brazil), 100 μg of ampicillin, and 5 μg of gentamicin per ml. When the cells reached confluence, the medium was removed, and the cell monolayer was infected with VSV at a multiplicity of 5 PFU/ml. The cultures were kept at 37°C for 16 to 20 h, and the virus were harvested and purified by differential centrifugation, followed by equilibrium sedimentation in a sucrose gradient as described elsewhere (13). Purified virions were stored at −70°C.

Preparation of liposomes. Phospholipids were dissolved in chloroform and evaporated under nitrogen. The lipid film formed was resuspended in 20 mM MES (morpholineethanesulfonic acid)–30 mM Tris buffer (pH 7.5 or 6.0) at a final concentration of 1 mM. The suspension was vortexed vigorously for 5 min. Small unilamellar vesicles were obtained by sonicating the turbid suspension with a Branson Sonifier (Sonic Power Company, Danbury, Conn.) equipped with a titanium microtip probe. Sonication was performed in an ice bath, alternating cycles of 30 s at 20% full power with 60-s resting intervals until a transparent solution was obtained (approximately 10 cycles). The vesicles used in this study were composed of phosphatidylcholine (PC), phosphatidylethanolamine (PE), and phosphatidylserine (PS) at a 3:1:1 ratio, with 10% cholesterol; PC and PS at different ratios, as indicated in the figure legends; PC and cardiolipin (CL), 3:1; and PC only. For fusion assays, 1% 1-hexadecanoyl-2-(1-pyrenedecanoyl)-*sn*-glycero-3-phosphocholine (10-PyPC; Molecular Probes Inc., Eugene, Oreg.) was incorporated in PC-PS vesicles by vortexing for 10 min. Phospholipids were purchased from Sigma Chemical Co.

Atomic force microscopy. The atomic force microscope used in this work was built in collaboration with the Ludwig-Maximilians-Universität Lehrstuhl für Angewandte Physik in Munich, Germany. For all the experiments, the atomic force microscope was used in force spectroscopy mode (18, 21, 58). Mica coverslips were glued to magnetic stainless steel punches and mounted in a fluid cell without using the O-ring. The mica surfaces were incubated with vesicles before transfer to the fluid cell (25, 35). Since the presence of calcium ions appears to facilitate as well as to increase the rate of planar membrane formation from vesicles (34, 38), mica surfaces were incubated with 20 μl of the vesicle suspension, containing 1 mM phospholipids, plus 10 μl of 20 mM MES–30 mM Tris buffer, pH 7.4, containing 1 mM $CaCl_2$, for approximately half an hour at room temperature (25 ± 0.5°C). After incubation, the slips were washed repeatedly with the same buffer used to prepare vesicles.

All experiments were performed at room temperature using standard V-shaped cantilevers, containing a silicon nitride tip with a 4-μm^2 pyramidal base (Digital Instruments Inc.). The cantilevers have a spring constant of 0.06 N/m (manufacturer's data) and were incubated with VSV as follows. The cantilevers were immersed in a virus suspension (total protein concentration, 0.28 mg/ml) for 24 h at 4 to 6°C. The instrument allows the performance of "approach-retraction" cycles, in which the maximal contact force, interaction time and the approach-retracting rates can be controlled independently. The maximal force was limited to approximately 3 nN, the interaction time was set to zero, and the approach-retracting rate was set to 7,500 nm/s.

Calorimetric measurements. The binding of VSV to lipid vesicles and the membrane fusion mediated by the G protein were studied at 35°C in an MCS-ITC microcalorimeter from MicroCal, Llc. (Northampton, Mass.). The implementation of ITC was previously described by Wiseman et al. (54). For the binding experiments, the samples were prepared at pH 7.5, and after equilibration at 35°C, several preparations (2 to 10 μl each) of a solution containing virus (28 μg of protein/ml) were injected into the cell (volume = 1.38 ml) containing the vesicles. The heat of dilution of the virus was measured by injecting the same solution of VSV into buffer only. The calorimetric thermograms ($\delta Q/\delta t$ as a function of time) were analyzed by integrating the area under each peak to determine the heat (Q) of injection.

For the membrane fusion experiments, the protein concentration in the VSV sample was 10-fold higher than that used for binding, and after a single 10-μl injection the fusion process was followed for 30 min. The experiments were done at pH 6.0 and pH 7.5, and the data were analyzed by integrating the calorimetric thermogram in order to obtain the heat released ($-Q$) as a function of time, which allows the analysis of the kinetics of fusion. Due to the high concentration of the virus suspension, the heat of VSV dilution was very intense, making it difficult to subtract from the raw data for fusion. In this case, the data were analyzed after the heat effect for the VSV dilution. In all the ITC experiments, the syringe was rotated at 400 rpm. The samples were degassed under vacuum prior to the titration. The data were analyzed with the Origin 5.0 software provided by MicroCal. The changes in enthalpy and entropy for the association (ΔH^{ass} and the ΔS^{ass}, respectively) were calculated according to Hyre and Spicer (24).

Intrinsic fluorescence measurements. G protein conformational changes during VSV interaction with membranes of different phospholipid composition were monitored by the changes in virus intrinsic fluorescence. VSV (final protein concentration, 70 μg/ml) was incubated with a liposome suspension containing 1 mM phospholipid in 20 mM MES–30 mM Tris buffer, pH 6.0. Intrinsic fluorescence data were recorded using a Hitachi F-4500 fluorescence spectrometer, exciting the samples at 280 nm and collecting emissions between 300 and 420 nm.

Liposome fusion assay. A suspension of liposomes of different phospholipid compositions containing equal amounts of unlabeled vesicles and vesicles labeled with 10-PyPC were prepared in 20 mM MES–30 mM Tris buffer, pH 6.0 or 7.5, with a final phospholipid concentration of 0.1 mM. The emission spectrum of pyrene-labeled vesicles exhibited a broad excimer fluorescence peak with maximal intensity at 480 nm and two sharp peaks at 376 and 396 nm due to monomer fluorescence emission (not shown). The fusion reaction was initiated by addition of purified VSV. Fusion was followed by the decrease in the 10-PyPC excimer/monomer fluorescence intensity ratio, which was measured by exciting the sample at 340 nm and collecting the fluorescence intensities of excimer and monomer at 480 and 376 nm, respectively.

RESULTS

VSV binding to membranes. Although the precise cellular receptor for VSV is still unknown, the finding that PS specifically inhibits VSV cell binding and infectivity suggested that PS is at least an important component of the VSV binding site (43). To study VSV binding to PS, we evaluated the interaction between the virus and membranes of different phospholipid composition using force spectroscopy (Fig. 1). This technique allows the direct determination of ligand-receptor interactions by measuring rupture forces between the cantilever and the surface, each of them covered with the molecules of interest.

For this study, we chose three different membrane compositions: PC-PS (3:1), PC only, and PC-CL (3:1). VSV was adsorbed on the cantilever, and several approach-retraction cycles were performed at a fixed rate of 7,500 nm/s. The contact between the tip containing adsorbed VSV and the PC-PS surface gave rise to force-distance curves with negative peaks, indicative of adhesion (Fig. 1A). At least 200 curves could be collected with the same tip. In order to ensure the reproducibility of the data, six to eight curves were collected with several tips and substrate.

Table 1 summarizes the values of the force of the adhesion peaks obtained with six different cantilevers with VSV adsorbed and three mica surfaces covered with PC-PS (3:1). The mean adhesion force was 690 pN, with a variation range of 200 to 1,920 pN. Most of the curves present peaks occurring from 200 nm onwards, which corresponds to the virus length. This result suggests that the whole virus particle bridges the tip and the lipid film. No interaction between the virus and the membrane of PC only was observed (Fig. 1B). Of 120 curves obtained with mica substrate covered with 100% PC, only two showed a single small adhesion peak at 293 and 310 pN, both

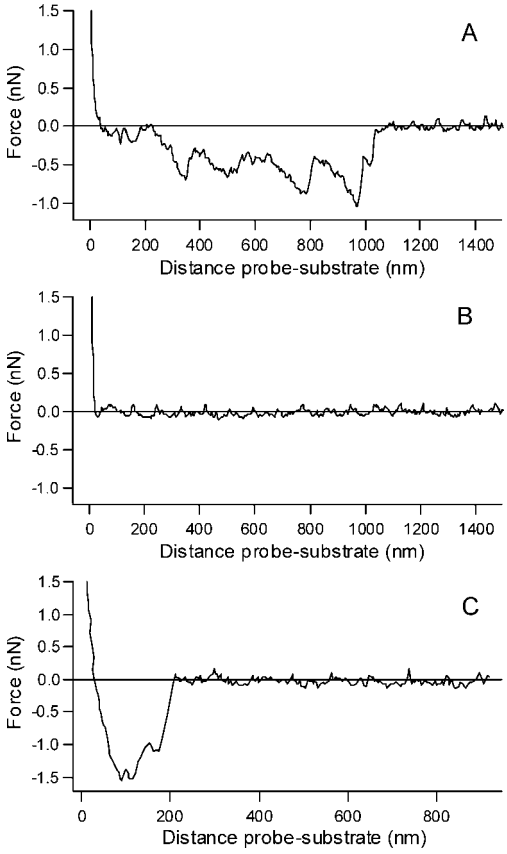

FIG. 1. Force-distance curves for VSV interaction with membranes. Force-distance curves were recorded on lipid-covered mica substrates. Retracting curves were obtained with VSV adsorbed on the tip and mica substrates covered with PC-PS (3:1) (A), PC only (B), or PC-CL (3:1) (C). The negative values for the force peaks in panels A and C indicate adhesion and are absent in panel B. Data were collected in 20 mM MES–30 mM Tris, pH 7.5, at room temperature.

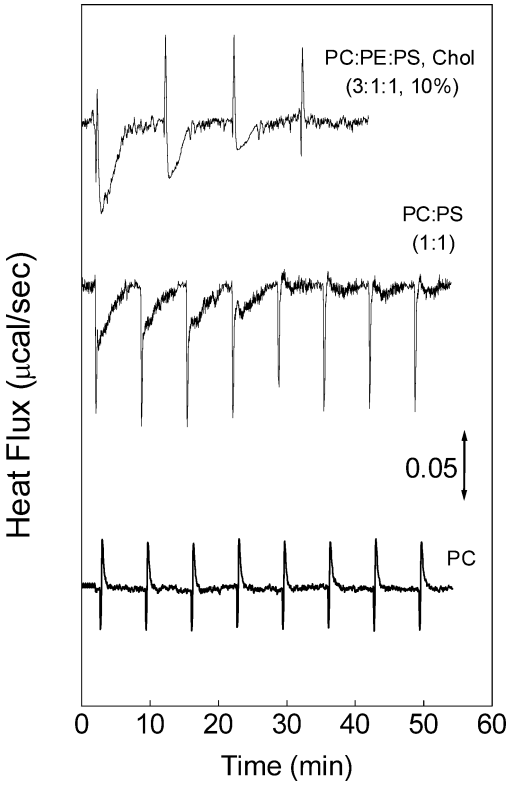

FIG. 2. Calorimetric measurement of VSV binding to liposomes at 35°C. Typical calorimetric traces (heat flow as a function of time) obtained for four to eight injections (5 μl each) of a VSV suspension (28 μg/ml) into the cell containing unilamellar vesicles of PC-PE-PS with cholesterol (3:1:1 and 10%), PC-PS (1:3), or PC only, in 20 mM MES–30 mM Tris, pH 7.5, at 35°C. The sharp peaks are due to the VSV dilution, as seen in control experiments of the injection of virus into buffer (not shown). The phospholipid concentration was 1 mM.

located very close to the surface, indicating nonspecific interactions. Again, to ensure reproducibility, the experiments were also performed using different tips and substrates, and the same results were obtained. No interaction was observed between bare tips and mica surfaces covered with PC or PC-PS membranes (not shown).

TABLE 1. Force of adhesion peaks obtained with VSV and PC-PS (3:1) films on mica

Expt	Force (pN)					
	Substrate[a] 1		Substrate 2		Substrate 3	
	Cant[b] 1	Cant 2	Cant 3	Cant 4	Cant 5	Cant 6
1	1,240	1,580	500	1,280	552	957
2	540	1,920	425	980	332	717
3	1,100	770	416	1,171	354	587
4	402	825	200	810	420	761
5	405	875	670	259	464	521
6	503	927	667	301	266	518
7	450	1,560		302		345
8						410

[a] Substrate, mica surface covered with membranes.
[b] Cant, cantilever.

In order to verify whether the interaction observed in force spectroscopy experiments was due to a specific binding between PS and VSV or due to an electrostatic interaction between positive charges in G protein and negatively charged phospholipids, we substituted PS with another negatively charged phospholipid, CL (Fig. 1C). The force-distance curve presented in Fig. 1C is representative of several experiments and showed a strong interaction between the virus and PC-CL membranes, as found for PC-PS membranes. The mean adhesion force was 1,500 pN, ranging from 620 to 2,900 pN. Multiple peaks were also obtained. This result suggests that, rather than being specific to PS, the interaction between VSV and the membranes probably depends on the presence of negatively charged phospholipids.

The interaction between VSV and vesicles of different phospholipid compositions was also studied by ITC at pH 7.5, at which G protein-induced membrane fusion is negligible (33, 52). As shown in the calorimetric traces in Fig. 2, each injection of VSV into vesicles of PC-PE-PS the cholesterol (3:1:1 and 10%) or PC-PS (1:1) results in a two-component reaction, one sharp exothermic peak followed by a broader exothermic component. A control experiment done by injecting VSV into

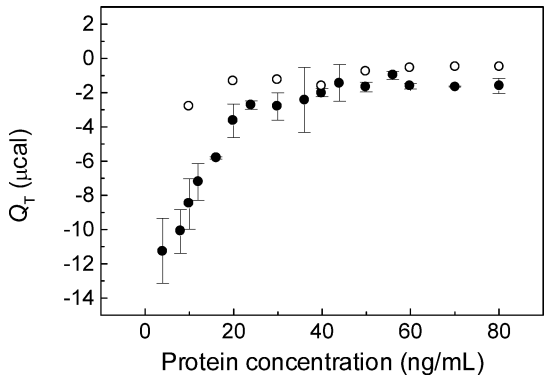

FIG. 3. Binding isotherms. The total heat (Q_T) was calculated for each peak of the calorimetric thermograms resulting from the injection of VSV into vesicles (see Fig. 1). Q_T is plotted as a function of the protein concentration in each injection, with the mean ± standard error (SE) for five different experiments with PC-PS (●) and the mean of two experiments with PC-only vesicles (○) obtained with the same VSV preparation. The data were essentially the same for the PC-PS vesicles containing 25, 50, or 75% PS. The conditions were the same as in Fig. 1. Bar, 0.05 μcal s^{-1}.

buffer showed that the sharp peaks were due to the heat of dilution of the virus suspension. Injection of buffer only into a cell containing vesicles gave rise to negligible heat effects and was not considered for subtraction. On the other hand, VSV injection into PC vesicles gave rise to sharp peaks similar to those observed in the control experiment of virus dilution (Fig. 2). Since no binding was observed with PC vesicles, the broader exothermic component was related to the binding of VSV to the PS-containing membranes. Several injections of VSV were done until saturation.

The plot of the total heat (Q_T) calculated for each peak shows that similar binding isotherms can be obtained with vesicles containing 25, 50, or 75% PS (Fig. 3). The exothermic nature of the binding indicates that this is an enthalpically driven reaction, probably derived from electrostatic interactions, as suggested by the need for negatively charged lipids for the binding to occur (Fig. 1). The Q_T calculated from the injections of VSV into PC-only vesicles was negligible in comparison with those obtained with vesicles containing PS (Fig. 3).

Interactions between G protein and PS drive the conformational changes involved in membrane fusion. It is well established that VSV induces membrane fusion at acidic pH. The fusion reaction depends on VSV G protein and was characterized by using isolated virus to promote fusion of model cells or liposomes in vitro (33, 52). We have recently shown that G protein interaction with liposomes at pH 6.0 resulted in dramatic protein conformational changes, which can be followed by intrinsic fluorescence (6). In the presence of vesicles composed of PC and PS, a great increase in the tryptophan fluorescence of G protein occurred upon acidification of the medium, while a pH decrease led to intrinsic fluorescence quenching in the absence of liposomes (6). The time course of fluorescence increase after VSV incubation with liposomes of different PS content, at pH 6.0, is shown in Fig. 4A. The extent of fluorescence increase was strongly dependent on the

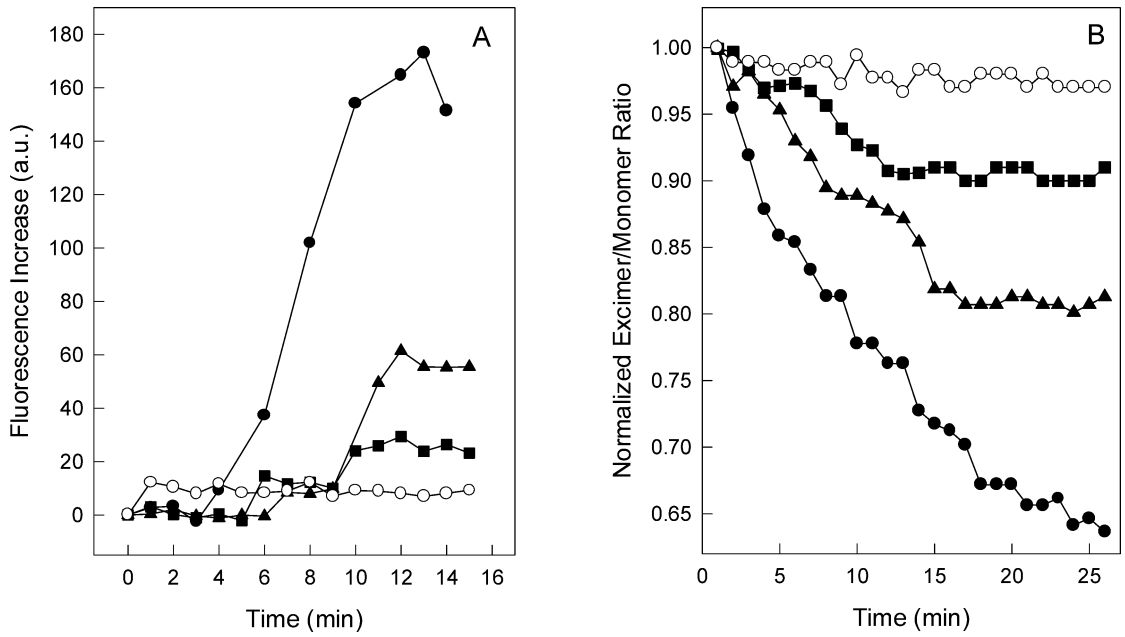

FIG. 4. VSV G protein conformational change during virus incubation with vesicles of different phospholipid compositions. (A) Intrinsic fluorescence of VSV was recorded after virus incubation with small unilamellar vesicles of PC-PS (1:3) (●), PC-PS (1:1) (▲), PC-PS (3:1) (■), and PC only (○). The vesicles were prepared in 20 mM MES–30 mM Tris buffer, pH 6.0, in a final phospholipid concentration of 0.1 mM. The excitation wavelength was 280 nm, and the emission was collected at 334 nm. The final protein concentration was 70 μg/ml. (B) Purified virus was added to a sample containing equal amounts of unlabeled vesicles and vesicles labeled with 10-PyPC. VSV-induced membrane fusion was measured by the decrease in the 10-PyPC excimer/monomer fluorescence intensity ratio. Vesicles used were PC-PS (1:3) (●), PC-PS (1:1) (▲), and PC-PS (3:1) (■) at pH 6.0 and PC-PS (1:3) at pH 7.5 (○). 10-PyPC was excited at 340 nm, and the intensities were collected at 480 and 376 nm for the excimer and monomer, respectively. Experimental conditions were the same as described in the legend to panel A.

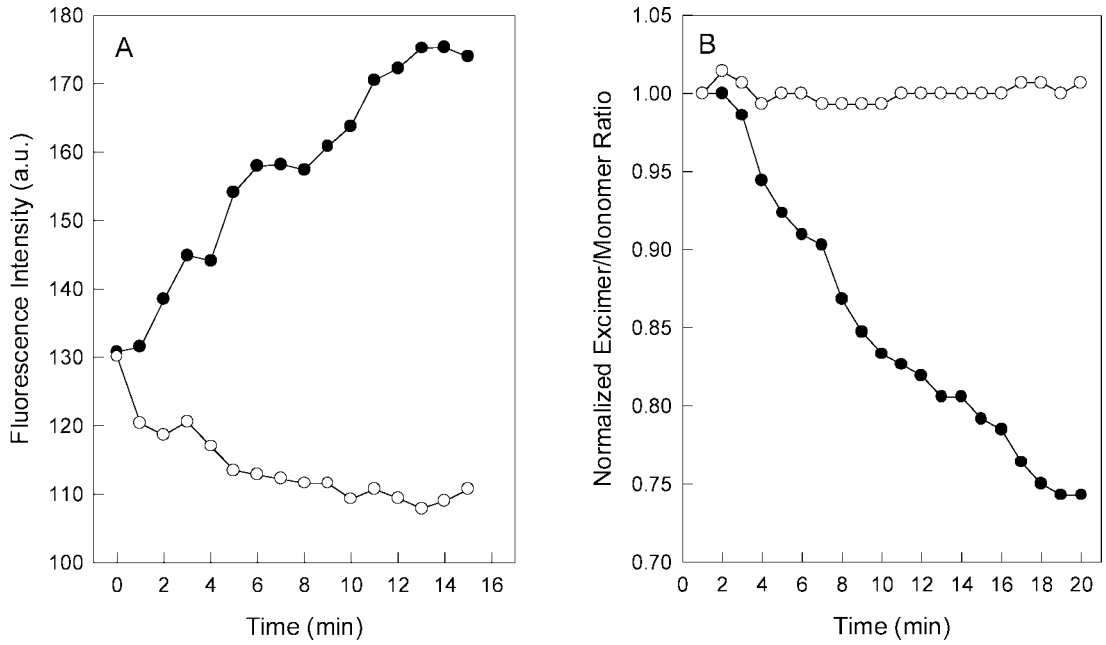

FIG. 5. Effect of high ionic strength on VSV G protein conformational changes during interaction with liposomes. (A) Intrinsic fluorescence of VSV was recorded after virus incubation with vesicles composed of PC-PS (1:3) in the absence (●) and in the presence (○) of 250 mM KCl. The vesicles were prepared in 20 mM MES–30 mM Tris buffer, pH 6.0, in a final phospholipid concentration of 0.1 mM. The excitation wavelength was 280 nm, and the emission was collected at 334 nm. The final protein concentration was 70 μg/ml. (B) VSV-induced membrane fusion measured as in Fig. 4 after virus incubation with vesicles composed of PC-PS (1:3) in the absence (●) and in the presence (○) of 250 mM KCl. Experimental conditions were the same as described in the legend to panel A.

amount of PS in the vesicle, and no increase in fluorescence was observed when the experiment was performed with vesicles of PC only. This result indicates that the G protein conformational changes that take place during protein-lipid interaction are mediated by VSV binding to PS at acidic pH, suggesting the requirement for negative charges in the membrane surface.

VSV-induced liposome fusion can be quantified by measuring the decrease in pyrene phospholipid excimer fluorescence (33). The ability of VSV to mediate fusion was highly dependent on PS content in the liposome (Fig. 4B), suggesting that interactions between G protein and negatively charged phospholipids are also involved in the fusion reaction.

In order to investigate the role of electrostatic interactions in G protein conformational changes during membrane fusion, we evaluated the effect of high ionic strength on G protein conformational changes and VSV fusion activity during incubation of the virus with PC-PS liposomes at pH 6.0. The kinetics of increase in VSV intrinsic fluorescence was followed in the presence of 250 mM KCl (Fig. 5A). At this salt concentration, the interaction between VSV and the vesicles was completely abolished. In addition, VSV-induced membrane fusion was also inhibited at this ionic strength (Fig. 5B). Taken together, these results corroborate the electrostatic nature of G protein-lipid interactions during VSV-induced membrane fusion.

Calorimetric studies of VSV-induced membrane fusion. Membrane fusion was also studied by ITC at 35°C by following the heat effect after injection of VSV into liposomes. The fusion was studied with membranes of different compositions in order to show the importance of negatively charged phospholipids in this process. At pH 6.0, at which the fusion occurs, there is a displacement of the heat flow to negative values relative to the baseline after the heat effects for the dilution (Fig. 6). This effect was related to the VSV fusion to the liposomes, which is a slow process and can be followed for several minutes (6, 33). The heat flow always returns to the baseline level, suggesting that the fusion is complete. The rate of the fusion reaction was dependent on the virus concentration. The negative heat effect was not observed with liposomes lacking negatively charged lipids, such as PC-PE (Fig. 7) or PC only (not shown) vesicles. In agreement with the force spectroscopy experiments, fusion can be studied with CL-containing vesicles (Fig. 7).

A control experiment was done with the same liposomes at pH 7.5 (Fig. 6). At this pH, essentially no fusion is observed (52), although several vesicles can bind to the virus surface (43). In this case, with the same vesicles studied before, the negative heat effect was not observed and a return of the heat flow to the baseline level was observed soon after the heat of VSV dilution. The calorimetric thermograms are similar to those obtained with PC or PC-PE liposomes, showing that the exothermic peak is a feature of systems in which fusion can be achieved.

In Fig. 8, we show the integration of the calorimetric thermograms obtained with PC-PS vesicles at both pH 6.0 and pH 7.5 (from Fig. 6) and with PC only vesicles at pH 6.0 after injection of VSV. At pH 6.0, as the PS content in the membrane increased, there was an increase in the rate of the exothermic reaction. In this particular case, the rate calculated in

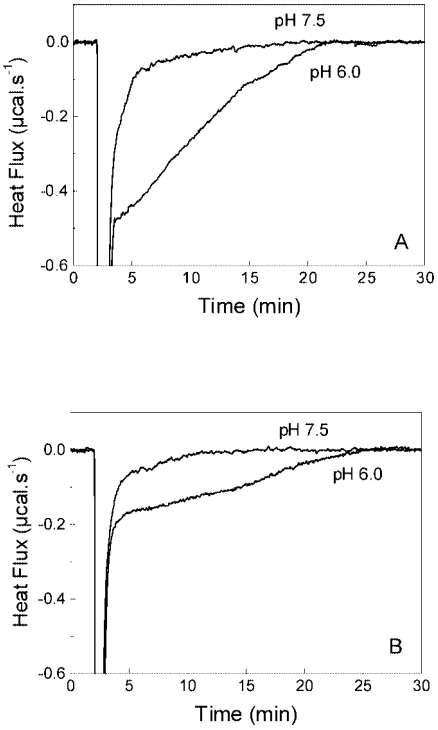

FIG. 6. Calorimetric traces of the fusion of VSV with vesicles of different PS content at 35°C. The calorimetric traces were obtained after the injection of 10 µl of VSV solution (0.28 mg/ml) into the cell containing 1 mM vesicles of PC-PS (1:3) (A) and PC-PS (3:1) (B) at pH 6.0 or pH 7.5, as indicated in each panel. After the heat due to the VSV dilution, there is a negative heat effect that can be associated with the fusion process. The return to the baseline level indicates that the fusion was complete. At pH 7.5, only the heat effect associated with the VSV dilution and binding to the vesicles is observed. The samples were prepared in 20 mM MES–30 mM Tris buffer, pH 7.5 or 6.0.

the steady state was 8.06 mcal min^{-1} for 25% PS, increasing to 20.75 mcal min^{-1} for 75% PS. The process reached a plateau at 18 min with 75% PS and 21 min with 25% PS. At pH 7.5, however, the initial rate of the exothermic process was 1.04 and 2.34 mcal min^{-1} for 25 and 75% PS, respectively, reaching a

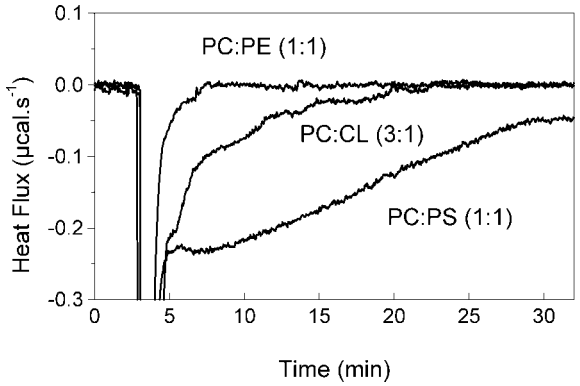

FIG. 7. Calorimetric traces of the fusion of VSV with vesicles of different PS content at 35°C. The calorimetric traces were obtained after the injection of 10 µl of VSV solution (0.28 mg/ml) into the cell containing 1 mM vesicles of PC-PE (1:1), PC-CL (3:1), and PC-PS (1:3). The vesicles were prepared in 20 mM MES–30 mM Tris buffer, pH 6.0.

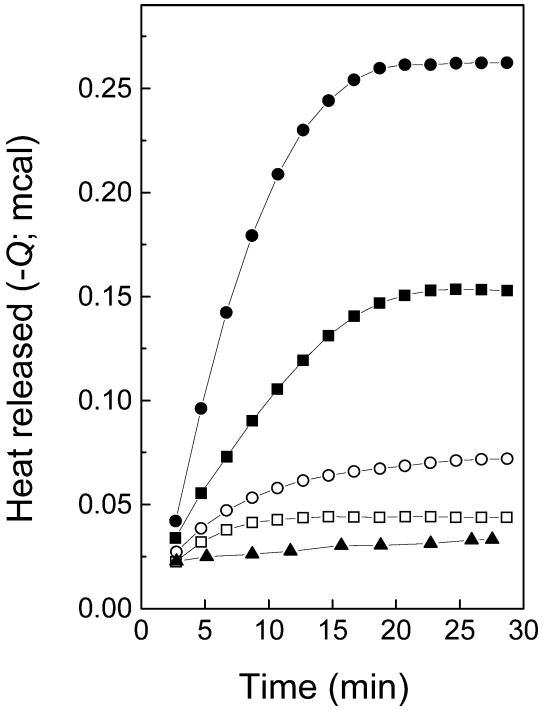

FIG. 8. Kinetics of VSV fusion with membranes at 35°C. The heat released after injection of VSV into the cell containing vesicles at pH 6.0 (●, ■) or at pH 7.5 (○, □) was calculated by integrating the calorimetric traces shown in Fig. 6 for PC-PS at ratios of 1:3 (●, ○) and 3:1 (■, □). Kinetics of the heat effects after VSV injection into vesicles of PC only at pH 6.0 (▲) was obtained from thermograms similar to those in Fig. 6 (not shown).

plateau at around 10 min. For PC-only vesicles at pH 6.0, the heat effect was less intense than those observed with PS-containing vesicles at pH 7.5. This is in agreement with the results found by force spectroscopy, where no binding was observed with PC only (Fig. 1B). Furthermore, when the virus was inactivated by incubation at 50°C for 10 min, no heat effect related to the fusion could be observed (not shown).

DISCUSSION

Enveloped-virus infection depends on a series of events, which comprise cell recognition, interaction between a viral surface protein and a cellular membrane, and membrane fusion induced by viral fusion proteins. Cell recognition by viruses is mediated by the interaction between a viral surface protein and a cellular receptor. Receptors used by viruses belong to different classes of macromolecules, including proteins, carbohydrates, and lipids (2), and virus-receptor interactions may determine the cell tropism and the viral host range. Membrane fusion is always mediated by viral glycoproteins and occurs either directly at the cell surface after virus binding to its receptor or at the acidic environment of the endosomal compartment.

In the case of VSV, cell recognition is mediated by its surface glycoprotein G, which also interacts with the target membrane at acidic pH and catalyzes the fusion reaction. VSV has a broad host range, extending from nearly all mammals to

insects, suggesting that the VSV receptor is a widely distributed molecule. Several efforts to identify the VSV binding site on the cell surface pointed to a lipid as the VSV receptor. Schlegel and coworkers found that VSV binds with high affinity in a saturable site on Vero cells (42) and that the binding could be inhibited by a membrane extract, which was resistant to protease, neuraminidase, and heating, and also inactivated by treatment with phospholipase C (43). These findings, together with the observation that only PS among various purified lipids was able to inhibit VSV binding, led the authors to suggest that PS could participate in the cellular binding site for VSV. Similar results were obtained with erythrocytes at acidic pH: only the lipid moiety of the cell membrane, specifically the negatively charged PS, phosphatidylinositol, and GM3 ganglioside, inhibited VSV attachment to cells (29). Removal of the charged groups from these molecules greatly reduced their inhibitory activities, suggesting an important role of electrostatic interactions during cell recognition by VSV.

Here we show direct evidences that VSV interacts very strongly with membranes containing negatively charged phospholipids at neutral pH. Force-distance curves obtained by using atomic force microscopy showed that VSV did not interact with membranes composed of PC only, whereas forces as strong as 1,900 to 2,900 pN were observed when PS or CL, both negatively charged phospholipids, was present in the lipid film. This suggests that electrostatic interactions between positively charged G protein amino acid residues and the negative charges present in the membrane surface are important for membrane recognition.

Similar results were found in the ITC studies, where binding isotherms were only observed with vesicles containing PS or CL. The binding gives rise to negative peaks, indicating that this process is enthalpically driven. ITC is the only technique that allows the direct thermodynamic analysis of biomolecular interactions, providing the binding constant and stoichiometry in addition to the enthalpy and entropy of binding. Several ITC studies showed that electrostatic binding is usually driven by enthalpy (3, 26, 31, 41, 50). However, it is important to point out that the calorimetric enthalpy is actually a sum of all the heat effects, endothermic and exothermic, taking place during the interaction. Nevertheless, another evidence that electrostatic interactions make a major contribution in the VSV interaction with membranes is the lack of binding and fusion at high ionic strength, as discussed below.

The requirement for electrostatic interactions for VSV binding to the cell surface has also been raised by Bailey et al., who showed that DEAE-dextran, a polycation, increased both VSV binding to BHK cells and G protein-mediated membrane fusion (1). It is possible that DEAE-dextran interacts with the negative charges on virus surface, increasing the density of the positive charges involved in binding to the host cell.

Identification of the amino acid residues involved in the membrane binding site requires further investigation. Although it is possible that the binding domain is formed in the three-dimensional structure of the G protein, recent studies demonstrated that the p2 peptide, a sequence presenting heptad repeats found in all rhabdovirus G proteins, binds PS (11). These heptad repeats (abcdefg) contain two hydrophobic amino acid residues at positions a and d, followed by a sequence containing positively charged amino acid residues, and are located in the amino-terminal part of the glycoproteins (10). For VSV, this sequence comprises the region between amino acid residues 134 and 161.

The components of biological membranes are asymmetrically distributed between the membrane surfaces, and PS is highly segregated to the inner leaflet of plasma membranes (40), suggesting that the G protein-PS interaction is a very improbable event. However, recent findings showing that the binding of a fragment of a salmonid rhabdovirus G protein to model membranes induces PS translocation from the inner to the outer leaflet of the membrane (16) indicate that VSV binding to PS could present more physiological relevance than was expected. Another possibility is that other negatively charged molecules, such as glycosaminoglycans and gangliosides, could act as the physiological binding site for VSV. The role of these molecules in VSV binding to cells and in the membrane fusion process is now under investigation.

The force involved in G protein interaction with membranes containing PS or CL was much stronger than that expected for single-molecule interactions ($\approx$100 pN) (35). This result could be explained if we consider that several G protein molecules interact with the membrane at a given point. Indeed, G protein is densely distributed in the viral envelope, suggesting that multiple binding occurs. It should be pointed out that several studies used force spectroscopy to determine the strength between molecular bonds (58) as well as to probe the adhesion forces between cells and surfaces (37). However, to our knowledge, the interaction between a virus and a target membrane has never been analyzed by this technique.

Viruses are much smaller than whole cells, and it is difficult to control the exact number of particles close to the tip apex. Considering the VSV dimensions (approximately 180 nm long and 65 nm wide), it should be expected that four to eight particles will adsorb on the sides of the tip apex. This also explains the multiple interaction peaks observed for the curves obtained with PC-PS and PC-CL membranes. Control experiments using VSV adsorbed on the tip and a clean mica surface (mica is negatively charged) showed many interacting peaks, indicating binding to the surface (not shown). The average force obtained in these experiments was 281 pN, which is enough to ensure that virus is adsorbed on the tip and sufficiently low to reinforce the specificity of the VSV interaction with membranes containing negative charges (much higher force values).

An attempt to calculate the calorimetric enthalpy (ΔH^{cal}) by dividing Q_T (from the data in Fig. 2) by the amount of G protein present in each injection showed that ΔH^{cal} values seems to be far from real, since they can be as low as $-1{,}400$ kcal/mol. As discussed before for the results with force spectroscopy, this is probably due to the fact that the G protein is densely distributed on the virus surface. Therefore, its local concentration in the binding reaction is actually much higher than that used for the calculations. If we consider the force spectroscopy data, at least seven proteins are involved in the binding, suggesting that the local concentration of G protein is at least seven times higher than that used for the calculations of ΔH^{cal}. Therefore, the values found for ΔH^{cal} will be decreased to around -200 kcal/mol. Although this value for enthalpy is large, it can be due to changes in the protein

conformation, which may contribute to values as large as −150 kcal/mol (47).

Kozlov and Lohman (27) also showed that the SSB protein-DNA interaction gives rise to a large negative enthalpy that was related to stacking interactions of aromatic amino acid residues and lysine-phosphate or arginine-phosphate interactions. There is also a possibility that protonation of the protein upon binding also contributes to a large negative ΔH^{cal} (14). From the analysis of the curve of ΔH^{cal} as a function of G protein concentration, it was found a large contribution for the association enthalpy ($\Delta H^{ass} = -1{,}185$ kcal/mol) and entropy ($\Delta S^{ass} = -3{,}839$ cal/mol · K). The thermodynamic parameters for the association were also calculated considering the local concentration of G protein as seven times higher, with $\Delta H^{ass} = -166$ kcal/mol and $\Delta S^{ass} = -525$ cal/mol · K. The unfavorable entropy can be due to different factors, such as the exposure of hydrophobic surfaces to the solvent as well as the decrease in conformational motion in the protein and/or the membrane (49). Nevertheless, there are some examples in the literature where hydrophobic interactions are driven by enthalpy and not by entropy, in the so-called nonclassical hydrophobic effect (for a review, see reference 44). Seelig (44) explains this binding enthalpy of hydrophobic solutes into lipid bilayers as possibly derived from (i) the van der Waals interaction energy and (ii) the increased hydration of the lipid-water interface.

VSV binding to membranes at neutral pH did not induce changes in VSV intrinsic fluorescence, suggesting that the binding itself did not alter the G protein tryptophan environment. On the other hand, G protein conformational changes induced when the pH was decreased after VSV binding to membranes can be followed by the increase in intrinsic fluorescence (6). Here, we found that the extent of these conformational changes depends on the number of negative charges in the target membrane. G protein-mediated membrane fusion can also be correlated to the PS content in the vesicles, probably because it is driven by G protein conformational changes. Indeed, the electrostatic nature of VSV-membrane interactions was also demonstrated by the inhibition of G protein conformational change and membrane fusion at high ionic strength. An increase in ionic strength can abolish electrostatic interactions by reducing charge-charge intermolecular or intramolecular interactions or even by decreasing the fraction of free water available to solvate the protein and/or the ligand. Although all these results unequivocally demonstrate the importance of electrostatic interactions for VSV fusion, we cannot discard the possibility that hydrophobic interactions are also involved in the VSV interaction with membranes. In fact, exposure of hydrophobic domains has already been shown to occur in G protein at low pH (6, 15).

The electrostatic nature of VSV interaction with membranes during fusion is an interesting result considering that for most of the viruses studied so far it is suggested that the binding to membrane occurs through hydrophobic interactions (22, 36). Very similar structures occur among several viral envelope glycoproteins, such as those of influenza virus, HIV-1, Moloney murine leukemia virus, and respiratory syncytial virus, which form a coiled-coil trimer that is inserted into the target membrane (5, 8, 17, 55, 57). Actually, since the ΔH^{cal} results from every single event, endothermic or exothermic, that is taking place during the binding, it is possible that hydrophobic interactions also occur in the case of VSV binding, but they are not the dominant energetic contribution for the overall process.

The ITC studies of VSV fusion to vesicles were done at pH 6.0. In these conditions, we clearly observed an exothermic effect following the heat effects due to the VSV dilution. This process was slow and could be followed for several minutes. The calorimetric pattern is related to fusion, and aggregation contributions can be excluded because the same pattern was not observed at pH 7.5. At this pH, the presence of multiple binding sites both on the virus surface, represented by G proteins, and in the vesicles containing negative charges probably causes aggregation. In fact, it was shown before by electron microscopy that several vesicles can bind to the surface of a single VSV (43). Nevertheless, the ITC experiments in such condition showed that, after the heat effects due to VSV dilution and binding to vesicles, there is a return to the baseline level, and the slow exothermic process is not observed.

It is interesting that our result is the opposite of that found in calorimetric studies of membrane fusion induced by influenza virus HA (32). This study showed that the fusion is an endothermic process, which could be explained by the increase in entropy upon both lipid mixing and the hydrophobic insertion of the fusion peptide into the lipid bilayer. It should be taken into account that the fusion process probably comprises several steps, such as the virus-membrane interaction, organization and/or destabilization of the outer monolayers of the membranes, and also the formation of a fusion pore, and other events (23). Thus, the heat released during the fusion process can be reflecting the result of all the changes that take place during this process as well as the mixing of virus and vesicle contents that results from the fusion. Nevertheless, our data suggest an alternative mechanism involved in VSV-induced membrane fusion compared to the calorimetric data for influenza virus HA-induced fusion, which is also supported by the fact that G protein does not contain an apolar fusion peptide. However, our results do not discard the participation of hydrophobic interactions during the VSV-induced fusion reaction.

Taken together, our results suggest that the interaction between VSV G protein and its target membrane seems to be more electrostatic than hydrophobic at both neutral and fusogenic pHs. We show that membrane recognition by VSV, G protein conformational changes induced by its interaction with the membranes, and the membrane fusion reaction itself are driven by electrostatic interactions between the viral G protein and negatively charged phospholipids present in the target membranes.

ACKNOWLEDGMENTS

This work was supported by grants from Conselho Nacional de Desenvolvimento Científico e Tecnológico (CNPq), Fundação de Amparo à Pesquisa do Estado do Rio de Janeiro (FAPERJ), Programa de Apoio ao Desenvolvimento Científico e Tecnológico (PADCT), Volkswagen Foundation, and Fundação Universitária José Bonifácio (FUJB).

We thank Leopoldo de Meis for the ITC facilities and Adalberto Vieyra for the use of the fluorometer. We also thank Paulo H. dos Santos for technical assistance.

REFERENCES

1. **Bailey, C. A., D. K. Miller, and J. Lenard.** 1984. Effects of DEAE-dextran on infection and hemolysis by VSV. Evidence that nonspecific electrostatic interactions mediate effective binding of VSV to cells. Virology **133:**111–117.

2. **Baranowski, E., C. M. Ruiz-Jarabo, and E. Domingo.** 2001. Evolution of cell recognition by viruses. Science **292:**1102–1105.
3. **Bathaie, S. Z., A. A. Moosavi-Movahedi, and A. A. Saboury.** 1999. Energetic and binding properties of DNA upon interaction with dodecyl trimethylammonium bromide. Nucleic Acids Res. **27:**1001–1005.
4. **Bonnafous, P., and T. Stegmann.** 2000. Membrane perturbation and fusion pore formation in influenza hemagglutinin-mediated membrane fusion. A new model for fusion. J. Biol. Chem. **275:**6160–6166.
5. **Bullough, P. A., F. M. Hughson, J. J. Skehel, and D. C. Wiley.** 1994. Structure of influenza haemagglutinin at the pH of membrane fusion. Nature **371:**37–43.
6. **Carneiro, F. A., A. S. Ferradosa, and A. T. Da Poian.** 2001. Low pH-induced conformational changes in vesicular stomatitis virus glycoprotein involve dramatic structure reorganization. J. Biol. Chem. **276:**67–72.
7. **Chan, D. C., and P. S. Kim.** 1998. HIV entry and its inhibition. Cell **93:**681–684.
8. **Chan, D. C., D. Fass, J. M. Berger, and P. S. Kim.** 1997. Core structure of gp41 from the HIV envelope glycoprotein. Cell **89:**263–273.
9. **Cleverley, D. Z., and J. Lenard.** 1998. The transmembrane domain in viral fusion: essential role for a conserved glycine residue in vesicular stomatitis virus G protein. Proc. Natl. Acad. Sci. USA **95:**3425–3430.
10. **Coll, J. M.** 1995. Heptad-repeat sequences in the glycoprotein of rhabdovirus. Virus Genes **10:**107–114.
11. **Coll, J. M.** 1997. Synthetic peptides from the heptad repeats of the glycoproteins of rabies, vesicular stomatitis and fish rhabdoviruses bind phosphatidylserine. Arch. Virol. **142:**2089–2097.
12. **Da Poian, A. T., A. M. O. Gomes, and T. Coelho-Sampaio.** 1998. Kinetics of intracellular viral disassembly and processing probed by Bodipy fluorescence dequenching. J. Virol. Methods **70:**45–58.
13. **Da Poian, A. T., A. M. O. Gomes, R. J. N. Oliveira, and J. L. Silva.** 1996. Migration of vesicular stomatitis virus glycoprotein to the nucleus of infected cells. Proc. Natl. Acad. Sci. USA **93:**8268–8273.
14. **de Haseth, P. L., T. M. Lohman, and M. T. Record.** 1977. The nonspecific binding of lac-repressor to DNA, an association reaction driven by counterion release. Biochemistry **16:**4783–4790.
15. **Durrer, P., Y. Gaudin, W. H. Ruigrok, R. Graf, and J. Brunner.** 1995. Photolabeling identifies a putative fusion domain in the envelope glycoprotein of rabies and vesicular stomatitis viruses. J. Biol. Chem. **270:**17575–17581.
16. **Estepa, A. M., A. I. Rocha, V. Mas, L. Pérez, J. A. Encinar, E. Nuñez, A. Fernandez, J. M. G. Ros, F. Gavilanes, and J. M. Coll.** 2001. A protein G fragment from the salmonid viral hemorrhagic septicemia rhabdovirus induces cell-to-cell fusion and membrane phosphatidylserine translocation at low pH. J. Biol. Chem. **276:**46268–46275.
17. **Fass, D., S. C. Harrison, and P. S. Kim.** 1996. Retrovirus envelope domain at 1.7 angstrom resolution. Nat. Struct. Biol. **3:**465–469.
18. **Florin, E. L., V. T. Moy, and H. E. Gaub.** 1994. Adhesion forces between individual ligand-receptor pairs. Science **264:**415–417.
19. **Fredericksen, B. L., and M. Whitt.** 1995. Vesicular stomatitis virus glycoprotein mutations that affect membrane fusion activity and abolish virus infectivity. J. Virol. **69:**1435–1443.
20. **Gaudin, Y., R. W. H. Ruigrok, and J. Brunner.** 1995. Low-pH induced conformational changes in viral fusion proteins: implications for the fusion mechanism. J. Gen. Virol. **76:**1541–1556.
21. **Gergely, C., J.-C. Voegel, P. Schaaf, B. Senger, M. Maaloum, J. K. H. Hörber, and J. Hemmerlé.** 2000. Unbinding process of adsorbed proteins under external stress studied by atomic force microscopy spectroscopy. Proc. Natl. Acad. Sci. USA **97:**10802–10807.
22. **Harter, C., P. James, T. Bachi, G. Semenza, and J. Brunner.** 1989. Hydrophobic binding of the ectodomain of influenza hemagglutinin to membranes occurs through the "fusion peptide." J. Biol. Chem. **264:**6459–6464.
23. **Hernandez, L. D., L. R. Hoffman, T. G. Wolfsberg, and J. M. White.** 1996. Virus-cell and cell-cell fusion. Annu. Rev. Cell Dev. Biol. **12:**627–661.
24. **Hyre, D. E., and L. D. Spicer.** 1995. Thermodynamic evaluation of binding interactions in the methionine repressor system of Escherichia coli using isothermal titration calorimetry. Biochemistry **34:**3212–3221.
25. **Jass, J., T. Tjärnhage, and G. Puu.** 2000. From liposomes to supported, planar bilayer structures on hydrophilic and hydrophobic surfaces: an atomic force microscopy study. Biophys. J. **79:**3153–3163.
26. **Jin, E., V. Katritch, W. K. Olson, M. Kharatisvili, R. Abagyan, and D. S. Pilch.** 2000. Aminoglycoside binding in the major groove of duplex RNA: the thermodynamic and electrostatic forces that govern recognition. J. Mol. Biol. **298:**95–110.
27. **Kozlov, A. G., and T. M. Lohman.** 1998. Calorimetric studies of E. coli SSB protein-single-stranded DNA interactions. Effects of monovalent salts on binding enthalpy. J. Mol. Biol. **278:**999–1014.
28. **Lu, M., S. C. Blacklow, and P. S. Kim.** 1995. A trimeric structural domain of the HIV-1 transmembrane glycoprotein. Nat. Struct. Biol. **2:**1075–1082.
29. **Mastromarino, P., C. Conti, P. Goldoni, B. Hauttecoeur, and N. Orsi.** 1987. Characterization of membrane components of the erythrocyte involved in vesicular stomatitis virus attachment and fusion at acidic pH. J. Gen. Virol. **68:**2359–2369.
30. **Matlin, K. S., H. Reggio, A. Helenius, and K. Simons.** 1982. Pathway of vesicular stomatitis virus entry leading to infection. J. Mol. Biol. **156:**609–631.
31. **Messana, I., M. Angeletti, M. Castagnola, G. De Sanctis, E. Di Stasio, B. Giardina, S. Pucciarelli, and M. Coletta.** 1998. Thermodynamics of inositol hexabisphosphate interaction with human oxyhemoglobin. J. Biol. Chem. **273:**15329–15334.
32. **Nebel, S., I. Bartoldus, and T. Stegman.** 1995. Calorimetric detection of influenza virus induced membrane fusion. Biochemistry **34:**5705–5711.
33. **Pal, R., Y. Barenholz, and R. R. Wagner.** 1988. Pyrene phospholipid as a biological fluorescent probe for studying fusion of virus membrane with liposomes. Biochemistry **27:**30–36.
34. **Puu, G., and I. Gustafson.** 1997. Planar lipid bilayers on solid supports from liposomes—factors of importance for kinetics and stability. Biochim. Biophys. Acta **1327:**149–161.
35. **Puu, G., E. Artursson, I. Gustafson, M. Lundstro, and J. Jass.** 2000. Distribution and stability of membrane proteins in lipid membranes on solid supports. Biosensors Bioelectronics **15:**31–41.
36. **Rabenstein, M., and Y.-K. Shin.** 1995. A peptide from the heptad repeat of human immunodeficiency virus gp41 shows both membrane binding and coiled-coil formation. Biochemistry **34:**13390–13397.
37. **Ratazos, A., Y.-L. Ong, M. M. Sharma, and G. Georgiou.** 1998. Molecular determinants of bacterial adhesion monitored by atomic force microscopy. Proc. Natl. Acad. Sci. USA **95:**11059–11064.
38. **Reviakine, I., and A. Brisson.** 2000. Formation of supported phospholipid bilayers from unilamellar vesicles investigated by atomic force microscopy. Langmuir **16:**1806–1815.
39. **Rose, J. K., and C. J. Gallione.** 1981. Nucleotide sequences of the mRNA's encoding the vesicular stomatitis virus G and M proteins determined from cDNA clones containing the complete coding regions. J. Virol. **39:**519–528.
40. **Rothman, J. E., and J. Lenard.** 1977. Membrane asymmetry. Science **195:** 743–753.
41. **Sanderson, N. M., B. Guo, A. E. Jacob, P. S. Handley, J. G. Cunniffe, and M. N. Jones.** 1996. The interaction of cationic liposomes with the skin-associated bacterium *Staphylococcus epidermidis*: effects of ionic strength and temperature. Biochim. Biophys. Acta **1283:**207–214.
42. **Schlegel, R., M. C. Willingham, and I. H. Pastan.** 1982. Saturable binding sites for vesicular stomatitis virus on the surface of Vero cells. J. Virol. **43:**871–875.
43. **Schlegel, R., T. S. Tralka, M. C. Willingham, and I. Pastan.** 1983. Inhibition of VSV binding and infectivity by phosphatidylserine: is phosphatidylserine a VSV-binding site? Cell **32:**639–646.
44. **Seelig, J.** 1997. Titration calorimetry of lipid-peptide interactions. Biochim. Biophys. Acta **1331:**103–116.
45. **Shokralla, S., Y. He, E. Wanas, and H. P. Ghosh.** 1998. Mutations in a carboxy-terminal region of vesicular stomatitis virus glycoprotein G that affect membrane fusion activity. Virology **242:**39–50.
46. **Skehel, J. J., P. M. Bayley, E. B. Brown, S. R. Martin, M. D. Waterfield, J. M. White, I. A. Wilson, and D. C. Wiley.** 1982. Changes in the conformation of influenza virus hemagglutinin at the pH optimum of virus-mediated membrane fusion. Proc. Natl. Acad. Sci. USA **79:**968–972.
47. **Spolar, R. S., and M. T. Record, Jr.** 1994. Coupling of local folding to site-specific binding of proteins to DNA. Science **263:**777–784.
48. **Stegmann, T., J. M. Delfino, F. M. Richards, and A. Helenius.** 1991. The HA2 subunit of influenza hemagglutinin inserts into the target membrane prior to fusion. J. Biol. Chem. **266:**18404–18410.
49. **Tame, J. R. H., R. O'Brien, and J. E. Ladbury.** 1998. Isothermal titration calorimetry of biomolecules, p. 27–38. *In* J. E. Ladbury and B. Z. Chowdhry (ed.), Biocalorimetry: applications of calorimetry in the biological sciences. John Wiley & Sons Ltd., London, England.
50. **Thomas, P. G., and J. Seelig.** 1993. Binding of the calcium antagonist flunarizine to phosphatidylcholine bilayers: charge effects and thermodynamics. Biochem. J. **291:**397–402.
51. **Weissenhorn, W., A. Dessen, L. J. Calder, S. C. Harrinson, J. J. Skehel, and D. C. Wiley.** 1999. Structural basis for membrane fusion by enveloped viruses. Mol. Membr. Biol. **16:**3–9.
52. **White, J., K. Matlin, and A. Helenius.** 1981. Cell fusion by Semliki Forest, influenza, and vesicular stomatitis viruses. J. Cell Biol. **89:**674–679.
53. **Wilson, I. A., J. J. Skehel, and D. C. Wiley.** 1981. Structure of the haemagglutinin membrane glycoprotein of influenza virus at 3 A resolution. Nature **289:**366–373.
54. **Wiseman, T., S. Williston, J. F. Brandts, and L. N. Lin.** 1989. Rapid measurement of binding constants and heats of binding using a new titration calorimeter. Anal. Biochem. **179:**131–137.
55. **Yu, Y. G., D. S. King, and Y.-K. Shin.** 1994. Insertion of a coiled-coil peptide from influenza virus hemagglutinin into membranes. Science **266:**274–276.
56. **Zhang, L., and H. P. Ghosh.** 1994. Characterization of the putative fusogenic domain in vesicular stomatitis virus glycoprotein G. J. Virol. **68:**2186–2193.
57. **Zhao, X., M. Singh, V. N. Malashkevich, and P. S. Kim.** 2000. Structural characterization of the human respiratory syncytial virus fusion protein core. Proc. Natl. Acad. Sci. USA **97:**14172–14177.
58. **Zlatanova, J., S. M. Lindsay, and S. H. Leuba.** 2000. Single molecule force spectroscopy in biology using the atomic force microscope. Prog. Biophys. Mol. Biol. **74:**37–61.

ANEXO B

Viral membrane fusion: is glycoprotein G of rhabdoviruses a representative of a new class of viral fusion proteins?

Andrea T. Da Poian, Fabiana A. Carneiro e Fausto Stauffer

Publicado em 2005 no periódico

Brazilian Journal of Medical and Biological Research

Brazilian Journal of Medical and Biological Research (2005) 38: 813-823
ISSN 0100-879X Review

Viral membrane fusion: is glycoprotein G of rhabdoviruses a representative of a new class of viral fusion proteins?

A.T. Da Poian, F.A. Carneiro and F. Stauffer

Programa de Biologia Molecular e Biotecnologia, Instituto de Bioquímica Médica, Universidade Federal do Rio de Janeiro, Rio de Janeiro, RJ, Brasil

Abstract

Enveloped viruses always gain entry into the cytoplasm by fusion of their lipid envelope with a cell membrane. Some enveloped viruses fuse directly with the host cell plasma membrane after virus binding to the cell receptor. Other enveloped viruses enter the cells by the endocytic pathway, and fusion depends on the acidification of the endosomal compartment. In both cases, virus-induced membrane fusion is triggered by conformational changes in viral envelope glycoproteins. Two different classes of viral fusion proteins have been described on the basis of their molecular architecture. Several structural data permitted the elucidation of the mechanisms of membrane fusion mediated by class I and class II fusion proteins. In this article, we review a number of results obtained by our laboratory and by others that suggest that the mechanisms involved in rhabdovirus fusion are different from those used by the two well-studied classes of viral glycoproteins. We focus our discussion on the electrostatic nature of virus binding and interaction with membranes, especially through phosphatidylserine, and on the reversibility of the conformational changes of the rhabdovirus glycoprotein involved in fusion. Taken together, these data suggest the existence of a third class of fusion proteins and support the idea that new insights should emerge from studies of membrane fusion mediated by the G protein of rhabdoviruses. In particular, the elucidation of the three-dimensional structure of the G protein or even of the fusion peptide at different pH's might provide valuable information for understanding the fusion mechanism of this new class of fusion proteins.

Correspondence
A.T. Da Poian
Instituto de Bioquímica Médica
UFRJ
21941-590 Rio de Janeiro, RJ
Brasil
E-mail: dapoian@bioqmed.ufrj.br

Presented at the XI Congresso Brasileiro de Biologia Celular, Campinas, SP, Brazil, July 15-18, 2004.

Research supported by CNPq, Centro Argentino-Brasileiro de Biotecnologia (CABBIO) and FAPERJ.

Received July 16, 2004
Accepted February 10, 2005

Key words
- Membrane fusion
- Fusion proteins
- Rhabdovirus
- G protein
- Glycoprotein

Introduction to viral-induced membrane fusion

The plasma membrane of eukaryotic cells serves as a barrier against invading parasites and viruses. To infect a cell, viruses must be capable of transporting their genome and accessory proteins into the host cell, bypassing or modifying the barrier properties imposed by the plasma membrane. Entry into the host cells always involves a step of membrane fusion for enveloped animal viruses. The fusion reaction may occur by two different general mechanisms (Figure 1): a) fusion between viral envelope and host cell plasma membrane, and b) fusion of endosomal mem-

brane with viral envelope, after virus particle internalization by receptor-mediated endocytosis (1,2). In both cases, membrane fusion is mediated by specific viral surface glycoproteins which undergo structural reorganization to be converted from the nonfusogenic to the fusogenic conformation.

The membrane of some enveloped viruses, such as paramyxoviruses, retroviruses or herpesviruses, fuses directly with the host cell plasma membrane after virus binding to their cell receptor. The best-characterized fusion mechanism that occurs at the plasma membrane level is that mediated by HIV gp120/gp41 glycoproteins (3). Interaction between gp120, the cellular CD4 molecule and a co-receptor protein leads to the insertion of gp41 hydrophobic fusion peptide into the plasma membrane. gp41 forms a trimeric coiled coil containing two interacting α-helical peptides that acquire a six-helical bundle structure (4).

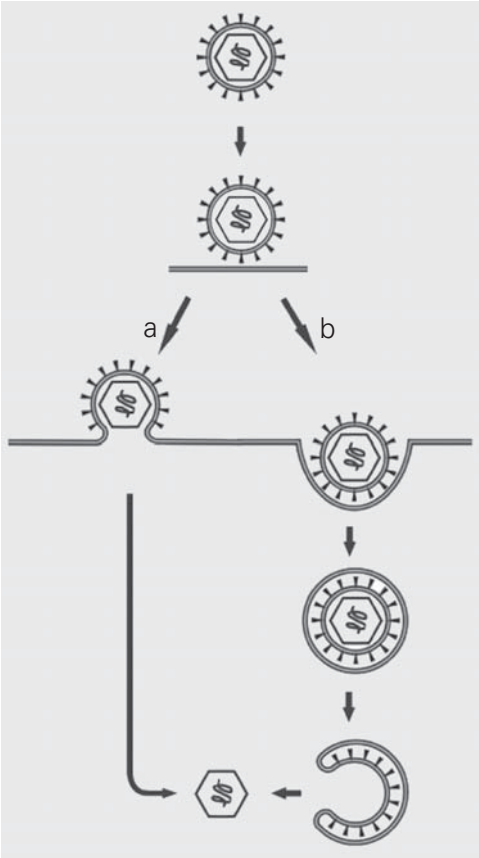

Figure 1. Entry of enveloped virus into the host cells. First, the virion attaches to the cell surface through the interaction between a viral envelope protein and a receptor molecule, leading to (a) pH-independent fusion between viral envelope and host cell plasma membrane or to (b) endocytosis of the virus particle, followed by fusion of the endosomal membrane with the viral envelope at low pH. After membrane fusion, the viral genome is released into the cytosol to be replicated, transcribed and translated. In both cases, membrane fusion is mediated by specific viral surface glycoproteins, which undergo structural reorganization to be converted from the nonfusogenic to the fusogenic conformation.

Other enveloped viruses such as orthomyxoviruses, alphaviruses or rhabdoviruses enter the cells by the endocytic pathway, and fusion depends on the acidification of the endosomal compartment. Fusion at the endosome level is triggered by conformational changes in viral glycoproteins induced by the low pH of this cellular compartment. The best-studied low pH-activated viral fusion protein is the influenza virus glycoprotein hemagglutinin (HA). The X-ray structure of influenza virus HA was determined at both neutral and fusogenic pH (5). The conformational changes observed suggest that the hydrophobic fusion peptide moves to the tip of the molecule and is delivered toward the target membrane. The conformational transition occurs in a narrow pH range, corresponding to the optimal pH of fusion, in which the protein acquires the ability to interact with detergent micelles and lipid vesicles. This interaction leads to the insertion of the fusion peptide into the membrane, where a pore is formed.

Viral fusion proteins

The viral fusion glycoproteins share a number of common features: a) they are type I integral membrane proteins presenting a large ectodomain, a single transmembrane sequence and a small C-terminal end inside the viral membrane; b) they contain an N-terminal signal sequence that is cleaved after directing the protein at the endoplasmic reticulum; c) they contain N-linked carbohydrates; d) they form oligomers and occur at high density in the viral membrane; e) they contain a specific segment involved in membrane fusion known as the fusion peptide.

Based on their molecular architecture, two classes of viral fusion proteins have been described. The main features that characterize the proteins of each class are summarized in Table 1. The HA from influenza

virus is the prototype of class I fusion proteins, which also include glycoproteins from myxo- and paramyxoviruses, retroviruses and filoviruses (5). These proteins form trimeric spikes of two-chain monomers generated by the cleavage of a precursor protein. The C-terminal end is anchored to the viral membrane and the N-terminal created by the precursor cleavage consists of a hydrophobic segment containing approximately 20 amino acids, which corresponds to the fusion peptide. After binding to a cellular receptor or on exposure to low pH, the protein assumes an extended conformation and the fusion peptide inserts into the target membrane. The post-fusion conformation is a hairpin-like structure in which the N-terminal central coiled coil is surrounded by a sheath of antiparallel chains, joining the fusion peptide and the membrane anchor at the same end (6).

Class II includes the E protein from flavivirus and E1 protein from alphaviruses (7). They have three domains that fold largely on ß-sheets and are arranged in a continuous protein lattice formed by dimers (8-10). The fusion peptide is an internal loop between two ß-strands, which is buried in the dimer interface. The class II fusion proteins are not proteolytically cleaved during virus maturation, but are associated with another viral membrane protein whose cleavage is required for fusion. The post-fusion structure of E protein of dengue virus (11), tick-borne encephalitis virus (12), and E1 protein of Semliki Forest virus (13) has been recently determined, revealing a surprising convergence of the class I and class II fusion mechanisms (14). The acidic pH of the endosome induces a disassembly of envelope protein dimers, which rearrange in trimers with the fusion peptide loops clustered at one end of an elongated molecule.

Despite their structural differences, both class I and class II fusion proteins are synthesized in a metastable conformation, and it is believed that the irreversible transition to the post-fusion state provides the energy for membrane fusion. However, several results suggest that there is at least one example of viral fusion protein that catalyzes fusion through a completely different mechanism. This is the case for the rhabdovirus fusion glycoprotein.

The rhabdoviruses

The viruses that belong to the Rhabdoviridae family are widely distributed in nature and their hosts range from vertebrate and invertebrate animals to many species of plants. The rhabdoviruses that infect mam-

Table 1. Characteristics of viral fusion protein classes.

	Class I	Class II
Oligomeric structure	Trimer	Dimer
Secondary structure	Predominantly α-helix	Predominantly ß-sheet
Fusion peptide	N-terminal	Internal
Proteolysis during maturation	Fusion protein	Associated membrane protein
Virus families	Retroviruses (HIV, SIV, MoLV, HTLV-1)	Alphaviruses (SFV)
	Orthomyxoviruses (influenza)	Flaviviruses (dengue, TBE)
	Paramyxoviruses (Sendai, SV5, HRSV)	
	Filoviruses (Ebola)	

HIV = human immunodeficiency virus; SIV = simian immunodeficiency virus; MoLV = Moloney murine leukemia virus; HTLV-1 = human T-cell leukemia virus-1; SV5 = simian virus 5; HRSV = human respiratory syncytial virus; SFV = Semliki Forest virus; TBE = tick-borne encephalitis virus.

mals have been classified into two genera: the *Lyssavirus* (rabies and rabies-like viruses) and the *Vesiculovirus* (whose name is derived from vesicular stomatitis virus (VSV), the prototype of the genus). Other rhabdoviruses include those that infect fish, arthropods and plants. All rhabdoviruses present a bullet-shaped structure measuring 200 x 70 nm that is formed by two major components: the nucleocapsid and the envelope. The nucleocapsid contains a negative single-stranded genomic RNA that is tightly packed by the nucleocapsid protein N. The viral RNA-dependent RNA polymerase, composed of L and P proteins, is also associated with the nucleocapsid core. The envelope is a lipid bilayer derived from the host cell containing approximately 400 trimeric transmembrane spikes consisting of the single viral glycoprotein G. The matrix protein is localized inside the viral envelope between the membrane and the nucleocapsid.

Entry of rhabdoviruses into host cells

The rhabdoviruses enter the cell by receptor-mediated endocytosis followed by low-pH-induced membrane fusion. Both the cell recognition and the fusion reaction are mediated by the surface glycoprotein G (15-19).

Structural features of rhabdovirus G protein

Rhabdoviruses possess a unique glycoprotein in their envelope, which presents a highly conserved structure (20). G proteins contain about 500 amino acids including a signal peptide, two sites of glycosylation, two acylated sites, and a hydrophilic cytoplasmic C-terminal tail. Rabies virus and VSV G proteins are organized as trimers anchored to the viral membrane via a single transmembrane sequence close to the C-terminus (21-24). The trimeric structure of VSV G protein is stabilized at mild acidic pH (22) but both rabies and VSV G protein trimers seem to be less stable than the other trimeric viral glycoproteins (24,25).

Rhabdovirus binding to the cell surface

The receptors for the attachment of rhabdoviruses have been difficult to identify because of the generally broad host range of these viruses. It has been hypothesized that the nicotinic acetylcholine receptor is the receptor for rabies virus (26,27), but recent evidence indicates that other proteins can also act as receptors for this virus (28,29).

Binding to phospholipids seems to be important for rhabdovirus infection. Phospholipids from cellular membranes inhibit attachment and infection of rabies virus and VSV (30-32). Indeed, the VSV host range extends from nearly all mammals to insects, suggesting that the receptor for this virus is a widely distributed molecule. A high affinity, saturable binding site has been described for VSV on Vero cells (30). The binding was inhibited by a membrane extract, which was resistant to protease, neuraminidase and heating, and was also inactivated by treatment with phospholipase C (33). These findings, taken together with the observation that only phosphatidylserine (PS) among various purified lipids was able to inhibit VSV binding, led the authors to suggest that PS could participate in the cellular binding site for VSV (33). The components of biological membranes are asymmetrically distributed between the membrane surfaces and PS is highly segregated to the inner leaflet of plasma membranes, suggesting that G protein-PS interactions were a very improbable event. However, recent findings showing that the binding of a fragment of a salmonid rhabdovirus G protein to model membranes induces PS translocation from the inner to the outer leaflet of the membrane (34) indicate that rhabdovirus binding to PS could have more physiological relevance than expected. Another possibility is that other negatively charged molecules such as glycosami-

noglycans and gangliosides could act as the physiological binding site for VSV. The results obtained by Mastromarino et al. (31) using erythrocytes at acidic pH showed that, besides PS, phosphatidylinositol and GM3 ganglioside also inhibited VSV attachment to cells. Removal of the charged groups from these negatively charged molecules greatly reduced their inhibitory activities, suggesting an important role of electrostatic interactions during cell recognition by VSV.

We found direct evidence that VSV interacts very strongly with membranes containing negatively charged phospholipids at neutral pH. Isothermal titration calorimetry experiments have shown that VSV binding to liposomes is an enthalpically driven process, suggesting that electrostatic interactions are important for membrane recognition (35). Using atomic force microscopy we determined the forces of VSV G protein binding to lipid films of different composition (35,36). We measured forces as strong as 2 nN after virus interaction with a PS-containing lipid film, whereas no interaction between the virus and membranes composed of neutral phospholipids was observed (35). Using other negatively charged phospholipids, we found that although G protein can bind to phosphatidylglycerol and cardiolipin, binding to PS seems to be much stronger (36), suggesting that membrane recognition by VSV occurs through a specific interaction between G protein positively charged amino acids and the negative charges of PS on the membrane surface (Figure 2A).

Viral hemorrhagic septicemia virus (VHSV), a fish rhabdovirus that infects salmonids, also binds PS (37). The PS-binding site of the VHSV G protein has been mapped using pepscan and solid-phase phospholipid binding assays. The major PS-binding regions were located between residues 79 and 113 of VHSV G protein. This sequence presents contiguous heptad repeats followed by a short segment containing positively charged amino acids, and led to the design of a peptide named p2 (from residues 82 to 109), which contains both the heptad repeat region and two arginine residues (Figure 2B). Antibodies against this peptide were able to inhibit both PS binding to VHSV and virus-induced cell to cell fusion, suggesting a direct participation of p2 peptide in virus

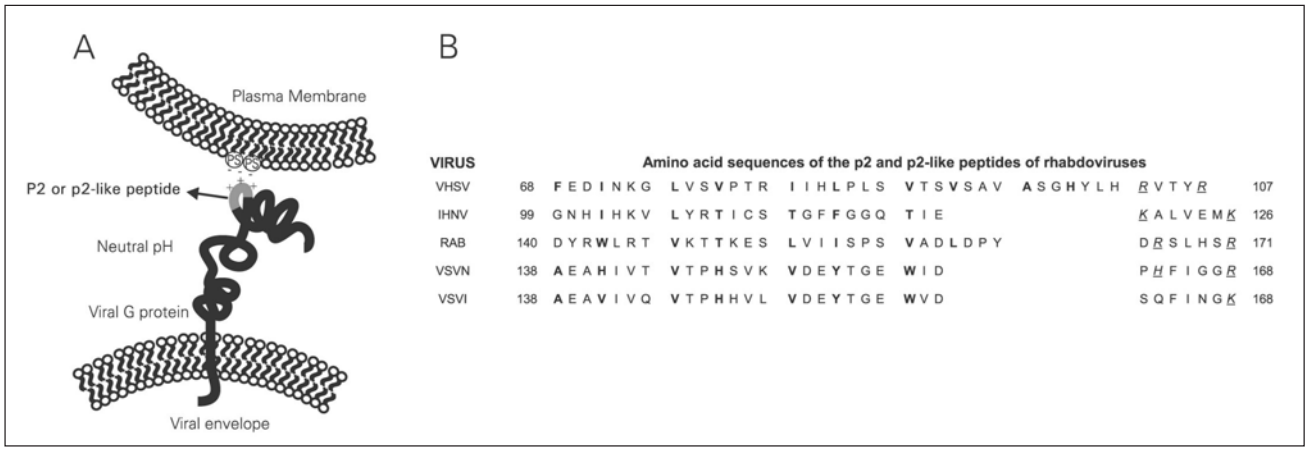

Figure 2. Binding of the G protein of rhabdoviruses to the cell surface. *A*, Schematic representation of the interaction between viral G protein and phosphatidylserine (PS) in the plasma membrane, at neutral pH, showing the importance of electrostatic interactions for the binding. A specific sequence of G protein directly involved in the binding to the negatively charged phospholipid PS is shown in gray. This sequence presents similar structural features in the G protein of all rhabdoviruses and is named p2 or p2-like peptide (20). *B*, PS-binding segments of rhabdovirus G protein contain heptad repeats followed by a short segment containing at least one positively charged residue (20). The heptads are separated by a space for better visualization. The numbers shown on the left or right correspond to the first and the last amino acid residue in each sequence, respectively. VHSV = viral hemorrhagic septicemia virus; IHNV = infectious hematopoietic necrosis virus RB-1 strain; RAB = rabies B19 strain; VSVN = vesicular stomatitis virus New Jersey strain; VSVI = vesicular stomatitis virus Indiana strain.

entry (37). p2-like regions have been found in other rhabdoviruses (38). These sequences contain heptad repeats followed by a short sequence of 5 to 7 amino acids with at least one positively charged residue, and show a high degree of sequence conservation within the same genus, but no sequence similarity among the different genera (Figure 2B).

p2-like peptides from rabies (residues 140 to 164), VSV (residues 134 to 161) and infectious hematopoietic necrosis virus, another fish rhabdovirus (residues 99 to 119), bind PS (39). The identification of these phospholipid-binding domains in several rhabdovirus G proteins suggests that PS binding is a common feature of rhabdovirus envelope protein. These observations led us to propose that the binding of VSV to PS-containing membranes occurs through its p2-like peptide (Figure 2A). Positive charges in this segment might participate in electrostatic interactions with the negatively charged phospholipid PS during membrane recognition.

Rhabdovirus-induced membrane fusion

G protein conformational changes

The low pH-induced conformational changes of rhabdovirus G protein were first investigated for VSV. It has been shown that the incubation of the protein at mild acidic pH leads to an exposure of a hydrophobic region (25). Binding of the fluorescent probe bis-ANS revealed that the exposure of hydrophobic domains was maximal at pH 6.2 (40). Between pH 6.0 and 5.6 a dramatic conformational change occurs, which includes loss of secondary and tertiary structures. For rabies virus G protein, it has been shown that immediately after acidification, at pH below 6.7, the viruses become more hydrophobic allowing the interaction with membranes (41). This conformation of G protein has been considered to be an activated state that may trigger the first step of membrane fusion. In the absence of membranes, however, the hydrophobic conformation of rabies and VSV G protein leads to its aggregation (18,40). Prolonged incubation at low pH leads rabies G protein to an inactive state, which become sensitive to proteases and is antigenically distinct from the native structure (18). For VSV, G trimers are stabilized in the inactive state (22).

Role of phosphatidylserine

It seems that PS is not only involved in membrane recognition but is also of crucial importance in membrane fusion, especially in the case of VSV. Membrane fusion mediated by VSV G protein reconstituted in lipid vesicles showed a large preference for target membranes containing PS or phosphatidic acid (42). We found that the extent of pH-induced conformational changes of G protein depends on the number of negative charges in the target membrane and that G protein-mediated membrane fusion may be correlated with the PS content in the vesicles (35). Although our results unequivocally demonstrate the importance of electrostatic interactions for VSV fusion, we cannot exclude the possibility that hydrophobic interactions are also involved in VSV interaction with membranes during fusion.

Role of histidines

We have shown that VSV-induced fusion depends on a dramatic structure reorganization of G protein, which occurs within a very narrow pH range, between 5.8 and 6.2 (40). This indicates that the protonation of a small number of ionizable groups is required for G protein structural changes, suggesting that the protonation of the imidazole ring of histidyl residue(s) (pK = 6.0) is involved in G protein conformational changes required for fusion. In addition, we have found that VSV binding to membranes as well as the

fusion reaction itself were highly dependent on electrostatic interactions between negative charges on the membrane surface and positively charged amino acids in G protein at the fusion pH (35), and His becomes positively charged after protonation (Figure 3). For rabies virus, Roche and Gaudin (43), showed that the pK of the transition from the native to the fusion-inactive state of G protein is 6.65, also suggesting that His residues are involved. To investigate the role of His protonation in VSV fusion, we modified these residues using diethyl pyrocarbonate, a compound that reacts with a nitrogen atom of the imidazole ring of His forming N-carbethoxyhistidyl derivatives (44) (Figure 3). His modification abolished pH-induced conformational changes on G protein and also the fusion reaction catalyzed by the virus, suggesting that His protonation drives G protein interaction with the target membrane at acidic pH (Figure 3). Mass spectrometry analysis of tryptic fragments of modified G protein, together with the use of synthetic peptides, allowed the identification of His 148 and His 149 of VSV G protein as the putative active residues (44). These His residues are located in the p2-like peptide of VSV, the PS-binding domain first identified in VHSV G protein and found among all rhabdoviruses (37,39).

Further evidence for the involvement of His protonation in rhabdovirus fusion was obtained in the study of the pH-dependent equilibrium between the native and the fusion-inactive states of rabies virus G protein

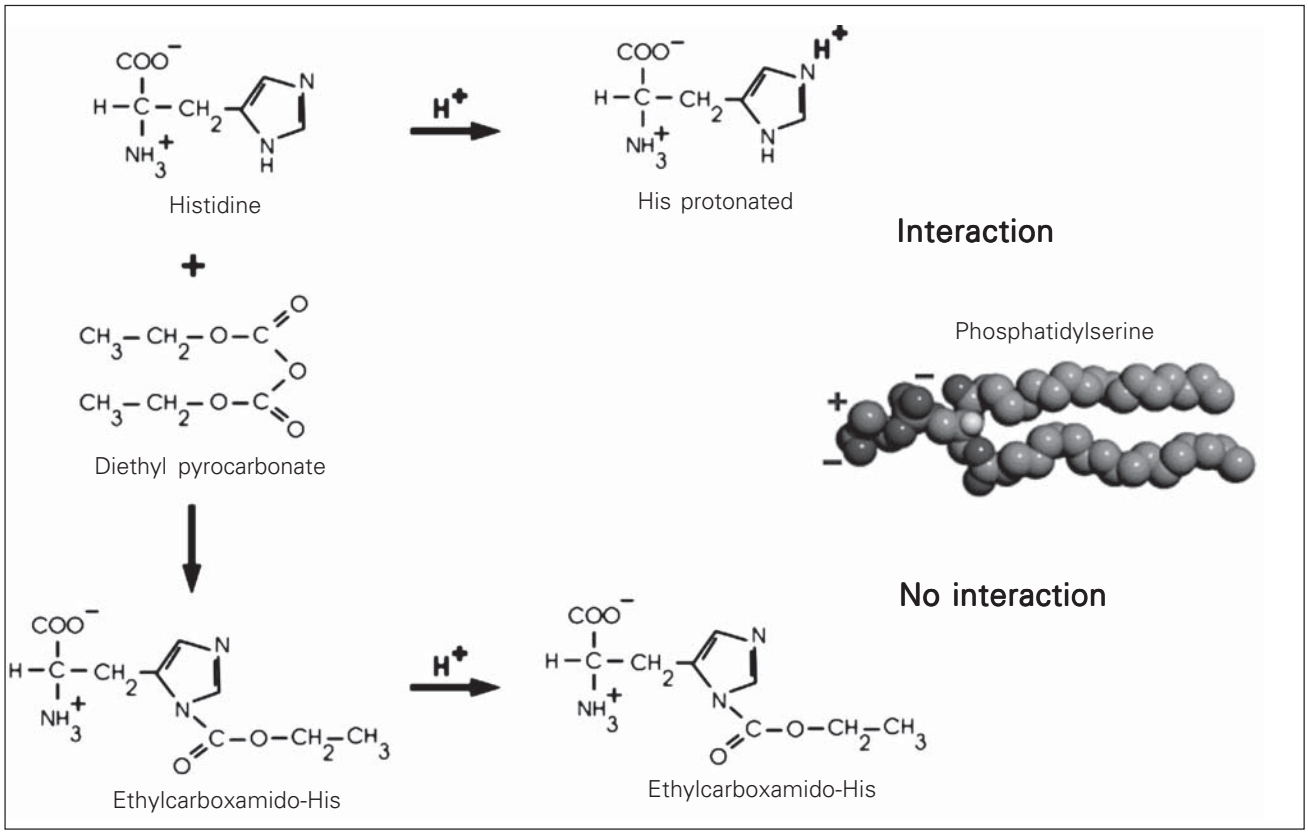

Figure 3. Role of His protonation in rhabdovirus-induced membrane fusion. His modification with diethyl pyrocarbonate (DEPC) abolishes pH-induced conformational changes in G protein and also the fusion reaction catalyzed by the virus. As demonstrated in this figure, treatment of vesicular stomatitis virus with DEPC impairs His protonation, which seems to be necessary for the interaction between G protein and the negative charges conferred by phosphatidylserine to the target membrane.

(43). Based on other studies using natural mutants (45), the authors suggested that the protonation of His 397 was required for the pH-dependent structural transitions. Thus, the protonation of this residue together with the protonation of His 148 and 149 would drive the complete conformational changes of G protein during membrane fusion mediated by the virus.

Determination of the rhabdovirus fusion peptide

The identification of the amino acid residues essential for membrane fusion mediated by viral glycoproteins might contribute to the elucidation of the molecular mechanisms underlying the fusion event.

Photolabeling studies of rabies and VSV G proteins have shown that interaction of these proteins with membranes strongly increased when the pH was lowered from 7.0 to 6.0 (46). At the pH of fusion, the labeling sites are contained in a segment in the ectodomain comprising amino acids 103 to 179 for rabies and 59 to 221 for VSV. In the case of VSV, mutational analysis has shown that substitution of conserved Gly, Pro, or Asp located in the region between amino acids 117 to 137 either abolished the fusion ability of G protein or shifted the optimum pH of fusion (47-49). Based on these results, the authors proposed that this segment contained VSV G protein internal fusion peptide. However, although this segment is highly conserved among the vesiculoviruses, there is less homology in the corresponding region in rabies glycoprotein (46) and direct evidence that this particular region interacts with the target membrane is still lacking. VSV putative fusion peptide contains no His, and thus it cannot be modified by diethyl pyrocarbonate. In addition, we found that a synthetic peptide corresponding to this segment failed to induce phospholipid vesicle fusion (44). Thus, further investigation is necessary to determine whether the segment between amino acids 117 to 137 of G protein directly participates in VSV fusion or whether the substitution of its conserved amino acids affects the conformation or the exposure of other membrane-interacting sequence in G protein.

In contrast, we found that VSV p2-like peptide was as efficient as the whole virus in catalyzing membrane fusion (44). In addition, peptide-induced fusion showed the same requirements as VSV-mediated fusion. It occurs at pH 6.0 but not at pH 7.5, and depends on the presence of PS on the target membrane. The data obtained with p2 peptide of VHSV also indicate that this peptide might play an active role in fusion: it mediates phospholipid vesicle fusion, lipid mixing, and leakage of liposome contents and inserts itself into liposome membranes (50). These results together suggest that p2-like peptides directly participate in membrane fusion mediated by rhabdoviruses probably through the protonation of their His residues.

Another region of G protein, encompassing residues 395 to 418 for VSV or containing residues 392 to 396 for rabies virus, has been identified as a segment that affects the fusogenic activity of the protein by influencing the low-pH-induced conformational changes (45,51). In addition, it has also been shown that not only the ectodomain segment but also the membrane anchoring domain is required for VSV fusion activity (52,53).

Reversibility

It has been suggested that the fusogenic conformation of viral fusion glycoprotein is thermodynamically more stable than the native structure of the protein, which is trapped in a metastable state (54). The native state is prevented from achieving the lower energy fusogenic conformation by a kinetic barrier imposed during the folding and/or maturation. In the case of influenza virus, for example, HA folds within the cell as the fu-

sion-incompetent precursor, which subsequently undergoes proteolytic cleavage to generate the mature, two-chain native state. This metastability allows the coupling of an energetically expensive membrane-fusion reaction to an energetically favorable conformational change, a fact that could drive the reaction toward complete membrane fusion (54).

The most striking observation with respect to the conformational changes of rhabdovirus G proteins is the reversibility of the structural transitions, suggesting that metastability is not absolutely required for viral membrane fusion. For rabies virus, it has been demonstrated that G protein can assume at least three different conformations: the native state detected on the viral surface at neutral pH, the activated hydrophobic state, and the fusion-inactive (I) state (41). These different conformations occur in a pH-dependent equilibrium and the low-pH triggered conformational changes are completely reversible (18,41). Although the metastability model predicts that any destabilizing reagent will cause the same conformational change and membrane-fusion activity as acidic pH, for VSV, neither heat nor urea induced the conformational changes leading to membrane fusion (55).

An even more interesting observation is that the low pH-induced conformational changes of rhabdovirus fusion proteins are reversible also after the interaction with the membrane (56,57). It has been shown that after the formation of the rabies virus prefusion complex, the lipids organized in this structure can be reversed to two bilayers (56). Photosensitized labeling experiments have shown that VSV binding to membranes and the subsequent interaction at low pH could be reversed after medium neutralization, suggesting a "velcro"-like attachment of VSV G protein to the target membrane (57). This indicates that G protein interaction with the target membrane during fusion occurs essentially on the membrane surface, and not through the insertion of a protein segment into the lipid bilayer. This hypothesis is in agreement with our results showing the electrostatic nature of G protein-lipid interactions (35), and suggests a mechanism of membrane destabilization resembling the one promoted by the antimicrobial peptides acting through a carpet model (58).

The increasing knowledge about virus-induced membrane fusion at the molecular level should provide new means to develop antiviral drugs. Indeed, although most of the antiviral drugs have been developed against viral enzymes involved in virus replication, recent studies have demonstrated that the entry events can also serve as a new target to block viral infection (59,60). As an example, the progress in understanding the mechanisms of HIV-1 cell entry into target cells permitted the design of a new class of anti-HIV-1 drugs: compounds that act as fusion or entry inhibitors that are currently being evaluated in clinical trials (60). Thus, new insights concerning the fusion mechanisms might be successfully applied to the development of entry inhibitors directed at other viruses. The data presented in this review suggest that the glycoprotein of the rhabdoviruses represents a new class of fusion proteins. The elucidation of the three-dimensional structure of this glycoprotein or even of its fusion peptide should provide valuable information for understanding the fusion mechanism of this new class of fusion proteins.

References

1. Hernandez LD, Hoffman LR, Wolfsberg TG & White JM (1996). Virus-cell and cell-cell fusion. *Annual Review of Cell and Developmental Biology*, 12: 627-661.
2. Eckert DM & Kim PS (2001). Mechanisms of viral membrane fusion and its inhibition. *Annual Review of Biochemistry*, 70: 777-810.
3. Chan DC & Kim PS (1998). HIV entry and its inhibition. *Cell*, 93: 681-684.
4. Chan DC, Fass D, Berger JM & Kim PS (1997). Core structure of gp41 from the HIV envelope glycoprotein. *Cell*, 89: 263-273.
5. Skehel JJ & Wiley DC (2000). Receptor binding and membrane fusion in virus entry: the influenza hemagglutinin. *Annual Review of Biochemistry*, 69: 531-569.
6. Skehel JJ & Wiley DC (1998). Coiled coils in both intracellular vesicle and viral membrane fusion. *Cell*, 95: 871-874.
7. Heinz FX & Allison SL (2001). The machinery for flavivirus fusion with host cell membranes. *Current Opinion in Microbiology*, 4: 450-455.
8. Rey FA, Heinz FX, Mandl C, Kunz C & Harrison SC (1995). The envelope glycoprotein from tick-borne encephalitis virus at 2 A resolution. *Nature*, 375: 291-298.
9. Lescar J, Roussel A, Wien MW, Navaza J, Fuller SD, Wengler G, Wengler G & Rey FA (2001). The fusion glycoprotein shell of Semliki Forest virus: an icosahedral assembly primed for fusogenic activation at endosomal pH. *Cell*, 105: 137-148.
10. Kuhn RJ, Zhang W, Rossmann MG et al. (2002). Structure of dengue virus: implications for flavivirus organization, maturation, and fusion. *Cell*, 108: 717-725.
11. Modis Y, Ogata S, Clements D & Harrison SC (2004). Structure of the dengue virus envelope protein after membrane fusion. *Nature*, 427: 313-319.
12. Bressanelli S, Stiasny K, Allison SL, Stura EA, Duquerroy S, Lescar J, Heinz FX & Rey FA (2004). Structure of a flavivirus envelope glycoprotein in its low-pH-induced membrane fusion conformation. *EMBO Journal*, 23: 728-738.
13. Gibbons DL, Vaney MC, Roussel A, Vigouroux A, Reilly B, Lepault J, Kielian M & Rey FA (2004). Conformational change and protein-protein interactions of the fusion protein of Semliki Forest virus. *Nature*, 427: 320-325.
14. Jardetzky TS & Lamb RA (2004). Virology: a class act. *Nature*, 427: 307-308.
15. Matlin KS, Reggio H, Helenius A & Simons K (1982). Pathway of vesicular stomatitis virus entry leading to infection. *Journal of Molecular Biology*, 156: 609-631.
16. Superti F, Derer M & Tsiang H (1984). Mechanism of rabies virus entry into CER cells. *Journal of General Virology*, 65: 781-789.
17. Wunner WH, Reagan KJ & Koprowski H (1984). Characterization of saturable binding sites for rabies virus. *Journal of Virology*, 50: 691-697.
18. Gaudin Y, Tuffereau C, Segretain D, Knossow M & Flamand A (1991). Reversible conformational changes and fusion activity of rabies virus glycoprotein. *Journal of Virology*, 65: 4853-4859.
19. Da Poian AT, Gomes AMO & Coelho-Sampaio T (1998). Kinetics of intracellular viral disassembly and processing probed by Bodipy fluorescence dequenching. *Journal of Virological Methods*, 70: 45-58.
20. Coll JM (1995). The glycoprotein G of rhabdoviruses. *Archives of Virology*, 140: 827-851.
21. Kreis TE & Lodish HF (1986). Oligomerization is essential for transport of vesicular stomatitis viral glycoprotein to the cell surface. *Cell*, 46: 929-937.
22. Doms RW, Keller DS, Helenius A & Balch WE (1987). Role for adenosine triphosphate in regulating the assembly and transport of vesicular stomatitis virus G protein trimers. *Journal of Cell Biology*, 105: 1957-1969.
23. Whitt MA, Buonocore L, Prehaud C & Rose JK (1991). Membrane fusion activity, oligomerization, and assembly of the rabies virus glycoprotein. *Virology*, 185: 681-688.
24. Gaudin Y, Ruigrok RW, Tuffereau C, Knossow M & Flamand A (1992). Rabies virus glycoprotein is a trimer. *Virology*, 187: 627-632.
25. Crimmins DL, Mehard WB & Schlesinger S (1983). Physical properties of a soluble form of the glycoprotein of vesicular stomatitis virus at neutral and acidic pH. *Biochemistry*, 22: 5790-5796.
26. Lentz TL, Burrage TG, Smith AL, Crick J & Tignor GH (1982). Is the acetylcholine receptor a rabies virus receptor? *Science*, 215: 182-184.
27. Gastka M, Horvath J & Lentz TL (1996). Rabies virus binding to the nicotinic acetylcholine receptor alpha subunit demonstrated by virus overlay protein binding assay. *Journal of General Virology*, 77: 2437-2440.
28. Reagan KJ & Wunner WH (1985). Rabies virus interaction with various cell lines is independent of the acetylcholine receptor. *Archives of Virology*, 84: 277-282.
29. Thoulouze MI, Lafage M, Schachner M, Hartmann U, Cremer H & Lafon M (1998). The neural cell adhesion molecule is a receptor for rabies virus. *Journal of Virology*, 72: 7181-7190.
30. Schlegel R, Willingham MC & Pastan IH (1982). Saturable binding sites for vesicular stomatitis virus on the surface of Vero cells. *Journal of Virology*, 43: 871-875.
31. Mastromarino P, Conti C, Goldoni P, Hauttecoeur B & Orsi N (1987). Characterization of membrane components of the erythrocyte involved in vesicular stomatitis virus attachment and fusion at acidic pH. *Journal of General Virology*, 68: 2359-2369.
32. Conti C, Mastromarino P, Ciuffarella MG & Orsi N (1988). Characterization of rat brain cellular membrane components acting as receptors for vesicular stomatitis virus. Brief report. *Archives of Virology*, 99: 261-269.
33. Schlegel R, Tralka TS, Willingham MC & Pastan I (1983). Inhibition of VSV binding and infectivity by phosphatidylserine: is phosphatidylserine a VSV-binding site? *Cell*, 32: 639-646.
34. Estepa AM, Rocha AI, Mas V et al. (2001). A protein G fragment from the salmonid viral hemorrhagic septicemia rhabdovirus induces cell-to-cell fusion and membrane phosphatidylserine translocation at low pH. *Journal of Biological Chemistry*, 276: 46268-46275.
35. Carneiro FA, Bianconi ML, Weissmuller G, Stauffer F & Da Poian AT (2002). Membrane recognition by vesicular stomatitis virus involves enthalpy-driven protein-lipid interactions. *Journal of Virology*, 76: 3756-3764.
36. Weissmüller G, Moraes MB, Prazeres GMP et al. (2003). Multiple application of atomic force microscopy in biology. *Acta Microscopica*, 12: 29-33.
37. Estepa AM & Coll JM (1996). Pepscan mapping and fusion-related properties of the major phosphatidylserine-binding domain of the glycoprotein of viral hemorrhagic septicemia virus, a salmonid rhabdovirus. *Virology*, 216: 60-70.
38. Coll JM (1995). Heptad-repeat sequences in the glycoprotein of rhabdoviruses. *Virus Genes*, 10: 107-114.
39. Coll JM (1997). Synthetic peptides from the heptad repeats of the

glycoproteins of rabies, vesicular stomatitis and fish rhabdoviruses bind phosphatidylserine. *Archives of Virology*, 142: 2089-2097.

40. Carneiro FA, Ferradosa AS & Da Poian AT (2001). Low pH-induced conformational changes in vesicular stomatitis virus glycoprotein involve dramatic structure reorganization. *Journal of Biological Chemistry*, 276: 67-72.
41. Gaudin Y, Ruigrok RW, Knossow M & Flamand A (1993). Low-pH conformational changes of rabies virus glycoprotein and their role in membrane fusion. *Journal of Virology*, 67: 1365-1372.
42. Eidelman O, Schlegel R, Tralka TS & Blumenthal R (1984). pH-dependent fusion induced by vesicular stomatitis virus glycoprotein reconstituted into phospholipid vesicles. *Journal of Biological Chemistry*, 259: 4622-4628.
43. Roche S & Gaudin Y (2002). Characterization of the equilibrium between the native and the fusion-inactive conformation of the rabies virus glycoprotein indicates that the fusion complex is made of several trimers. *Virology*, 297: 128-135.
44. Carneiro FA, Stauffer F, Lima CS, Juliano MA, Juliano L & Da Poian AT (2003). Membrane fusion induced by vesicular stomatitis virus depends on histidine protonation. *Journal of Biological Chemistry*, 278: 13789-13794.
45. Gaudin Y, Raux H, Flamand A & Ruigrok RW (1996). Identification of amino acids controlling the low-pH-induced conformational change of rabies virus glycoprotein. *Journal of Virology*, 70: 7371-7378.
46. Durrer P, Gaudin Y, Ruigrok WH, Graf R & Brunner J (1995). Photolabeling identifies a putative fusion domain in the envelope glycoprotein of rabies and vesicular stomatitis viruses. *Journal of Biological Chemistry*, 270: 17575-17581.
47. Li Y, Drone C, Sat E & Ghosh HP (1993). Mutational analysis of the vesicular stomatitis virus glycoprotein G for membrane fusion domains. *Journal of Virology*, 67: 4070-4077.
48. Zhang L & Ghosh HP (1994). Characterization of the putative fusogenic domain in vesicular stomatitis virus glycoprotein G. *Journal of Virology*, 68: 2186-2193.
49. Fredericksen BL & Whitt M (1995). Vesicular stomatitis virus glycoprotein mutations that affect membrane fusion activity and abolish virus infectivity. *Journal of Virology*, 69: 1435-1443.
50. Nuñez E, Fernandez AM, Estepa A, Gonzalez-Ros JM, Gavilanes F & Coll JM (1998). Phospholipid interactions of a peptide from the fusion-related domain of the glycoprotein of VHSV, a fish rhabdovirus. *Virology*, 243: 322-330.
51. Shokralla S, He Y, Wanas E & Ghosh HP (1998). Mutations in a carboxy-terminal region of vesicular stomatitis virus glycoprotein G that affect membrane fusion activity. *Virology*, 242: 39-50.
52. Odell D, Wanas E, Yan J & Ghosh HP (1997). Influence of membrane anchoring and cytoplasmic domains on the fusogenic activity of vesicular stomatitis virus glycoprotein G. *Journal of Virology*, 71: 7996-8000.
53. Cleverley DZ & Lenard J (1998). The transmembrane domain in viral fusion: essential role for a conserved glycine residue in vesicular stomatitis virus G protein. *Proceedings of the National Academy of Sciences, USA*, 95: 3425-3430.
54. Carr CM, Chaudhry C & Kim PS (1997). Influenza hemagglutinin is spring-loaded by a metastable native conformation. *Proceedings of the National Academy of Sciences, USA*, 94: 14306-14313.
55. Yao Y, Ghosh K, Epand RF, Epand RM & Ghosh HP (2003). Membrane fusion activity of vesicular stomatitis virus glycoprotein G is induced by low pH but not by heat or denaturant. *Virology*, 310: 319-332.
56. Gaudin Y (2000). Rabies virus-induced membrane fusion pathway. *Journal of Cell Biology*, 150: 601-611.
57. Pak CC, Puri A & Blumenthal R (1997). Conformational changes and fusion activity of vesicular stomatitis virus glycoprotein: [^{125}I]-iodonaphthyl azide photolabeling studies in biological membranes. *Biochemistry*, 36: 8890-8896.
58. Shai Y (1999). Mechanism of the binding, insertion and destabilization of phospholipid bilayer membranes by alpha-helical antimicrobial and cell non-selective membrane-lytic peptides. *Biochimica et Biophysica Acta*, 1462: 55-70.
59. Stoll V, Stewart KD, Maring CJ et al. (2003). Influenza neuraminidase inhibitors: structure-based design of a novel inhibitor series. *Biochemistry*, 42: 718-727.
60. Moore JP & Doms RW (2003). The entry of entry inhibitors: a fusion of science and medicine. *Proceedings of the National Academy of Sciences, USA*, 100: 10598-10602.

ANEXO C

Probing the interaction between vesicular stomatitis virus and phosphatidylserine

Fabiana A. Carneiro, Pedro A. Lapido-Loureiro, Sandra M. Cordo, Fausto Stauffer, Gilberto Weissmüller, M. Lucia. Bianconi, Maria A. Juliano, Luiz Juliano, Paulo M. Bisch e Andrea T. Da. Poian

Publicado em 2006 no periódico

European Biophysics Journal

Eur Biophys J (2006) 35: 145–154
DOI 10.1007/s00249-005-0012-z

ARTICLE

**Fabiana A. Carneiro · Pedro A. Lapido-Loureiro
Sandra M. Cordo · Fausto Stauffer
Gilberto Weissmüller · M. Lucia. Bianconi
Maria A. Juliano · Luiz Juliano · Paulo M. Bisch
Andrea T. Da. Poian**

Probing the interaction between vesicular stomatitis virus and phosphatidylserine

Received: 20 May 2005 / Revised: 30 June 2005 / Accepted: 20 July 2005 / Published online: 24 September 2005

Abstract The entry of enveloped animal viruses into their host cells always depends on membrane fusion triggered by conformational changes in viral envelope glycoproteins. Vesicular stomatitis virus (VSV) infection is mediated by virus spike glycoprotein G, which induces membrane fusion between the viral envelope and the endosomal membrane at the acidic environment of this compartment. In this work, we evaluated VSV interactions with membranes of different phospholipid compositions, at neutral and acidic pH, using atomic force microscopy (AFM) operating in the force spectroscopy mode, isothermal calorimetry (ITC) and molecular dynamics simulation. We found that the binding forces differed dramatically depending on the membrane phospholipid composition, revealing a high specificity of G protein binding to membranes containing phosphatidylserine (PS). In a previous work, we showed that the sequence corresponding amino acid 145–164 of VSV G protein was as efficient as the virus in catalyzing membrane fusion at pH 6.0. Here, we used this sequence to explore VSV–PS interaction using ITC. We found that peptide binding to membranes was exothermic, suggesting the participation of electrostatic interactions. Peptide–membrane interaction at pH 7.5 was shown to be specific to PS and dependent on the presence of His residues in the fusion peptide. The application of the simplified continuum Gouy–Chapman theory to our system predicted a pH of 5.0 at membrane surface, suggesting that the His residues should be protonated when located close to the membrane. Molecular dynamics simulations suggested that the peptide interacts with the lipid bilayer through its N-terminal residues, especially Val^{145} and His^{148}.

Fabiana A. Carneiro and Pedro A. Lapido-Loureiro contributed equally to this work

F. A. Carneiro · S. M. Cordo · F. Stauffer · M. L. Bianconi
A. T. Da. Poian (✉)
Instituto de Bioquìmica Médica,
Universidade Federal do Rio de Janeiro,
Rio de Janeiro, 21941-590 Brazil
E-mail: dapoian@bioqmed.ufrj.br
Tel.: +55-21-22706264
Fax: +55-21-22708647

P. A. Lapido-Loureiro · G. Weissmüller · P. M. Bisch
F. A. Carneiro
Laboratório de Física Biológica,
Instituto de Biofísica Carlos Chagas Filho,
Universidade Federal do Rio de Janeiro,
Rio de Janeiro, RJ, 21949-900 Brazil

S. M. Cordo
Laboratorio de Virología, Departamento de Quimica Biológica,
Facultad de Ciencias Exactas y Naturales,
Universidad de Buenos Aires, Buenos Aires, Argentina

M. A. Juliano · L. Juliano
Departamento de Biofísica, Escola Paulista de Medicina,
UNIFESP, Rua Trêsde Maio, 100,
SãoPaulo, 04044-020 Brazil

Introduction

The plasma membrane of eukaryotic cells serves as a barrier against invading parasites and viruses. To infect a cell, viruses must be capable of transporting their genome and accessory proteins into the cytosol or, in some cases, into the nucleus of the host cell, thus bypassing or modifying the barrier properties imposed by the plasma membrane. Enveloped viruses always gain entry to the cytoplasm by fusion of their lipid envelope with the plasma or endosomal membranes (Hernandez et al. 1996; Skehel and Wiley 2000; Eckert and Kim 2001), whereas nonenveloped viruses must use alternative strategies to cross the membrane. Membrane fusion induced by viruses is mediated by viral fusion glycoproteins, which have already been identified for a number of different viruses (Hernandez et al. 1996). The fusion reaction depends on conformational changes in the fusion glycoproteins that can be triggered either by

the interaction with a specific virus receptor on cell surface, or by the acidic pH of the endosomal environment.

Vesicular stomatitis virus (VSV) belongs to the *Rhabdoviridae* family, a group of enveloped negative single strand RNA viruses. The VSV envelope contains approximately 1,200 molecules of a single transmembrane glycoprotein, the G protein, that form about 400 trimeric spikes on the virus surface. VSV G protein is involved in both virus attachment to the host cell surface and in the membrane fusion mediated by the virus. VSV-induced membrane fusion occurs at the endosomal compartment where the acidic pH induces conformational changes on G protein, leading to the exposure of hydrophobic domains (Crimmins et al. 1983; Durrer et al. 1995; Pak et al. 1987), followed by dramatic structural reorganization (Carneiro et al. 2001).

The cellular receptor for VSV is still to be determined. There are several evidences in the literature suggesting an important role for phospholipids in the rhabdovirus entry into the host cell (Schlegel et al. 1982, 1983; Superti et al. 1984; Mastromarino et al. 1987). A high affinity, saturable binding site has been described for VSV on Vero cells, indicating that the binding occurs through a specific receptor (Schlegel et al. 1982). The binding could be inhibited by membrane extracts, which were resistant to protease, neuraminidase and heating, but inactivated by treatment with phospholipase C (Schlegel et al. 1983). These findings, together with the observation that only phosphatidylserine (PS) among various purified lipids was able to inhibit VSV binding to membranes, led the authors to suggest that PS could participate in the cellular binding site for VSV (Schlegel et al. 1983). On the other hand, a recent work from Coil and Miller (2004) provided consistent evidences supporting that the VSV binding to PS is not a determinant event in the context of the cellular plasma membrane. For the authors, virus recognition at cell surface must occur through an unknown cellular receptor, and the binding to PS should be important in a subsequent step of the entry process. Despite this controversy regarding the participation of PS in VSV binding site at the host cell surface, several findings indicate that PS is essential for VSV–membrane interactions. Membrane fusion mediated by VSV G protein reconstituted in lipid vesicles showed a large preference for target membranes containing phosphatidylserine or phosphatidic acid (Eidelman et al. 1984). In a previous work, we showed that the extent of pH-induced G protein conformational changes and the membrane fusion mediated by this protein could be correlated to the PS content in the vesicles (Carneiro et al. 2002). A PS-binding segment was mapped in G protein from several rhabdoviruses (Coll 1997). This sequence was first identified in viral hemorrhagic septicemia virus (VHSV), a fish rhabdovirus that infects salmonids (Estepa and Coll 1996), and then found in rabies, VSV and infectious haematopoietic necrosis virus (IHNV), another fish rhabdovirus (Coll 1997). We have demonstrated that a synthetic peptide corresponding to the VSV PS binding site (amino acids 145 to 164 of G protein) was as efficient as the whole virus to mediate fusion (Carneiro et al. 2003). This segment contains two His residues, whose substitution by Ala or modification with diethylpyrocarbonate (DEPC) inhibits the fusogenic properties of the peptide.

In the present work, we compared the interaction forces between VSV and membranes of different phospholipid composition and we found a high specificity for PS on VSV binding to vesicles. We evaluated the role of this His residues on membrane recognition at neutral bulk pH, a condition in which no fusion occurs. We show that the high specificity of VSV binding to membranes containing PS was due to His–PS interaction. In addition, a model for this interaction is proposed.

Materials and methods

Chemicals

Phosphatidylserine (PS), phosphatidylcholine (PC) and phosphatidylethanolamine (PE) from bovine brain, phosphatidylglycerol (PG) from egg yolk lecithin, phosphatidylinositol (PI) from bovine liver, and diethylpyrocarbonate (DEPC) were purchased from Sigma Chemical Co., St. Louis, MO, USA. All other reagents were of analytical grade.

Virus propagation and purification

VSV Indiana was propagated in monolayer cultures of BHK_{21} cells. The cells were grown at 37°C in petri dishes containing Dulbecco's modified Eagle medium supplemented with 10% fetal bovine serum, 100 μg/ml penicillin, 0.0085% streptomycin sulfate. When the cells reached confluence, the medium was removed, and the cell monolayer was infected with VSV at a multiplicity of infection (MOI) of 0.1. The cultures were kept at 37°C for 16–20 h and the virus was harvested and purified by differential centrifugation followed by equilibrium sedimentation in a sucrose gradient as described elsewhere (Da Poian et al. 1996). For all the experiments the purified virus was dialyzed against Tris 10 mM buffer, pH 7.4 for 4 h. Purified virions were stored at −70°C.

Peptides synthesis

The VSV G protein peptide corresponding to the sequence between amino acids 145 and 164, VTPHHVLVDEYTGEWVDSQF, and the same peptide except for the substitution of then two His for Ala residues, VTPAAVLVDEYTGEWVDSQF, were synthesized by solid phase using the Fmoc methodology

and all protected amino acids were purchased from Calbiochem–Novabiochem (San Diego, USA) or from Neosystem (Strasbourg, France). The syntheses were done in an automated bench-top simultaneous multiple solid-phase peptide synthesizer (PSSM 8 system from Shimadzu). The final deprotected peptides were purified by semipreparative HPLC using an Econosil C-18 column (10 μm, 22.5 × 250 mm) and a two-solvent system: (a) trifluoroacetic acid/H_2O (1:1000, v/v) and (b) trifluoroacetic acid/acetonitrile/H_2O (1:900:100, v/v/v). The column was eluted at a flow rate of 5 ml min^{-1} with a 10 or 30 to 50 or 60% gradient of solvent B over 30 or 45 min. Analytical HPLC was performed using a binary HPLC system from Shimadzu with a SPD-10AV Shimadzu UV/vis detector, coupled to an Ultrasphere C-18 column (5 μm, 4.6 × 150 mm), which was eluted with solvent systems A1 (H_3PO_4/H_2O, 1:1000, v/v) and B1 (acetonitrile/H_2O/H_3PO_4, 900:100:1, v/v/v) at a flow rate of 1.7 ml min^{-1} and a 10–80% gradient of B1 over 15 min. The HPLC column eluted materials were monitored by their absorbance at 220 nm. The molecular mass and purity of synthesized peptides were checked by MALDI-TOF mass spectrometry (TofSpec-E, Micromass) and/or peptide sequencing using a protein sequencer PPSQ-23 (Shimadzu Tokyo, Japan).

Sample modification with DEPC

DEPC solutions were freshly prepared by dilution of the reagent in cold ethanol. The concentration of stock DEPC solution was determined by reaction with 10 mM imidazole (Miles 1977). For modification with DEPC, VSV (0.6 mg/ml) was incubated with DEPC at final concentration of 0.5 mM for 15 min at room temperature. Then VSV was diluted in 20 mM MES, 30 mM Tris buffer, pH 7.5 to a final protein concentration of 60 μg/ml. For modification of peptides, the process was carried out under the same conditions except that the initial and final protein concentrations were 10 mg/ml and 400 μg/ml, respectively.

Preparation of liposomes

Phospholipids were dissolved in chloroform and evaporated under nitrogen. The lipid film was resuspended in 20 mM MES, 30 mM Tris buffer (pH 7.5 or 6.0) in a final lipid concentration of 1 mM. The suspension was vortexed vigorously for 5 min. Small unilamellar vesicles were obtained by sonicating the turbid suspension using a Branson Sonifier (Sonic Power Company, Danbury, CT, USA) equipped with a titanium microtip probe. Sonication was performed in an ice bath, alternating cycles of 30 s at 20% full power, with 60 s resting intervals until a transparent solution was obtained (approximately ten cycles). The phospholipids used in this study were composed of PC only, PC:PE, PC:PS, PC:PI and PC:PG at the proportions indicated in the figure legends.

Atomic force microscopy

The AFM used in this work was built in collaboration with the Ludwig-Maximilians-Universität, Lehrstuhl für Angewandte Physik in München, Germany. For all the experiments, the AFM was used in force-spectroscopy mode (Florin et al. 1994; Gergely et al. 2000; Zlatanova et al. 2000). Mica coverslips were glued to magnetic stainless steel punches, and mounted in a fluid cell without using the O-ring. The mica surfaces were pre-incubated with vesicles before transferring to the fluid cell (Jass et al. 2000; Puu et al. 2000). Since the presence of calcium ions appears to facilitate as well as to increase the rate of planar membrane formation from vesicles (Puu et al. 1997; Reviakine et al. 2000), mica surfaces were incubated with 20 μl of the vesicle suspension containing 1 mM phospholipids, plus 10 μl of 20 mM MES, 30 mM Tris buffer, pH 7.4 containing 1 mM $CaCl_2$, for approximately half an hour at room temperature (25 ± 0.5°C). After incubation, the slips were washed repeatedly with the same buffer used to prepare vesicles. All experiments were performed at room temperature using standard V-shaped cantilevers, containing a silicon nitride tip with a 4 μm^2 pyramidal base (Digital Instruments Inc.). The cantilevers have a spring constant of 0.06 N/m (manufacturer's data) and were pre-incubated with VSV as follows. The cantilevers were immersed in a virus suspension (total protein concentration of 0.28 mg/ml) for 24 h at 4–6°C. The instrument allows the performance of "approach-retraction" cycles, in which the maximal contact force, interaction time and the approach-retracting rates can be controlled independently. The maximal force was limited to approximately 3 nN, the interaction time was set to zero and the approach-retracting rate was set to 7,500 nm/s. Tips can be reused but they should be cleaned soon and should not dry out before the cleaning procedure.

Calorimetric studies

Binding to lipid vesicles and membrane fusion induced by VSV or wild type and mutant peptide [145–164] were studied by isothermal titration calorimetry (ITC) using a MCS-ITC from MicroCal, Llc. (Northampton, MA, USA). Membrane fusion was studied by following the heat effect of four injections of 5 μl of a VSV suspension (60 μg/ml) or peptide solution (400 μg/ml) into the sample cell containing 1 mM PC:PS (1:3) vesicles in 20 mM MES, 30 mM Tris buffer (pH 6.0), after equilibration at 37°C. For the binding experiments, the samples were prepared at pH 7.5, and four injections (5 μl each) of the virus suspension or peptide solution were done into the sample cell (V = 1.38 ml) containing

1 mM PC:PS (1:3) or PC:PG (1:3) vesicles in 20 mM MES, 30 mM Tris buffer (pH 7.5), after equilibration at 37 ° C. The heat of dilution of the peptides was measured by injecting the same solutions into buffer only.

Molecular dynamics simulations

Initially, we decided to simulate the peptide [145–164] in solution by molecular dynamics (MD) in order to evaluate the consistency of the force field and compare it with experimental NMR data in aqueous environment (C.S. Lima et al., unpublished results). The starting atomic coordinates were parameterized with the GROMOS96 united atom force field implemented in the GROMACS MD program (Lindahl et al. 2001). The peptide [145–164] with protonated His^{148} and His^{149} was solvated in a SPC water box (Berendsen et al. 1987) with 4,737 water molecules and two sodium ions, to neutralize the -2 e net charge. After energy minimization with constraints of 1,000 kJ/mol applied on C, N and O atoms, we performed an unconstrained MD simulation in the NPT ensemble (fixed number of particles and constant pressure/temperature) (Berendsen et al. 1984) for 10 ns, at 298 K and 1 bar.

To gain insight into the interaction between the peptide [145–164] and charged membranes at an atomistic resolution, we chose to simulate a dimyristoylphosphosphatidylserine (DMPS) bilayer in the liquid-crystalline phase. The last configuration of the peptide [145–164] in the previous simulation was inserted in the aqueous phase of a pre-equilibrated 126 DMPS bilayer, with 7,347 SPC water molecules and 126 sodium counterions. The system was energy minimized with constraints (see above) applied on the protein. The lipids were simulated with the parameters taken from Pandit et al. (2002) and Chandrasekhar et al. (2003) in the NPT ensemble, with anisotropic pressure scaling (i.e., six box dimensions *xx, yy, zz, xy/yx, xz/zx* and *yz/zy* were independently coupled to pressure "baths") for 10 ns. In both systems, bonds were constrained with the SHAKE algorithm (Ryckaert et al. 1977) allowing a 2 fs integration step. Electrostatic forces were calculated using the particle mesh Ewald method (Darden et al. 1993) with 1.2 Å grid spacing and a fourth-order spline for interpolation. Van der Waals forces were computed with a cut-off radius of 14 Å .

Continuum electrostatics models

Assuming that the electrostatics of model lipid membranes is well described by the Gouy–Chapman approximation for interfaces of the generalized Poisson–Boltzmann equation (Cevc 1990), we can calculate the surface potential as:

$$\psi_0 = \left(\frac{2k_BT}{Ze}\right)\sinh^{-1}\left(\frac{Ze\sigma_{el}\lambda}{2\varepsilon\varepsilon_0 k_BT}\right)$$

where, Ψ_0 is the surface potential, Z is the co- and counter-ion valency, ε, ε_0 and k_B are the dielectric constant of water, the permittivity of free space and the Boltzmann constant, respectively. σ_{el} is the surface charge density and λ is the Debye screening length (or the width of the double layer), defined as:

$$\lambda = \left(\frac{\varepsilon\varepsilon_0 k_BT}{10^3 N_A e^2 \Sigma Z_i^2 c_i}\right)^{\frac{1}{2}} \quad (2)$$

According to the Boltzmann distribution, we have:

$$[\text{ion}]_0 = [\text{ion}]_{\text{bulk}} \exp\left(-\frac{Ze\Psi_0}{k_BT}\right) \quad (3)$$

where, $[\text{ion}]_0$ and $[\,ion]_{bulk}$ are the ionic species concentration near the surface and in the bulk, respectively.

Results

Probing the VSV–membrane interaction using atomic force microscopy

Force spectroscopy was used to measure the interaction forces between VSV and membranes of different phospholipid composition at pH 7.5, a condition that simulates binding to membrane but not fusion; and at pH 6.0, the optimum pH for VSV fusion. A set of five lipid film compositions was used: three negatively charged, composed of PC:PS (3:1), PC:PI (3:1), and PC:PG (3:1), and two neutral, composed of PC only and PC:PE (3:1). Sets of scans were acquired with delay times increasing from 0 to 800 ms between the approach and the retraction of the scanner (Figs. 1, 2).

At pH 7.5, the binding between the virus and lipid films containing PS was remarkably stronger when compared to that observed for other lipid compositions (Fig. 1). Moreover, as shown in Table 1, the retraction curves obtained for the interaction between VSV and PC:PS showed several rupture events that extended for hundreds of nanometers, while for other lipid films the interaction peaks appear much closer to the contact point. The interaction between the virus and films of PC:PS and PC:PG increased with contact time (Fig. 1). Although PC:PG films exhibited force curves with several rupture events after longer contact times, the force peaks were considerably smaller than that observed for PC:PS films. For PC:PI films, no significant interaction was observed even after increasing the contact time, indicating that not only the charge is important for virus–membrane interaction, but also the specific lipid head group. Films containing PC:PE showed a very small interaction peak, close to the contact point, exhibiting only a small variation with contact time. Furthermore, films containing PC only did not show any detectable interaction even after 800 ms of contact (not shown).

In order to analyze the interactions under conditions reflecting the protein–lipid interaction events that take

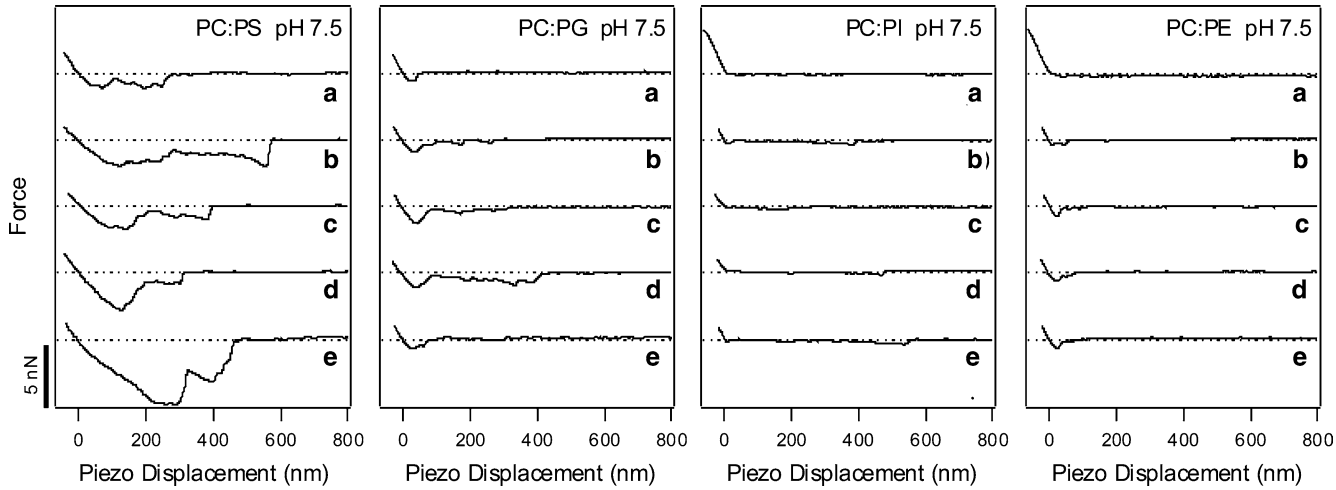

Fig. 1 Interaction forces between VSV and membranes of different phospholipid composition probed by atomic force microscopy at pH 7.5. Force–distance curves were recorded on lipid-covered mica substrates. Retracting curves were obtained with VSV adsorbed on the tip and mica substrates covered with PC:PS (3:1), PC:PG (3:1), PC:PI (3:1) or PC:PE (3:1) after a delay time of 0 (a), 200 (b), 400 (c), 600 (d) and 800 (e) ms. Data were collected in 20 mM MES, 30 mM Tris, pH 7.5, at room temperature

place during membrane fusion reaction, similar experiments were performed at pH 6.0 (Fig. 2). As observed at pH 7.5, for PS and PG containing lipid films, the interaction forces increased with the increase in the contact time and no interaction was detected between the virus and PC:PI films. A small interaction close to the contact point was observed with PC:PE films and a small increase in the force peak was observed with longer contact times. The films containing PC only did not show any response to the pH change (not shown).

All experiments were repeated with different lipid and tip preparations where a set of at least ten scans was acquired for each pH and delay time. With short contact times, we did not observe a significant variation in the adhesion peaks even after a large set of scans (20–30 scans). However, as the contact time increased, the number of reproducible scans obtained with PC:PS films was reduced when the interaction peaks become as large as 3–4 nN. One explanation for this could be a strong interaction between the virus and PS at pH 6.0 that probably involves insertion of VSV G protein into the lipid bilayer, resulting in the removal of VSV from the tip during retraction.

Calorimetric studies of VSV and peptide [145–164] interaction with vesicles

The role of PS in the interaction between membranes and VSV or G protein peptide [145–164] was also studied using microcalorimetry at the pHs of fusion and binding. Membrane fusion was studied by ITC at 37° C, by following the heat flow after injection of VSV or the peptide [145–164] into PC:PS (1:3) vesicles at pH 6.0.

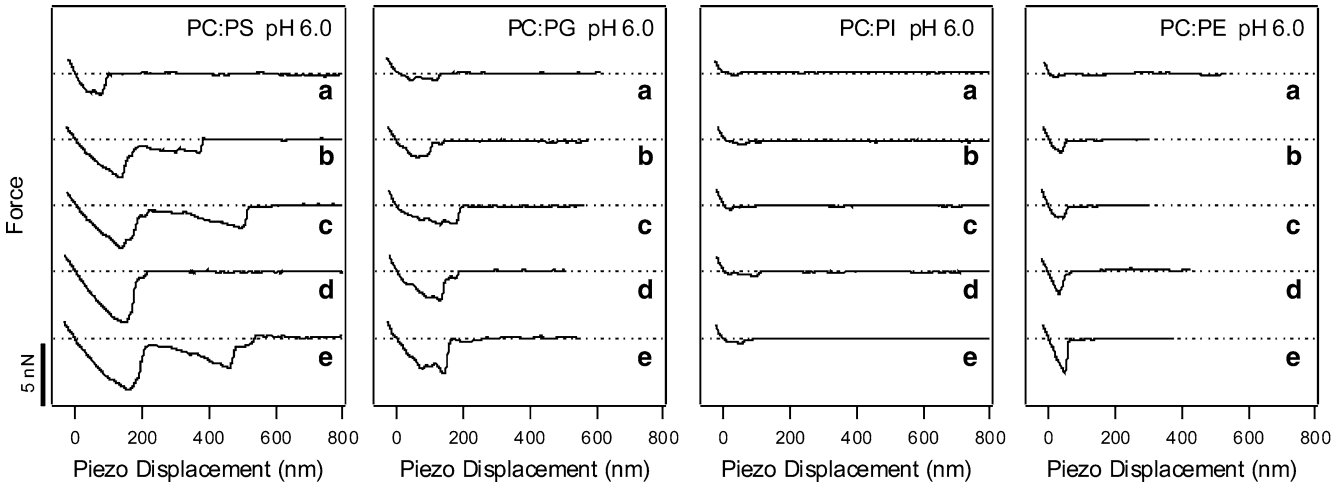

Fig. 2 Interaction forces between VSV and membranes of different phospholipid composition probed by atomic force microscopy at pH 6.0. Force–distance curves were recorded on lipid-covered mica substrates. Retracting curves were obtained with VSV adsorbed on the tip and mica substrates covered with PC:PS (3:1), PC:PG (3:1), PC:PI (3:1) or PC:PE (3:1) after a delay time of 0 (a), 200 (b), 400 (c), 600 (d) and 800 (e) ms. Data were collected in 20 mM MES, 30 mM Tris, pH 6.0, at room temperature

Table 1 Interaction between VSV and membranes of different lipid composition at pH 7.5

Film composition	Force (pN)	Maximal rupture distance (nm)	Rupture events
PC:PS	1400 ± 400	520 ± 430	Up to 8
PC:PG	660 ± 140	68 ± 22	Up to 2
PC:PI	160 ± 80	150 ± 120	2
PC:PE	450 ± 90	40 ± 15	1
PC	Not detected	–	–
Mica	250 ± 200	30 ± 25	2

Figure 3a shows that either the virus or the peptide were able to cause membrane fusion in a similar way. The kinetics of the fusion also seems to be very similar occurring in a time frame of about 10 min, in agreement with our previous observation using other techniques (Carneiro et al. 2001; 2003; Da Poian et al. 1998). The calorimetric thermograms obtained with VSV or with the peptide showed a negative displacement of the heat flow from the baseline after sample injection. Intriguingly, fusion stopped after one or two injections of viruses, suggesting the newly injected viruses were not able to fuse with the virosomes resulting from previous fusion events. This was also observed when we measured fusion by fluorescence energy transfer in labeled liposomes (not shown). However, the fusion process is probably complex. It is probably causing a change in macromolecular level to have a mixture of VSV proteins and phospholipids, resulting in a different structure than that of a lipid bilayer.

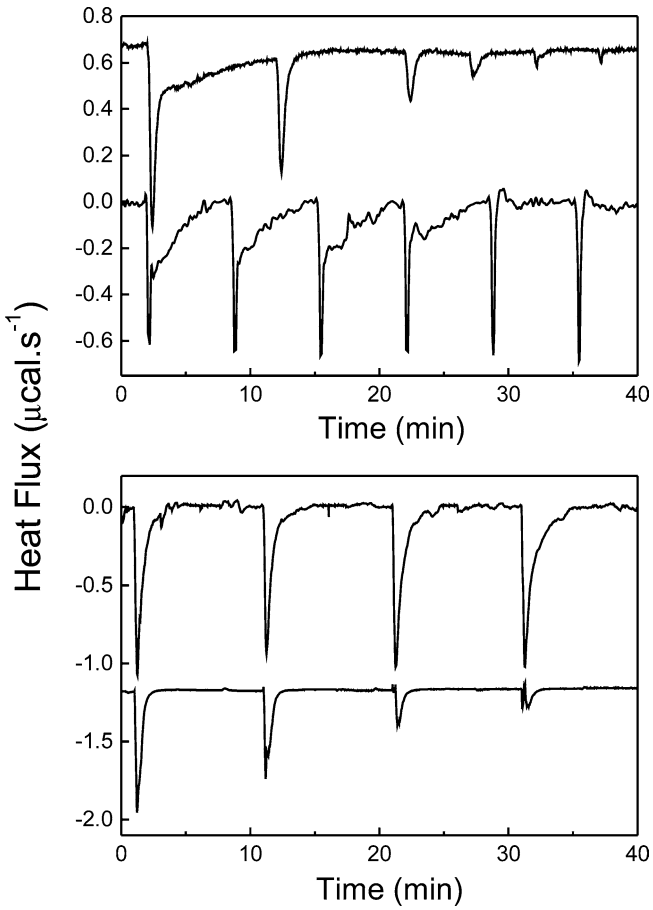

Fig. 3 Calorimetric measurements of membrane fusion (*upper panel*) and binding (*lower panel*) by VSV or peptide [145–164] at 37°C. *Upper panel*: Typical calorimetric traces (heat flow as a function of time) obtained from 6 × 5 μL injections of VSV (0.06 mg/ml) or PEP (0.4 mg/ml) into the sample cell containing 1 mM PC:PS (1:3) vesicles in 20 mM MES, 30 mM Tris, pH 6.0. The sharp peak that follows the injection is due to dilution effects, and the following slow heat effect is associated with the fusion process (broader peak). The negative heat effects indicate that the fusion is exothermic in nature. *Lower panel*: calorimetric traces for membrane binding of VSV (0.06 mg/ml) or PEP (0.4 mg/ml) into the sample cell containing 1 mM PC:PS (1:3) vesicles in vesicles in 20 mM MES, 30 mM Tris, pH 7.5. The negative peaks observed after subtraction of the heat of dilution indicate the exothermic nature of the binding

On the other hand, when the VSV or the peptide was injected into vesicles prepared at pH 7.5, no fusion was observed and the binding could be measured. In both cases we observed negative peaks indicative of an exothermic binding to the vesicles. In this case, after 2×5 μL injections of the peptide (corresponding to 4 μg of peptide in the cell), there was no significant heat effect in the thermogram indicating a binding saturation. These results suggest that besides acting in membrane fusion, the binding of peptide [145–164] to PS-containing membranes at pH 7.5 is similar to the exothermic binding between the whole VSV and membranes containing PS. This encouraged us to explore the role of His^{148} and His^{149} on membrane recognition at neutral pH. We had shown earlier that the protonation of these two His was involved in VSV fusion, since blocking these His through their reaction with DEPC or substituting these residues for Ala completely abolished peptide fusion activity (Carneiro et al. 2003). To address this point, binding experiments were done using the peptide modified with DEPC or a mutant peptide containing two Ala residues replacing His^{148} and His^{149} (Fig. 4). In both cases, as compared to the intact peptide, after the injection of either peptide to the cells containing PC:PS (1:3) vesicles at 37°C, no significant heat effect could be observed after subtraction of the heat of dilution of the peptides (Fig. 4b, c). These results are indicative that the His^{148} and His^{149} are also essential for the binding to occur. Changing PS for PG in the vesicles abolished peptide binding (Fig. 4d), indicating that Peptide–membrane interaction occurs through the binding between His and PS.

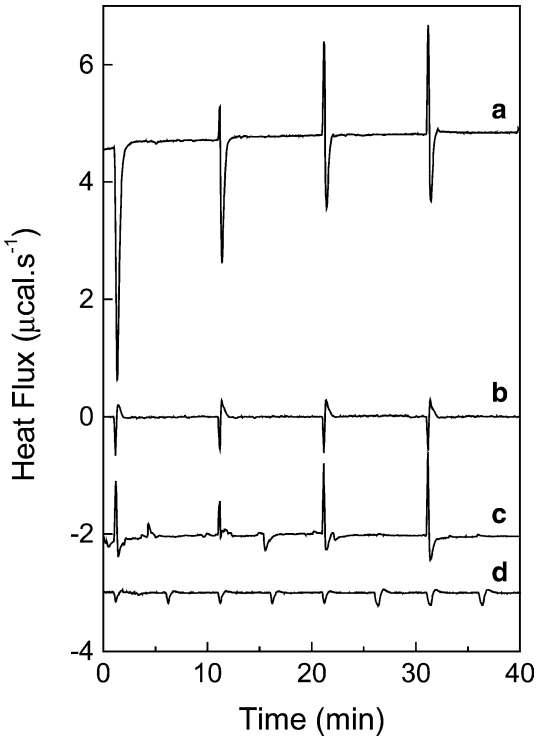

Fig. 4 Specificity of the peptide interaction with phospholipid vesicles. The heat flow as a function of temperature is shown after subtraction of the heat of dilution of the peptides. The calorimetric traces were obtained at 37°C where the peptide [145–164] was injected in the sample cell containing 1 mM PC:PS 1:3 (**a**) or PC:PG 1:3 (**d**) vesicles. Traces b and c show the importance of the His residues for the interaction as the mutant peptide (b) and the DEPC-modified peptide (**c**) since no significant heat effect is observed

Simulation of peptide [145–164] interaction with PS-containing membranes

Since classical MD techniques are carried out with fixed partial atomic charges, it was necessary to make a choice regarding the protonation state of the His[148] and His[149] residues. By using the simplified continuum Gouy-Chapman theory (see Material and methods) an interfacial H_3O^+ concentration was calculated and the His imidazol ring protonation state was inferred, assuming a pK_a of 6.0. Applying Eqs. 1 and 2, a Debye screening length of approximately 10 Å and a surface potential in the range of −120 mV were obtained. The parameters used in the calculations were: surface charge density, σ_{el}, of 0.2 Cm^{-2}, and ionic strength, $\Sigma\ Z_i^2\ c_i$, of 100 mM. The surface charge density was calculated assuming an ideal mixture of the PS and PC molecules and an area per lipid of 55 and 64 $Å^2$, respectively. Inserting these values into the Boltzmann distribution (Eq. 3) of H_3O^+ ion and neglecting changes in H_3O^+ ion activity coefficient, a 10^{-5} mol l^{-1} hydronium concentration was obtained, which corresponds to a local surface pH of 5.0 (Boström et al. 2004). At this pH, the His imidazol ring is mostly protonated, displaying a net charge of $+1e$.

Although the starting structure of the DMPS + peptide [145–164] system was somewhat arbitrary, a 10 ns-long MD simulation was probably sufficient to minimize any major artifacts arising from this initial choice. Moreover, using the last 2 ns of simulation, an area per lipid of 55 ± 0.7 $Å^2$ was calculated (data not shown), in accordance with other simulations (Pandit and Berkowitz 2002). This value, together with the fact that we used fully anisotropic pressure coupling (i.e., the bilayer was free to adjust its area), underlines the consistency of the lipid model.

As can be observed in Fig. 5, the peptide seems to interact with the simulated membrane patch mainly through its N-terminal residues. The rest of the peptide chain displays larger fluctuations, with the negatively charged residues (Asp and Glu) initially repelled from and afterwards approximating the water-DMPS interface. In fact, by analyzing the distance between the centers of mass of titratable aminoacids and the bilayer center (see Fig. 6), it can be seen that Val[145] and His[148] are stabilized in their positions. On the contrary, at least in the 10 ns time frame, the other charged residues (His[149], Asp[153,161] and Glu[154,158]) have not reached a stable position along the normal to the membrane.

Discussion

The early events of envelope virus infection comprise at least three distinct steps: (a) the cell recognition, which occurs generally through the interaction between the virus and a specific receptor on cell surface; (b) the interaction between a viral surface protein and a cellular membrane; and (c) membrane fusion reaction induced by the viral fusion proteins. In this work, we focused on dissecting the interaction between VSV and the membrane at neutral pH, which might take place after binding to the receptor but before the events involved in the membrane fusion reaction. We have taken advantage of our previous demonstration that atomic force microscopy (AFM) operating in the force spectroscopy mode could efficiently measure the interaction forces between a virus particle and a lipid bilayer (Carneiro et al. 2002). Using this technique, we showed that VSV interacts very strongly with membranes containing PS, while no interaction was observed with membranes composed of PC only. A question not completely answered was whether VSV–membrane interaction depends only on electrostatic interaction or it was specific for PS. Although VSV fusion has already been tested varying the phospholipid composition (Eidelman et al. 1984; Hermann et al. 1990), the binding events at neutral pH were not explored so far. To address this point we measured the interaction forces between virus particles and lipid films supported on mica surfaces at pH 7.5, a condition in which binding but not fusion could occur. These experiments revealed a high specificity for membrane-containing PS, suggesting that PS is

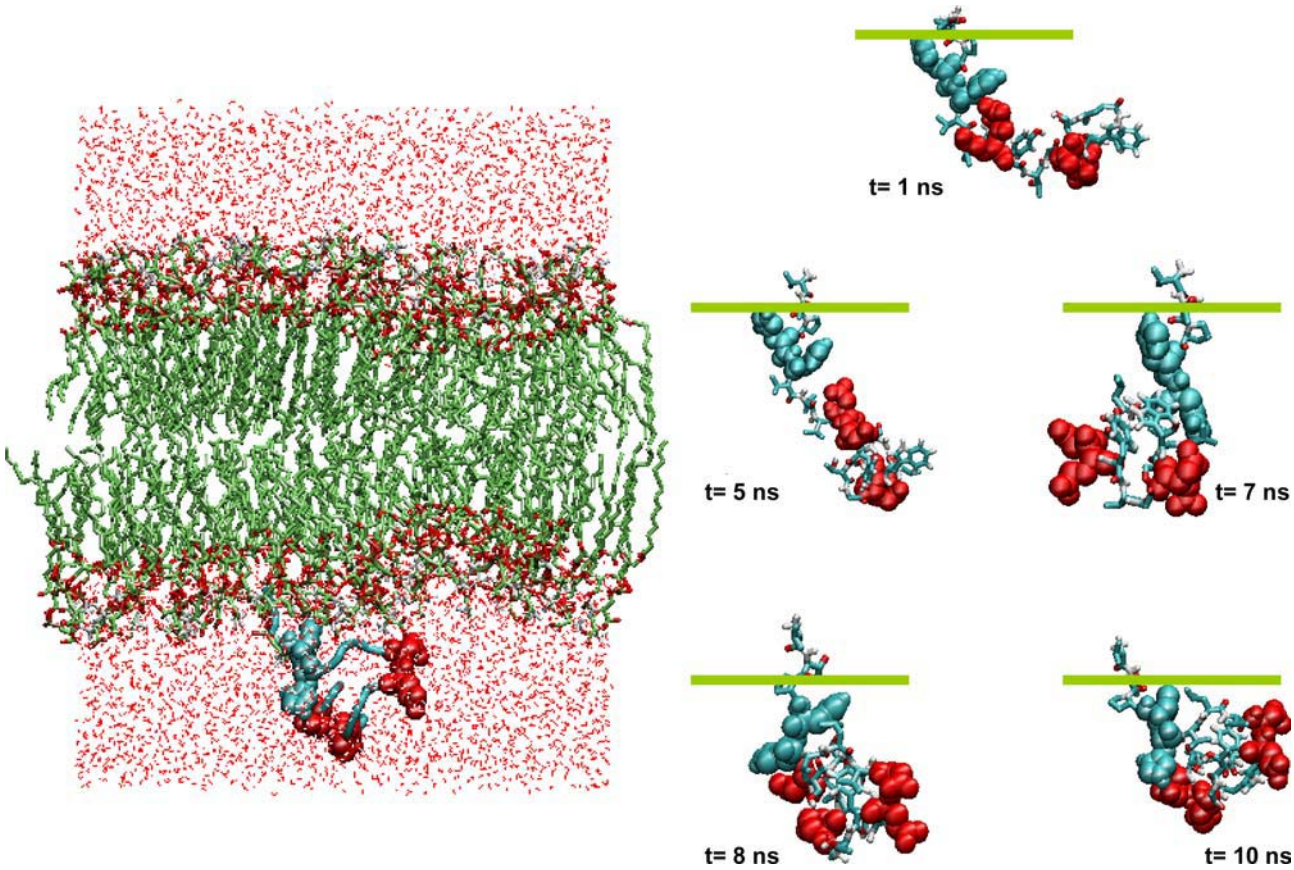

Fig. 5 Snapshots of the system configuration during 10 ns MD simulation. The protein backbone is represented as a cyan tube, except that the titratable residues are depicted as van der Waals spheres (cyan for the His and red for the Asp/Glu residues). Water is represented as *red lines*. The peptide is seen in detail along the simulation time. A representation of the water–DMPS interface is depicted as a *green line*. The DMPS bilayer is shown with the lipid tails in green, after 10 ns of simulation

also important for VSV–membrane interactions at neutral pH. This does not mean that the receptor for the virus is PS, but suggests that although other components in the cell surface might act as the VSV receptors, as indicated by the results from Coil and Miller (2004), a direct interaction between G protein and PS in the membrane could take place before the acidification inside the endosome.

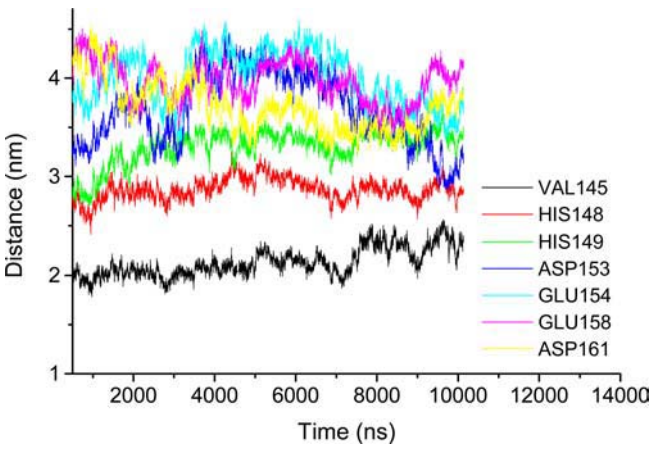

Fig. 6 Distance between titratable aminoacids and the bilayer center during the 10 ns simulation. It can be seen that Val^{145} and His^{148} display stable center of mass distances to the DMPS bilayer. The negatively charged aminoacids, on the contrary, display unstable positions in relation to the membrane as well as being more distant to the bilayer center of mass

The identification of G protein amino acid residues directly involved in VSV binding to membranes is an important point in the understanding of VSV–membrane interaction. Photolabeling studies of VSV G protein showed that its interaction with membranes strongly increases when the pH is lowered from 7.0 to 6.0 (Durrer et al. 1995). At the pH of fusion, the labeled site was located in the ectodomain comprising the amino acids 59 to 221. Based on several mutagenesis studies, the sequence between the residues 117 and 136 has been proposed as the putative fusion peptide of VSV G protein (Li et al. 1993; Zhang and Ghosh 1994; Fredericksen and Whitt 1995). However, direct evidence that this particular region interacts with the target membrane is still lacking and further investigation will be necessary to provide unambiguous evidence whether the segment between amino acids 117 and 136 of the G protein directly participates in VSV fusion or whether the substitution of its conserved amino acids affects the conformation or the exposure of other membrane-

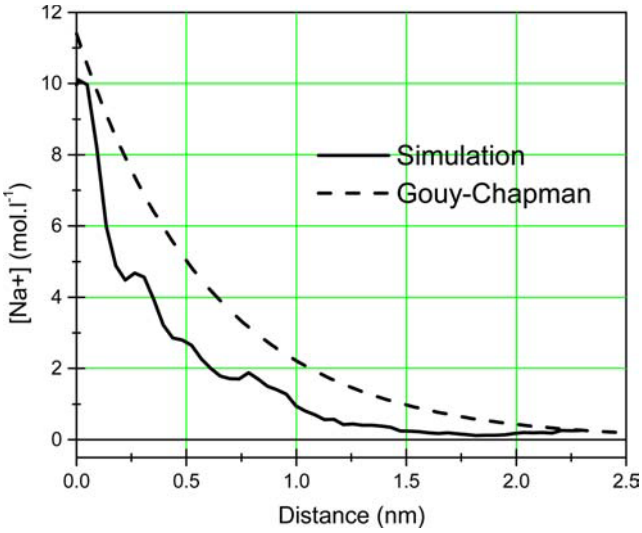

Fig. 7 Comparison of Gouy–Chapman theory and MD simulation. We divided the simulation box in slices normal to the membrane and measured the counterion Na+ concentration (*line*). Applying the Gouy–Chapman formalism we calculated the expected theoretical value (*dashed line*).

interacting sequence in the G protein. Another region of the G protein, encompassing residues 395–418 for VSV has been identified as a segment that affects the fusogenic activity of the protein by influencing the low-pH-induced conformational changes (Shokralla et al. 1998). In addition, it has also been shown that not only the ectodomain segment but also the membrane anchoring domain is required for VSV fusion activity (Odell et al. 1997; Cleverly and Lenard 1998).

Recently, we identified a specific sequence in the VSV G protein directly involved in membrane interaction and fusion (Carneiro et al. 2003). This segment has been previously characterized as the PS-binding site in the VSV G protein together with similar regions of G proteins from other rhabdoviruses (Coll et al. 1997). We showed that this segment, which corresponds to the sequence between amino acids 145 to 164 of the VSV G protein, is very efficient in catalyzing membrane fusion (Carneiro et al. 2003). Here we used the peptide 145–164 to explore G protein–membrane interaction. The study of the interaction between membrane and synthetic peptides corresponding to the fusogenic domain of the fusion protein is sometimes an important strategy to adopt. Although the results obtained with the peptides have to be considered cautiously since many features of the complex viral full length protein are not present in the isolated peptide–vesicle model system, analysis of the molecular mechanisms underlying fusion peptide activity in the whole protein would be not viable in most cases. As revised by Nieva and Agirre (2003), several findings support the view that synthetic peptides are useful models to study viral cell fusion. In our case, we were encouraged to use this peptide by the similarity between peptide- and whole virus-induced fusion. Besides showing the same kinetics of whole virus fusion, the peptide-induced fusion was dependent on pH and on the presence of PS in the target membrane.

Here we have shown that the peptide [145–164] binding to PS-containing vesicles is exothermic, suggesting the electrostatic nature of the binding. Therefore, taking into account the requirement of the negatively charged PS in the vesicles for VSV binding, our results suggest that the binding process may be mediated by a direct interaction between the positively charged His and the negative charges of PS in the membranes. Indeed, calorimetric experiments using the mutant peptide or the wild-type peptide modified with DEPC revealed that PS–peptide interaction occurs through the His residues. This proposition is further substantiated by the results of MD simulations, which show that His^{148} interacts strongly with the DMPS bilayer. The positive charge of His residues at pH 7.5 could be explained by the proximity of the peptide to the negativelly charged headgroups of the lipids, which can lower the pH at membrane surface, as suggested by the Gouy–Chapman theory. Despite the simplicity of the Gouy–Chapman theory and its mean-field nature, its use seems justifiable because the charge density σ_{el} of 0.2 C m^{-2} is in accordance with reported values by Cevc (1990) and with our own MD simulations. In fact, integrating the average charge density per 1 Å -long slices of the system along the bilayer normal in the last 2 ns of simulation, we obtained a value of 0.3 C m^{-2} concentrated in the phosphate region of the DMPS lipid (data not shown), in accordance with a mean charge of 1 *e* per 55 $Å^2$ for a pure PS bilayer. In addition, to further check the validity of the Gouy-Chapman model, we applied it to the calculation of Na^+ counter ion concentration near a surface of 0.3 C m^{-2} charge density and compared it to the MD simulation. As can be seen in Fig. 7, the agreement is reasonable.

Taking together, our results suggest that during VSV entry into the host cell binding to the receptor at cell surface could be essential for bringing the active His of G protein fusion peptide to the proximity of membrane surface, allowing its protonation and the interaction of the fusion protein with the target membrane.

Acknowledgements This work was supported by grants from Conselho Nacional de Desenvolvimento Científico e Tecnológico (CNPq), Centro Argentino-Brasileiro de Biotecnologia (CABBIO), Fundação Carlos Chagas Filho de Amparo à Pesquisa do Estado do Rio de Janeiro (FAPERJ) and Fundação Amparo à Pesquisa do Estado de São Paulo (FAPESP). S. C. was recipient of a fellowship from the International Center for Genetic Engineering and Biotechnology (ICGEB).

References

Berendsen HJC, Postma JPM, Dinola A, Haak JR (1984) Molecular dynamics with coupling to an external bath. J Chem Phys 81:3684–3690

Berendsen HJC, Grigera JR, Straatsma TP (1987) The missing term in effective pair potentials. J Phys Chem 91:6269–6271

Boström M, Williams DRM, Ninham BW (2004) Specific ion effects: Role of salt and buffer in protonation of cytochrome c. Eur Phys J 13:239–245

Carneiro FA, Ferradosa AS, Da Poian AT (2001) Low pH-induced conformational changes in vesicular stomatitis virus glycoprotein involve dramatic structure reorganization. J Biol Chem 276:62–67

Carneiro FA, Bianconi ML, Weissmuller G, Stauffer F, Da Poian AT (2002) Membrane recognition by vesicular stomatitis virus involves enthalpy-driven protein-lipid interactions. J Virol 76:3756–3764

Carneiro FA, Stauffer F, Lima CS, Juliano MA, Juliano L, Da Poian AT (2003) Membrane fusion induced by vesicular stomatitis virus depends on histidine protonation. J Biol Chem 278:13789–13794

Cevc G (1990) Membrane electrostatics. Biochim Biophys Acta 1031(3):311–382

Chandrasekhar I, Kastenholz M, Lins RD, Oostenbrink C, Schuler LD, Tieleman DP, van Gunsteren WF (2003) A consistent potential energy parameter set for lipids: dipalmitoylphosphatidylcholine as a benchmark of the GROMOS96 45 A3 force field. Eur Biophys J 32:62–67

Cleverley PZ, Lenard J (1998) The transmembrane domain in viral fusion: essential role for a conserved glycine residue in vesicular stomatitis virus G protein. Proc Natl Acad Sci USA 95:3425–3430

Coil DA, Miller AD (2004) Phosphatidylserine is not the cell surface receptor for vesicular stomatitis virus. J Virol 78:10920–10926

Coll JM (1997) Synthetic peptids from the heptad repeats of the glicoproteins of rabies, vesicular stomatitis and fish rhabdoviruses bind phosphatidylserine. Arch Virol 142:2089–2097

Crimmins DL, Mehard WB, Schlesinger S (1983) Physical properties of a soluble form of the glycoprotein of vesicular stomatitis virus at neutral and acidic pH. Biochemistry 22:5790–5796

Da Poian AT, Gomes AMO, Oliveira RJN, Silva JL (1996) Migration of vesicular stomatitis virus glycoprotein to the nucleus of infected cells. Proc Natl Acad Sci USA 93:8268–8273

Da Poian AT, Gomes AMO and Coelho-Sampaio T (1998) Kinetics of intracellular viral disassembly probed by bodipy fluorescence dequenching. J Virol Meth 70:45–58

Darden T, York D, Pedersen L (1993) Particle Mesh Ewald: an *N*log (*N*) method for Ewald sums in large systems. J Chem Phys 98:10089–10092

Durrer P, Gaudin Y, Ruigrok RW, Graf R and Brunner J (1995) Photolabeling identifies a putative fusion domain in the envelope glycoprotein of rabies and vesicular stomatitis viruses. J Biol Chem 270:17575–17581

Eckert DM, Kim PS (2001) Mechanisms of viral membrane fusion and its inhibition. Annu Rev Biochem 70:777–810

Eidelman O, Schlegel R, Tralka TS, Blumenthal R (1984) pH-dependent fusion induced by vesicular stomatitis virus glycoprotein reconstituted into phospholipid vesicles. J Biol Chem 259:4622–4628

Estepa A, Coll JM (1996) Pepscan mapping and fusion related properties of the major phosphatidylserine-binding domain of the glycoprotein of viral hemorragic septicemia virus, a salmonid rhabdovirus. Virology 216:60–70

Florin EL, Moy VT, Gaub HE (1994) Adhesion forces between individual ligand-receptor pairs. Science 264:415–417

Fredericksen B, Whitt MA (1995) Vesicular stomatitis virus glycoprotein mutations that affect membrane fusion activity and abolish virus infectivity. J Virol 69:1435–1443

Gergely C, Voegel J-C, Schaaf P, Senger B, Maaloum M, Hörber JKH, Hermmerlé J (2000) Unbinding process of adsorbed proteins under external stress studied by atomic force microscopy spectroscopy. Proc Natl Acad Sci USA 97:10802–10807

Hernandez LD, Hoffman LR, Wolfsberg TG, White JM (1996) Virus-cell and cell-cell fusion. Annu Rev Cell Dev Biol 12:627–661

Herrmann A, Clague MJ, Puri A, Morris SJ, Blumenthal R and Grimaldi S (1990) Effect of erythrocyte transbilayer phospholipid distribution on fusion with vesicular stomatitis virus. Biochemistry 29:4054–4058

Jass J, Tjärnhage T, Puu G (2000) From liposomes to supported, planar bilayer structures on hydrophilic and hydrophobic surfaces: an atomic force microscopy study. Biophys J 79:3153–3163

Li Y, Drone C, Sat E, Ghosh HP (1993) Mutational analysis of the vesicular stomatitis virus glycoprotein G for membrane fusion domains. J Virol 67:4070–4077

Lindahl E, Hess B, van der Spoel D (2001) GROMACS 3.0: A package for molecular simulation and trajectory analysis. J Mol Mod 7:306–317

Mastromarino P, Conti C, Goldoni P, Hauttecoeur B, Orsi N (1987) Characterization of membrane components of the erythrocyte involved in vesicular stomatitis virus attachment and fusion at acidic pH. J Gen Virol 68:2359–2369

Miles EW (1977) Modification of histidyl residues in proteins by diethyl pyrocarbonate. Meth Enzymol 47:431–442

Nieva JL, Agirre A (2003) Are fusion peptides a good model to study viral cell fusion? Biochim Biophys Acta 1614(1):104–115

Odell D, Wanas E, Yan J, Ghosh HP (1997) Influence of membrane anchoring and cytoplasmic domains on the fusogenic activity of vesicular stomatitis virus glycoprotein G. J Virol 71:7996–8000

Pak CC, Puri A, Blumenthal R (1987) Conformational changes and fusion activity of vesicular stomatitis virus glycoprotein: [^{125} I]iodonaphtyl azide photolabeling studies in biological membranes. Biochemistry 36:8890–8896

Pandit SA, Berkowitz ML (2002) Molecular dynamics simulation of dipalmitoylphosphatidylserine bilayer with Na+ counterions. Biophys J 82:1818–1827

Puu G, Gustafson I (1997) Planar lipid bilayers on solid supports from liposomes-factors of importance for kinetics and stability. Biochim Biophys Acta 1327:149–161

Puu G, Artursson E, Gustafson I, Lundstro M, Jass J (2000) Distribution and stability of membrane proteins in lipid membranes on solid supports. Biosensors Bioelectronics 15:31–41

Reviakine I, Brisson A (2000) Formation of supported phospholipid bilayers from unilamellar vesicles investigated by atomic force microscopy. Langmuir 16:1806–1815

Ryckaert JP, Ciccott GI, Berendsen HJC (1977) Numerical integration of the cartesian equations of motion of a system with constraints: molecular dynamics of n-alkanes. J Comp Phys 23:327–341

Schlegel R, Willingham MC, Pastan IH (1982) Saturable binding sites for vesicular stomatitis virus on the surface of Vero cells. J Virol 43:871–875

Schlegel R, Tralka TS, Willingham MC, Pastan I (1983) Inhibition of VSV binding and infectivity by phosphatidylserine: is phosphatidylserine a VSV-binding site? Cell 32:639–646

Shokralla S, He Y, Wanas E, Ghosh HP (1998) Mutations in a carboxy-terminal region of vesicular stomatitis virus glycoprotein G that affect membrane fusion activity. Virology 256:119–129

Skehel JJ, Wiley DC (2000) Receptor binding and membrane fusion in virus entry: the influenza hemagglutinin. Annu Rev Biochem 69:531–569

Superti F, Seganti L, Tsiang H, Orsi N (1984) Role of phospholipids in rhabdovirus attachment to CER cells. Arch Virol 81:321–328

Zhang L, Ghosh HP (1994) Characterization of the putative fusogenic domain in vesicular stomatitis virus glycoprotein G. J Virol 68:2186–2193

Zlatanova J, Lindsay SM, Leuba SH (2000) Single molecule force spectroscopy in biology using the atomic force microscope. Prog Biophys Mol Biol 74:37–61

CURRICULUM VITAE

Nome: Fausto Stauffer Junqueira de Souza
Nascimento: 20 de Março de 1981
Naturalidade: Rio de Janeiro

FORMAÇÃO ACADÊMICA

- Graduação em Medicina pela Universidade Federal do Rio de Janeiro, de Fevereiro de 1999 a Dezembro de 2004.
- Doutorado em Bioquímica Médica no Instituto de Bioquímica Médica da Universidade Federal do Rio de Janeiro (programa MD-PhD), orientação pela Profa. Dra. Andrea T. Da Poian, de Agosto de 2003 a Julho de 2007, com financiamento da Fundação de Amparo a Pesquisa do Estado do Rio de Janeiro (FAPERJ). Bolsista FAPERJ nota 10 no período de Agosto de 2006 a Julho de 2007.
- Doutorado Sandwich no Laboratório de Biofísica Molecular, Departamento de Química e Bioquímica, Faculdade de Ciências da Universidade de Lisboa (programa CAPES-GRICES), orientação pelo Prof. Dr. Miguel A. R. B. Castanho, de Agosto de 2005 a Abril de 2006, com financiamento da Coordenação de Aperfeiçoamento de Pessoal de Nível Superior (CAPES).

ORIENTAÇÃO DE ESTUDANTE

- Marcos Coutinho Schechter - iniciação científica de julho de 2004 a janeiro de 2006 (aluno da faculdade de medicina).
- Nathalia Oliveira Santos - iniciação científica de agosto de 2006 a julho de 2007.
- Fernando Avila Queiroz - iniciação científica de agosto de 2006 a julho de 2007.

PUBLICAÇÕES

- Carneiro, F. A., Bianconi, M. L., Weissmüller, G., **Stauffer, F.**, Da Poian, A. T. (2002). Membrane recognition by vesicular stomatitis virus involves enthalpy-driven protein-lipid interactions. *J. Virol.* **76**, 3756-3764.
- Carneiro, F. A., **Stauffer, F.**, Lima, C. S., Juliano, M. A., Juliano, L., Da Poian, A. T. (2003). Membrane fusion induced by vesicular stomatitis virus depends on histidine protonation. *J. Biol. Chem.* **278**, 13789-13794.
- Da Poian, A. T., Carneiro, F. A., **Stauffer, F.** (2005). Viral Membrane Fusion: is the Glycoprotein G of Rhabdovirus a New class of Viral Fusion Protein? *Brazilian Journal of Medical and Biological Research*, **38**(6): 813-23.
- Carneiro, F. A., Lapido-Loureiro, P. A., Cordo, S. M., **Stauffer, F.**, Weissmuller, G., Bianconi, M. L., Juliano, M.A., Juliano, L., Bisch, P. M., Da Poian, A.T. (2006). Probing the interaction between vesicular stomatitis virus and phosphatidylserine. *Eur Biophys J.*, **35**: 145-154.
- **Stauffer, F.**, El-Bacha, T. P., Da Poian, A. T. (2006). Advances in the development of inactivated virus vaccines. *Recent Patents on Anti-Infective Drug Discovery*, **3**: 291-296.
- **Stauffer, F.**, De Miranda, J. M., Schechter, M. C., Carneiro, F. A., Salgado, L. T., Machado, G., Da Poian, A. T. (2007). Inactivation of vesicular stomatitis virus through inhibition of membrane fusion by chemical modification of the viral glycoprotein. *Antiviral Research*, **73**: 31-39.
- **Stauffer, F.**, De Miranda, J. M., Schechter, M. C., Queiroz, F. A., Santos, N. O., Alves, A. M. B., Da Poian, A. T. (2007). New chemical method of viral inactivation for vaccine development. *Vaccine*, **25**: 7885-7892.
- **Stauffer, F.**, Melo, M. N., Carneiro, F. A., Sousa, F. J. R., Juliano, M.A., Juliano, L., Mohana-Borges, R., Da Poian, A.T., Castanho, M. A. R. B. (2007). Interaction between dengue virus fusion peptide and lipid bilayers depends on peptide clustering. *Molecular Membrane Biology. In press*.

Patentes depositadas:

- **Stauffer, F.**, Carneiro, F. A., De Miranda, J. M., Machado, G., Da Poian, A. T. (2004). Composição para inativação viral, processo de inativação viral, vacina e processo de produção de vacina. Depósito número BR0401466, publicada em 29 de Novembro de 2005.

Livros Grátis

(http://www.livrosgratis.com.br)

Milhares de Livros para Download:

Baixar livros de Administração
Baixar livros de Agronomia
Baixar livros de Arquitetura
Baixar livros de Artes
Baixar livros de Astronomia
Baixar livros de Biologia Geral
Baixar livros de Ciência da Computação
Baixar livros de Ciência da Informação
Baixar livros de Ciência Política
Baixar livros de Ciências da Saúde
Baixar livros de Comunicação
Baixar livros do Conselho Nacional de Educação - CNE
Baixar livros de Defesa civil
Baixar livros de Direito
Baixar livros de Direitos humanos
Baixar livros de Economia
Baixar livros de Economia Doméstica
Baixar livros de Educação
Baixar livros de Educação - Trânsito
Baixar livros de Educação Física
Baixar livros de Engenharia Aeroespacial
Baixar livros de Farmácia
Baixar livros de Filosofia
Baixar livros de Física
Baixar livros de Geociências
Baixar livros de Geografia
Baixar livros de História
Baixar livros de Línguas